Enzyme Recovery from Biological Wastewater Treatment

Ziyi Liu

Supervisor: Professor Stephen R. Smith

June 2021

Department of Civil and Environmental Engineering

Imperial College London

A thesis submitted to Imperial College London for the degree of Doctor of Philosophy

Declaration of originality and copyright

I declare that this thesis is my own original work. Any material from the published or unpublished work of others is appropriately referenced.

Abstract

Enzymes are high value industrial bio-catalysts with extensive applications in a wide range of manufacturing and processing sectors. The catalytic efficiency of enzymes can be several orders higher compared to inorganic chemical catalysts under mild conditions. However, the nutrient medium necessary for biomass culture represents a significant cost to industrial enzyme production. Activated sludge (AS) is a waste product of biological wastewater treatment and consists of microbial biomass that degrades organic matter by producing substantial quantities of hydrolytic enzymes. Therefore, enzyme recovery from AS offers an alternative, potentially viable approach to industrial enzyme production. Enzyme extraction from disrupted AS flocs is technically feasible and has been demonstrated at experimental scale.

However, no consistent, optimal approach is available for the enzyme extraction from AS and the production of bio-enzymes from this biomass source can be affected by a range of factors, such as the operational extraction parameters. Moreover, free enzymes in the crude extract exhibit poor storage and operational stability, and are readily inactivated and difficult to recycle and reuse, which limits their large-scale commercial applications. The aim of this study is to develop a robust technology for enzyme recovery from AS and to explore the potential applications of recovered enzymes.

A protocol for harvesting crude enzyme extracts from AS, by using sonication treatment to disrupt AS flocs, was set up; the impact of the sonication operational parameters and sludge sampling location on the enzyme extraction efficiency was investigated. A carrier-free, immobilised enzyme product, cross-linked enzyme aggregates (CLEA), was produced from the crude AS enzyme extract for the first time; the CLEA technique essentially combines purification and stabilisation of crude AS enzyme in a single step, and avoids introducing a large amount of inert carrier into the enzyme product. The AS CLEA contained a variety of hydrolytic enzymes and demonstrated high potential to be used for bioconversion of complex organic substrates.

Acknowledgements

I would like to express my deepest gratitude to my supervisor, Professor Stephen R. Smith, who always has confidence in me and supported me throughout my journey of this project. His expertise and guidance were invaluable for this research project.

I am grateful to China Scholarship Council and Yorkshire Water Services Ltd to sponsor this research. Thanks to Tom Taylor for his advice and comments on this project at each steering group meeting.

Thanks to Geoff Fowler and Ángel Nievas Pino for their assistance, advice and creativity to solve every problem I encountered during the experimental works at the Roger Perry lab. Thanks to Steve Oxtoby for his kind help during the sludge sample collections. Thanks to Marcus Yio for helping me with the SEM. Thanks to Liying Jiang for helping me with the microbial culture works.

Thanks to all my colleagues and friends: Yang Yu, Yiran Fan, Amanda Larasati, Marc Heitmann, Jin Liu, and others in the lab and Office 411, for making my life so much fun.

Finally, I would like to thank my parents, Li Ai and Qinghua Liu, and my husband, Yang Xue, for their care, concern and support. Without them, I would not have been able to fulfil my PhD studies.

Table of contents

Declaration of originality and copyright....1
Abstract....2
Acknowledgements....3
Table of contents....4
List of tables....12
List of figures....13
Acronyms....18
Chemical formulae and abbreviations....20
1 Introduction....22
1.1 Background....22
1.2 Aims and objectives....25
1.3 Overview of the research strategy....25
2 Literature review....27
2.1 Wastewater treatment and sludge management....27
2.1.1 Conventional process description....27
2.1.2 Sustainability of the Water Industry....28
2.2 Fundamentals of enzymology....29
2.2.1 Structure of enzymes and their classification....29
2.2.2 Mechanisms of enzyme catalysis....29
2.2.3 Enzyme kinetics....30
2.3 Enzyme location in activated sludge....31
2.3.1 Extracellular enzyme distribution patterns within activated sludge flocs....31
2.3.2 Influence of substrate incorporation....34
2.4 Crude enzyme extraction from activated sludge....35
2.4.1 Extraction protocol....35
2.4.2 Physical disruption....39
2.4.2.1 Sonication....39
2.4.2.2 Milling....44

2.4.2.3 Advantages and disadvantages 46
2.4.3 Chemical extractants 47
2.4.3.1 Cation removal agents 47
2.4.3.2 Formaldehyde 48
2.4.3.3 Surfactants 48
2.4.4 Factors influencing enzyme extraction from activated sludge 49
2.4.4.1 Enzyme location in sludge flocs 49
2.4.4.2 Upstream wastewater management 50
2.5 General Enzyme purification and stabilisation 53
2.5.1 Purification and consolidation 53
2.5.2 Stabilisation and immobilisation 55
2.6 Cross-linked enzyme aggregates 55
2.6.1 Background 55
2.6.2 Fundamental principles of CLEA preparation. 58
2.6.3 Precipitants 60
2.6.3.1 Hydration layer of proteins 60
2.6.3.2 Neutral salts 61
2.6.3.3 Water miscible organic solvents 61
2.6.3.4 Nonionic polymers 62
2.6.3.5 Effect of operational mode on CLEA activity 62
2.6.4 Cross-linkers 63
2.6.4.1 Glutaraldehyde 63
2.6.4.2 Macromolecular saccharide derivatives: poly-aldehydes 67
2.6.4.3 Others 69
2.6.5 Additives 70
2.6.5.1 Protein feeder: bovine serum albumin 70
2.6.5.2 Ionic polymer: polyethyleneimine 71
2.6.5.3 Surfactant 72
2.6.5.4 Saccharides 73

2.6.5.5 Metal ions 73
2.6.5.6 Others 74
2.6.6 Recent innovations in enzyme immobilisation by cross-linking 74
2.6.6.1 Co-immobilisation of different types of enzymes in CLEAs 74
2.6.6.2 Magnetic CLEAs 75
2.6.6.3 Post stabilisation of CLEAs by carrier bound immobilisation 76
2.7 Potential application of recovered enzymes from activated sludge 77
2.7.1 Wastewater treatment 77
2.7.2 Pre-treatment of waste for anaerobic digestion 78
2.7.3 Organic micropollutant degradation 79
2.7.4 Biofuel production 81
2.7.5 Other applications 81
2.8 Secondary benefits of enzyme recovery from activated sludge 83
3 General materials and methods 85
3.1 Materials 85
3.2 Sludge sample collection 85
3.3 Sludge characterisation 87
3.3.1 pH 87
3.3.2 Total solids & volatile solids 87
3.4 General enzyme extraction and recovery procedures 88
3.5 Indicators of cell disruption 90
3.5.1 Protein 90
3.5.2 Deoxyribonucleic acid 90
3.6 Enzyme activity assays 91
3.6.1 Protease activity 91
3.6.2 Lipase activity 91
3.6.3 Amylase activity 91
3.6.4 Cellulase activity 92
3.6.5 Dehydrogenase activity 92

3.7 Statistical analysis 92
4 Optimisation of crude enzyme extraction from activated sludge 93
4.1 Introduction 93
4.2 Materials and methods 94
4.2.1 Sludge sampling 94
4.2.2 Preliminary comparison of enzyme extraction methods 94
4.2.3 Optimising probe sonication for activated sludge disruption and enzyme extraction 97
4.2.3.1 Summary of experimental optimisation conditions 97
4.2.3.2 Effect of sonication duration and energy level 98
4.2.3.3 Effect of solids content 98
4.2.3.4 Effect of surfactant addition 98
4.2.4 Effect of activated sludge sampling location on enzyme extraction 99
4.2.5 Enzyme recovery rate 99
4.3 Results 100
4.3.1 Preliminary comparison of activated sludge disruption methods 100
4.3.2 Effect of Sonication conditions 101
4.3.2.1 Duration and energy level 101
4.3.2.2 Solids content 104
4.3.2.3 Surfactant addition 105
4.3.2.4 Summary of optimum sonication protocol for activated sludge disruption and enzyme extraction 106
4.3.3 Effect of activated sludge sampling location on enzyme extraction 106
4.3.4 Enzyme recovery rate 107
4.3.5 Energy consumption 108
4.3.6 Reproducibility of enzyme activities in different batches of activated sludge 108
4.4 Discussion 110
4.4.1 Comparison of cell disruption methods 110
4.4.1.1 Bead milling 110

4.4.1.2 Sonication 111
4.4.2 Sonication device 112
4.4.3 Effect of operational conditions on enzyme extraction efficiency by sonication probe 114
4.4.3.1 Duration, amplitude and energy level 114
4.4.3.2 Solids content of sludge 116
4.4.3.3 Surfactant addition 117
4.4.4 Effect of activated sludge sampling location on enzyme extraction 118
4.4.5 Summary of crude enzyme extraction from sludge 119
5 Consolidation and stabilisation of crude enzymes by cross-linking 120
5.1 Introduction 120
5.2 Materials and methods 122
5.2.1 Enzyme preparation 122
5.2.2 CLEA preparation methodology 123
5.2.2.1 General CLEA preparation process 123
5.2.2.2 Chemical precipitation of soluble enzyme 123
5.2.2.3 Cross-linking of the precipitated enzymes 124
5.2.3 Preliminary tests 124
5.2.3.1 Precipitation of AS enzymes by $(NH_4)_2SO_4$ 124
5.2.3.2 CLEA preparation from commercial protease with $(NH_4)_2SO_4$ precipitation 124
5.2.3.3 CLEA preparation from commercial amylase with acetone precipitation .125
5.2.4 CLEA preparation from crude AS enzyme extracts 126
5.2.4.1 Enzyme cross-linking by glutaraldehyde 126
5.2.4.2 Enzyme cross-linking by dextran aldehyde 126
5.2.5 Fourier-transform infrared spectroscopy 126
5.2.6 CLEA morphology 127
5.2.7 Preservation of prepared CLEAs 127
5.3 Results 128
5.3.1 Preliminary tests 128

5.3.1.1 Precipitation of AS enzymes by $(NH_4)_2SO_4$ 128
5.3.1.2 CLEAs of commercial protease with $(NH_4)_2SO_4$ precipitation 128
5.3.1.3 CLEAs of commercial amylase with acetone precipitation 130
5.3.1.4 Summary of the preliminary experiments 131
5.3.2 CLEAs of AS extracted enzymes 132
5.3.2.1 Cross-linking with glutaraldehyde 132
5.3.2.2 Cross-linking with dextran aldehyde 133
5.3.2.3 Summary of optimal conditions for CLEA preparation from crude enzyme extracts from AS 136
5.3.3 FTIR analysis 136
5.3.4 Morphology and micro-structure of AS CLEAs 138
5.3.5 Preservation of prepared CLEAs 139
5.4 Discussion 141
5.4.1 Precipitants 141
5.4.2 Cross-linker 143
5.4.2.1 Glutaraldehyde 143
5.4.2.2 Dextran aldehyde 145
5.4.3 Additives 147
5.4.4 Micro-structure/morphology of CLEAs and its enzyme activity 147
5.4.5 CLEA preservation 148
5.4.5.1 Buffer suspension 148
5.4.5.2 Freeze drying 148
5.4.5.3 Selection of preservation conditions 150
5.4.6 Summary of CLEA preparation from AS 150
6 Substrate hydrolysis activity of CLEAs prepared from activated sludge 152
6.1 Introduction 152
6.2 Materials and methods 154
6.2.1 Wheat flour and primary sludge 154
6.2.2 CLEA preparation 155

6.2.3 Substrate preparation 155
6.2.3.1 Wheat flour 155
6.2.3.2 Sludge 155
6.2.4 Hydrolysis of organic materials 156
6.2.5 Inhibition of sludge matrix on CLEA activity 156
6.2.6 Sludge cell culture 156
6.2.7 Indicators of the progress of enzymatic hydrolysis 157
6.2.7.1 Soluble total organic carbon 157
6.2.7.2 Reducing sugar and tyrosine 157
6.2.8 Progress curve of enzymatic hydrolysis 158
6.3 Results 160
6.3.1 Hydrolysis of flour 160
6.3.1.1 Accumulation of hydrolysis products 160
6.3.1.2 Hydrolysis kinetics of wheat flour 162
6.3.2 Hydrolysis of activated sludge 166
6.3.2.1 CLEA activity in sludge supernatant 166
6.3.2.2 Whole AS 166
6.3.2.3 Autoclaved AS 168
6.3.2.4 γ-Irradiated AS 169
6.3.2.5 Sonicated AS 170
6.3.2.6 Sludge cell culture 172
6.3.2.7 Hydrolysis kinetics of γ-irradiated AS and sonicated AS 173
6.4 Discussion 174
6.4.1 Quantifying the kinetics of enzymatic hydrolysis reactions 174
6.4.2 Hydrolysis of wheat flour 176
6.4.2.1 Factors influencing the CLEA hydrolysis of wheat flour 176
6.4.2.2 Competitive reactions to CLEA hydrolysis 179
6.4.3 Effect of sludge chemical environment on CLEA hydrolysis activity 179
6.4.4 Hydrolysis of activated sludge 182

6.4.4.1 Whole sludge....182
6.4.4.2 Autoclaved AS....183
6.4.4.3 Gamma-irradiated AS....183
6.4.4.4 Sonicated AS....184
6.4.5 Summary....185
7 General discussion....187
7.1 Multi-CLEA preparation from crude activated sludge enzyme extracts....187
7.1.1 Enzyme activity in AS CLEA....187
7.1.2 Impact of enzyme characteristics on CLEA activity....194
7.1.2.1 Physical and chemical features....194
7.1.2.2 Enzyme source....195
7.1.2.3 Summary....195
7.1.3 Factors influencing cross-linking chemistry and CLEA properties....196
7.1.3.1 Random binding sites and enzyme orientation....196
7.1.3.2 Intramolecular cross-linking....197
7.1.3.3 Centrifugation and mass transfer limitations....198
7.1.3.4 Summary....199
7.2 Hydrolysis of complex organic substrates by AS CLEA....199
7.2.1 Wheat flour and activated sludge hydrolysis....199
7.2.1.1 Pattern of enzymatic hydrolysis product yield....199
7.2.1.2 Factors influencing CLEA hydrolysis of complex organic matrices....200
7.2.1.3 Feasibility of CLEA pretreatment of sludge....200
7.2.2 Feasibility of CLEA hydrolysis of complex organic waste materials into valuable commodities and products....202
7.2.3 Operational attributes and advantages of CLEAs for industrial application....204
7.3 High-value enzyme product recovery from biological wastewater treatment....206
8 Conclusions and recommendations for future research....208
9 References....212
Appendix....255

List of tables

Table 2-1 Enzymes detected in activated sludge and their distribution in sludge flocs 32

Table 2-2 Methods for crude enzyme extraction from activated sludge 36

Table 2-3 Examples of reactive amino acids/functional groups in proteins (corresponding reactive residues are shown in blue circles) that can react with aldehydes 59

Table 4-1 Summary of the specific conditions for different enzyme extraction methods tested 96

Table 4-2 Summary of different experimental conditions for the optimisation of probe sonication extraction of enzymes from activated sludge 97

Table 4-3 Effect of surfactant addition on activated sludge disruption and extracted enzyme activity 106

Table 5-1 Summary of experimental conditions for CLEA preparation from commercial protease enzyme, with 80% saturated $(NH_4)_2SO_4$ as the precipitant and glutaraldehyde as the cross-linker 125

Table 5-2 Precipitation efficiency and residual activity of protease and α-amylase in the precipitate 128

Table 5-3 FTIR peaks and bands relevant to the conformational changes after CLEA preparation of AS enzymes 137

Table 5-4 Residual enzyme activity of freeze-dried CLEA prepared from crude AS extracts before and after storage at -20 °C (% relative to the fresh prepared CLEA suspension before freeze drying) 141

Table 6-1 First order kinetic model of soluble total organic carbon (sTOC), reducing sugar and tyrosine accumulation from the enzymatic hydrolysis of wheat flour by AS CLEA at two addition rates and incubated at 40 °C for 6.5 h (best-fit coefficients in 95% confidence interval ± standard deviation) 164

Table 6-2 Average CLEA activities (%) in primary sludge supernatant compared to the activity in standard buffer solution, which was set as 100% 166

Table 6-3 First order kinetic model of tyrosine accumulation from the enzymatic hydrolysis of γ-irradiated AS and sonicated AS by CLEA at 1:10 v/v dosage rate and incubated at 40 °C for 6.5 h (best-fit coefficients in 95% confidence interval ± standard deviation) 173

Table 7-1 Comparison of enzyme activities and recovery rate in carrier-free CLEAs (% of original soluble enzymes) at optimum conditions 189

Table 7-2 Recyclability of various CLEAs in bioconversion processes 205

List of figures

Figure 1-1 General structure and linkage between different phases of the research 26

Figure 2-1 Schematic of a conventional wastewater treatment and sludge management process (grey shadowed area representing biological AS process, adapted from (Tchobanoglous et al., 2014)) 28

Figure 2-2 Organisation of enzyme structure using lysozyme as an example (binding sites in blue, catalytic site in red and peptidoglycan substrate in black) (Shafee, 2015) 30

Figure 2-3 (a) Chemical structure of microbial extracellular polymeric substances (EPS); (b) Spatial distribution of different EPS fractions and the relationship with a bacteria cell (tightly bound EPS (TB-EPS) is the fraction that is closely associated with the cell; loosely bound EPS (LB-EPS) diffuses from TB-EPS and is located at the outer region of AS flocs) (Lin et al., 2014) 33

Figure 2-4 Typical stages to extract enzymes from activated sludge 35

Figure 2-5 Representation of the three stages of cell disruption by sonication: (a) Stage 1: pores form on the outer cell wall due to the external mechanical forces exerted by cavitation, releasing some periplasmic enzymes; (b) Stage 2: chemical agents diffuse from the external solution into the cell, generating a combined disruptive effect with the mechanical forces from sonication; and (c) Stage 3: cell membranes are destroyed by the continuous exposure to cavitation (“fatigue failure” of the cell structure) causing more severe cell disruption, releasing intracellular enzymes and substances (adapted from (Balasundaram and Harrison, 2006)) 39

Figure 2-6 Mechanisms of bead milling in microbial cell disruption (adapted from (Koubaa et al., 2020)) 44

Figure 2-7 Stepwise purification of enzymes 53

Figure 2-8 Enzyme immobilisation by cross-linking; the cross-linker is represented by the orange line; CLEA can be prepared with (a) original enzyme solutions or via co-precipitation with additives (see Section 2.6.5), such as (b) bovine serum albumin (green triangles) and (b) polyethyleneimine (dark blue lines). 57

Figure 2-9 Reaction of enzyme amino groups (e.g. lysine residues) with aldehyde groups of a cross-linker, followed by reduction of the Schiff bases (imines) into more stable single bonds, during CLEA preparation 59

Figure 2-10 Protein folding in aqueous solution under hydrophobic interactions, to allow polar regions (blue) to interact with water, while non-polar hydrophobic regions (red) not interact with the water (Than, 2020) 61

Figure 2-11 Formation of different glutaraldehyde derivatives in solution under different pH conditions (Migneault et al., 2004).....66

Figure 2-12 Sodium periodate oxidation of α-1,6 glycosidic linkages in dextran to form the cross-linking agent, dextran aldehyde (Orrego et al., 2018).....68

Figure 2-13 Glutaraldehyde and its analogues (Schoevaart et al., 2005) 69

Figure 3-1 Waste activated sludge sampling from sludge thickening belt in WWTP1 85

Figure 3-2 Five sampling points (P1-5) of mixed liquor along the aeration tank in WWTP2 .86

Figure 3-3 Sampling mixed liquor and dosing Flopam on-site.....86

Figure 3-4 (a) Wasted activated sludge sample from sludge thickening belt; (b) mixed liquor sample from aerated tank 86

Figure 3-5 General procedures of enzyme extraction and recovery.....89

Figure 4-1 Apparatus used for activated sludge disruption: (a) water-bath type sonication, (b) probe-type sonication, and (c) bead milling 97

Figure 4-2 Volume activity of protease and lipase enzymes and protein content in the crude extracts from activated sludge extracted by different cell disruption methods (vertical bars represent the standard deviation, n=3; see Table 4-1 for explanation of disruption methods 101

Figure 4-3 Effect of sonication duration (minutes) on protein and DNA release from activated sludge at 40% amplitude (vertical bars represent the standard deviation, n=3).....103

Figure 4-4 Effect of sonication duration (minutes) on specific enzyme activities at 40% amplitude (vertical bars represent the standard deviation, n=3).....103

Figure 4-5 Effect of sonication power density (for 10 min duration) on specific enzyme activities (vertical bars represent the standard deviation, n=3) 104

Figure 4-6 Effect of solids content on enzyme activity after sonication treatment for 10 min duration and 40% amplitude (vertical bars represent the standard deviation, n=3) 105

Figure 4-7 Hydrolytic enzyme activities (on left axis) and sludge microbial activity (on right axis) at different sampling points along the length of an activated sludge aeration reactor (point 1-5); sample point 6 was taken from the activated sludge thickening belt (vertical bars represent the standard deviation, n=3).....107

Figure 4-8 Activities of major hydrolytic enzymes extracted from different batches of activated sludge (see Appendix A-1) under optimal conditions (*Note: for measuring α-amylase only, preheat treatment was applied to inactivate the β-amylase contained in the crude enzyme solution, see Section 3.6.3) 109

Figure 5-1 FTIR spectra in 4000–500 cm $^{-1}$ region of glutaraldehyde (red line), periodate oxidised and dialysed dextran aldehyde (blue line), and untreated dextran (green line).....127

Figure 5-2 Distribution of protease activity in CLEA, and supernatants after the 1st, 2nd and 3rd wash (volume activity in original enzyme solution was set as 100%); group number corresponds to the experimental conditions shown in Table 5-1; mean values of two replicate measurements 130

Figure 5-3 CLEA of commercial protease enzyme prepared with 5 mg/mL BSA addition, 80% saturated $(NH_4)_2SO_4$ precipitation, and 0.2% glutaraldehyde cross-linking for 3.5 h at room temperature 130

Figure 5-4 Effect of glutaraldehyde concentration on amylase activity of CLEA prepared from crude AS extracts with 5 mg/mL BSA addition and precipitation with 80% saturated $(NH_4)_2SO_4$ (R_{CLEA}: volume activity in original enzyme solution was set as 100%; error bars represent the standard deviation) 132

Figure 5-5 Effect of glutaraldehyde concentration on solid-liquid separation of CLEAs prepared from AS extracts with 5 mg/mL BSA addition and precipitation with 80% saturated $(NH_4)_2SO_4$. Glutaraldehyde concentrations (% w/v) (left to right): 0.005, 0.01, 0.02, 0.03, 0.04, 0.05, 0.1, 0.15, 0.2, 0.25 and 0.3. 133

Figure 5-6 Effect of dextran aldehyde cross-linker concentration on activities of four different enzymes in CLEA prepared from AS extracts with 5 mg/mL BSA addition and precipitation with (a) 80% saturated $(NH_4)_2SO_4$ or (b) 4:1 acetone (R_{CLEA}: volume activity in original enzyme solution was set as 100%; error bars represent the standard deviation).....135

Figure 5-7 FTIR spectra in 4000–500 cm $^{-1}$ region of freeze-dried crude AS enzyme solution (blue line), and the CLEA prepared under optimal conditions (red line) 137

Figure 5-8 SEM images of: (a) freeze dried crude AS enzyme extract (magnification = 6320×); (b) CLEAs of AS extracted enzymes with irregular ball-shape structure (magnification = 4440×); (c) CLEAs of AS extracted enzymes with amorphous structure (magnification = 7160×) 139

Figure 5-9 Residual enzyme activity in CLEA prepared from crude AS extracts and maintained in Tris-HCl buffer (10 mM, pH 7.0) for 12, 20 and 27 days (% relative to the activities of the fresh prepared CLEA suspension; error bar: standard deviation) 141

Figure 6-1 Effect of AS CLEA at rates of (a) 1:100 v/v and (b) 1:10 v/v on the accumulation of soluble total organic carbon (sTOC) from the hydrolysis of wheat flour incubated at 40 °C (error bars indicate the standard deviation) 160

Figure 6-2 Effect of AS CLEA at rates of (a) 1:100 v/v and (b) 1:10 v/v on the accumulation of reducing sugar from the hydrolysis of wheat flour (error bars indicate the standard deviation) 161

Figure 6-3 Effect of AS CLEA at rates of (a) 1:100 v/v and (b) 1:10 v/v on the accumulation of tyrosine from the hydrolysis of wheat flour (error bars indicate the standard deviation)..... 162

Figure 6-4(a) Sediments in the filtrate at 6.5h, compared to (b) the clear filtrate at 5.5h (the bottles with transparent filtrate were control groups at corresponding time) 162

Figure 6-5 First order kinetic model of (a) sTOC, (b) reducing sugar and (c) tyrosine accumulation from the enzymatic hydrolysis of wheat flour by AS CLEA at two addition rates (1:100 and 1:10 v/v) and incubated at 40°C showing the maximum potential yield of each product (solid line: model prediction for the incubation period 0-6.5 h based on experimental data; dashed line: extrapolation beyond the available experimental data for the period 6.5-26 h; solid symbols: experimental data; error bars: standard deviation) 166

Figure 6-6 Effect of CLEA addition (1:10 v/v) on (a) sTOC and (b) reducing sugar release from the hydrolysis of whole AS (error bars indicate the standard deviation; reducing sugar content shown as average values of two replicate measurements) 167

Figure 6-7 Effect of CLEA addition (1:10 v/v) on (a) sTOC and (b) reducing sugar release from the hydrolysis of autoclaved AS (error bars indicate the standard deviation; reducing sugar content shown as average values of two replicate measurements) 168

Figure 6-8 Effect of CLEA addition (1:10 v/v) on (a) sTOC, (b) reducing sugar and (c) tyrosine release from the hydrolysis of γ-irradiated AS (error bars indicate the standard deviation). 170

Figure 6-9 Effect of CLEA addition (1:10 v/v) on (a) sTOC, (b) reducing sugar and (c) tyrosine release from the hydrolysis of sonicated AS (error bars indicate the standard deviation)... 172

Figure 6-10 Microbial cultures of (a) whole AS, (b) by γ-irradiated AS and (c) sonicated AS 172

Figure 6-11 Predicted data by first order reaction model and its comparison to the experimental data (solid lines-predicted data within 0-6.5 h; dash lines: predicted data within 6.5-26 h; solid dots: experimental data; error bars: standard deviation) 174

Figure 7-1 (a) Random orientation of enzymes in carrier-free CLEAs; (b) directed orientation of carrier-bound enzymes using a functionalised solid carrier (orange lines: cross-linker; green triangles: active catalytic site) 197

Figure 7-2 Intramolecular and intermolecular cross-linking of enzymes by a di-aldehyde cross-linker (adapted from (Ayhan et al., 2012)) 198

Acronyms

Abs	Absorbance
AD	Anaerobic digestion
AMP	Amplitude
ANOVA	One-way analysis of variance
AS	Activated sludge
BNR	Biological nutrient removal
BSA	Bovine serum albumin
CER	Cation exchange resin
CLEA	Cross-linked enzyme aggregate
CLEC	Cross-linked enzyme crystal
CMC	Carboxymethyl cellulose
COD	Chemical oxygen demand
Combi-CLEA	Combined cross-linked enzyme aggregate
DF	Dilution factor
DNA	Deoxyribonucleic acid
DNS	3,5-Dinitrosalicylic acid
DS	Dry solids
EC	Enzyme Commission
EDTA	Ethylene diamine tetraacetic acid
EG-NHS	Ethylene glycolbis(succinimidylsuccinate)
EPS	Extracellular polymeric substances
F/M	Food to microorganism ratio
FDA	Fluorescein diacetate
FTIR	Fourier-transform infrared
HDPE	High-density polyethylene
LB-EPS	Loosely bound extracellular polymeric substances

ML	Mixed liquor
MLSS	Mixed liquor suspended solids
MNP	Magnetic nanoparticles
Multi-CLEA	Multi-purpose cross-linked enzyme aggregate
MW	Molecular weight
NAD+	Nicotinamide adenine dinucleotide
NADP+	Nicotinamide adenine dinucleotide phosphate
OLR	Organic loading rate
OUR	Oxygen uptake rate
PBS	Phosphate-buffered saline
PDA	Potato dextrose agar
PEG	Polyethylene glycol
PEI	Polyethyleneimine
PMSF	Phenylmethylsulfonylfluoride
pNP	p-Nitrophenol
pNPP	p-Nitrophenol palmitate
RNA	Ribonucleic acid
RO	Reverse-osmosis
rpm	Revolutions per minute
RT	Room temperature
sCOD	Soluble chemical oxygen demand
SEM	Scanning electron microscopy
sTOC	Soluble total organic carbon
STPP	Sodium tripolyphosphate
TB-EPS	Tightly bound extracellular polymeric substances
TCA	Trichloroacetic acid
TF	Triphenyl formazan

Tris	Tris(hydroxymethyl)aminomethane
TS	Total solids
TTC	2,3,5-Triphenyltetrazolium chloride
TX100	Triton X100
VFA	Volatile fatty acid
VS	Volatile solids
WAS	Waste activated sludge
WCO	Waste cooking oil
WWTP	Wastewater treatment plant

Chemical formulae and abbreviations

Al^{3+}	Aluminium ion
C	Carbon
Ca^{2+}	Calcium ion
CH_2O	Formaldehyde
$CaSO_4$	Calcium sulphate
CH_3COCH_3	Acetone
CO_2	Carbon dioxide
Cs	Caesium
Cu^{2+}	Copper ion
Fe^{3+}	Ferric ion
Fe_3O_4	Ferrous ferric oxide
H	Hydrogen
$H\cdot$	Hydrogen atoms
H_2SO_4	Sulfuric acid
HCl	Hydrogen chloride
Hg^{2+}	Mercury ion

$KNaC_4H_4O_6 \cdot 4H_2O$	Rochelle salt/Potassium sodium tartrate tetrahydrate
Mg^{2+}	Magnesium ion
N	Nitrogen
Na_2CO_3	Sodium carbonate
Na_2SO_3	Sodium sulphite
$NaBH_4$	Sodium borohydride
NaCl	Sodium chloride
$NaCNBH_3$	Sodium cyanoborohydride
$NaIO_4$	Sodium periodate
NaOH	Sodium hydroxide
NH_3	Ammonia
NH_4^+	Ammonium
$(NH_4)_2SO_4$	Ammonium sulphate
NO_3^-	Nitrate
O	Oxygen
$OH\cdot$	Hydroxyl radicals
$OHC(CH_2)_2CHO$	Succinaldehyde
$OHC(CH_2)_3CHO$	Glutaraldehyde
$OHC(CH_2)_4CHO$	Adipaldehyde
$OHCCH_2CHO$	Malonaldehyde
OHCCHO	Glyoxal
P	Phosphorus
$R\text{-}NH_2$	Amine
S	Sulphur
Zn^{2+}	Zinc ion
ZrO_2	Zirconium dioxide

1 Introduction

1.1 Background

Enzymes are biocatalysts produced by cells and are involved in almost all metabolic processes performed by living organisms. Most enzymes are proteins or polypeptides with a morphological structure and functional groups that provide unique active sites, which are usually highly specific for binding to, and catalysing the reaction of, a particular substrate (Jaeger and Eggert, 2004; Robinson, 2015). Enzymes accelerate biochemical reactions by similar mechanisms to inorganic chemical catalysts (e.g., metals, metal oxides and metal ions), by enabling molecules to overcome the energy barrier necessary for a reaction to proceed and increasing the correct orientation collision of molecules (Berg et al., 2002).

The global market for industrial enzymes was approximately $5.5 billion in 2018 and is expected to rise to $7.0 billion by 2023, representing an annual growth rate of 4.9% (Li and Zong, 2010; BCC Research, 2018). Hydrolytic enzymes, such as protease, amylase and lipase, constitute the majority of the world market (Haki and Rakshit, 2003) and are used extensively in various industries including food, leather and biodiesel production (Zhou et al., 2018a; Khan et al., 2019; Nadeem et al., 2019; Wang et al., 2020), where they reduce dependency on environmentally-harmful chemicals (e.g. sodium sulphide in leather tanning (Zhou et al., 2018a)).

Enzymes offer several key advantages over inorganic catalysts (Hermes et al., 1987; Bisswanger, 2011d). For instance, they can be extremely effective under mild conditions (i.e., ambient/physiological temperatures, atmospheric pressure and neutral pH) and possess a catalytic efficiency several orders greater compared to inorganic catalysts. Furthermore, enzymatic reactions usually induce fewer side-reactions and generate less waste by-products. Therefore, enzymes can provide an effective, environmentally sustainable alternative to inorganic chemical catalysts in a wide range of industrial processes.

Commercial enzymes are typically extracted from microbial biomass, including different types of fungi, such as yeast, produced in an industrial fermentation process, using carefully formulated culture media to provide the essential nutrients necessary for microbial growth, followed by further consolidation and purification (Gibson and Koch, 2019). Enzymes are extracted by disrupting the biomass and formulated into marketable solid or liquid products by the addition of stabilisers (neutral salts such as ammonium sulphate or low molecular weight (MW) polyols such as glycerol, and sorbitol), designed to maintain the protein conformation, and standardising agents (salts or carbohydrates such as starch, maltodextrins and sugar alcohols), to dilute the extracted enzymes to a standardised activity (Aberer et al., 2002). In particular, polysaccharide-containing substrates are frequently used as the substrate for

fermentation and growth of microorganism, providing both carbon and energy for the microbial growth; typical materials include unrefined sugar, hydrolysates of wood and starch, fruit juices, starch from various grains (barley, corn, rice, rye, and wheat) or potatoes, etc (Aberer et al., 2002). However, these synthetic culture media represent one of the most significant costs for commercial enzyme production, equivalent to 30-40% of the total manufacturing cost (Tyagi and Lo, 2013). Therefore, high costs of production translate into a high market retail price and, consequently, enzymes produced by standard industrial methods are generally too expensive for wide adoption in large-scale and continuous industrial processes. Moreover, consumption of these materials in enzyme production could compete with food production and bio-fuel generation (Lee and Lavoie, 2013), and potentially cause an increase in food prices (Kurowska et al., 2020). Thus, alternative, cost-effective approaches to producing hydrolytic microbial biomass, avoiding the need for synthetic growth media, would offer significant commercial advantages for industrial enzyme production.

Wastewater treatment is essential to protect human health and the environment, and involves a series of physico-chemical and biological processes to remove pollutants from the wastewater stream, producing a residual by-product, sewage sludge. The main stages of wastewater treatment include: primary sedimentation, followed by biological treatment by the activated sludge (AS) process. Total sludge production from wastewater treatment within the European Union is almost 10 M t dry solids (DS) (Eurostat, 2021) and the treatment and management of sewage sludge residues is a highly topical subject (Gherghel et al., 2019). Recycling to farmland as a fertiliser and soil conditioner is the main approach to sludge management adopted in the majority of countries globally, however, other significant opportunities exist to recover potentially more valuable resources from sludge (Smith, 2014). Drivers to increase value recovery in wastewater and sludge treatment systems include offsetting the significant costs associated with sludge handling and management (Shaddel et al., 2019), which account for up to 60% of the total operating cost of wastewater treatment plant (WWTP), as well as supporting circular economy as a whole.

Recently, biological sludge generated during wastewater treatment by the AS process has been identified as potentially an alternative source of biomass for industrial enzyme extraction (Liu and Smith, 2020a). Within the AS process, a diverse community of prokaryotic and eukaryotic microorganisms develop in suspended floc structures (up to 2 mm diameter) and degrade non-settable organic substrates in wastewater by producing substantial quantities of hydrolytic enzymes (e.g. protease, lipase, α-glucosidase, α-amylase, cellulase, dehydrogenase and phosphatases). These enzymes specifically cleave the sensitive linkage bond of large organic polymer molecules to produce simpler monomer units that can transfer across the cell membrane to be metabolised by bacteria (Boczar et al., 1992; Szilveszter et

al., 2009). The majority of hydrolytic enzymes are either adsorbed to the cell surface or are embedded in extracellular polymeric substances (EPS) surrounding bacterial cells (Wingender et al., 1999). Several studies (Jung et al., 2001; Gessesse et al., 2003; Nabarlatz et al., 2010) report the extraction of crude enzymes from biological wastewater treatment by disrupting AS flocs, representing the first steps towards developing the potential commercial scale recovery of hydrolytic enzyme products from this waste biomass source. However, no consistent, optimal approach is available for enzyme extraction from AS and the production of bio-enzymes from this biomass source can be affected by a range of factors, including the operational parameters for disrupting the AS cells and upstream wastewater treatment conditions (e.g. income wastewater composition, wastewater treatment reactor type, sludge age, etc). In addition, few studies reported the maximum potential enzyme recovery rate from AS and no information is available in terms of the hydrolytic enzyme activities in the AS in the presence of varying levels of organic substrates.

Crude extracted enzyme solutions from the sludge biomass inevitably contain a large amount of co-extracted materials (e.g. inhibitory chemicals, cellular substances, etc.) and often show poor storage and operational stability. They are also readily inactivated and are difficult to recycle and reuse, which limits their large scale commercial application (Sahutoglu and Akgul, 2015). Therefore, purification and stabilisation is necessary to upgrade crude AS extracts to develop marketable, high value commercial products from this secondary biomass source. Conventional purification and stabilisation of enzyme extracts via the consolidation of the active content (e.g. by dialysis, chemical precipitation, ultrafiltration, chromatography, electrophoretic systems and gel separation), is followed by immobilisation of the consolidated enzymes onto inert carriers by adsorption, entrapment or encapsulation (Sharma et al., 2001; Bisswanger, 2011b).

Recently, a novel technique to produce carrier-free immobilised enzyme products, cross-linked enzyme aggregates (CLEAs), has attracted increasing attention since it essentially combines consolidation and stabilisation of crude enzyme in a single step, and avoids introducing a large amount of inert content (i.e. the carrier) into the enzyme product and diluting the enzyme activity. Enzymes formulated into CLEAs show enhanced mechanical strength and increased resistance to denaturation under extreme conditions (e.g. pH and temperature) or exposure to organic solvents, compared to the corresponding soluble enzyme (Cui et al., 2017; Asgher et al., 2018). This technique has been successfully applied to an increasing number of hydrolytic enzymes including laccases, amylase, lipase, and cellulase, amongst others (Sheldon, 2011a), demonstrating its significant potential for enhancing and upgrading enzyme products from AS. However, highly purified, commercially available enzyme products are used in most of the previous studies (e.g. (Shah et al., 2006; Wang et

al., 2011; Sinirlioglu et al., 2013; Torabizadeh et al., 2014; Zhu et al., 2021)). CLEA preparation from the crude and highly complex enzyme source, i.e. AS, has not been previously reported, and new approaches of formulating the AS enzymes into a product that can be applied in practice need to be set up. In addition, the performance of the produced CLEA for bioconversion of organic substrates needs to be assessed.

1.2 Aims and objectives

This project aims to determine the technical feasibility of recovering hydrolytic enzymes from wastewater treatment process, develop a robust and sustainable technology for enzyme recovery from the complex AS matrix, and explore the impacts of different operational conditions on recovery performance. A further aim is to examine the potential applications of recovered bio-enzymes for wastewater and sludge treatment process enhancement.

The specific objectives are to:

- Develop an extraction-consolidation protocol for enzyme recovery from AS;
- Optimise the crude enzyme extraction process;
- Quantify the impacts of different extraction operational conditions on enzyme activity recovery in the final product;
- Develop a consolidation and stabilisation method for extracted AS enzymes via the cross-linking technique;
- Determine the optimum storage methods for the AS enzyme product;
- Assess potential applications of the recovered enzymes at laboratory scale, including hydrolysing complex organic materials as a pretreatment for anaerobic digestion (AD).

1.3 Overview of the research strategy

The general structure of this study is summarised in Figure 1-1. Based on the literature review (Chapter 2), laboratory experiments were carried out to develop the protocol of producing crude enzyme extract from AS (Chapter 4) and impacts of operational conditions, including sludge cell disruption method, treatment duration, energy input, solids content and chemical additive, on the enzyme extraction process were examined. Production of a carrier-free immobilised enzyme CLEA product from the crude extract, was investigated in Chapter 5, involving selection of chemical reagents (precipitant, cross-linker and additive) and the corresponding reaction conditions, as well as the preservation method of the CLEA. The potential application of the CLEA in hydrolysing complex organic materials was explored in Chapter 6, and wheat flour and AS were selecting representing complex organic substrates with contrasting physicochemical and biological properties.

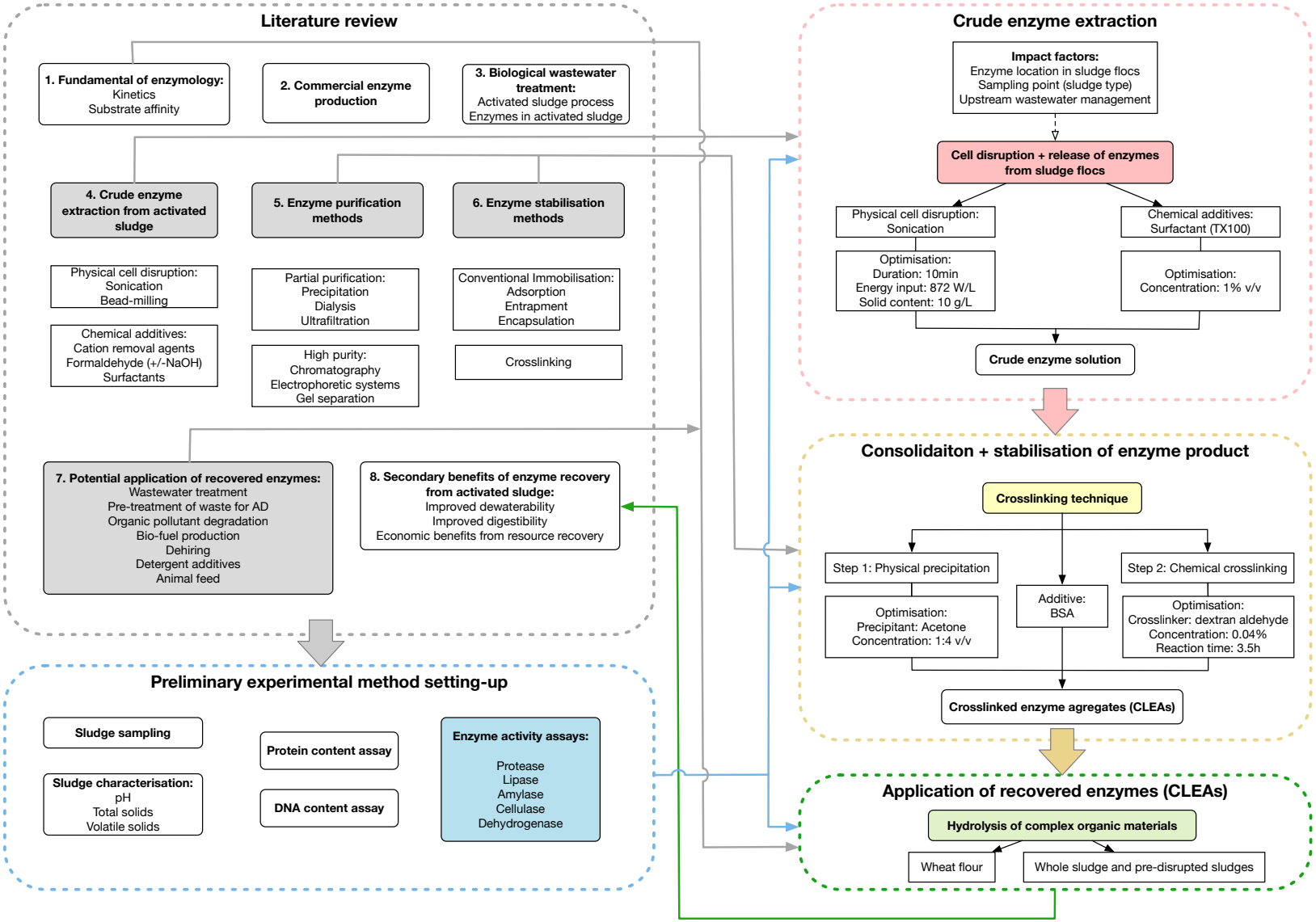

Figure 1-1 General structure and linkage between different phases of the research

2 Literature review

2.1 Wastewater treatment and sludge management

2.1.1 Conventional process description

Wastewater treatment is critical to sustainable urban development to protect human health, water resources and the environment. A central objective of wastewater treatment is to improve and protect the natural water environment, as well as the health and well-being of downstream communities (Pan et al., 2019). The system comprises a series of unit processes to remove gross solids by gravity settlement and suspended and soluble pollutants by biological treatment. The main biological wastewater treatment technology is the AS process, in which aerobic microorganisms metabolise the organic fraction present in the wastewater under elevated oxygen supply. Figure 2-1 illustrates a typical wastewater treatment. In general, the influent undergoes screening, grit removal and primary sedimentation to removal inorganic particulates, followed by biological degradation of organic pollutants and oxidation of inorganic ammonium (NH_4^+) ions by nitrification to nitrate (NO_3^-). The biological process can also be configured for the removal of nitrogen (N) and phosphorus (P). Sludge flocs, as a flocculated mass of active microorganisms that capable of utilising organic substances under aerobic conditions, as well as microbial extracellular polymeric substances (EPS) and other adsorbed organic and inorganic materials, play an important role in the AS process (Wilén et al., 2003). The treated wastewater is separated from the sludge flocs by secondary clarification and the effluent is discharged or subjected to further, tertiary treatment processes, such as disinfection. A proportion of the secondary sludge is returned to the process (typically 25-75% v/v of the influent for a conventional plug flow reactor (Tchobanoglous et al., 2014)) to maintain biological activity in the reactor, and the remaining sludge is taken from the process as waste activated sludge (WAS).

Waste activated sludge, is a complex heterogenous mixture of microorganisms, undigested organic matter (e.g. paper), vegetable residues or faeces, inorganic materials and water (Durdevic et al., 2020). The waste sludge is blended with the primary sludge and is treated by various physical, chemical, biological or thermal methods, typically including, for example, conditioning, anaerobic digestion, followed by dewatering, for spreading to agricultural land; alternative methods include composting or heat drying, also for land application, or incineration and landfill disposal of the ash residue (Tchobanoglous et al., 2014).

Land application for soil improvement, incineration and landfill are the main management routes for sludge in Europe (European Council, 2009). In UK, land application of treated sludge

is considered as the Best Practicable Environmental Option for sludge management, and 96% of sewage sludge generated in the UK is recycled to land (Environment Agency, 2020).

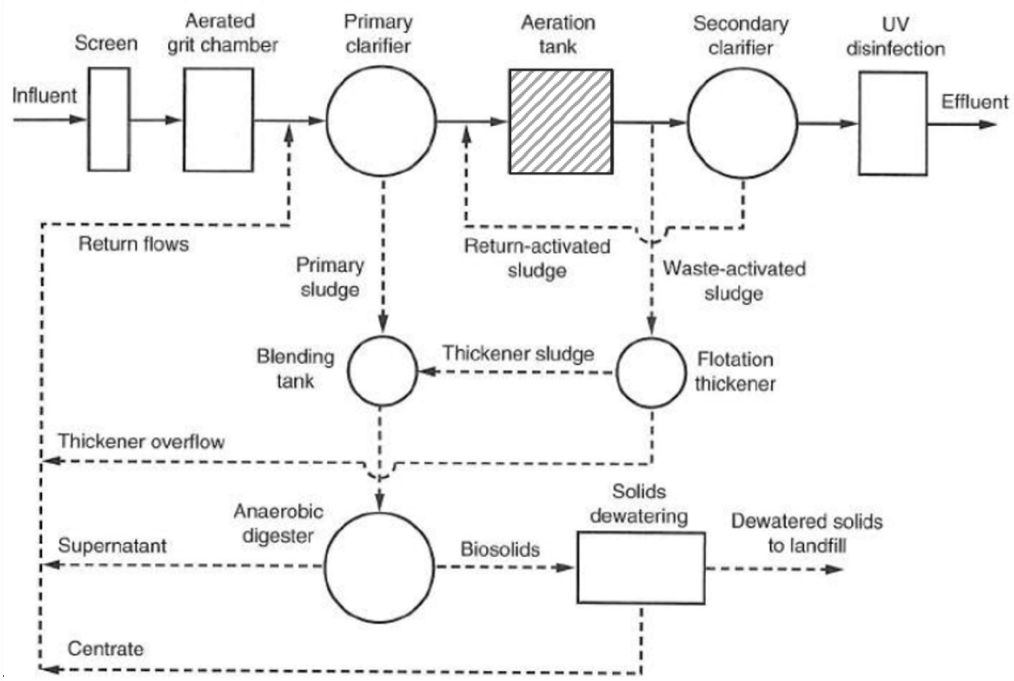

Figure 2-1 Schematic of a conventional wastewater treatment and sludge management process (grey shadowed area representing biological AS process, adapted from (Tchobanoglous et al., 2014))

2.1.2 Sustainability of the Water Industry

Conventional wastewater and sludge treatment comply with environmental legislation requirements, however, the energy demand and environmental footprint can be large. Thus, conventional WWTPs are one of the major energy consumers at the municipal level worldwide, with the energy consumption constituting about 1-3% of the total electrical energy output of a country (Bauer, 2014). Whilst resource recovery and cost effectiveness are improving, for example, through increased anaerobic digestion (AD) of sludge and renewable energy generation from biogas, there remains considerable scope to increase income and sustainability by recovering valuable materials and resources from wastewater and sludge (Verstraete and Vlaeminck, 2011; Kehrein et al., 2020).

Thus, increasingly, sewage sludge is recognised as a resource rather than a waste stream, and that WWTPs not only function to remove environmental pollutants, but also as resource recovery centres (Kehrein et al., 2020). Indeed, resource recovery facilities can be integrated into current treatment units, so that the Water Industry can establish more circular resource flows, contributing to national sustainable development goals and circular economy.

Activated sludge consists a high concentration of total organic carbon, N, P and sulphur (S), polyhydroxyalkanoate polymers and also hydrolase enzymes (Smith, 2014), and several

opportunities for resource recovery from waste AS are identified. For example, biogas and energy generation from AD (Han et al., 2017; Aragon-Briceno et al., 2021) and nutrient recovery as fertiliser (Rigby et al., 2016; Muller-Stover et al., 2021) are highly successful strategies for sludge management. Recovering enzymes from the wastewater treatment process is an alternative approach with significant potential industrial, treatment and economic advantages, although the technology development is at an early stage (Liu and Smith, 2020b).

2.2 Fundamentals of enzymology

2.2.1 Structure of enzymes and their classification

The majority of enzymes (except ribozymes, which are ribonucleic acid (RNA) molecules that facilitate gene expression within microbial cells) are globular, bio-catalytic proteins comprising a tertiary amino acid conformation, which may, in some cases, be bound to a non-protein coenzyme or metal ion cofactors. The size of enzymes can range from less than 100 to over 2500 amino acid residues (Robinson, 2015). Specific mixtures of amino acids undergo condensation reactions to form a peptide chain, which subsequently folds forming a three-dimensional structure that is stabilised by non-covalent interactions such as hydrogen bonding, ionic interactions, and Van der Waals forces (Bugg, 2012).

In general, the categorisation of enzymes depends on the type of catalysed chemical reaction and they are described as: oxidoreductases, transferases, hydrolases, lysases, isomerases, ligases or translocases and each specific type is given a unique Enzyme Commission (EC) number (Bisswanger, 2011a). Enzymes present in microbial cells can also be classified as:

- Intracellular or extracellular, depending on the location; extracellular enzymes are secreted and exist outside the cell (usually in the vicinity of a cell), whereas intracellular enzymes exist inside the cell membrane.
- Constitutive or inducible; constitutive types are produced in the cell regardless of the external environment, whereas inducible forms are only expressed under specific conditions, for instance, the main one being the presence of a particular or unique substrate type.

2.2.2 Mechanisms of enzyme catalysis

The enzyme catalysis of a reaction initially involves the substrate (*S*) binding to the active site of the enzyme (*E*) to form an enzyme-substrate complex (*ES*) as an intermediate state. The process of enzyme catalysis is thus shown as follows:

$$E+S \rightleftharpoons ES \longrightarrow E+P_r$$

As the reaction progresses, the enzyme detaches from the products (P_r) without being consumed itself (Price and Stevens, 1999). The active sites of an enzyme consist of a small

proportion of the total amino acid content (usually <10 (Robinson, 2015)), and the specificity of an enzyme is determined by the arrangement of these amino acids and the shape of the active site (Stank et al., 2016) (Figure 2-2). The active functional groups also show a degree of mobility and flexibility, and can orientate to their counterparts within a substrate molecule in a favourable way (Rupley et al., 1983).

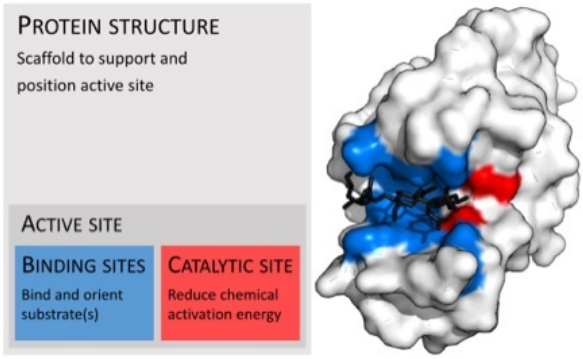

Figure 2-2 Organisation of enzyme structure using lysozyme as an example (binding sites in blue, catalytic site in red and peptidoglycan substrate in black) (Shafee, 2015)

2.2.3 Enzyme kinetics

The progress curve of enzymatic reaction (against time) can be divided into three stages (Bisswanger, 2011c): (1) pre-steady stage (usually less than a second), during which the product accumulation increases with time in a nonlinear pattern; (2) steady-state stage (usually s to min), during which the product concentration increases linearly with time (i.e. the enzymatic reaction rate is regarded as constant) in the presence of excessive amount of substrate, and most of the enzyme activity assays (see Section 3.6) are carried out within this period; and (3) substrate depletion stage, which could be obtained with prolonged time period, with product concentration levelling off and eventually reaching a plateau due to substate depletion and/or product inhibition.

The velocity of an enzymatic reaction (v), i.e. the amount of product increase (or substrate decrease) per unit time, which is numerically equivalent to the slope of the progress curve, can be described by the Michaelis-Menten equation:

$$v = \frac{V_{max}[S]}{K_{m+}[S]} \quad \text{(Eq 2-1)}$$

Where, V_{max} represents the maximum velocity of the reaction; [S] represents the substrate concentration; K_m is the Michaelis-Menten constant and represents the substrate binding affinity of the enzyme, which is numerically equivalent to the substrate concentration that delivers an enzymatic reaction at half of V_{max}. The Michaelis–Menten model provides information about the dependence upon substrate concentration of the enzyme.

In the presence of excess substrate, the velocity of an enzymatic reaction is directly proportional to the enzyme concentration (Bisswanger, 2011c). In many cases, the molar concentration of an enzyme is difficult to measure following standard chemical recording protocols, either because the enzyme is not purified or because the molecular mass of the target enzyme is unknown (Cornish-Bowden, 2012). Therefore, an enzyme concentration in solution is commonly measured and expressed in terms of its activity, which is defined as an enzyme unit (U). Thus, one enzyme unit (1 U) represents the amount of enzyme that converts 1 μmol of substrate or generates 1 μmol of products per unit time period (e.g. min or hour) under standard conditions.

2.3 Enzyme location in activated sludge

2.3.1 Extracellular enzyme distribution patterns within activated sludge flocs

Microorganisms assimilate organic substrates in the AS process by producing a wide range of enzymes to catalyse the hydrolysis of large organic polymer molecules into smaller units that can be transported across the microbial cell membrane to be metabolised (Wingender et al., 1999). Various extracellular enzymes (including amylase, glucosidase, phosphatase, lipase, etc.) have been detected in AS flocs (Table 2-1). Therefore, AS provides an excellent matrix for recovery of complex enzyme mixtures that may be formulated into compound enzyme products for industrial application.

However, enzymes are not evenly distributed within AS flocs. Hydrolytic enzymes are not usually found in the free water phase of sludge flocs but are mainly detected outside of the cell (and are therefore extracellular), either attached to the cell wall or embedded within the EPS fraction of microbial cells. EPS represents a complex mixture of bacterial metabolites (including proteins, polysaccharides, lipids, humic compounds, nucleic acids, etc.) that locate outside the bacteria cell (Wingender et al., 1999). The EPS forms a negatively-charged, three-dimensional gel-like structure due to hydrogen bond and cation bridging effects between the polysaccharide and protein components (Liu and Fang, 2003). The gel-like EPS fills the void space between adjacent microbial cells (Figure 2-3), acting as an “adhesive” material that maintains the structural integrity and mechanical stability of the floc; it also provides a protective layer for the embedded microbial biomass against extreme external environmental conditions (for instance, sudden changes in pH or the presence of toxic substances) (Wang et al., 2014; Zou et al., 2018; He et al., 2019).

Table 2-1 Enzymes detected in activated sludge and their distribution in sludge flocs

Enzymes	Bulk aqueous fraction	Microbial cells +EPS	Reference
Phosphatase, cyclic phosphodiesterase, glycosidase and aminopeptidase	<5%	>95%	Teuber and Brodisch (1977)
α-Amylase	Negligible	Detected	Dold et al. (1995)
Protease and α-glucosidase	~4%	~96%	Goel et al. (1998a)
Leucine aminopeptidase	<=3%	97%	Confer and Logan (1998)
α-Glucosidase	7%	93%	
Phosphatase	1%	99%	Kloeke and Geesey (1999)
Leucine aminopeptidase	15.5%	84.5%	Li and Chrost (2006a)
β-Glucosidase	11.2%	88.8%	
Lipase	18.3%	81.7%	
Protease, α-amylase and α-glucosidase	Negligible	~100%	Yu et al. (2007)

(a) (b)

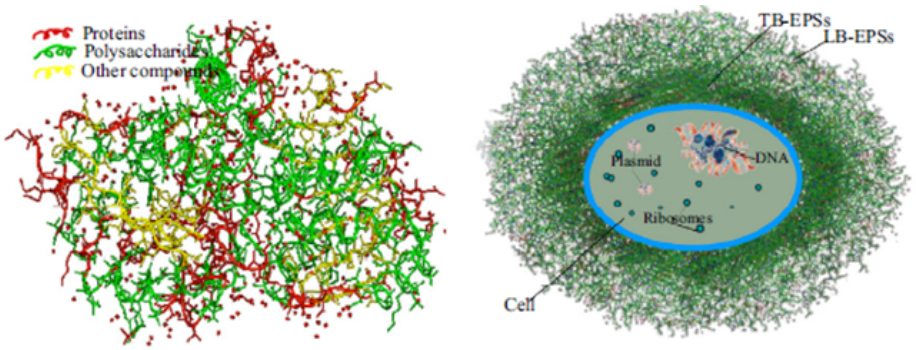

Figure 2-3 (a) Chemical structure of microbial extracellular polymeric substances (EPS); (b) Spatial distribution of different EPS fractions and the relationship with a bacteria cell (tightly bound EPS (TB-EPS) is the fraction that is closely associated with the cell; loosely bound EPS (LB-EPS) diffuses from TB-EPS and is located at the outer region of AS flocs) (Lin et al., 2014)

Different hydrolytic enzymes have been found within the tightly bound and loosely bound EPS (TB-EPS and LB-EPS, respectively) fractions present in sludge flocs (Figure 2-3(b)). For example, Boczar et al. (1992) detected esterase, lipase and leucine aminopeptidase in the easily extracted EPS (and presumably, therefore, although not specifically assigned to, the LB-EPS fraction); other enzymes (including phosphatase, valine aminopeptidase, phosphohydrolase and some glucosyl hydrolases) were mainly tightly bound to microbial cells. Cadoret et al. (2002) showed that 9-24, 4-6, 15-28 and 21-67% of the total leucine aminopeptidase, α–glucosidase, protease and α-amylase was detected in LB-EPS, respectively. Indeed, Yu et al. (2007) indicated that protease (98.4%) was mainly tightly bound to the cell surface, whereas α-amylase (44-65%) and α-glucosidase (59-100%) activities were largely associated with LB-EPS, and only limited protease, α-amylase, or α-glucosidase activity was detected within the TB-EPS fraction.

The mechanism of enzyme stabilisation in the extracellular fraction of sludge flocs is not clearly understood (Karn et al., 2013). It is possible that ionic and hydrophobic interactions contribute to the immobilisation and stabilisation of hydrolytic enzymes within the sludge matrix (Trzcinski, 2018). Wingender et al. (1999) suggested that the interaction between enzymes and polysaccharides was responsible for the preservation of enzymes within EPS. Frolund et al. (1995) proposed that complexation with humic compounds in EPS was also involved in enzyme stabilisation.

The majority of published literature, summarised in Table 2-1, indicates the glycolytic enzyme activity resides mainly in the sludge floc EPS, with relatively little or no activity in the bulk aqueous fraction. Interestingly, however Guellil et al. (2001) found the opposite behaviour to be the case. Guellil et al. (2001) argued that readily bio-hydrolysable substrates were

depolymerised by free enzymes present in the wastewater colloidal fraction. Presumably the enzymes were released by free, non-floc forming bacteria, and/or originated and survived from hydrolysis reactions that took place during transportation of raw wastewater in-sewer. Consequently, only recalcitrant, slowly biodegradable polymers (such as cellulose and lipopolysaccharides) were identified, and these were removed by physicochemical adsorption onto the sludge matrix, rather than bio-degradation, forming structural elements that contributed to sludge floc stability. Evidently, the enzyme distribution patterns in biological wastewater treatment systems are dynamic and complex. However, it would appear that the biomass in AS flocs is capable of producing glycolytic enzymes and these are present in the EPS, in response to degradable polysaccharides in settled sewage.

2.3.2 Influence of substrate incorporation

Organic substances with a particle size <0.001 μm (soluble) are rapidly degraded by AS microorganisms whereas materials >1 μm (supracolloidal and/or non-settable), which constitute approximately 50-60% of the total organic matter in settled primary effluent (Levine et al., 1991), are assimilated at a much slower rate (Levine et al., 1985; Chrost, 1991). The EPS fraction of sludge flocs acts as the primary surface contacting the settled primary effluent and provides sites for physical removal followed by preliminary degradation of insoluble organic substrates. The extremely large surface area of EPS, and the presence of a large number of hydrophobic groups (Hou et al., 2015), means that exogenous macromolecules and particulates are effectively scavenged and adsorbed into the sludge floc matrix from the free aqueous phase of wastewater. Subsequently, the hydrolytic enzymes accumulated within the EPS matrix rapidly react with adsorbed materials, producing smaller molecular units that can be absorbed by cells for metabolism.

However, the distribution of different enzymes is greatly influenced by the mobility of substrates, which is determined by the MW and the extent to which they transmit through the EPS matrix (Hoppe et al., 1988). Thus, substrates of higher MW are less mobile, compared to smaller molecules, and accumulate within the outer EPS fraction resulting in the corresponding increase in hydrolytic enzyme activity (Cadoret et al., 2002). Consequently, sludge flocs, in suspended growth, biological wastewater treatment reactors, develop an efficient, diverse, stable enzyme pool, which operates synergistically and/or synchronously to degrade polymeric organic compounds without extra substrate or metabolic energy transfer for enzyme consumption and production.

2.4 Crude enzyme extraction from activated sludge

2.4.1 Extraction protocol

As most hydrolytic enzymes in sludge flocs are extracellular, and are either attached to the cell wall or embedded within the sludge EPS, crude enzyme extraction from AS can be achieved by disrupting the sludge flocs and harvesting microbial EPS. Figure 2-4 shows the general steps and procedures to extract enzymes from AS. Typically, AS is centrifuged to remove the bulk water fraction that contains little extracellular enzymes. The solid sediment is subjected to floc disruption (with either physical or chemical methods, alone or in combination); dilution of the sludge may be necessary prior to disruption depending on the conditions. The crude enzyme product, after solid/liquid separation, is subsequently concentrated and stabilised for application.

A wide range of techniques have been reported in the literature to extract crude enzymes from AS (Table 2-2), and the optimum conditions tend to be specific for different enzymes. The most frequently applied techniques, shown in Table 2-2, and their mechanisms of action, are critically discussed in the following sections.

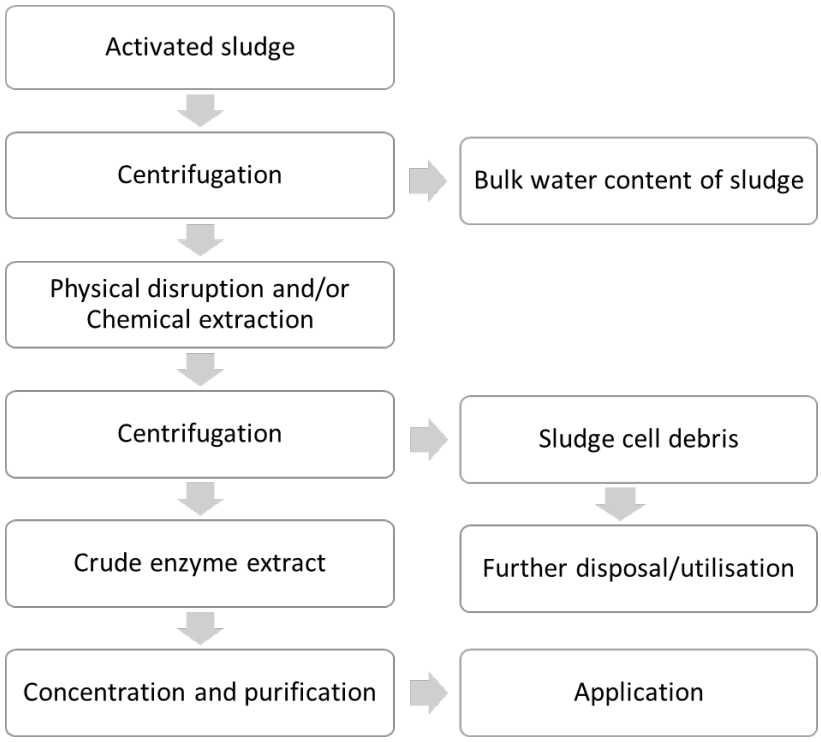

Figure 2-4 Typical stages to extract enzymes from activated sludge

Table 2-2 Methods for crude enzyme extraction from activated sludge

Method	Optimum extraction conditions	Target enzymes	Enzyme activity (U) in crude extract	Reference
End-over-end rotation with PBS and FDA solution; incubation at room temperature	Direct detection in AS without optimisation	Esterase Ala-aminopeptidase α-Glucosidase	120 U/g VS 1060 U/g VS 40 U/g VS (1 U: 1 μmol product released/h)	Nybroe et al. (1992)
Stirring with CER	Dosage = 70-75 g/g VS Stirring at 600 rpm for 1 h 4°C	Esterase Leucine aminopeptidase α-Glucosidase β-Glucosidase Lipase β-Glucuronidase Chitinase	35 U/g VS 13 U/g VS <10 U/g VS ~10 U/g VS <10 U/g VS <10 U/g VS <10 U/g VS (1 U: 1 μmol product released/h)	Frolund et al. (1995)
Fractionation by Dyno Mill	Glass beads (diameter = 0.5 mm) Bead loading = 60% (v/v) Agitating speed of milling = 3200 rpm	Protease	~5 U/g protein for diary sludge 40 U/g protein in municipal sludge (1 U: undefined)	Jung et al. (2001)
Stirring with CER	Dosage = 60–70 g/g VS Stirring at 900 rpm for 1 h	Lipase Protease	~210 U/g VS ~300 U/g VS	Gessesse et al. (2003)
Stirring with TX100	Dosage = 0.1% for lipase, 0.5% for protease Stirring at 900 rpm for 1 h	Lipase Protease	~320 U/g VS ~4000 U/g VS	Gessesse et al. (2003)
Stirring with EDTA	Dosage = 10 mM Stirring at 900 rpm for 1 h	Lipase Protease	~250 U/g VS ~1700 U/g VS	Gessesse et al. (2003)
Sonication with TX100	Frequency = 15 kHz Duration = 30 min Power = ~200 W Dosage = 0.1% TX100	Lipase	335.0 U/g VS (1 U for lipase: 1 mmol product released/min; 1 U for protease: UV absorbance increase of 0.01 at 440 nm)	Gessesse et al. (2003)

Sonication	Frequency = 20 kHz Duration = 10 min Specific power input = 552 W/g DS 4°C	Protease α -Amylase β-Glucosidase Alkaline phosphatase Acid phosphatase	~3 U/g VS ~20 U/g VS <1 U/g VS ~10 U/g VS ~4 U/g VS (1 U: 1 μmol product released/min)	Yu et al. (2009)
Stirring with EDTA	Dosage = 2% EDTA Stirring at 600 rpm for 3 h 4°C	Protease α-Amylase β-Glucosidase Alkaline phosphatase Acid phosphatase	<1 U/g VS ~40 U/g VS Very low Very low ~1 U/g VS (1 U: 1 μmol product released/min)	Yu et al. (2009)
Sonication with 2% TX100	Frequency = 24 kHz Power intensity = 4 W/cm^2 Duration = 10 min for protease, 20 min for lipase	Protease Lipase	~53 U/g VS ~21 U/g VS (1 U: 1 μmol product released/min)	Nabarlatz et al. (2010)
Stirring with CER and TX100	Dosage = 0.48 g/mL CER, 0.5% TX100 Stirring at 500 rpm for 1 h Ice-water bath	Protease Lipase	7.0 U/g VS 15.5 U/g VS (1 U: 1 μmol product released/min)	Nabarlatz et al. (2010)
Sonication with TX100	Frequency = 24 khz Duration = 30 min Power intensity = 3.9 W/cm^2 Dosage = 2% TX100 Ice-water bath	Protease Lipase	52 U/g VS ~21 U/g VS (1 U: 1 μmol product released/min)	Nabarlatz et al. (2012)
Sonication with TX100	Frequency = 24 kHz Duration = 30 min Power intensity = 3-7.4 W/cm^2 Dosage = 0.1% TX100 Ice-water bath	Lipase	450 U/g VS (1 U for lipase: 1 mmol product released/min)	Karn et al. (2013)
Stirring with CER	Dosage = 40–60 g/g VS. Stirring at 1000 rpm for 1 h Ice-water bath	Lipase Protease	200 U/g VS 700 U/g VS (1 U for lipase: 1 mmol product released/min;	Karn et al. (2013)

			1U for protease: UV absorbance increase of 0.01 at 440 nm)	
Stirring with TX100	Dosage = 0.1% for lipase, 1.0% for protease Stirring at 1000 rpm for 1 h Ice-water bath	Lipase Protease	400 U/g VS 3600 U/g VS (1 U for lipase: 1 mmol product released/min; 1U for protease: UV absorbance increase of 0.01 at 440 nm)	Karn et al. (2013)
Sonication	Frequency = 20 kHz Duration = 10 min Power density = 1 W/mL	Phosphatase Galactosidase Glucuronidase	~38 U/mg protein ~15 U/mg protein ~10 U/mg protein (1 U: 1 μg product released/h)	Krah et al. (2016)
Stirring with TX100	Dosage = 1.0% TX100 60 min (agitating speed not specified) 4°C	Protease	5.1 U/g (1 U: 1 mol product released/min)	Ni et al. (2017)

Note: U is the enzyme activity and is based on either the amount of product formed or substrate consumed within a specified, standard time period under defined experimental conditions; rpm, revolutions per minute, is a measure of rotational speed; VS, volatile solids; DS, dry solids; PBS, phosphate-buffered saline; FDA, fluorescein diacetate; CER, cation exchange resin; TX100, Triton X100, is a non-ionic surfactant; EDTA, ethylene diamine tetraacetic acid, is a chelating agent

2.4.2 Physical disruption

2.4.2.1 Sonication

2.4.2.1.1 Mechanisms of enzyme release by ultrasonic treatment

Sonication is a practicable technology (Rubin et al., 2018) that has been applied at full-scale in the wastewater industry for waste sludge pretreatment to improve the AD of sewage sludge. This is achieved by disrupting the biomass to shorten the hydrolytic phase of fermentation, increase the production of biogas as a source of renewable energy and to improve the mineralisation (stability) of fermented sludge (Rubin et al., 2018; Zielinski et al., 2019). As sonication causes cellular disruption it is also a suitable technique for extracting enzymes from AS.

The initial direct effect of sonication treatment of AS is the breakdown of sludge flocs, exposing microbial cells to the aqueous environment and increasing the vulnerability to further ultrasonic destruction. The release of extracellular and intracellular substances containing enzymes from the sludge occurs upon cellular destruction. Balasundaram and Harrison (2006) suggested that enzymes are released following the stepwise breakdown of the cell structure by sonication treatment, as illustrated in Figure 2-5. Cadoret et al. (2002) found that the ultrasound treatment of AS significantly shifted the floc size distribution of disrupted sludge towards the smaller size classes, reducing the median diameter of the flocs from 91 to 37 μm. The frequency of small flocs was, therefore, also increased; 99% of the particles had a mean diameter of <4 μm in the disrupted sludge, compared to 6 to 600 μm in untreated flocs. Zielewicz (2016a) indicated that disrupted microbial flocs with a particle size smaller than 100 μm was more likely to release cellular substances compared to larger flocs. Thus, reducing the floc size by sonication also aids the mechanism of enzyme extraction from AS.

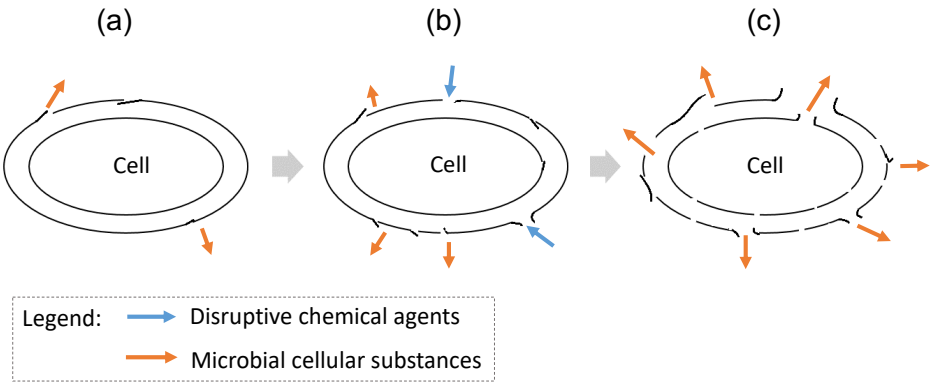

Figure 2-5 Representation of the three stages of cell disruption by sonication: (a) Stage 1: pores form on the outer cell wall due to the external mechanical forces exerted by cavitation, releasing some periplasmic enzymes; (b) Stage 2: chemical agents diffuse from the external solution into the cell, generating a combined disruptive effect with the mechanical forces from sonication; and (c) Stage 3: cell membranes are destroyed by the continuous exposure to cavitation ("fatigue failure"

of the cell structure) causing more severe cell disruption, releasing intracellular enzymes and substances (adapted from (Balasundaram and Harrison, 2006))

The disruption of sludge flocs and cells is caused by the cavitation effect of ultrasound treatment (Onyeche et al., 2002; Vardanega et al., 2014). High frequency acoustic signals pass through the liquid medium and the compression and expansion cycles of the sound waves creates bubbles or cavities in the liquid. Two types of cavities, stable and inertial, form depending on the pressure level and other ambient conditions (Coussios et al., 2007). Stable cavities typically oscillate non-linearly around an equilibrium size and for many cycles of the acoustic pressure without collapse. By contrast, inertial cavities expand significantly before violently collapsing and, consequently, are much more important for cell disruption (Lee, 2016). Inertial cavities can expand to many times their original size in response to the applied acoustic pressure (Neppiras, 1984). When the negative pressure exerted exceeds the local tensile strength of the liquid, the implosive collapse of the bubbles releases a shock wave. Shock waves propagate in the surrounding medium, forming jet streams initiating hydrodynamic shear forces that disrupt cell membranes. The size of the inertial cavities at which collapse occurs is described as the linear resonance size (R_0) (Avvaru and Pandit, 2009; Lee, 2016) as follows:

$$R_0 = \sqrt{\frac{3\gamma P_\infty}{\rho \omega^2}} \qquad \text{(Eq 2-2)}$$

where, γ is the specific heat ratio of the gas; P_∞ is the ambient liquid pressure; ρ is the liquid density; and ω is the driving frequency of the acoustic field.

2.4.2.1.2 Factors influencing the efficiency of enzyme extraction by sonication

The performance of ultrasound at extracting enzymes from cellular biomass depends on several critical operational conditions, including:

- Ultrasound frequency

Ultrasound includes a wide range of frequencies between 20 kHz and 10 MHz (Dewil et al., 2006). As shown in Eq 2-2, the size of the cavities is directly related to the frequency of the generating ultrasound (ω). Dewil et al. (2006) indicated that ultrasound of high frequencies (>1 MHz) tends to produce stable, oscillating cavities that do not implode; whereas low frequencies (<1 MHz) can generate inertial cavities, and the energy release by implosion of inertial bubbles is positively corelated to the size of cavities.

- Duration

Several studies (Zhang et al., 2007; Monique et al., 2008; Hong et al., 2017) consistently show that effective cellular disruption and enzyme release by sonication requires a minimum treatment period >10 min. For example, Arun and Sivashanmugam (2017) found that

increasing the sonication duration from 5 to 20 min significantly improved the recovery of protease, lipase and amylase from fruit waste and measured maximum activity values equivalent to approximately 43, 17 and 27 U/ml, respectively. However, extending the sonication period to 50 min reduced the enzyme activity by 76, 41 and 81%, respectively. This can be caused by a number of factors, but, released enzymes are particularly sensitive to thermal damage from the increase in energy dissipation as heat from excessive energy inputs to biomass associated with prolonged sonication times (see below). Thus, an uncontrolled increase in temperature by sonication treatment could have a detrimental impact on the protein structure of most enzymes, but can be effectively avoided by: (1) applying an optimal sonication duration, (2) carrying out the sonication treatment in the laboratory in an ice-water bath (see Table 2-2) or with a coolant circulation system outside the treatment chamber for larger-scale, industrial processes, and/or (3) adopting a pulse-cycle mode of on/off operation (for example, see Section 4.2.2).

- Energy level

The energy supplied for cellular disruption by sonication treatment can be expressed in several ways, shown as follows (Tyagi et al., 2014):

$$Specific\ energy\ (kJ/kg) = \frac{P_o \times t}{V \times S} \quad \text{(Eq 2-3)}$$

$$Energy\ dose\ (kJ/L) = \frac{P_o \times t}{V} \quad \text{(Eq 2-4)}$$

$$Power\ density\ (W/L) = \frac{P_o}{V} \quad \text{(Eq 2-5)}$$

$$Power\ intensity\ (W/cm^2) = \frac{P_o}{A} \quad \text{(Eq 2-6)}$$

Where, P_o is the power input (kW); t is the sonication duration (s); V is the sample volume (L); S represents the solids content of the sample (kg/L); and A is the area of the emitting surface of the sonication probe (cm^2).

The energy supplied by sonication treatment may be represented by any one of these different quantitative units in published studies. However, they are not readily transferrable; therefore, it is not always possible to directly or quantitatively compare the amount of sonication energy delivered for cell disruption between different reports in the literature.

Show et al. (2007) argued that the impact of cavitation bubble formation, and their subsequent implosion, on AS disruption, can be viewed as a competition between the structural strength of sludge particles and the sonication intensity. Consequently, there is a critical energy intensity level above which the mechanical forces delivered by sonication will disrupt sludge flocs. However, uncontrolled sonication energy intensities can be detrimental to enzyme conformation, due to irreversible breakage/formation of specific chemical bonds and over-heating of the samples (Mawson et al., 2011). The sonication intensity is directly proportional

to the amplitude of vibration of the ultrasonic source. Thus, high sonication amplitudes generate excessive amounts of cavitation bubbles, and the shock wave from the implosion of cavities can trigger extreme shear forces in the aqueous solution. Under these conditions, the hydrogen bonds and van der Waals' interactions of the polypeptide chains can be disrupted, which are vital to maintaining the structural integrity of enzymes (Subhedar and Gogate, 2013; Huang et al., 2017).

Zielewicz (2016a) recommended that a sonication device with a power density of 880 W/L was necessary for maximum sludge floc disintegration. For continuous commercial application, Zielewicz (2016b) suggested that the sonication duration, which is associated with the hydraulic retention time in the disintegration chamber, should provide an energy density ranging from 5 to 25 kWh/m^3 (equivalent to an energy dose of 18-90 kJ/L).

- Solids content in sludge

Ultrasonic conditions for effective cell disruption are often specific to the characteristics of the target material (Rubin et al., 2018). The core principle of sonication treatment is the conversion of electrical energy into mechanical vibrations that generate cycles of cavitation bubble formation and collapse, producing biologically disruptive shear forces at the cellular level. Consequently, sonication devices (typically a sonication probe) have an effective functioning range over which the energy is gradually dissipated, depending on the physicochemical characteristics of the sample material (Abramov, 1999).

Particularly, sonication disruption of AS for enzyme extraction is performed on sludge suspension and so it is necessary to consider the optimum solids content of the sludge for cell disruption. Optimum DS contents reported for AS disruption by sonication are in the range of 2-4%. For example, Show et al. (2007) found that, at a power density of 520 W/L, significant particle size reduction of AS flocs occurred for sludge samples at <2.9% DS, however, there was only minor disruption at higher DS contents (3.8%). Zhang et al. (2008) found the optimum DS concentration for ultrasonic treatment of AS at a power density of 80 W/L was 2%. By comparison, sonication of sludge with lower solids content (0.5% DS) consumed 137% more energy, while a higher solids content (3% DS) absorbed the sound energy and reduced the disruption efficiency. Zielewicz (2016a) also confirmed that lower dry matter concentrations (ranging from 2.8-4.2% DS) were more susceptible to ultrasonic disruption compared to more concentrated sludge (6.3% DS).

The apparent range of optimum solids contents reported in the literature may be explained because sludge samples from different sources exhibit contrasting physicochemical properties with distinct structural strength characteristics that influence the susceptibility to cavitation. Activated sludge flocs represent a multiphase, complex matrix containing

microorganisms, EPS, gas bubbles and dissolved and particulate organic and mineral matter. Abbasi et al. (2015) and Pilli et al. (2011) indicated that gas entrapment in sludge flocs can lower the cavitation pressure and thus reduce the sludge floc disruption efficiency, since part of the energy released from implosion of the cavities is utilised to collapse the gas bubbles, rather than the solid fraction of the sludge. Richard (2003) found that small flocs (usually with diameter <50 μm), consisting only of floc-forming bacteria without a filament backbone, which commonly occur under starvation (typically when the food to microorganism ratio (F/M) (Tchobanoglous et al., 2014) is very small (Li et al., 2011)) or the sludge age is extended (Li and Stenstrom, 2018)) or chronic toxicity conditions, are particularly susceptible to disruption by external forces such as ultrasound, which is consistent with other work on the effects of floc size (see Section 2.4.2.1.1). Zielewicz (2016a) suggested that the mineral/organic matter ratio of sludge was another important factor influencing the efficiency of ultrasound disruption, due to its effect on the mechanical strength, but did not explain how they were related. The mineral/organic matter ratio of AS ranges from 0.17 to 0.67 (typical value = 0.4) (Tchobanoglous et al., 2014). As the sludge becomes more mineralised with increasing sludge age, the EPS content in AS flocs decreases, and the mineral/organic matter ratio and proportion of recalcitrant cellular, structural material increase (Eriksson et al., 1992). Therefore, the efficiency of sonication treatment may decrease with increasing mineral/organic matter ratio of AS flocs due to the greater dissipation and absorbance of ultrasound energy by larger, non-disruptable inorganic and recalcitrant, structural organic fractions, compared to sludge with smaller ratios.

2.4.2.1.3 Ultrasound treatment and enzyme activity

Interestingly, ultrasound has been found to have a direct, positive effect on enzyme activity if the treatment is carried out in a controlled manner. For example, Liu et al. (2006) investigated the effect of ultrasound on the activity of calcium ATPase (an enzyme attached to the plasma membrane that is responsible for regulating the intracellular calcium (Ca^{2+}) concentration via expulsion of Ca^{2+} from the cytosol of cells) in callus cells of *Aloe arborescens*. Plasma membrane, containing Ca^{2+}-ATPase, was extracted by physical chopping and homogenisation of *Aloe* callus cells, followed by centrifugation and chemical purification using a two-phase, aqueous polymer system. Exposing the extracted plasma membrane to a pulsed ultrasound treatment (20 kHz, 2 W, 10 s duration with a pulse cycle of 0.1 s on and 0.9 s off) increased the Ca^{2+}-ATPase activity by 26% compared to the control condition without sonication. However, increasing the ultrasound energy intensity to 10 W, delivered as a continuous wave, decreased the enzyme activity by approximately 25%.

The mechanism and reason why ultrasound treatment can increase enzyme activity is not fully understood. A possible explanation is that controlled sonication treatment may induce

conformational changes to the protein structure of the enzyme, by breaking covalent bonds (Ladole et al., 2017). This may release and expose more active sites in the interior of the protein to substrate molecules in the aqueous solution, increasing the apparent enzyme activity. Capelo et al. (2004) suggested that sonication may also increase the efficiency of mixing and diffusion of reaction components, resulting in a higher frequency of collision between reaction substrates and active sites of the enzyme.

2.4.2.2 Milling

2.4.2.2.1 Mechanisms of cell disruption by bead milling

Milling treatment is an effective, alternative method of cell disruption to release cellular substances from AS (Baier and Schmidheiny, 1997; Wett et al., 2010; Postma et al., 2015). A typical bead mill consists of a grinding chamber (vertical or horizontal) filled with small beads (e.g. glass (Clavijo Rivera et al., 2018) or ZrO_2 beads (Safi et al., 2017)), and a rotating shaft (fitted with several agitator disks) through its centre, imparting kinetic energy to the small beads. During the rotary movement of the cells and the beads, the energy is released by the collisions between beads and cells (Figure 2-6), destroying the cell wall (Geciova et al., 2002). Suarez Garcia et al. (2019) indicated that approximately 95% of the total energy released from collisions in the mill occurs in the vicinity of the agitators, where the beads are moving at the maximum speed. By contrast, the beads are almost static close to the shaft or chamber wall, where they have lower potential to collide with adjacent cells. Furthermore, layers of rolling beads (Figure 2-6) moving at different speeds can induce shear forces and the grinding effect also contributes to cellular disruption (Koubaa et al., 2020).

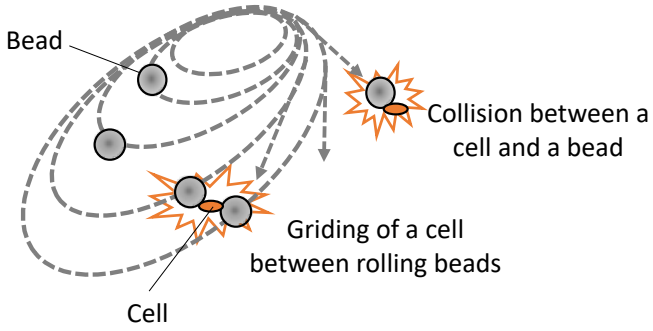

Figure 2-6 Mechanisms of bead milling in microbial cell disruption (adapted from (Koubaa et al., 2020))

2.4.2.2.2 Factors influencing the efficiency of enzyme extraction by milling

- Operational conditions influencing bead milling

The progress of cell disruption against time (t) by milling can be described by a first order kinetic model (Currie et al., 1972; Montalescot et al., 2015), shown as follows:

$$Cell\ disruption\ rate\ =\ 1\ -\ e^{-kt} \qquad \text{(Eq 2-7)}$$

Where, the first-order rate constant, *k*, represents the efficiency of the milling process at cell disruption, and can be affected by bead size, loading rate and agitation speed; in particular, the first-order rate constant (*k*) is proportional to the square of the bead loading rate and increases with decreasing bead diameter (Currie et al., 1972; Montalescot et al., 2015). Jung et al. (2001) found that the disruption rate constants (*k*) of diary and municipal sewage sludge, under optimum conditions, were 0.22/min and 0.20/min, respectively.

The efficacy of milling as an approach to sludge and cellular disruption largely depends on the collision frequency between agitated beads and cells. Consequently, bead size and loading rate (i.e., the ratio of the total bead volume to sample volume, v/v %) are critical metrics for optimisation. For example, Jung et al. (2001) used a continuous Dyno mill and glass beads to disrupt AS to solubilise the sludge and recover cellular proteins. An optimum solubilisation ratio (i.e., the ratio of total soluble organic carbon to total carbon of the disrupted AS) of 53% was obtained with 0.5 mm diameter beads, a loading rate of 60% (v/v), and agitation speed of 3200 rpm.

The diameter of the beads used in milling has a major influence on the amount of energy required to achieve the effective disruption of AS flocs and bacterial cells. Thus, Lehne et al. (2001) found the minimum, optimum specific energy value was obtained with decreasing bead diameter to 0.2 mm. However, reducing the bead size further (for example, to <0.1 mm) limited the kinetic energy carried by the beads to a level that was insufficient to cause cellular damage at every bead-bead or bead-cell wall collision, thus, increasing the specific energy demand for effective disruption. For example, beads with a diameter of 1.5 mm required a specific energy of >10000 kJ/kg DS to achieve 60% of the disruption obtained at 0.2 mm. This represented an energy consumption almost an order of magnitude higher compared to the smaller bead size. Rai et al. (2008) similarly reported that the specific energy required for maximum cell disruption (89%) using 0.77 mm diameter beads was equivalent to 15301 kJ/kg DS.

The speed of agitation is another important parameter influencing the performance of milling, and the first-order rate constant (*k*) additionally increases with agitation speed (Melendres et al., 1991). However, an optimal agitation speed is always required from a practical point of view, since the total energy demand could become significant at a high agitation speeds compared to lower speeds. Suarez Garcia et al. (2019) assessed the power consumption of a bead mill under several scenarios including running the mill empty, with beads (0.5 mm, 65% v/v loading rate) and/or microalgae cells (concentration ranging 30-155 g/L). The power consumption over a period of 20 min showed an exponential increase, from <50 W in all scenarios to 100-350 W as the agitation speed increased from 1500 rpm to 5500 rpm, respectively. Similarly, the heat dissipation (mainly due to friction) also increased from 17.8 to 60.8 % of the total power consumed. This was probably because the movement of the beads

is more chaotic at higher agitation speeds, which forces the agitator to demand more power to keep a constant stirring speed in the chamber (Suarez Garcia et al., 2019).

- Cell concentration

Postma et al. (2015) investigated the effectiveness of a Dyno mill (filled with 1 mm ZrO_2 beads with 65% v/v loading rate) at disrupting microalgae cells of *Chlorella vulgaris*. The soluble protein yield after cell disruption was significantly influenced by the concentration of biomass fed into the unit, regardless of the agitation speed (ranging from 6 to 12 m/s). The yield was the highest (42%) at the smallest biomass concentration (25 g dry weight/kg) and decreased by 25% as the biomass concentration increased to 145 g dry weight/kg. This was explained by the formation of insoluble protein aggregates at the high biomass concentration due to increased local protein concentrations, shear forces and interactions with other cellular substances/components. Furthermore, microbial cell suspensions with higher concentrations often show increased viscosity, and handling such material is practically limiting due to greater biomass losses and reduced mixing properties, compared to lower biomass concentrations (Postma et al., 2015).

- Microbial cell type

Middelberg (1995) indicated that bead milling is more effective for disrupting microorganisms with larger cells (e.g. yeast and fungi) compared to smaller cell types (e.g. bacteria, which is typically 1/10 that of a yeast cell (Geciova et al., 2002)), due to the enhanced collision frequency between beads and larger cells. Indeed, multiple passes of operation of bead milling bacteria cells are often required to achieve a similar degree of disruption achieved after a single pass operation for yeast cells.

Furthermore, the strength of the cell wall and its resistance to shear forces/bead collisions varies between biomass materials, resulting in different disruption efficiencies and *k* values. For example, higher shear stress may be required to achieve the complete destruction of bacterial cell walls, which contain a rigid peptidoglycan network, compared with yeast cell walls that are mainly composed of short and branched saccharide molecules (such as glucans and mannans) (Middelberg, 1995).

2.4.2.3 Advantages and disadvantages

Bead milling has several advantages for cell disruption and recovery of cellular materials, such as a continuous mode of operation, high disruption efficiency, simple biomass loading, and applicability to various types of biomass from lab- to industrial-scale (Koubaa et al., 2020). However, the vigorous friction in the chamber converts a significant portion of the available energy into heat during the milling process. This can lead to inefficient energy transfer to individual cells (Koubaa et al., 2020) and also may require an intensive, energy-demanding

cooling system to allow the recovery of functionally fragile products (e.g. enzymes) (Günerken et al., 2015). Moreover, continuous mode operation requires extra measures, such as sieving and centrifugation to separate the beads from the disrupted sludge cells. These additional process requirements may explain why milling has not been adopted as extensively for industrial enzyme recovery compared to sonication.

2.4.3 Chemical extractants

2.4.3.1 Cation removal agents

Cation exchange resin (CER) (Li and Xi, 2019; Lv et al., 2019), ethylene diamine tetraacetic acid (EDTA) (Lu et al., 2015; Felz et al., 2016), and sodium tripolyphosphate (STPP) (Wawrzynczyk et al., 2007) have been applied as chemical agents to extract both EPS and cellular enzymes from AS. The mechanism of enzyme extraction is similar for all of these chemical agents and involves removing multivalent cations from sludge EPS to disrupt AS flocs. Cations, such as: Ca^{2+}, Mg^{2+}, Fe^{3+} and Al^{3+}, play a significant role in maintaining the structural stability of AS flocs by forming ionic bridges and stabilising proteins (which are usually negatively charged under neutral conditions due to ionization of carboxyl groups) and also small fractions of carbohydrate and nucleic acids (Park et al., 2008; Merrylin et al., 2013). EDTA and STPP are chelating agents and form complexes with metal ions, whereas CER is a polymer and acts as a cation exchange medium that binds with multivalent, bridging cations, to release EPS components into solution.

Chemical extractants damage cell membranes and eventually lead to cell lysis, but are much less aggressive compared to physical methods of cell disruption. For example, Frolund et al. (1995) found that 90% of the extracellular enzyme, esterase, was rapidly released within 1 h when extracting microbial EPS with CER. By contrast, <40% of the intracellular enzyme, dehydrogenase, was detected during this period; however, the majority of dehydrogenase was released by extending the treatment time up to 8 h. The differences in the patterns of detection of these extra- and intracellular enzymes suggested minimal cell lysis occurred during the initial period of CER treatment. Therefore, potential advantages of chemical extractants are that they can: (1) specifically target the recovery of extracellular enzymes, and (2) reduce cell disintegration and contamination with intracellular enzymes or other cellular components.

As may be expected, the dose rate of a chemical extractant can significantly affect the extraction efficiency. Sheng et al. (2005) used EDTA to extract EPS proteins from the bacteria *Rhodopseudomonas acidophila*. They found that EPS extraction increased markedly (from 29.9 to 84.3 mg/g dry cells) with the EDTA dose (from 0.8 to 2.8 g/g dry cells). However, raising the dose further did not improve protein extraction, presumably because the maximum removal of divalent ions from EPS had been achieved. Similarly, Merrylin et al. (2013) observed a stepwise improvement in EPS release, without cell lysis, with increasing EDTA

dose up to 0.4% (equivalent to 0.71 g/g VS of sludge), which gave the maximum EPS content of 38 mg DS/L in the crude extract. Larger doses, ≥0.5% of EDTA (equivalent to ≥0.89 g/g VS of sludge), had no further effect on EPS release, but increased cell lysis.

2.4.3.2 Formaldehyde

Formaldehyde (systematic name: methanal (CH_2O)) is the simplest aldehyde compound (R−CHO) and is widely used in various industries as a common precursor for producing more complex compounds and materials (e.g. polyoxymethylene and phenol formaldehyde resins) (Franz et al., 2016). It has also been used as a chemical agent for crude enzyme and EPS extraction (in combination with, or without sodium hydroxide (NaOH)) (Yu et al., 2007). In aqueous solution, formaldehyde binds to macromolecules (e.g. proteins in EPS) by reacting with various functional groups (Khoirunnisa et al., 2016). Formaldehyde also reacts with amino, hydroxyl, carbonyl and sulfhydryl groups of proteins and nucleic acids of the cell membrane, forming cross-linked complexes. The addition of NaOH increases the pH of the mixture, dissociating the acidic groups in EPS and increasing the solubility of EPS in water. Comte et al. (2006) found that a formaldehyde-NaOH process (involving the incubation of microbial cells from AS with 36.5% formaldehyde at 4°C for 1 h, followed by addition of 1 M NaOH and incubation for a further for 3 h) was more effective than EDTA and CER at extracting EPS from AS cells. For example, the EPS yield (dry weight of EPS/sludge DS expressed as %) obtained for the different extractants: formaldehyde, EDTA and CER, was 47.0, 19.2 and 3.1%, respectively. Similar results were also reported by Alasonat and Slaveykova (2012) investigating different methods of EPS extraction from the bacterium, *Sinorhizobium meliloti*. In this case, an equivalent formaldehyde-NaOH process applied to a suspension culture of the bacteria increased the protein content in extracted EPS by 1.6-1.8 times compared to an EDTA extraction technique (2% EDTA and incubation at 4°C for 3 h).

2.4.3.3 Surfactants

Surfactants (e.g. Triton X100 (Anbazhagan and Palani, 2018) and Tween 20 (Monique et al., 2008)) are often used as additives to enhance the efficiency of EPS and enzyme extraction from AS cells. For example, Triton X100 (TX100) is a non-ionic surfactant that is widely used in cell lysis protocols. It can permeabilise microbial cell membranes and consequently improve the release of cellular proteins and enzymes (Koley and Bard, 2010). Karn and Kumar (2019) suggested the addition of TX100 weakens the hydrophobic interaction between enzymes and the sludge floc components they attach to, facilitating the release of extracellular enzymes from the cell by shearing forces induced by simple continuous stirring.

However, TX100 can have both positive and negative effects on extraction performance, depending on the concentration used and type of enzyme. For example, Nabarlatz et al. (2010) combined TX100 addition with sonication treatment to recover protease and lipase from AS.

They found that, under the equivalent sonication treatment (8 W/cm^2 power intensity, 20 kHz frequency and 10 min duration), protease extraction was significantly improved with increasing TX100 concentration, achieving the maximum enzyme activity (52.9 U/g VS) at 2% v/v TX100. However, lipase extraction followed a different pattern and, in this case, the maximum activity (11 U/g VS) was obtained with 0.5-1% v/v TX100 and increasing the TX100 concentration to >1% v/v reduced the enzyme activity. Other researchers (e.g. (Gessesse et al., 2003; Karn et al., 2013)) also report the greater sensitivity of lipase to TX100 concentration compared to protease.

Bio-surfactants offer a novel alternative to standard chemical surfactants for enzyme recovery from AS. For example, Sethupathy and Sivashanmugam (2019) used rhamnolipid (a bio-surfactant produced by the bacterial strain, *Pseudomonas pachastrellae*) in combination with sonication to extract a crude compound enzyme product from AS. The optimum extraction conditions were obtained with 2% v/v of rhamnolipid and ultrasound treatment at 100W for 15 min, providing a specific energy intensity of 30,456 kJ/kg DS. The maximum activity of protease, α-amylase, cellulase, lipase and α-glucosidase in the crude product was 42, 52, 34, 24, and 11 U/g VS, respectively. This was comparable with the extraction efficiencies of hydrolytic enzymes obtained with the standard chemical surfactant, TX100, at 1% v/v combined with sonication treatment (75 W ultrasound energy, 10 min duration and 27,027 kJ/kg DS specific energy).

2.4.4 Factors influencing enzyme extraction from activated sludge

2.4.4.1 Enzyme location in sludge flocs

As discussed in Section 2.3.1, extracellular enzymes are located in different EPS fractions of AS flocs and, consequently, the degree of floc and cell disruption required to harvest them depends on whether they are associated with LB-EPS or TB-EPS, or whether they are attached to cell walls. Thus, enzymes located in the EPS fraction (so called “exo-enzymes”) can be readily extracted by harvesting the EPS. In contrast, enzymes that are closely attached to the cell surface (“ecto-enzymes”) may remain after removing EPS from the cell (Cadoret et al., 2002) and, therefore, require more physically or chemically aggressive methods for their effective extraction. Cadoret et al. (2002) suggested that, in general, the distribution of enzymes between the exo- and ecto- pools was approximately in the proportions: 5-44% and 56-95%, respectively. Different exo-enzymes are distributed between the LB-EPS or TB-EPS fractions and, consequently, also vary in extractability (Feng et al., 2019). Thus, LB-EPS can be readily separated by shearing detachment from sludge flocs from exposure to turbulence within the extraction solution, whereas TB-EPS is less affected by physical agitation because it exhibits stronger hydrophobic properties.

Yu et al. (2007) investigated the effectiveness of different methods at extracting crude hydrolytic enzymes from AS. The maximum amount of protease (an ecto-enzyme) obtained by formaldehyde extraction (AS was incubated with 36.5% formaldehyde at 4°C for 1 h) from both LB-EPS and TB-EPS was 2.3 U/g VS. However, more than 60% of the total protease was still closely associated with the cell surface after EPS removal. In contrast, up to 84% and 79% of the exo-enzymes: α-amylase and α-glucosidase, were extracted, respectively, by a formaldehyde-NaOH process (incubation with 36.5% formaldehyde for 1 h, followed by addition of 1 M NaOH and incubation for a further 3 h) and sonication (120 W, 40 kHz, 2 min). Gessesse et al. (2003) also found that extracting protease was more difficult than lipase (another example of an exo-enzyme present in LB-EPS (Boczar et al., 1992)). They observed the maximum protease activity in the crude extract after extraction treatment for 1h (60-70 g/g VS of CER addition, in the presence of 0.1% TX100). In contrast, maximum lipase activity occurred after 10 min under equivalent conditions.

2.4.4.2 Upstream wastewater management

Microorganisms react dynamically to changes in environmental conditions within the aquatic ecosystem of the biological wastewater treatment process, including pH, temperature, organic substrates in the influent, the hydraulic regime and presence of toxic substances/enzyme inhibitors (Ye et al., 2011). These conditions determine the microbial physiology and, therefore, the nature of enzyme secretion. The major factors that potentially influence the types and properties of hydrolytic enzymes in AS include:

- Wastewater composition

The enzyme activity profile of AS is strongly affected by the composition of the influent wastewater. For example, Nybroe et al. (1992) found that addition of readily degradable starch to wastewater increased the activity of α-glucosidase in sludge flocs (0.2-0.4 μmol/mg VS/h) compared to the control group without starch addition (<0.1 μmol/mg VS/h). Li and Chrost (2006b) compared the activities of four extracellular enzymes, including: leucine aminopeptidase, β-glucosidase, alkaline phosphatase and lipase, in communal, dairy and petroleum wastewater treatment systems. The AS from each system showed a wide range of activities for each enzyme type investigated, equivalent to: 27.8-41.5, 32.9-57.8, 31.0-47.0 and 86.0-161.2 μmol/L/h, respectively. The relative activity of each enzyme was largely related to the composition of the influent wastewater and the abundance of particular substrates. Thus, lipase activity was highest, and leucine aminopeptidase and β-glucosidase activities were lowest, for AS from petroleum wastewater, which was richer in lipids, but had reduced protein and carbohydrate contents, compared to the other wastewater types. Yu et al. (2008) investigated the activity of extracellular enzymes in AS samples collected from 14 WWTPs.

Activities of α-amylase and α-glucosidase were significantly ($P < 0.05$) correlated with the polysaccharide concentration in the wastewater (Pearson's correlation coefficients were >0.74 and >0.76, respectively). Similarly, protease activity was significantly ($P < 0.05$) correlated with the protein concentration for WWTPs treating wastewater with a high-protein content (Pearson's correlation coefficient > 0.79).

Furthermore, anthropogenic chemical compounds (e.g. organic micropollutants) in wastewater can lead to the expression of specific enzyme types (so-called "inducible enzymes", see Section 2.2.1) by microbial cells in AS. For example, Liu et al. (2002) found that the presence of anilines, a group of environmental pollutants associated with the manufacture of dye materials and herbicides, induced the expression of aniline dioxygenase (1.094 U/mg protein) and catechol 2,3-dioxygenase (5.224 U/mg protein) by the bacteria, *Delftia* sp., isolated from municipal AS. Similarly, *Sphingomonas* sp. Y2, isolated by Bai et al. (2016) from sewage sludge, produced inducible enzymes and degraded 99.2% of the surfactant, nonylphenol polyethoxylate, which is an environmentally active anthropogenic compound with oestrogenic and mutagenic properties.

Inducible enzymes can also be produced by the addition of secondary materials to AS. Hao and Jahng (2019) found that a biodrying process was accelerated by adding spent coffee grounds as a bulking agent to dewatered AS, which increased the water removal rate to 81% in 8 days, compared to 65% removal in the control treatment without coffee grounds. The improved drying rate was not only explained by the better structural conditions, which increased microbial biodrying activity, but also because the abundance of mannan (a plant storage polysaccharide that constitutes more than 50% of total hemicellulose) in coffee grounds induced the significant production of mannanase. Indeed, the specific activity of mannanase was undetectable in the control, but increased to approximately 3100 μg/min/g DS by the second day of biodrying with coffee grounds. The large amount of induced mannanase interacted synergistically with protease, amylase and cellulase, to accelerate the aerobic biodegradation of protein and lignocellulose, thus increasing heat generation and the associated biodrying rate.

These various examples illustrate the potential flexibility and capacity of AS, and biological waste treatment systems in general, to produce a wide variety of commercially important enzymes. The research suggests the addition of particular organic chemical substrates, or secondary materials, such as industrial organic wastes rich in certain substances, to AS under controlled conditions as "stimulating agents" would offer a practically feasible and viable approach to induce the production of an array of high value, specific, novel enzyme products.

- Sludge age

Sludge age represents the average residence time of active microorganisms in a biological wastewater treatment reactor; it is one of the main parameters influencing the operation of the AS process and has a significant impact on the treatment performance of a WWTP (Clara et al., 2005). A sludge age of 3-6 days is typical for WWTP where only removal of carbonaceous matter in wastewater is necessary. However, most WWTP must also remove ammonia (NH_3), which is an extremely harmful pollutant of natural water systems, and this is achieved concomitantly with organic carbon mineralisation in the AS process through biological oxidation by nitrifying bacteria. Nitrifiers are relative slow growing chemoautotrophic bacteria, therefore, a longer sludge age, typically up to 18 days, is necessary, depending on the ambient temperature and influent composition, to main nitrification activity (Tchobanoglous et al., 2014). Sludge age can also influence the activity of hydrolytic enzymes in AS. For example, sludge hydrolase activity increased by a factor of two when the sludge age was extended from 6 days to 14 days, at 20 ± 3 °C (Garcia et al., 1997). This may be explained because, at longer sludge ages, dead microbial biomass may be utilised as an energy source by the remaining viable cells. Consequently, the increased availability of organic substrates, mainly in the form of rigid cellular components such as gelatin, stimulated the production of hydrolytic enzymes in the viable microbial fraction.

- Activated sludge reactor type

In general, biological wastewater treatment processes can be classified into suspended growth systems (such as the conventional AS process) and attached growth systems (which include trickling filters, moving bed biofilm reactors, membrane biofilm reactors, etc.). In conventional AS, sludge flocs, which are agglomerations of microorganisms that are flocculated together and embedded in EPS, are suspended by physical agitation within the treatment process. By contrast, attached growth systems develop a fixed biofilm of microorganisms that is attached to a solid support medium. Therefore, attached growth systems typically have longer sludge retention times and a higher diversity of microorganisms than conventional AS processes, which also enables them to perform more efficiently at higher organic loading rate (OLR) (Loupasaki and Diamadopoulos, 2013). This behaviour also has implications for enzyme production since increasing OLR stimulates the expression of extracellular hydrolytic enzymes in microbial cells. For example, Hassard et al. (2018) found the activity of amino-peptidase, α-glucosidase and phosphatase increased by 4.6, 13.5 and 6.3 times, respectively, in a rotating biofilm reactor (a semi-submerged attached growth reactor with a rotating support material of high porosity mesh plates) compared to a conventional AS system. However, excess OLR can limit enzyme expression, because diffusion of compounds of large MW and electron acceptors may decline under high OLR conditions (Hassard et al., 2018).

2.5 General Enzyme purification and stabilisation

2.5.1 Purification and consolidation

Crude enzyme extracts from AS inevitably contain a large amount of water, and their stability in storage and for industrial application is relatively limited. The presence of inhibitory substances, co-extracted from the sludge biomass, can reduce the activity of crude enzyme mixtures, however, whilst purification can increase stability and enzymic specificity, it can also cause performance losses to a certain extent compared to the crude enzyme extract. Nevertheless, the benefits of consolidating and purifying enzymes to upgrade crude AS extracts will further facilitate the development of marketable, high value commercial products from this secondary biomass source.

Purification of enzymes is usually achieved by a multi-step series of non-specific techniques (Figure 2-7). The first step is clarification of the crude extract to remove remaining cell debris. The sedimentation rate of a bacterial cell with a diameter of 0.5 mm is less than 1 mm/h (Aberer et al., 2002). Therefore, rapid separation can be achieved by centrifugation and filtration, to separate soluble proteins (including enzymes) from organelle-sequestered proteins and retain them in the supernatant or filtrate (Ramos and Malcata, 2011).

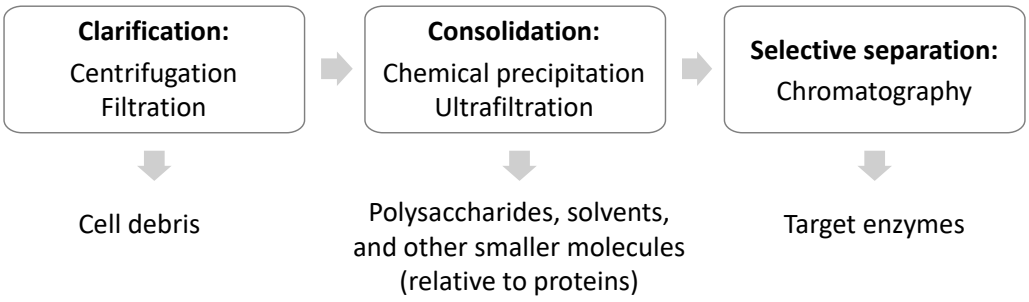

Figure 2-7 Stepwise purification of enzymes

However, the total volume of the clarified enzyme solution is generally very large, but the concentration of enzymes is relatively low. Therefore, the enzyme concentration in the solution can be consolidated by chemical precipitation. Enzymes are complex protein molecules possessing both ionic and hydrophobic groups (see Section 2.2.1) and are readily susceptible to precipitation by a number of different reagents including: (1) neutral salts (followed by a dialysis step for salt removal), e.g. ammonium sulphate, which change the electrostatic forces responsible for the solubility by acting on the water molecules surrounding the protein; (2) organic solvents, e.g. acetone, ethanol and butanol, which reduce the dielectric constant of the water solution, causing aggregation of proteins; and (3) polymers, e.g. polyethylenimines and polyethylene glycols, which precipitate proteins by inducing steric exclusion effects (Atha and Ingham, 1981). Alternatively, consolidation can be achieved by ultrafiltration (e.g. (Qin et al.)), by separating large enzyme molecules from smaller solvent molecules through a

semipermeable membrane (pore size ranging from 0.008 to 0.2 μm (Tchobanoglous et al., 2014)).

Purification treatment of crude AS extracts generally leads to a diminution of enzyme activity (on an equivalent volumetric base) to some extent for several reasons (Hmidet et al., 2008). Jung et al. (2002) observed a reduction in protease activity, equivalent to approximately 30%, following precipitation of a crude enzyme extract from disrupted AS with 40-50% saturated ammonium sulphate, compared to the original extract, and explained that this was probably due to the loss of protein content (approximately 36.2% protein) during chemical precipitation. Nabarlatz et al. (2012) purified lipase obtained from AS by precipitation with 40% saturated ammonium sulphate and dialysis (12-14 kDa), and obtained an activity recovery rate for each step equivalent to 74% and 45%, respectively. Ni et al. (2017) extracted a crude enzyme product from AS using 1% TX100 and sonication treatment, followed by precipitation in 80% acetone and vacuum drying at 40°C, and found that 47, 45, 34, and 32% of the activity in the original crude enzyme extract of collagenase, lipase, amylase, and cellulase, respectively, was preserved in the final dried enzyme product.

Higher degrees of purification can be obtained by applying chromatographic techniques after the basic clarification and consolidation stages (Sharma et al., 2001), and this is usually necessary for analytical or medical applications. Enzyme molecules can be selectively separated chromatographically based on their size and shape, total charge, hydrophobic groups present on the surface, and binding capacity with the stationary phase (Coskun, 2016). For example, Erat et al. (2005) purified glutathione reductase extracted from chicken liver and precipitated with ammonium sulphate, using Sepharose affinity chromatography, and Sephadex gel filtration chromatography. The enzyme was purified 1714-fold relative to the original crude enzyme solution, and the specific activity of the final enzyme product was 120 U/mg protein. Ion-exchange chromatography for enzyme purification is also frequently reported (Batista et al., 2020; D'Souza et al., 2020; Vidya et al., 2020).

In summary, the purification/consolidation steps necessary to develop commercial products from AS may reduce the enzyme activity by 30-70% compared to the original crude extract. However, this is the case with all enzyme recovery/purification systems from microbial biomass (Aberer et al., 2002) and, in practice, only small quantities of enzymes are used to catalyse process reactions, so it is unlikely that this is a significant barrier to the development of commercially viable, industrial enzyme products from AS produced by biological wastewater treatment. Indeed, consolidation and purification of AS enzymes would increase the flexibility and range of industrial end-uses and marketability of the product.

2.5.2 Stabilisation and immobilisation

Free enzymes often show poor storage and operational stability, they are readily inactivated and are difficult to recycle and reuse, which limits their large scale commercial application (Sahutoglu and Akgul, 2015). Immobilisation of free enzymes is a promising approach to overcome these drawbacks, by enhancing mechanical strength, increasing resistance to denaturation and facilitating recycling of the enzyme catalyst within a reaction system (Katchalskikatzir, 1993; Sheldon and van Pelt, 2013).

Conventional enzyme immobilisation is by chemical or physical binding to an inert carrier (e.g. sephorose, zeolites, silica, agarose, alginate, polyacrylamide, hollow fibres and acrylic resins) by adsorption, entrapment or encapsulation (Bisswanger, 2011b). However, the carrier introduces a large amount of non-catalytic material, typically representing 90 to 99% of the total mass of the enzyme product (Schoevaart et al., 2004), which significantly dilutes the enzyme activity. Recently, carrier-free immobilisation, by intermolecular cross-linking between adjacent enzyme molecules (to be discussed in Section 2.6), has emerged as an alternative method to conventional carrier-bound enzyme immobilisation (Cao et al., 2000; Cui et al., 2017; Asgher et al., 2018). This technique combines purification and stabilisation into a single step, and can be performed directly on crude enzyme extracts, such as those obtained from AS (Yamaguchi et al., 2018). Furthermore, immobilising enzymes by cross-linking to the surface of a membrane or micro-reactor for use within a continuous reaction process (Jannat and Yang, 2018) offers significant potential opportunities and is an exciting area for future research and development. For instance, Barber et al. (2020) recently proposed that oxidoreductase enzymes cross-linked with flexible spacers (e.g. polyethylene glycol) could provide an effective approach to organic micropollutant degradation in municipal wastewater treatment.

2.6 Cross-linked enzyme aggregates

2.6.1 Background

Conventional enzyme immobilisation is by chemical or physical binding to an inert carrier (e.g. sephorose, zeolites, silica, agarose, alginate, polyacrylamide, hollow fibres and acrylic resins) via adsorption, entrapment or encapsulation (Bisswanger, 2011b). However, the carrier introduces a large amount of non-catalytic material, typically representing 90 to 99% of the total mass of the enzyme product (Schoevaart et al., 2004), which significantly dilutes the enzyme activity.

Quiocho and Richards (1964) introduced an alternative method to conventional carrier-bound enzyme immobilisation based on the intermolecular cross-linking of crystallised carboxypeptidase (a proteolytic enzyme that is synthesised in the pancreas and cleaves the

carboxy-terminal amino acid residue from polypeptide substrates (Bukrinsky et al., 1998)) to produce carrier-free, immobilised, cross-linked enzyme crystals (CLECs). In this process, soluble enzymes are initially crystallised, followed by fixation with glutaraldehyde treatment. CLEC show reduced, but nevertheless, substantial enzymatic activity (approximately 30% of the initial soluble enzyme activity), as well as an increased mechanical strength (compared to crystallised enzymes without glutaraldehyde treatment). Bayne and Ottesen (1976) produced CLEC of lactate dehydrogenase using octanediimidic acid dimethyleste (a bifunctional diimidate that reacts specifically with N-terminal residues and lysine ε-amino groups of proteins) as the fixative. The enzyme activity of the CLEC was 34% of the initial activity in the crude extract, however, the stability of the CLECs after exposure to urea (an example compound for testing the stability of CLEC in the presence of organic chemicals) was much improved with 50% activity loss after 300-min exposure to 2mol/L urea, compared to soluble enzymes which lost almost 1005 activity under equivalent conditions. St Clair and Navia (1992) also found that CLEC of thermolysin (a thermostable Zn^{2+}-metalloprotease that specifically hydrolyses peptide bonds on the imino side of large hydrophobic residues (Pelmenschikov et al., 2002)) showed significantly enhanced stability under harsh catalytic conditions. Thus, the CLEC was able to produce the aspartame precursor in buffer-saturated ethyl acetate at 55 °C over a period of 18 days without significant loss of enzyme activity, whereas free thermolysin was completely inactivated by day four of the experiment.

Higher operational stability and mechanical strength of CLECs offer major operational advantages and improved functionality compared to soluble enzymes, however, CLEC production is considered a time-consuming and laborious process. This is because highly purified enzyme solutions are usually necessary for efficient crystallisation of proteins, which severely limits its application for large-scale enzyme production and industrial application (Haring and Schreier, 1999; Sheldon, 2007). Consequently, the CLEC technique has been applied only to a limit extent and enzymes, including: ribonuclease, subtilisin, carboxypeptidase, alcohol dehydrogenase and some lipases (Cui and Jia, 2015).

An alternative strategy to novel, carrier-free enzyme production, is to develop cross-linked enzyme aggregates (CLEAs), and this approach has emerged recently and overcomes the drawbacks of CLEC preparation. Crystallisation is replaced by enzyme precipitation, by the addition of inorganic salts or organic solvents/polymers, followed by treatment with a cross-linking reagent (Figure 2-8). Thus, purification and immobilisation of the enzyme are combined into a single unit operation, and the need for highly purified enzyme is avoided (Cao et al., 2003; Yamaguchi et al., 2018). Therefore, the CLEA technique can be used to directly isolate and immobilise enzymes from complex matrices (such as a crude fermentation broth, or, indeed, AS). Cao et al. (2000) reported the first example of CLEAs prepared from penicillin G

amidase (the free enzyme is readily and irreversibly inactivated if exposed to organic solvents) via precipitation with tert-butyl alcohol followed by cross-linking with glutaraldehyde. The CLEA maintained catalytic activity in a wide range of organic solvents, and its catalysing efficiency (expressed as turnover frequency, i.e. the number of molecular reactions or catalytic cycles occurring at one catalytic centre per unit time (Bisswanger, 2011c)) was 50% higher compared to the equivalent CLEC during the synthesis of ampicillin in acetonitrile. The simplicity and robustness of CLEA preparation has attracted increasing attention over the past decade. The technique has been successfully applied to an increasing number of enzymes including: laccases, amylase, lipase, and cellulase (Sheldon, 2011a). It has also been applied to enzyme extraction, purification and immobilisation from crude sources, such as fermentation broths of microorganisms (Lai et al., 2012; Bashir et al., 2018), mung bean extract (Yu et al., 2013), and fresh fruit extracts (Tandjaoui et al., 2015).

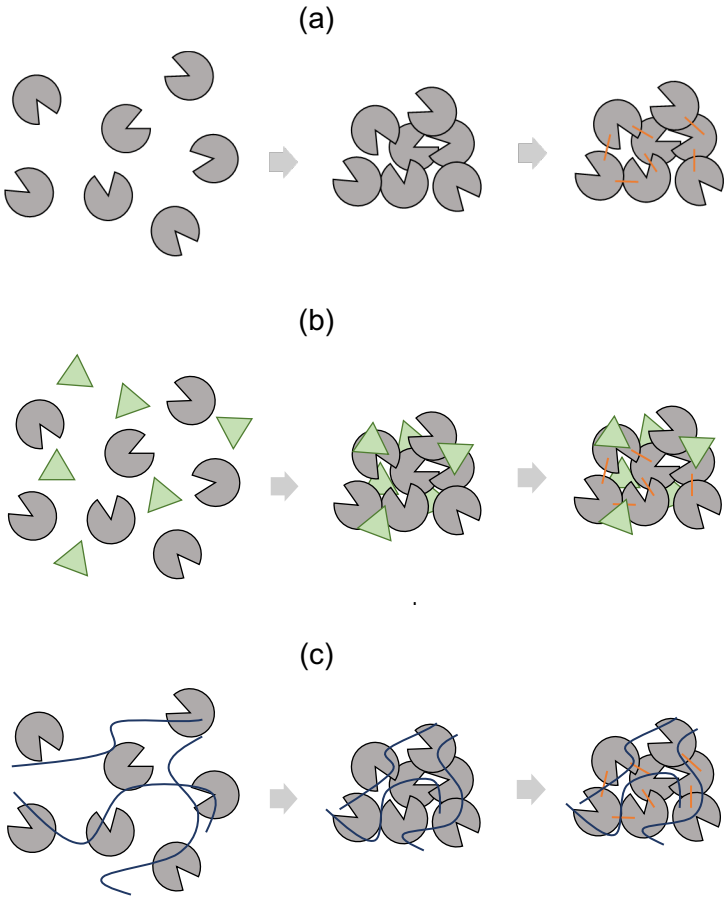

Figure 2-8 Enzyme immobilisation by cross-linking; the cross-linker is represented by the orange line; CLEA can be prepared with (a) original enzyme solutions or via co-precipitation with additives (see Section 2.6.5), such as (b) bovine serum albumin (green triangles) and (b) polyethyleneimine (dark blue lines).

2.6.2 Fundamental principles of CLEA preparation.

The first step in CLEA preparation involves the aggregation and precipitation of the enzyme from aqueous solution, which is essentially equivalent to the mechanism of protein precipitation by inorganic salts, organic solvents or non-ionic polymers (i.e. the precipitant). The second step is chemical cross-linking of the precipitated enzyme, via adding a bifunctional reagent (i.e. the cross-linker) containing reactive groups that can respond to the functional groups on the surface of the enzymes and consequently knit the enzymes together. A simplified procedure, with the precipitant and the cross-linker simultaneously added to the enzyme solution (instead of the step-wise manner), can also be adopted without affecting the overall CLEA activity recovery rate (Lopez-Serrano et al., 2002; Aytar and Bakir, 2008).

The bifunctional reagents can be classified as either homobifunctional or heterobifunctional, with the two reactive moieties being identical or different, respectively. The most commonly used cross-linkers are carbonyl-based reagents, for example, aldehydes, which form Schiff bases upon nucleophilic attack by the amino groups of the enzymes (Figure 2-9) (Okuda et al., 1991; Salem et al., 2010). The resulting Schiff base after cross-linking is not stable if exposed to the buffer solution for an extended period, and they tend to break down into the constituent aldehyde and amine at acidic pH, which may cause the gradual release of the enzyme into solution (Migneault et al., 2004). Some researchers (e.g. Sheldon (2007)) suggested that dosing a reducing agent after the cross-linking reaction can effectively reduce the Schiff base intermediate and stabilise CLEAs; sodium borohydride ($NaBH_4$) sodium or cyanoborohydride ($NaCNBH_3$) are often used for this purpose (Garcia-Galan et al., 2013; Hermanson, 2013a; Sahutoglu and Akgul, 2015; Perzon et al., 2017). Fernandez-Lafuente et al. (1995) showed that reduction of the Schiff base by $NaBH_4$, following cross-linking of penicillin G acylase onto glyoxyl agarose gel, significantly enhanced the stability of the enzymes, and approximately 80% of the activity was preserved after a 20-h incubation at pH 9 and 20°C; whereas only 10-30% of the activity was detected in non-reduced samples; however, Schiff base reduction did not increase the activity recovery rate of the immobilised enzyme.

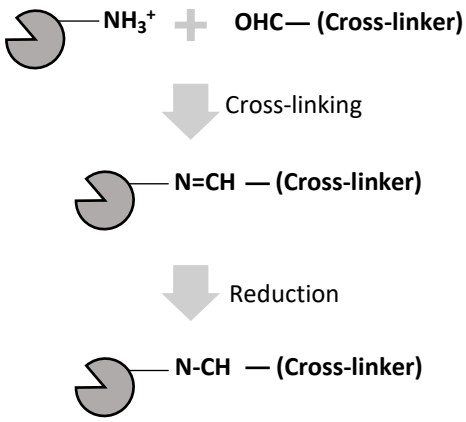

Figure 2-9 Reaction of enzyme amino groups (e.g. lysine residues) with aldehyde groups of a cross-linker, followed by reduction of the Schiff bases (imines) into more stable single bonds, during CLEA preparation

Various types of amino groups are able to react with aldehydes, such as lysine, tyrosine, tryptophan, histidine, cysteine, proline, serine, glycine and arginine (Bowes and Cater, 1966; Migneault et al., 2004), and several examples are shown in Table 2-3. Regarding their reactivity towards the aldehydes, these moieties can be ranked in decreasing order as follows: ε-amino, α-amino, guanidino, secondary amino, and hydroxyl groups (Migneault et al., 2004). Lysine, in particular, appears to play a significant role in enzyme cross-linking reactions (Wine et al., 2007). Lysine residues (i.e. the remaining lysyl side chain after the formation of peptides via dehydration condensation of the amino acids) exhibit a great abundance in most proteins (ranging from 3.6-7.0% for different source of protein (Gorissen et al., 2018)). Lysine residues contain three methylene groups that are generally located inside the protein molecule because of its high hydrophobicity. It also contains one reactive terminal ε-amino group that is often positively changed under physiological conditions and is located on the surface of the protein, exposed to the aqueous medium and is, therefore, highly available to react with the cross-linker (Srere and Uyeda, 1976; Mateo et al., 2005).

Table 2-3 Examples of reactive amino acids/functional groups in proteins (corresponding reactive residues are shown in blue circles) that can react with aldehydes

Amino group	Molecular structure	Type of the reactive residue
Lysine	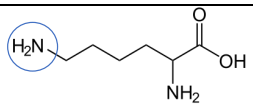	ε-Amino group
Arginine	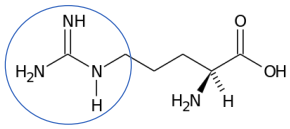	Guanidino group

Histidine	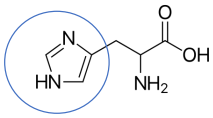	Imidazole group (containing secondary amine)
Tryptophan	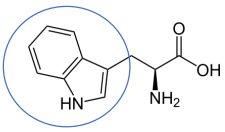	Indole group (containing secondary amine)
Tyrosine	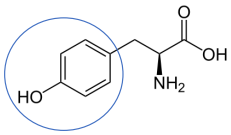	Phenolic group (aromatic + hydroxyl group)
Cysteine	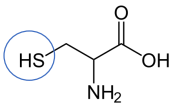	Thiol group

Cross-linking of an enzyme by the reaction between aldehyde groups and amine residues produces additional covalent bonds in the tertiary structure of the (immobilised) enzyme. Therefore, the original ionisation of the basic amino acid side chains in the micro-environment around the enzyme active site can be modified (Chui and Wan, 1997; Lai et al., 2012). Indeed, shifting of the optimum pH of the cross-linked enzymes is often reported for this reason (e.g. (Bashir et al., 2018)). Furthermore, the molecular structure of the enzyme proteins may be also altered. Lai et al. (2012) indicated that the immobilised enzymes can be protected from distortion or inactivation due to the more rigid structure of the aggregate, compared to free enzymes. Therefore, enhanced operational stability of CLEAs against extreme conditions (such as pH, temperature and exposure to organic substances), as well as storage stability and reusability, was also frequently observed.

2.6.3 Precipitants

2.6.3.1 Hydration layer of proteins

Protein molecules in aqueous media are surrounded by water molecules, i.e. the “hydration layer”, which shows slower dynamics compared to how quickly water molecules move in bulk solvent (Sinha et al., 2008). The hydration layer is an intrinsic part of protein structure (about 0.38 g water/g protein (Rupley et al., 1983)), maintaining the protein solubility and conformational stability. It can be further classified into bound waters, buried waters and diffusive waters (Dahanayake and Mitchell-Koch, 2018; Dahanayake et al., 2019). The hydration layer binds to the protein surface mainly through hydrogen bonds and long-range electrostatic forces between water and the polar or ionic groups of the protein, and also hydrophobic interactions, which are also relevant to aggregation of hydrophobic moieties and/or protein folding (Laage et al., 2017; Camisasca et al., 2018) (Figure 2-10).

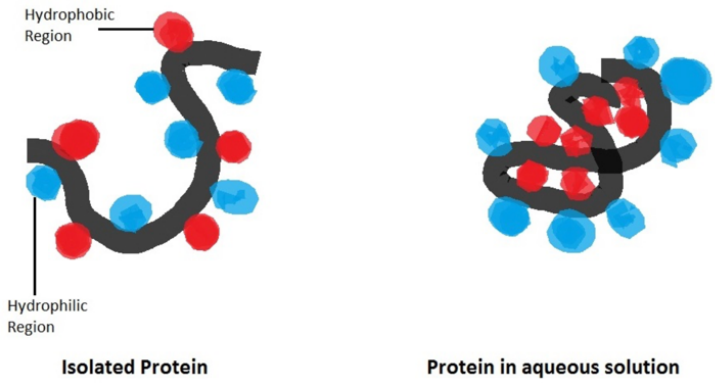

Figure 2-10 Protein folding in aqueous solution under hydrophobic interactions, to allow polar regions (blue) to interact with water, while non-polar hydrophobic regions (red) not interact with the water (Than, 2020)

2.6.3.2 Neutral salts

Protein precipitation from aqueous solution can be induced by adding neutral salts to the solution. As the salt concentration increases, water molecules that are initially attached to the charged part of the protein are preferably attracted to the charged inorganic ions, causing self-association and aggregation of the protein due to hydrophobic interactions between adjacent molecules. Among various inorganic salts used for protein precipitation, ammonium sulphate ($(NH_4)_2SO_4$) is the most widely used because it is readily soluble in water, it is relatively inexpensive and is a highly efficient precipitant, and does not cause severe denaturation of the protein structure (Burgess, 2009). Most of the lower molecular proteins begin to precipitate when the concentration of $(NH_4)_2SO_4$ in solution is over 50% saturation; precipitation of larger multi-proteins is possible below 20% saturation (Wingfield, 2001).

2.6.3.3 Water miscible organic solvents

Water miscible organic solvents, such as dimethoxyethane (Shah et al., 2006), acetone (Tandjaoui et al., 2015) and some alcohols (e.g. isopropanol (Graebin et al., 2018), and tert-butanol (Dong et al., 2010)), have been be used as precipitants for several enzymes in CLEA preparation. After addition to the crude enzyme extract solution, these organic solvents decrease the dielectric constant of water, progressively displacing water from the protein surface and binding it in hydration layers around the organic solvent molecules. Consequently, proteins with thinner hydration layers tend to aggregate by attractive electrostatic and dipole forces. The advantage of organic solvent precipitation is that salt removal from the final product is not required, which is particularly important in cases where the presence of salts in the product may interfere with the catalytic reaction of the enzyme.

However, organic solvents can readily disrupt the structure of enzymes due to strong dipole forces (Zhou et al., 2017b), or the penetration of the solvent into deep layers of the enzyme molecule (Graebin et al., 2018). Therefore, a cautious approach to the selection of a suitable

organic precipitant is necessary. Zhen et al. (2013) reported that alcohols with a longer aliphatic chain (e.g. iso-propanol) tend to preserve more enzyme activity in CLEA preparation than those with a shorter chain (e.g. methanol). Alcohols with a longer chain often show a higher hydrophobicity and, therefore, weaker capacity to capture water from the surface of enzymes. Consequently, the protein structure can be protected during precipitation, without excessive displacement of surface-bound water. Optimising the volume ratio of organic solvent to enzyme solution is required to obtain complete precipitation and avoid enzyme inactivation. For example, in the case of acetone, a volume ratio of at least 4:1 (acetone : protein solution) is required (Nie et al., 2018).

Mixing organic solvents into aqueous solutions is exothermic, which may cause a loss of enzyme activity if the rise in temperature is not controlled below the critical point for inactivation. Therefore, precipitation with organic solvents is usually performed at low temperature (e.g. -20°C for acetone). By contrast, where $(NH_4)_2SO_4$ is used to precipitate proteins, temperature control is not critical in this case, because dissolution of $(NH_4)_2SO_4$ is endothermic and thus cools the solution.

2.6.3.4 Nonionic polymers

Polyethylene glycol (PEG) is the most common non-ionic hydrophilic polymer used for protein precipitation. The theory of steric exclusion has been widely accepted as the mechanism for this reaction, where proteins are sterically excluded from the regions that are occupied by the inert synthetic polymer (i.e. PEG) and are thus concentrated until their solubility is exceeded, and aggregation and precipitation occurs (Atha and Ingham, 1981). The MW of PEG has a profound influence on the protein precipitation. Linear PEG 6000 or PEG 4000, with a concentration in the range: 3% to 20% v/v, are recommended for protein precipitation in practice (Ingham, 1984; Lovrien and Matulis, 1997). PEG with a higher MW (>6000 Da) showed similar precipitation efficiency compared to PEG 6000, but the higher viscosity reduced the ease of recovering precipitated enzyme sediments (Sim et al., 2012); on the other hand, for PEG with lower MW (<4000 Da), usually concentrations of 20%-50%, which also exhibits extremely high viscosity, are necessary for effective protein precipitation of target proteins (Honig and Kula, 1976; Lovrien and Matulis, 1997; Perzon et al., 2017).

2.6.3.5 Effect of operational mode on CLEA activity

The mode of adding precipitants to a soluble enzyme during CLEA preparation can influence the final enzyme activity. During chemical precipitation of the enzymes (Figure 2-8), they can be potentially inactivated because of the mechanism of enzyme precipitation is closely related to removal of the essential hydration layer (see above). Schoevaart et al. (2004) suggested that shock-wise aggregation of the enzymes, via quenching with precipitant of high concentration (e.g. 90% saturated $NH_4(SO_4)_2$) or adding enzyme to precipitant, can facilitate

attachment to neighbouring protein molecules and, consequently, preserve the enzyme tertiary structure. CLEA of glucose oxidase with almost 100% activity recovery rate was produced by Schoevaart et al. (2004) by quenching the soluble enzyme with 90% v/v $NH_4(SO_4)_2$. By contrast, the slow addition of precipitant, which is more analogous to a protein crystallisation process, caused partial inactivation of the enzyme.

2.6.4 Cross-linkers

2.6.4.1 Glutaraldehyde

Glutaraldehyde ($OHC(CH_2)_3CHO$) is a homo-bifunctional reagent that contains an aldehyde residue at both ends of the 5-carbon chain. The two carbonyl ends can react with different protein moieties, including not only amino groups but also thiols, phenols, and imidazoles (Barbosa et al., 2014) (see Table 2-3). Glutaraldehyde has been widely used as a surface disinfectant (Al Shikh and Milosevic, 2020), medical treatment for warts (Dall'Oglio et al., 2012), leather tanning agent (Rachmawati and Anggriyani, 2018) and protein fixative in microscopy (Woods and Stirling, 2019), preservative for tissue samples (Yamaguchi et al., 2020) and also cross-linker for a wide range of industrial enzymes (Sheldon, 2011a). Bowes and Cater (1966) indicated that the stability of protein-aldehyde bonds formed with glutaraldehyde was increased compared to other dialdehyde compounds, including glyoxal (OHCCHO), malonaldehyde ($OHCCH_2CHO$), succinaldehyde ($OHC(CH_2)_2CHO$) and adipaldehyde ($OHC(CH_2)_4CHO$), and this was probably explained by the differing solubility and molecular size of these aldehydes.

Schoevaart et al. (2004) prepared CLEA of a commercial lipase product from *Candida antarctica* (containing 308 U of activity and 10mg protein per mL), by adding dimethoxyethane to the enzyme solution with a volume ratio of 9:1 for precipitation, followed by adding glutaraldehyde (final concentration = 150 mM) for a 3-hour reaction at room temperature. The CLEA showed almost 100% of the activity recovery relative to the free enzyme solution. Aytar and Bakir (2008) also prepared CLEA of tyrosinase from crude mushroom extract via precipitation with $(NH_4)_2SO_4$ (60% saturation) and cross-linking with 2% glutaraldehyde for 3 h at room temperature, and also achieved almost a 100% activity recovery rate compared to the original free enzyme. The CLEA also showed high storage stability, and 81% of the initial activity was retained after 80 days storage at 4 °C, whereas the free soluble enzyme only exhibited 2% of its initial activity under the same conditions.

Lai et al. (2012) produced CLEA of *Penicillium expansum* lipase directly from the crude fermentation broth, by precipitation with $(NH_4)_2SO_4$ (50% saturation, 30min at 4 °C), followed by glutaraldehyde addition (final concentration = 0.125% w/w) for a 24-h reaction period at 4 °C, followed by freeze drying to obtain a solid CLEA product. The CLEA showed higher stability in aqueous solution under extreme conditions compared to the free enzyme, and the

optimal reaction temperature and pH for the CLEA were 40 °C and pH 7, respectively, compared to 35 °C and pH 9, respectively for the free enzyme. The produced CLEA also showed high tolerance to nonaqueous media, such as hexane (an organic solvent) and [BMIm][PF6] (an organic salt, or ionic liquid, that is considered as a more sustainable alternative to traditional volatile organic solvents (Liu et al., 2012)). The CLEA was used to catalyse biodiesel production from microalgal oil in [BMIm][PF6] media, and the yield of biodiesel first increased with increasing CLEA dosage, with the highest conversion rate after 48 h (85.7%) obtained at dosage = 100mg dried solids/0.5 g microalgal oil. Further increasing the CLEA dosage (200 mg/g) resulted in decreased conversion rate (59%) under the same conditions, which was explained by possible clumping of CLEAs at high dosage and consequent shielding of enzyme active sites.

Yu et al. (2013) produced CLEAs of epoxide hydrolases (an enzyme that catalyse the synthesis of enantiopure diols) from a crude mung bean extract. Under optimal condition (80% saturated $(NH_4)_2SO_4$, 25mM glutaraldehyde, 12 h reaction time, at 4 °C), 92.5% of the free enzyme activity was retained in the CLEA, and the specific activity was 66.6 U/g CLEA. The CLEA showed enhanced stability and tolerance to various organic solvents (including *n*-hexane, *n*-octane, isopropyl ether, dimethyl benzene, *n*-octyl alcohol and ethylacetate), and the activity relative to the initial value (prior to incubation in organic solvents at 35 °C for 4h) was 20-40% higher compared to the free enzymes. Furthermore, the CLEA was able to retain >50% of its initial activity after 8 batches of reuse in either aqueous solution (phosphate buffer, 100 mM, pH 7.5) or in a biphasic system (*n*-hexane/buffer = 1:1).

Perzon et al. (2017) produced CLEA of cellulase using various precipitants, including $(NH_4)_2SO_4$ (40% w/v), PEG (MW=1500 Da, 50% w/v), and tert-butyl alcohol (60% w/v) under different reaction conditions, glutaraldehyde as the cross-linker (at dose rates of: 5, 30, or 200 mmol/L). Tert-butyl alcohol inactivated the enzyme, and the highest activity recovery rate, obtained with $(NH_4)_2SO_4$ and PEG precipitation, was equivalent to 16.7% (with 5 mmol/L glutaraldehyde, cross-linking at 4 °C for 2 h) and 28.7% (with 30 mmol/L glutaraldehyde, cross-linking at room temperature for 2 h), respectively. However, PEG-CLEA showed better reusability compared to $(NH_4)_2SO_4$, and 40 and 10% of the activity was retained after 4 cycles of reactions for each precipitant type, respectively. The activity of $(NH_4)_2SO_4$-CLEA was negatively correlated with the increasing amounts of glutaraldehyde and prolonged cross-linking time. However, the activity of PEG-CLEAs was positively correlated with increasing glutaraldehyde dose for cross-linking, and there was no effect on the time period required to complete the cross-linking reaction. Perzon et al. (2017) suggested that this behaviour may be explained by a competitive reaction between the enzyme cross-linking with glutaraldehyde and the solubilised $(NH_4)_2SO_4$ salt at high glutaraldehyde concentrations, forming excessive

amounts of a gel-like structure which can trap the active site of cellulase. This would reduce access to the substrate and therefore lower the apparent enzyme activity.

Graebin et al. (2018) prepared a CLEA of dextransucrase by isopropanol precipitation and glutaraldehyde cross-linking (100 mM, 3h at 5 °C) and found the activity was equivalent to 22% of the free enzyme. The CLEA showed a shift in optimal pH and temperature from pH 5.2 and 30 °C (free enzyme) to pH 3.0 and 60 °C, and the operational stability of the CLEA retained approximately 30-40% of residual activity after 10 cycles of reuse for the production of oligosaccharides (precursors of dextran) with 100mM sucrose and/or 600 mM maltose as the substrate (at 30 °C and 3 h for each cycle).

Although glutaraldehyde has been successfully used for cross-linking in enzyme immobilisation, the molecular structure of CLEAs has not been elucidated (Barbosa et al., 2014). Some researchers (Ruijgrok et al., 1990; Hermanson, 2013b; Barbosa et al., 2014) suggested that the reaction of glutaraldehyde with enzyme moieties is not limited to just one mechanism. Indeed, glutaraldehyde shows highly complex chemical behaviours in aqueous solution and the main reactive species of monomeric and polymeric forms are found in equilibrium.

The pH of the solution significantly affects the extent of polymerisation of glutaraldehyde in dilute solution (<25%). Figure 2-11 shows several possible forms of glutaraldehyde in solution at different pH. Under acidic conditions, glutaraldehyde monomers are in equilibrium with the cyclic hemiacetals and aldol ring structure as pH increases to a more basic range, the monomers begin to polymerise via intermolecular condensation reactions, forming α-, β-unsaturated aldehyde polymers that contain carbon–carbon double bonds (Walt and Agayn, 1994; Migneault et al., 2004). Gas chromatography and nuclear magnetic resonance (Peters and Richards, 1977) showed that, at pH 3, a commercial solution labelled as 25% glutaraldehyde contained approximately 79% H_2O, 3% glutaraldehyde, and 18% of higher MW derivatives that could be broken down into the glutaraldehyde monomer. At a pH value in the neutral or slightly basic range, large aldehyde polymers were detected in the solution. Furthermore, Peters and Richards (1977) found that the degree of polymerisation (i.e. the n value in Figure 2-11) increased as the pH was raised, until the polymer precipitated from the solution.

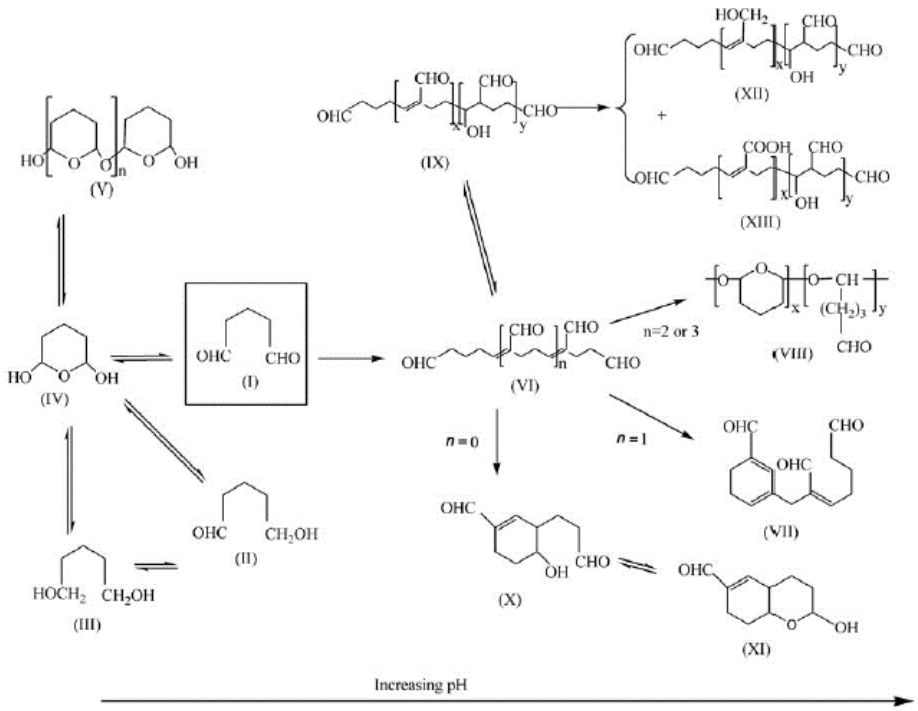

Figure 2-11 Formation of different glutaraldehyde derivatives in solution under different pH conditions (Migneault et al., 2004)

The balance of the reactive species also differs with varying concentration of glutaraldehyde in solution. Kawahara et al. (1992) investigated the structure of glutaraldehyde in aqueous solution by UV absorption and light scattering and found that 70% v/v glutaraldehyde mainly contained polymeric species with cyclic hemiacetal structure (V in Figure 2-11), which undergo depolymerisation with increased dilution. In contrast, in more diluted solutions (20% v/v or less), glutaraldehyde exists mainly in its monomeric form with cyclic hemiacetal structure (IV in Figure 2-11), under a range of pH conditions including acidic, neutral and slightly basic (pH 3-8); in this state the monomer can remain stable in solution for more than a week without significant transformation.

Furthermore, the molecular structure of glutaraldehyde may change during storage. Hermanson (2013b) indicated that old, prepared solutions were more likely to contain appreciable amounts of polymer polymerised species than freshly prepared solutions. The impact of storage temperature on glutaraldehyde structure has also been reported. Gillett and Gull (1972) found increasing temperature during storage caused an equilibrium shift from pure glutaraldehyde monomers, which have an absorbance peak at wavelength = 280 nm (Abs_{280}), towards the formation of α-, β-unsaturated polymers, which was demonstrated by an increase in absorption at 235 nm wavelength (Abs_{235}). Rasmussen and Albrechtsen (1974) continuously measured the UV absorbance of a 20.8% aqueous solution of glutaraldehyde stored at varying temperatures (-14 to 60 °C) for up to 5 months (or until Abs_{235} value exceeded the detection limit). No polymerisation of monomeric glutaraldehyde was detected at -14 °C

for the entire testing period. However, the polymerisation rate (expressed by the ratio of Abs_{235}/Abs_{280}) showed an exponential rise with temperature, and the rate increased by factor 3 with a 10 °C lift in temperature. However, Ruijgrok et al. (1990) showed that, after heating a 0.85% w/w glutaraldehyde solution from 25 to 60 °C, no peak was observed at 235nm over a 2 h period. This was explained because the polymerisation reaction occurs relatively slowly and that a significant conversion to the unsaturated polymer only occurs after prolonged exposure to high temperatures.

Therefore, in most cases of protein/enzyme cross-linking, which is often carried out with <1% glutaraldehyde at neutral pH and room temperature or 4 °C, it is reasonable to speculate that the concentration of polymeric forms will be relatively small compared to the monomers. However, Kawahara et al. (1992) indicated that polymeric species containing an ethylenic double bond (structure VI in Figure 2-11) may also exist from the reaction between monomeric glutaraldehyde and trace amounts of amino groups such as n-amylamine (an analogue of the side chain of lysine residue), which are also involved in cross-linking reactions.

2.6.4.2 Macromolecular saccharide derivatives: poly-aldehydes

Glutaraldehyde is generally one of the most common choices of cross-linker for CLEA production, as it is relatively inexpensive and readily available (Sheldon and van Pelt, 2013). However, the MW of monomeric glutaraldehyde is relatively small and equivalent to 100.11 Da, compared to an average enzyme which may be in the range of 12000 to 300000 Da (Ogston, 1962). Therefore, glutaraldehyde can interfere with enzyme activity as it may penetrate recessed part of the enzyme structure where the active catalytic sites are often located (Figure 2-2). Glutaraldehyde molecules may react with the essential active sites of enzymes, resulting in reduced or, indeed, no enzymatic activity retained in the produced CLEA.

Therefore, macromolecular polymers with higher MW than glutaraldehyde that contain numerous reactive aldehyde groups (i.e. poly-aldehydes) have been used as alternatives for enzyme cross-linking. Macromolecular cross-linkers can be easily prepared through sodium periodate ($NaIO_4$) based oxidation of a polysaccharide, which introduces reactive aldehyde groups onto the carbon skeleton (Drobchenko et al., 1993). Adjacent carbon atoms containing hydroxyl groups are influenced by the presence of periodate, and the corresponding carbon–carbon bonds are cleaved and hydroxyl groups are transformed into aldehydes (Hermanson, 2013b). Other methods for producing macromolecular cross-linkers include ozonolysis (Schoevaart et al., 2005) or enzymatic oxidising (Schoevaart and Kieboom, 2001).

Dextran is a complex branched polysaccharide derived from the condensation of glucose, containing α-1,6 glycosidic linkages between glucose monomers. It has varying chain length and molecular weights (3-2000 kDa) depending on the extent of condensation (E. Polifka and

Habermann, 2015). Modified dextran, i.e. dextran aldehyde (Figure 2-12), is one of the most frequently used macromolecular cross-linkers.

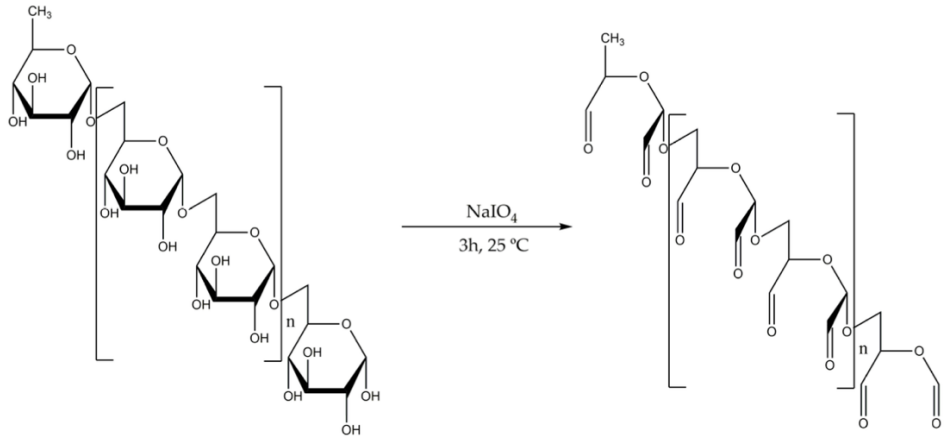

Figure 2-12 Sodium periodate oxidation of α-1,6 glycosidic linkages in dextran to form the cross-linking agent, dextran aldehyde (Orrego et al., 2018)

Sahutoglu and Akgul (2015) compared the effectiveness of glutaraldehyde and dextran aldehyde for the preparation α-amylase and glucoamylase CLEAs under different conditions. The maximum activity recovery rate of glutaraldehyde cross-linking was 21.8% for α-amylase (5 mM glutaraldehyde, 1 h reaction) and 41.2% for glucoamylase (50 mM glutaraldehyde, 2 h). In the case of dextran aldehyde, 60.0% of the α-amylase activity was recovered at 0.126% w/v dextran aldehyde and 2 h reaction time; however, no activity was observed for glucoamylase CLEA. In this case, the functional groups of glucoamylase (such as tryptophan 144, asparagine 200 and glutamine 203), involved in the cross-linking reaction, were probably also responsible for substrate binding as these functional sites show high affinity for both polysaccharides (e.g. starch, the testing substrate in this study) and polysaccharide derivatives (dextran aldehyde). It can be inferred, therefore, that the active site of glucoamylase had been saturated by excessive dextran aldehyde during CLEA preparation, and therefore had very low affinity for starch test substrate.

Valdes et al. (2011) prepared CLEA from lipase solution (activity = 2220 U/mL) containing bovine serum albumin (an inert protein source, to be discussed later, with mass ratio of enzyme/albumin = 5 or 15) and TX100 (a surfactant mentioned in 2.4.3.3, at a final concentration = 0.05% v/v), via acetone precipitation (30 min at 4 °C), followed by glutaraldehyde (concentration = 1.5-3.5 g/L) or dextran aldehyde (MW = 100-200 kDa, concentration = 1.7-2.7 g/L) cross-linking at pH 4.5 and 9.5. In general, CLEAs prepared with dextran aldehyde showed higher specific activity (3186-4800 U/g CLEA) and larger CLEA

particle size (52.6-126.2 μm) compared to glutaraldehyde (the specific activity and particle size in this case were: 882-2874 U/g and 21.2-83.4 μm, respectively).

The MW of dextran has been reported to affect the CLEA preparation. Zhen et al. (2013) found that the activity recovery rate of β-mannanase increased from 11.12% to 32.01% with the MW of dextran aldehyde increasing from 42 kDa to 2000 kDa. However, Zhou et al. (2017b) argued that dextran with different MW (10, 100, 500kDa) did not make much difference in the activity recovery of nitrile hydratase; all of the dextran CLEAs showed activity recovery around 36-39%. Orrego et al. (2018) found that CLEA of lipase prepared by dextran with high MW (25 kDa) showed a higher thermal stability than the ones with lower MW (1.5 and 6 kDa), with the inactivation half-life equivalent to 36.7, 28.1 and 20.5 for dextran MW = 25, 6, 1.5 kDa, respectively, at 70 °C and pH 7.

2.6.4.3 Others

Schoevaart et al. (2005) indicated that saccharide derivatives that possess a 1,5-dialdehyde moiety, which resembles the functional groups/structure of glutaraldehyde (Figure 2-13), have high potential for cross-linking. The effectiveness of glutaraldehyde and its various analogues, including diglycolaldehyde (prepared via ozonolysis of 2,5-dihydrofuran), was compared to periodate oxidised lactose, sucrose, and dextran, for CLEA preparation of *Candida antarctica* lipase. At a concentration of 100 mM and under room temperature conditions, diglycolaldehyde was the most reactive glutaraldehyde analogue, and achieved maximum cross-linking (>90% of the activity recovery) within 1 h. Nevertheless, the reaction rate was approximately ten times slower compared to glutaraldehyde under equivalent conditions. Oxidized dextran (i.e. dextran aldehyde) also recovered >80% activity compared to the initial free enzyme, although a longer reaction time (>4 h) was required compared with diglycolaldehyde.

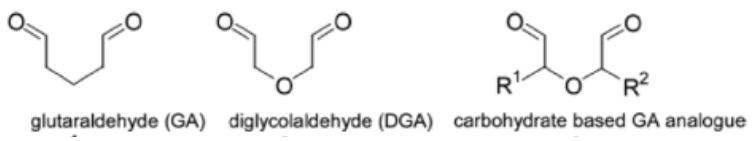

Figure 2-13 Glutaraldehyde and its analogues (Schoevaart et al., 2005)

Rehman et al. (2016) used ethylene glycolbis(succinimidylsuccinate) (EG-NHS, a homobifunctional cross-linker with a 12-atom skeleton that contains two N-hydroxysuccinimide ester ends reactive towards amino groups of proteins, forming amide bonds) as a milder alternative cross-linker to glutaraldehyde, to immobilise *Pencilluim notatum* lipase. Under optimum conditions (saturated $(NH_4)_2SO_4$ precipitation and 150 min cross-linking at room temperature), CLEA prepared with EG-NHS (150 mM) showed a hydrolytic activity of 96.5 U/mL, which was almost twice that obtained with glutaraldehyde (200 mM).

The relatively higher hydrolytic activity with EG-NHS was explained by visual examination of the product through fluorescence and scanning electron microscopy. CLEA with EG-NHS showed smaller particle size, but with larger surface area compared to glutaraldehyde CLEA. The presence of more available active sites may contribute to a higher mass transfer rate of the substrate and thus increase the CLEA activity. Both glutaraldehyde and EG-NHS CLEAs showed improved thermal stability, with half-lives of 3.44-4.30 and 3.44-6.93 times longer, respectively, compared to free lipase when exposed to increased temperature (40-70 °C). They also had comparable reusability, and 63.6% and 70.9% of their original activities were preserved after ten reaction cycles in and aqueous medium, respectively.

Interestingly, Hermanson (2013a) indicated that enzymes with glycosidic residues can be oxidised, resulting in the transformation of hydroxyl groups (R-OH) into aldehyde groups (R-CHO). Therefore, "Self-cross-linking" of these types of enzyme is possible under certain conditions (Schoevaart et al., 2005). For example, Ayhan et al. (2012) successfully produced CLEAs of glucose oxidase, peroxidase and urease, which contain hydrolxyl groups, via precipitation in the presence of bovine serum albumin (BSA, to be discussed in Section 2.6.5.1) followed by $NaIO_4$ oxidation of the enzymes to obtain aldehydes and cross-linking (2 h at 25 °C) with either 1,8-octanediamine (4% v/v) or L-lysine (4% v/v) to provide neutrophilic functional groups reactive towards aldehydes. The produced CLEAs showed 40-60% activity recovery, relative to the original soluble enzymes.

2.6.5 Additives

2.6.5.1 Protein feeder: bovine serum albumin

The availability of sufficient lysine residues on an enzyme is crucial for covalent bond formation with the cross-linker. Enzymes that are deficient in lysine groups, often require the addition of an inert protein feeder. For example, BSA is a small, stable, moderately non-reactive and lysine rich protein that is widely used to quantify other proteins (Lowry et al., 1951) and to stabilise enzymes against thermal inactivation (Chang and Mahoney, 1995). Co-precipitating enzymes with BSA (Figure 2-8(b)) can effectively increase the accessibility of reactive lysine groups, and protect essential active sites of the enzyme from attack by excessive amounts of cross-linker (Dong et al., 2010; Bashir et al., 2018). The formation of intermolecular, rather than intramolecular, cross-linkages is favoured in the presence of BSA, which can avoid occupation of active sites of enzymes that may reduce substrate affinity (Habeeb and Hiramoto, 1968).

Aytar and Bakir (2008) showed that CLEA preparation for tyrosinase from crude mushroom extract, via 60% saturated $(NH_4)_2SO_4$ and 2% v/v glutaraldehyde reacting for 3 h at room temperature, recovered approximately 100% and 31% activity with and without BSA addition (dosage = 50 mg/mL), respectively. Shah et al. (2006) used BSA (5 mg BSA/50 mg enzyme

addition) to facilitate CLEA preparation of *Pseudomonas cepacia* lipase with acetone precipitation and glutaraldehyde cross-linking (25 mM, 3 h at 4 °C). The apparent activity of the CLEA was 12 times that of free enzyme (compared on the weight of dry powder, with which the CLEA was prepared); on the contrary, CLEA without BSA addition showed almost zero activity. The BSA-assisted CLEA showed a higher catalytic efficiency than free enzyme powder for biodiesel production from Jatropha seed oil (500 mg, mixed with ethanol with molar ratio = 1:4); a conversion rate of >90% and 77% was obtained with 6.25mg CLEA and 50mg free enzyme, respectively, after 8 h incubation at 40 °C. Furthermore, the positive effect of BSA in improving the thermal stability of CLEAs was also proved by Shah et al. (2006). CLEA of penicillin acylase (containing 5 mg BSA/125μl enzyme solution) was prepared via dimethoxyethane precipitation and 25 mM glutaraldehyde cross-linking (3 h at 4 °C) and retained 70% activity after 8 h incubation at 50 °C, whereas CLEA without BSA addition retained only 40% activity under the same conditions.

2.6.5.2 Ionic polymer: polyethyleneimine

Polyethyleneimine (PEI) is a polymer abundant in terminal amino groups and is often positively charged at neutral pH and therefore can bind with negatively charged proteins through ionic interactions (Burgess, 2009). Lopez-Gallego et al. (2005) found that mixing *Pseudomonas* sp. glutaryl acylase solution (25 mg/mL) with PEI (MW = 600,000 Da, concontration = 100mg/mL) at mass ratio of protien/PEI = 1:1, followed by PEG (MW = 600 Da) precipitation and glutaraldehyde cross-linking (75mM, 1h), recovered 57% of the free enzyme activity in the CLEA, with the specific activity being 341 U/g dry CLEA, which was 5.5 times that without PEI. This improved CLEA production by PEI addition (Figure 2-8(c)) may be probably due to: (1) the electrostatic forces between positively charged groups in the polymer and negatively charged surface of enzymes, which stabilise the aggregate structure (Yan et al., 2012); (2) the presence of a protection layer of PEI, which effectively “coat” the enzyme and preserve its quaternary structure and active sites during cross-linking reactions (Bolivar et al., 2009); (3) hydrogen bonds within the aggregates induced by PEI (Zhang et al., 2016).

Zheng et al. (2014) prepared CLEA of trehalose synthase from *Meiothermus ruber* (0.5mg protein/mL) via co-aggregation with PEI (75 kDa) and precipitation with PEG (8000 Da, 25% w/v), followed by cross-linking with glutaraldehyde (mass ratio of enzyme/glutaraldehyde = 1:0.5). The highest activity recovery (62.3%) and aggregation rate (97.5%) was obtained at1:0.8 enzyme to PEI mass ratio. Stable aggregates are produced at the optimum dose rate of PEI due to the balance of electrostatic forces between the positive charge of PEI and the negative charge of the enzyme. However, the addition of excessive amounts of PEI may introduce strong electronic repulsion, leading to re-dissolution of the CLEAs.

It should be noted that PEI addition may cause partial precipitation of enzymes before the precipitant is added, due to the formation of ionic bonds and also the electrical neutralisation of enzymes (Burgess, 2009). In this case, however, addition of a precipitant (such as PEG (Wilson et al., 2004; Lopez-Gallego et al., 2005) or acetone (Yan et al., 2012)) is still necessary to complete enzyme precipitation. Visual observation results from scanning electron microscopy (SEM) by Zheng et al. (2014) showed that CLEAs with both PEI and PEG were much smaller with a more uniform structure, compared to CLEAs with PEI only, which showed a more "bulky" appearance that can lead to mass-transfer limitations in reaction catalysis.

2.6.5.3 Surfactant

Use of surfactant addition is often reported for lipase cross-linking. For example, Lopez-Serrano et al. (2002) immobilised seven commercially available microbial lipases by glutaraldehyde cross-linking and $(NH_4)_2SO_4$ precipitation (55% saturation) and two additive surfactants (sodium dodecyl sulphate, an anionic surfactant, or TX100, a nonionic surfactant) were supplied at a dose rate of 25 mg/mL. Effectiveness of surfactant addition varied for the different enzymes. For example, hyperactivation of the immobilised enzymes (i.e. activity recovery > 100%) was observed with sodium dodecyl sulphate addition for *Candida antarctica* lipase A (162%), *Thermomyces lanuginosus* lipase (327%) and *Rhizomucor miehei* lipase (218%), or with TX100 for *C. antarctica* lipase A (240%) and *C. antarctica* lipase B (129%). However, in other cases, the surfactant generally reduced the activity of the CLEAs or inactivated lipase (e.g. TX100 added to *Thermomyces lanuginosus* lipase).

Gupta et al. (2009) immobilised lipase from *Thermomyces lanuginose* through $(NH_4)_2SO_4$ precipitation (60% saturation) followed by glutaraldehyde cross-linking (concentration not mentioned by the author, at 4 °C for 12-14 h), with different surfactant additions (including sodium dodecyl sulphate, TX100 and Tween-80, dosage = 100mg/5mL lipase). The activity recovery increased from 68.7% (without surfactant) to 137.0% and 78.2% with sodium dodecyl sulphate and Tween-80, respectively. TX100, on the other hand, partially inactivated the enzyme, and in this case the recovered activity decreased to 17.6%.

The mechanism of surfactant hyperactivation and/or inactivation of CLEAs can be explained by the special molecular structure of lipases (Lopez-Serrano et al., 2002; Fernandez-Lorente et al., 2006; De Rose et al., 2017; Henriques et al., 2018). Active sites of lipases are usually hydrophobic and only have high affinity for other hydrophobic substances. In aqueous medium, lipases adopt a closed conformation, and the active sites are isolated by a helical polypeptide chain that acts as a "lid". The "lid" can be displaced in the presence of a surfactant, which opens the enzyme conformation that can be fixed by the cross-linking reaction. As may be expected, hyperactivation could be observed due to increased exposure of the active sites to

the substrate in the solution. However, inactivation may also occur since exposed active sites have less protection from aggressive chemical species (e.g. glutaraldehyde).

2.6.5.4 Saccharides

The effect of glucose, sucrose and trehalose on CLEA preparations of *Penicillin G* acylase (156 U/mg) was examined by Wang et al. (2011). The initial enzyme solution was mixed with 20% w/v of the sugars followed by acetone precipitation and glutaraldehyde cross-linking (0.375% w/v, 2 h at 4 °C). The highest specific activity of the produced CLEA (123.7 U/mg) was obtained with acetone precipitation and trehalose addition, which achieved a recovery equivalent to 79.3% of the activity obtained for free enzyme, followed by glucose (71.3%) and sucrose (66.9%). The lowest activity recovery rate, equivalent to 54.4% of the free enzyme was obtained by cross-linking without sugar addition. Amaral-Fonseca et al. (2018) prepared magnetic CLEAs (to be discussed in Section 2.6.6.2) of *Aspergillus niger* amyloglucosidase by ethanol precipitation, with/without starch (1% w/v) co-precipitation, followed by glutaraldehyde cross-linking (500 mM, 16 h at 4 °C). The activity recovery rate (40%) obtained with starch addition was almost double that without starch.

The increased performance with saccharide addition was explained because (1) the saccharide molecules protect proteins from excessive dehydration during enzyme precipitation, thus preserving the conformation of the enzymes before cross-linking reactions (Wang et al., 2011), (2) saccharide molecules are abundant in hydroxyl groups, which can react with aldehyde groups of the cross-linker (Table 2-3), forming stable covalent cross-linkages (Mehde et al. (2018a), (3) significant degree of hydrogen bonding can form between these hydroxyl groups and other functional groups of the enzymes, further stabilising the produced CLEAs (Mehde et al., 2018a). Amaral-Fonseca et al. (2018) also indicated that the use of polysaccharides like starch during enzyme aggregation can facilitate formation of large pores of the CLEA, which may reduce mass-transfer limitation of the substrate and thus increase the catalytic efficiency of the CLEA.

However, in a study by Yu et al. (2013), where CLEA of mung bean epoxide hydrolases was prepared with 80% saturated $(NH_4)_2SO_4$ precipitation and 20mM glutaraldehyde cross-linking for 12 h at 4 °C, no significant improvement was obtained with sugar addition (data not shown by the author).

2.6.5.5 Metal ions

Metal ions can induce the formation of coordination bonds between immobilised enzymes, and enhance the stability of CLEAs compared to free soluble enzymes (Zhang et al., 2016). Torabizadeh et al. (2014) investigated the impact of calcium (Ca^{2+}) and sodium ion (Na^{+}) addition on CLEA of *Bacillus licheniformis* α-amylase (α-amylase is a metalloenzyme that

requires Ca^{2+} as a cofactor to stabilise the protein structure (Hsiu et al., 1964)). Dosing both cations at a Ca:Na ratio of 3:1 (final concentration = 1200 and 400 mg/L, respectively), approximately equivalent to the ratio of Ca^{2+}/Na^{+} naturally present in amylase, increased the specific activity of the CLEA from 1.95 (without cations) to 2.25 U/mg (which was similar to the activity of the free enzymes), under optimum preparation conditions (tert-butanol precipitation and 5 mM glutaraldehyde cross-linking overnight at 2-3 °C).

2.6.5.6 Others

Other additives, such as soil humates for cross-linking of glucosidase and carboxymethyl cellulase (Busto et al., 1997), soy protein for cross-linking of invertase (Mafra et al., 2018), and egg white as protein feeder for cross-linking of nitrile hydratase (Zhou et al., 2017b) are reported. However, these substances are less frequently used compared to the main types identified above and are therefore, not discussed further.

2.6.6 Recent innovations in enzyme immobilisation by cross-linking

2.6.6.1 Co-immobilisation of different types of enzymes in CLEAs

Co-immobilised enzymes can be identified as either multi-purpose CLEAs (multi-CLEAs) or combined CLEAs (combi-CLEAs). A multi-CLEA is a single aggregate that can catalyse unconnected reactions for multi-purposes in one application. Ozacar et al. (2019) produced a multi-CLEA of protease, lipase, and catalase from sunflower seeds, via $(NH_4)_2SO_4$ precipitation (55% w/v), glutaraldehyde cross-linking (100 mM, 17 h at 4 °C) and starch addition (8 mg/mL); the activity recovery of protease, catalase, and lipase in the multi-CLEA was 87, 61, and 60%, respectively. The multi-CLEA showed increased pH- and thermo-stability compared to free enzymes, and was used to improve the washing efficiency of a commercial detergent in removing food stains (mixed chocolate, coffee, yolk, oil, ketchup and chicken blood) from cotton. The stain removal (expressed as the difference in the absorbance at 518 nm wavelength of acetone extract before and after washing, relative to the absorbance before washing) was enhanced from 38% (without enzyme addition) to 83%.

Combi-CLEAs refer to co-aggregated enzymes for multi-step cascade reaction systems. Here, the product or by-products of the first enzymatic reaction act as a substrate for the second reaction, providing a continuous catalysis process towards a target compound (Henriques et al., 2018). Talekar et al. (2013) prepared a combi-CLEA from a commercially available mixture of glucoamylase and pullulanase, via $(NH_4)_2SO_4$ precipitation (saturated) followed by glutaraldehyde cross-linking (2% v/v, 8 h at 30 °C). The produced combi-CLEA showed a nearly 100% conversion rate of starch (10 mg/mL) into glucose after 180 min incubation at 65 °C, with enzyme dosage = 45 U for glucoamylase and 15 U for pullulanase; whereas only 80 and 30% conversion was obtained by dosing mixture of separate CLEAs and free enzymes under equivalent conditions.

Dal Magro et al. (2016) produced a combi-CLEA from a commercial enzyme mixture (containing various enzymes including pectinase, polygalacturonase, pectin lyase, pectin methyl esterase and cellulase), for depectinisation of fruit juice to produce a clear final product. Optimal cross-linking conditions were: isopropanol precipitation, 110 mM glutaraldehyde cross-linking at room temperature at 4 °C, with 2.4 mg/mL BSA addition. The combi-CLEA showed a depectinisation activity of 14 U/mL, which was smaller and equivalent to 18% of the free enzyme activity. The low enzyme activity recovery to free enzyme was probably explained because the pores inside the CLEA particles were relatively small compared to pectin, which is a macromolecule. Therefore, accessibility of the substrate to enzyme active sites was reduced; furthermore, glutaraldehyde may also have had a detrimental impact on the enzyme essential functional groups. The CLEA improved the grape juice clarification process and reduced the turbidity by 56.7% compared to free enzymes, which achieved a 47.9% reduction in turbidity at the same enzyme dosage rate (5 U/mL). The improved clarification efficiency was attributed to the relatively high pH and thermo-stability of the combi-CLEA. The presence of other enzymes in the vicinity of the first enzyme was also a suggested as a possible mechanism, which may facilitate the substrate transfer among the enzymes, resulting in improved efficiency of the cascade reactions.

2.6.6.2 Magnetic CLEAs

Magnetic CLEAs are prepared by co-precipitation of enzymes with ferrosoferric oxide (Fe_3O_4) magnetic nanoparticles (MNPs), followed by the cross-linking reaction. One of the advantages of magnetic CLEAs over standard CLEA preparation is that separation of the biocatalysts from the reaction system is possible by simply applying an external magnetic field. Separation of standard CLEAs is usually by centrifugation or filtration which can cause unwanted clustering of the enzyme aggregates and increase mass transfer limitations (Schoevaart et al., 2004).

Surface modification, to introduce a large number of biocompatible reactive groups (shown in Table 2-3, e.g. aldehyde, hydroxyl and amines) onto the MNPs, is an essential step in the CLEA preparation. This increases the “protein retention capacity”, and facilitates cross-linking with biomolecules such as proteins/enzymes (Reza et al., 2010). Furthermore, the coating can effectively shelter the magnetic dipole interaction between adjacent particles, avoiding formation of large MNP clusters (Khosroshahi and Ghazanfari, 2010; Mehde et al., 2018a). Organic materials, such as 3-aminopropyltriethoxysilane (an aminosilane containing a -NH_2 group) (Nadar and Rathod, 2016) and tannic acid (a polyphenol extracted from plants) (Mehde et al., 2018b) have been reported as effective coatings for magnetic CLEA preparation.

Talekar et al. (2012) prepared a magnetic CLEA of α-amylase by cross-linking the enzyme with aminosilane-functionalised MNPs, using saturate $(NH_4)_2SO_4$ as the precipitant and glutaraldehyde (40 mM) as the cross-linker (3 h cross-linking at 4 °C). The enzyme activity of

the magnetic CLEA was equivalent to almost 100% of free amylase. By contrast, the activity after CLEA prepared without aminated MNPs was reduced to 45% of the free enzyme. Furthermore, the magnetic CLEA showed higher reusability compared to standard CLEAs and no activity was lost after six cycles of reuse of the magnetic CLEAs, whereas a 75% loss of activity was observed for the conventional CLEA under equivalent condition. This was explained because the surface amine groups in α-amylase were not sufficient for efficient cross-linking of all enzyme molecules in the standard CLEA preparation. However, the addition of aminated MNPs provided adequate functional groups for cross-linking, to produce CLEAs of high operational stability and reduce enzyme release from the aggregates.

Amaral-Fonseca et al. (2018) used aminosilane-functionalised MNPs to produce a magnetic CLEA of *Aspergillus niger* amyloglucosidase (an enzyme with a low content of surface lysine groups, commonly used in industrial starch saccharification for hydrolysing maltodextrins, amylose, and amylopectins to produce glucose syrup). The magnetic CLEA was prepared by precipitation with 90% v/v ethanol, 300 mM glutaraldehyde cross-linking for 16 h at 4 °C and 1% w/v starch addition and exhibited more than 40% of the original free enzyme activity. A standard CLEA was also prepared by replacing the MNPs with 20 mg/mL BSA, which also gave a similar activity recovery rate (36%) under equivalent conditions. The BSA-CLEA, magnetic CLEA and free enzymes were evaluated for the hydrolysis of amylase-pretreated starch (3% w/v) at 55 °C and pH 4.5 under 300 rpm stirring and a starch-to-glucose conversion of >95% after 6 h was found in all cases. However, the efficient separation and handling of the magnetic CLEAs was a potential advantage for large-scale industrial application compared to other immobilised enzyme formulations.

Mehde et al. (2018b) synthesised a magnetic CLEA of *Candida antarctica* lipase B using tannic acid modified MNPs and, under the optimum preparation conditions (50% saturation $(NH_4)_2SO_4$ precipitation followed by 100 mM glutaraldehyde cross-linking for 17 h at 4 °C, with 8 mg/mL starch addition), the CLEA retained 98.5% of the free enzyme activity. The CLEA showed higher tolerance to organic solvents compared to free enzymes and catalysed the transesterification of sunflower oil (mixed with 2-propanol in a ratio of 1:6) to biodiesel at a conversion rate equivalent to 85.9% compared to 42.8% for free enzymes.

2.6.6.3 Post stabilisation of CLEAs by carrier bound immobilisation

Carrier bound immobilisation has been reported as technique for the post stabilisation of CLEAs. For example, Zeinali and Lenjannezhadian (2018) produced CLEA of urease, via $(NH_4)_2SO_4$ precipitation (80% saturation) followed by 7 mM glutaraldehyde cross-linking for 4 h at 4 °C with 20% w/v trahalose additive. The carrier-free immobilised enzyme was further entrapped into an 8% polyacrylamide gel. Entrapped CLEAs showed higher operational stability under extreme conditions compared to conventional CLEA preparation. For example,

the optimum temperature and pH for the standard CLEA was 60 °C and pH 7 compared to 70 °C and pH 5 with entrapment. Moreover, the reusability of entrapped CLEAs was much higher than the conventional form and approximately 90% of the initial activity was obtained after 15 cycles of reuse at 50 °C, compared to the activity of the standard CLEA which decreased markedly by 75% after eight cycles of reuse under equivalent conditions. The improved performance achieved by CLEA entrapment in polyacrylamide gel was explained because leaching of enzymes into the reaction media was prevented. Furthermore, the separation and regeneration of the biocatalyst in the reaction system was simplified, providing economic advantages for the industrial scale urea degradation process.

2.7 Potential application of recovered enzymes from activated sludge

2.7.1 Wastewater treatment

Jung et al. (2002) extracted compound enzymes from laboratory-cultured AS by milling disruption of sludge flocs and ammonium sulphate precipitation, followed by re-suspension. The compound enzyme product (containing protease at 5.4 U/ml) was mixed with an artificial milk wastewater at a volume ratio of 1:1, and rapidly hydrolysed the protein content within 2 h, releasing the degradation product, tyrosine (a main constituent amino acid of milk protein), at a yield of 103 μg/mg protein. The results therefore demonstrated the potential application of AS enzymes for the treatment of waste streams high in protein and lipid content, such as diary wastewater.

Damasceno et al. (2008) dosed crude, solid, lipase-rich compound enzymes, obtained from the solid-state fermentation of agro-industrial wastes by *Penicillium restrictum*, into a wastewater reactor treating an artificial, high-fat dairy wastewater (with 1200 mg oil and grease per L) and found the removals of both chemical oxygen demand (COD) and turbidity were improved. Dosing the enzyme at a rate of 0.1% w/v increased the overall COD removal from 83% (in the control) to 90%, and the effluent turbidity decreased by 50% compared to the control, without enzyme dosing.

Mackul'ak et al. (2016) applied an enzymatic pretreatment unit (using a commercial mixture of various redox enzymes, transferases and hydrolases, with an enzyme activity equivalent to 4881 U/mL, dosed at 2 mg/L, and a treatment duration of 60 min) to an industrial paintshop wastewater with a high content of organic nitrogen (COD = 5100 mg/L, total nitrogen = 184 mg/L), followed by a 24 h lab-scale AS process. The COD and total nitrogen content of the treated wastewater decreased to 200 and 20 mg/L, respectively, compared to 840 and 45 mg/L, respectively, for the control without enzymatic pretreatment.

Mobarak-Qamsari et al. (2012) obtained a crude enzyme extract from *Pseudomonas aeruginosa* KM110 (a bacterium strain isolated from wastewater collected from an oil

processing plant), with lipase activity = 0.3 U/mL. The enzyme extract was applied as a hydrolysis pretreatment to synthetic dairy wastewater (dose rate = 10% v/v and incubation at 45°C for 48 h), followed by anaerobic wastewater treatment (37°C, retention time = 13 days). Enzymatic prehydrolysis significantly increased the COD removal and biogas output by approximately 1.5 and 2 times, to 90% and 4710 mL/L wastewater, respectively, compared to the control.

2.7.2 Pre-treatment of waste for anaerobic digestion

Anaerobic digestion is the preferred treatment method for a wide variety of municipal, industrial and agricultural organic waste materials, and particularly those with high moisture contents, as it is effective at stabilising organic matter, reducing odour nuisance and potential human pathogens, and produces a biogas rich in methane that is a valuable renewable energy source (Smith, 2014; Lohri et al., 2017). However, the initial hydrolysis step of AD is often rate-limiting to the treatment of complex organic substrates, such as sewage sludge (Donoso-Bravo et al., 2009; Lindeboom et al., 2014). Enzymatic pretreatment of sewage sludge can enhance the anaerobic digestibility by increasing lysis of microbial cells and the release of protein and carbohydrate substrates from sludge flocs, and also by accelerating the biodegradation of recalcitrant materials, such as humic and fulvic acid-like substances (Chen et al., 2018).

Arun and Sivashanmugam (2015) used a crude compound enzyme extract from the fermentation of fruit peel waste (pineapple and orange) to solubilise the polymeric organic compounds in waste AS. The sludge was incubated with enzymes at 35 °C and pH 7 for 60 h and the VS reduction and COD solubilisation following enzymatic treatment were approximately 22% and 25%, respectively, compared to 5% and 6%, respectively, for the control treatment (without enzyme addition).

Yin et al. (2016) applied a fungal mash (rich in hydrolytic enzymes) to pretreat AS, mixed with food waste, prior to AD. The pretreatment produced a soluble COD equivalent to 7.65 g/L within 24 h, which was approximately 1.7 times larger compared to the control, and the biomethane yield from AD of pretreated sludge increased 2.5 times compared to AS without pretreatment.

Bonilla et al. (2018) pretreated pulp and paper biosludge with protease extracted from *Bacillus licheniformis* (ratio of protein/biosludge DS, 1:100) for AD and measured the effects on the biogas yield. The pretreatment enhanced the anaerobic digestibility of the sludge, increasing the specific biogas yield (measured in a 62-day biomethane potential test) by up to 26% to approximately 160 mL/g COD compared to the control supplied with inactivated enzyme, which produced approximately 130 mL/g COD of biogas.

Bahreini et al. (2020) dosed a commercial enzyme product (containing cellulase and xylanase, with 20% active protein content) into primary sludge at a rate of 1% of the DS in the feed, prior to fermentation at 35°C for 2 days. The specific soluble COD and volatile fatty acid (VFA) yields during the fermentation process were 316 mg/g VS and 201 mg COD/g VS, respectively, for the control group, and increased with enzymatic treatment by 68% and 35% to 532 mg/g VS and 272 mg COD/g VS, respectively.

2.7.3 Organic micropollutant degradation

Compound enzymes extracted from AS can also significantly improve the biodegradation of organic micropollutants in municipal wastewater treatment. For example, crude, cell-free compound enzymes from AS degraded the pharmaceutical compounds: acetaminophen (an analgesic), N-acetyl-sulfamethoxazole (an antibiotic), atenolol (a beta blocker) and bezafibrate (a lipid-lowering agent), with average removal efficiencies of 85, 59, 26 and 20%, respectively, compared to the control with heat deactivated enzymes, which showed no removal (Krah et al., 2016). The majority of enzymes involved in the degradation of organic pollutants are hydrolytic (e.g. phosphatase, galactosidase and glucuronidase), and these are abundant in AS, but, other, minor non-hydrolase enzymes, such as oxidoreductase, have a strong and critical influence on pollutant destruction and may also be extracted, or inducible, in AS (Krah et al., 2016) (see Section 2.2.1 and 2.4.4.2).

Zhou et al. (2017a) investigated the effects of enzyme addition on the removal of four pharmaceutically active compounds during sewage sludge AD. The pharmaceutical compounds included: clofibric acid (a lipid regulating agent), triclosan (a broad-spectrum antibacterial agent), diclofenac (an anti-inflammatory painkiller) and carbamazepine (an epilepsy drug) and each compound was added to raw sewage sludge at a concentration of 5 µg/L. Different enzymes were mixed with sludge, including: papain (a proteolytic enzyme extracted from the papaya plant), lysozymes or cellulase, at dose rates of 30 mg/g DS, prior to mesophilic AD (35 ± 2°C and solids retention time = 15 days). The effects of enzyme dosing on the removal rates of the target pharmaceuticals varied depending on the type of enzyme and the specific compound type. In general, triclosan and carbamazepine were the most susceptible to enzymatic degradation, and cellulase was the least effective enzyme at organic micropollutant removal. Dosing with papain and lysozymes increased the removal of triclosan to 60 and 82%, respectively, compared to 50% for the control treatment, and carbamazepine removal increased from 51% in the control to 64 and 58% by papain and cellulase addition, respectively. However, enzymatic treatment had no positive effect on the concentrations of clofibric acid or diclofenac and the largest removals of these compounds obtained with lysozyme dosing were 53% and 58%, respectively, compared to 61% and 60%, respectively, in the control condition). Sonication treatment of the sludge (20 kHz, power density at 0.05

W/mL for 30 min) significantly improved contaminant removal, by increasing the accessibility and biodegradation of organic pollutants by AD.

Therefore, Zhou et al. (2018b) proposed an integrated AD system, comprising of both hydrolytic enzyme dosing and pretreatment with ultrasound. Lysozymes and papain, which gave the best overall removal performance in the previous study, were mixed at a mass ratio of 1:1 and added to sludge at a rate of 30 mg/g DS prior to sonication and mesophilic AD (solids retention time = 15 days). In this case, the micropollutants were dosed into the sludge at a higher rate equivalent to 7.5 µg/L. Enzyme dosing also showed variable effects in the integrated system, however, a comparison with sonication without enzyme addition was not possible because this treatment was not included in the experimental design. Nonetheless, comparison with the earlier results (Zhou et al., 2017a) suggested the degradation of clofibric acid and carbamazepine was increased to 77 and 68%, respectively, with combined enzyme dosing and sonication, compared to ultrasound alone (68 and 63%, respectively (Zhou et al., 2017a)). On the same basis, there was little or no change in the removal of triclosan in the integrated system (69%), compared to sonication alone (73% (Zhou et al., 2017a)), and diclofenac degradation declined with enzyme dosing to 47% compared to 72% with ultrasound alone (Zhou et al., 2017a). Increasing the digestion temperature of the integrated system to the thermophilic range (55 ± 2°C), had no effect on diclofenac degradation (48%) compared to mesophilic conditions (47%), but removals of the other compounds decreased (71, 65 and 51% for clofibric acid, triclosan and carbamazepine, respectively) relative to mesophilic temperatures (Zhou et al., 2018b). Thus, enzyme dosing had variable effects on the degradability of pharmaceutical compounds during AD of sewage sludge and this may be explained because: (1) enzymes demonstrate a high degree of specificity at cleaving chemical bonds of available substrates (Hoppe et al., 1983) (see Section 2.2), (2) free enzymes may be vulnerable to and be inactivated by the AD environment, and (3) ultrasound exposure may damage the enzyme structure at thermophilic temperatures, causing the breakage of essential bonds at active sites (e.g. the disulfide bonds of lysozyme (Mañas et al., 2006)).

Thus, specific enzymes may be required to degrade particular, unique contaminant compounds, and general hydrolytic enzymes, similar to those supplied by Zhou et al. (Zhou et al., 2017a; Zhou et al., 2018b), may not be effective at removing all types of organic pollutant. Thus, the general hydrolytic enzymes extracted from AS will have variable effects on degrading a broad range of organic contaminants, but specific inducible enzymes can also be expressed to target the degradation of particular micropollutant compounds (Section 2.4.4.2). The sensitivity of free enzymes to treatment process conditions can also be reduced to enhance the longevity of activity by preparing stabilised/immobilised formulations (Section

2.5.2). Furthermore, the operational conditions (including temperature and reaction time) need to be optimised to facilitate the enzymatic hydrolysis treatment of organic micropollutants.

2.7.4 Biofuel production

Selvakumar and Sivashanmugam (2019) produced lipase from the anaerobic fermentation of organic waste, including: pomegranate, orange and pineapple fruit peels, followed by ammonium sulphate precipitation of the crude enzyme solution. The partially purified lipase (56.5 U/mL) was used as the catalyst for biodiesel production from yeast lipid. Under optimum conditions for lipase-catalysed transesterification (6.4 methanol/oil molar ratio, 20% enzyme concentration, 35 °C and 16 h treatment time), 97 % of the original lipid source was transformed into biodiesel.

2.7.5 Other applications

In addition to the cases mentioned above, recovered compound enzymes from secondary materials, such as AS, have potential applications in many other areas, for example:

- Leather industry

Abu Yazid et al. (2016) produced alkaline protease from the fermentation of hair waste, followed by partial purification of the crude enzyme solution using ultrafiltration and lyophilisation techniques. The effectiveness of the lyophilised enzymes at dehairing high pigmentation cowhides was examined by incubating sections of the cowhide with the enzyme for 24 h, supplied at dose rates of 7556 to 9373 U per cm^2. The performance of enzymatic dehairing was similar to a standard chemical treatment (22 h soaking with sodium carbonate and a non-ionic surfactant for 22 h, followed by reaction with calcium hydroxide for 1 h and sodium hydrosulphide for 30 min) with a relative effectiveness of 90-95% compared to the chemical method. This study emphasised the significant potential of using enzymatic treatments as alternatives to chemical dehairing in the leather industry.

- Detergent additives

Purified proteases, amylases, lipase and cellulase are used as biodegradable, non-toxic additives to detergents to improve the effectiveness of stain removal from fabrics, without damaging the textile quality (Hasan et al., 2010; Niyonzima, 2019). A major advantage of using enzymes in bulk detergent formulations is that they do not have harmful residues and, therefore, the environmental loading of synthetic chemicals from large scale detergent use is reduced (Hasan et al., 2010).

Zhang et al. (2014b) investigated the washing performance of several phosphate and non-phosphate detergents that were reformulated by adding alkali protease (280 U/mg) and/or amylase (300 U/mg). They found that the efficiency of stain removal was marginally increased with the addition of mixed enzymes compared to single enzymes, probably due to a synergistic

reaction between protease and amylase. For example, the stain removal from a polyester/cotton fabric soiled with blood, milk and ink was 28% for protease addition (0.5% w/w) alone and this increased to 32% for the combined enzymatic treatment (protease: amylase = 1:1, 0.5% w/w dosage for each enzyme).

Some microorganisms in sludge are naturally able to produce enzymes that can remain active under the harsh conditions that are usually applied during detergent use (such as high temperature, alkaline pH and high salt concentration (Thebti et al., 2016)). For example, El Hadj-Ali et al. (2007) found that a thermostable, alkaline serine-protease, produced by a bacterium isolated from fishery sewage sludge (identified as *Bacillus licheniformis* NH1), could maintain 93% of its initial activity after incubation at 40 °C for 60 min in the presence of commercial laundry detergents (7 mg/mL). This suggested that the protease derived from secondary waste biomass may be suitable as an effective enzyme additive in detergent manufacture. Stabilised enzymes (mentioned in Section 2.5.2) may also be suitable for use in detergent formulation. For example, Soleimani et al. (2012) formulated a detergent powder containing 0.1% of α-amylase, either as free enzyme or in immobilised form on silica nanoparticles, and examined the effect on the removal of starch stains from cotton fabrics, compared to the same formulation, but without enzyme addition. The presence of immobilised or free α-amylase increased the cleaning efficiency (measured as the difference in the reflectance light intensity (%) between washed and unwashed fabric, at a wavelength of 460 nm) by approximately 2.3 and 1.5 times, respectively, compared to the control.

- Animal feed

Increasing the digestibility and nutritional value of animal feeds (e.g. for pig and poultry production) is an area of expanding interest for the utilisation and application of compound enzymes (BCC Research, 2018). The digestive systems of pigs and poultry tend to lack certain important enzymes that are necessary to break down complex organic substrates (such as barley, rye and oats) (Ojha et al., 2019). The use of endolytic enzymes as supplementary ingredients in animal feed formulations can effectively degrade cell wall polysaccharides in the feed and reduce the viscosity of the intestinal contents, resulting in improved digestion, absorption and nutritive value of feed stuffs (Campbell and Bedford, 1992; Brufau et al., 2006).

Kalmendal and Tauson (2012) investigated the effect of mixed xylanase and protease (alone and/or in combination) supplied to broiler chickens fed a wheat-soybean meal-based diet. The digestibility coefficients of starch and fat were enhanced with enzyme addition, from 93.1 to 97.3% and 89.3 to 92.5%, respectively, and the retention of crude protein was also improved from 59.7 to 64.3%. Woyengo et al. (2018) fed pigs with a corn-soybean based diet, supplemented with a compound enzyme product (with 4000 U of xylanase, 150 U of β-

glucanase and 3000 U of protease per kg of diet). The digestibility of “acid detergent fibre” and “neutral detergent fibre” (which are indicators of structural carbohydrate components such as the cell wall fraction of the feed) was improved by 21.1 and 42.0%, respectively, compared to the control group without enzyme supplementation. The feed conversion ratio of the pigs (measured as gained body mass to feed mass ratio, G:F) also increased by 6.64% for the enzyme treated diet. Similar results were reported by Zhang et al. (2014a) using a commercial multi-enzyme product (containing amylase, protease and xylanase) as a dietary supplementation for a corn-soybean based feed supplied to 35 to 65 day old piglets. It was found that the nutrient digestibility was improved and the G:F ratio increased from 0.59 (in the control group) to 0.65 by the addition of the multi-enzyme product to the diet at a rate of 350 mg/kg. Although the numerical increases in feed digestibility with enzyme addition reported in the literature appear relatively modest, they are considered to provide significant benefits in terms of the uptake and utilisation of dietary nutrients by animals (Montoya-Mejía et al., 2016).

The use of AS-recovered enzymes as animal feed additives has not yet been advocated, but is a technically feasible application for compound enzyme products derived from secondary resources. The potential adoption in feed manufacture would require the development of highly refined compound enzymes and would be subject to animal feed quality regulations to ensure livestock safety and to also protect the human food chain (European Parliament and Council of the European Union, 2003).

2.8 Secondary benefits of enzyme recovery from activated sludge

Physical disruption of AS for enzyme recovery has several important secondary benefits for the subsequent treatment, management and utilisation of the residual sludge. The large amount of EPS in AS has a major influence on the sludge properties and LB-EPS, in particular, is responsible for the high content of bound water in sludge flocs, which reduces the compressibility and dewaterability of sludge (Li and Yang, 2007). Enzyme recovery is accompanied by sludge floc disruption, and EPS removal from microbial cells reduces the bound water content in the disrupted sludge, improving the overall settlement and dewaterability characteristics (Atay and Akbal, 2016; Iritani et al., 2016). Physical disruption of sludge flocs also increases organic matter solubilisation and anaerobic digestibility (Salsabil et al., 2009b). Martin et al. (2015) showed that sonication treatment of mixed, and dehydrated, primary and secondary sludge prior to AD (carried out in an ultrasonic water bath with 150 W power input for 45 min at 25 °C) almost doubled the specific biogas yield from 88 L/kg VS for the control (without pretreatment) to 172 L/kg VS. Similarly, Chatterjee et al. (2019) found the methane production of septic tank sludge increased from 299 L/kg VS destroyed (specific methane yield: 224 L/kg VS) in the control to 410 L/kg VS destroyed (specific methane yield:

337 L/kg VS) after sonication pretreatment (ultrasound frequency of 20 kHz at a power of 100 W for 5 min).

The disrupted sludge after enzyme extraction may also open other opportunities for resource recovery. For example, the AS residue contains a large fraction of cytoskeletal macromolecules and Ni et al. (2017) proposed that this was suitable as a raw material for the production of superabsorbent polymers.

3 General materials and methods

3.1 Materials

Commercial pure enzymes were purchased from Sigma-Aldrich, including protease from *Aspergillus melleus* (product No. P4032, activity ⩾3 U/mg solid), lipase from *Candida rugosa* (product No. 62316, activity ⩾2 U/mg solid), α-amylase from *Aspergillus oryzae* (product No. 86250, activity up to 1.5 U/mg solid), cellulase from *Aspergillus niger* (product No. 22178, activity up to 0.8 U/mg solid) and dehydrogenase from rabbit muscle (product No. L2500, activity = 800-1,200 U/mg protein).

Other chemicals were all reagent grade and purchased from various commercial sources.

3.2 Sludge sample collection

Sludge samples were collected from two major WWTPs in the UK, WWTP1 and WWTP2, with treatment capacities of 180,000 m^3/day and 53,000 m^3/day, respectively:

WWTP1 operated a standard AS process: the settled sewage after primary clarification was subjected to biological treatment comprising an aerated, plug flow reactor, followed by secondary sedimentation. Waste activated sludge (WAS) samples were collected from the thickening belts after flocculant dosing (Flopam, 0.24% w/w active) (Figure 3-1).

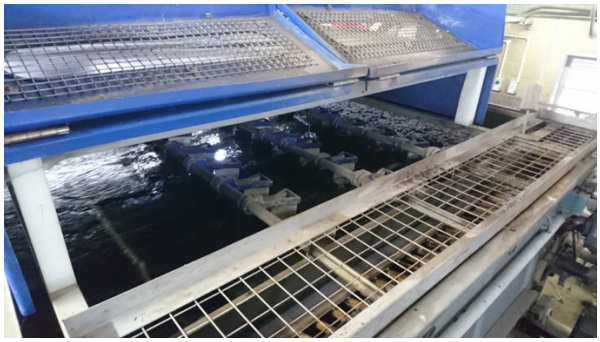

Figure 3-1 Waste activated sludge sampling from sludge thickening belt in WWTP1

WWTP2 treated the settled sewage with a biological nutrient removal (BNR) process, comprising anaerobic, anoxic and aerobic zones. Mixed liquor (ML) samples were collected directly at five equidistant positions along the aeration tank, which is a plug flow reactor (Figure 3-2). The mixed liquor suspended solids (MLSS) concentration at WWTP2 was typically in the range of 3,800-4,300 mg/L. The ML samples were collected with a bucket and dosed with polyacrylamide (Flopam, 0.24% w/w active) at a rate of 200 ml/20 L. The mixture was filtered after 30 minutes through a strainer bag and the flocculated sludge was collected (Figure 3-3). A WAS sample was also collected from the thickening belt, after polymer dosing.

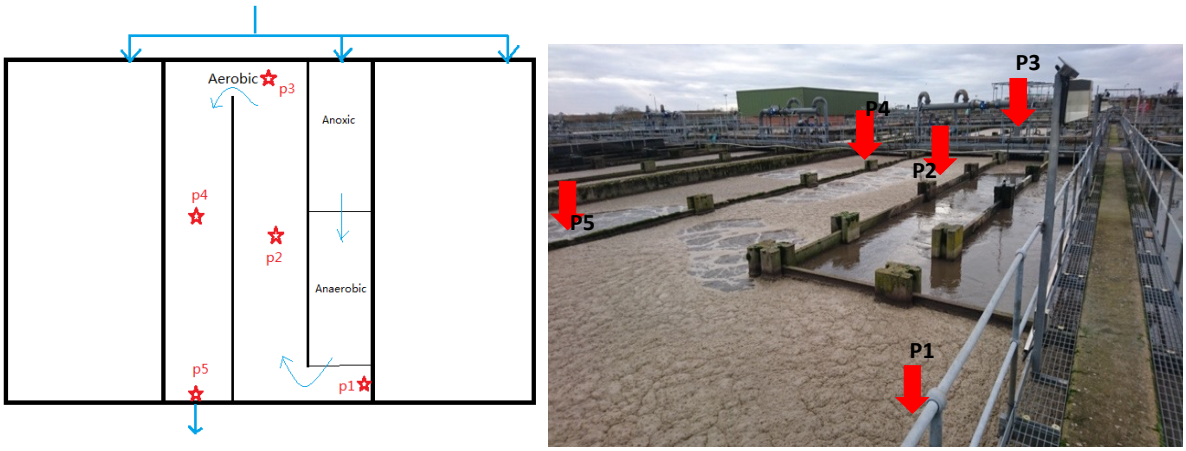

Figure 3-2 Five sampling points (P1-5) of mixed liquor along the aeration tank in WWTP2

Figure 3-3 Sampling mixed liquor and dosing Flopam on-site

Sludge samples were collected in 500 mL HDPE bottles (with a lid, air-tight, Figure 3-4) and transported to the lab in a portable insulated cool box (24 L, containing ice packs) on the day of collection and were stored in a fridge overnight at 4 °C. Enzyme extractions and other assays were performed the following day unless otherwise specified.

(a) (b)

Figure 3-4 (a) Wasted activated sludge sample from sludge thickening belt; (b) mixed liquor sample from aerated tank

3.3 Sludge characterisation

3.3.1 pH

Sludge samples were placed on a magnetic stirrer, mixed thoroughly but gently and the pH value was measured by a pH meter (Fisherbrand Hydrus 500 pH meter with HI01230 pH electrode probe) according to standard method (APHA, 2017b). For sludge with more than 99% water content, the pH electrode was placed directly into the sample for at least 30 seconds before the recoding the reading. For thickened sludge, the sludge was centrifuged at 2000 g for 15 min (Sorvall RC6 Centrifuge) and the supernatant was collected for pH measurement, following the same approach.

3.3.2 Total solids & volatile solids

The total solids (TS) and volatile solids (VS) of the sludge samples were measured according to standard methods (APHA, 2017a). A clean evaporation dish was ignited at 550°C for 1 h in a muffle furnace and cooled in a desiccator, charged with fresh silica gel dehydrant. The dish was weighed and stored in the desiccator until ready for use.

Sample were homogenised by continuous stirring and 5 to 10 g was placed in the prepared evaporation dish and weighed. The sample was subjected to evaporation in a drying oven at 103 to 105 °C for 1 h, followed by cooling to room temperature in an individual desiccator containing fresh desiccant, and was weighed. This procedure was repeated until the weight change was less than 4% or 50 mg, whichever was the smaller value.

The dried residue was transferred to a muffle furnace and ignited at 550 °C for 1 h, and the residue was cooled in a desiccator to ambient temperature and weighed. This procedure was also repeated using the equivalent criteria to TS determination.

The TS content was calculated as:

$$TS\ mg/L = \frac{(A-B)\times 1000}{Sample\ volume,mL} \quad \text{(Eq 3-1)}$$

Where,

A is the total weight of the evaporation dish and the oven-dried residue (mg); *B* is the weight of the ignited evaporation dish (mg).

The VS content was calculated as:

$$VS\ mg/L = \frac{(C-D)\times 1000}{sample\ volume,mL} \quad \text{(Eq 3-2)}$$

Where,

C is the total weight of the evaporation dish and the oven-dried residue before ignition (mg); *D* is the total weight of evaporation dish and the oven-dried residue after ignition (mg).

3.4 General enzyme extraction and recovery procedures

The protocol for enzyme extraction and recovery from AS is illustrated in Figure 3-5. The sludge was centrifuged at 2000 g for 15 min to remove excess water content, and the sediment was washed with 10mM Tris-HCl (pH 7.0) buffer and centrifuged again at 5,000 g for 15 min. The sediment was collected and re-suspended in 10 mM Tris-HCl buffer (pH 7.0) to its original volume. The suspension was diluted with buffer and subjected to a cell disruption process for a certain time period (as prescribed by the experimental design – see Chapter 4), after which the suspension was shaken at 120 rpm for 45 min and centrifuged at 12000 g for 15 min. To prevent warming of the samples and to preserve biological activity in the extract, the process of cell disruption, centrifugation and washing of the sludge were carried out at 4°C in an ice-water bath.

The supernatant C was collected as crude enzyme extract, which was subjected to consolidation and stabilization procedures (to be discussed in Chapter 5). The recovered enzyme product was applied to accelerate hydrolysis of wasted biomass and/or organic substrate (to be discussed in Chapter 6). Collected AS samples were stored in a fridge (at 4°C) and further assays (described in Section 3.5 and 3.6) were performed the following day unless otherwise specified.

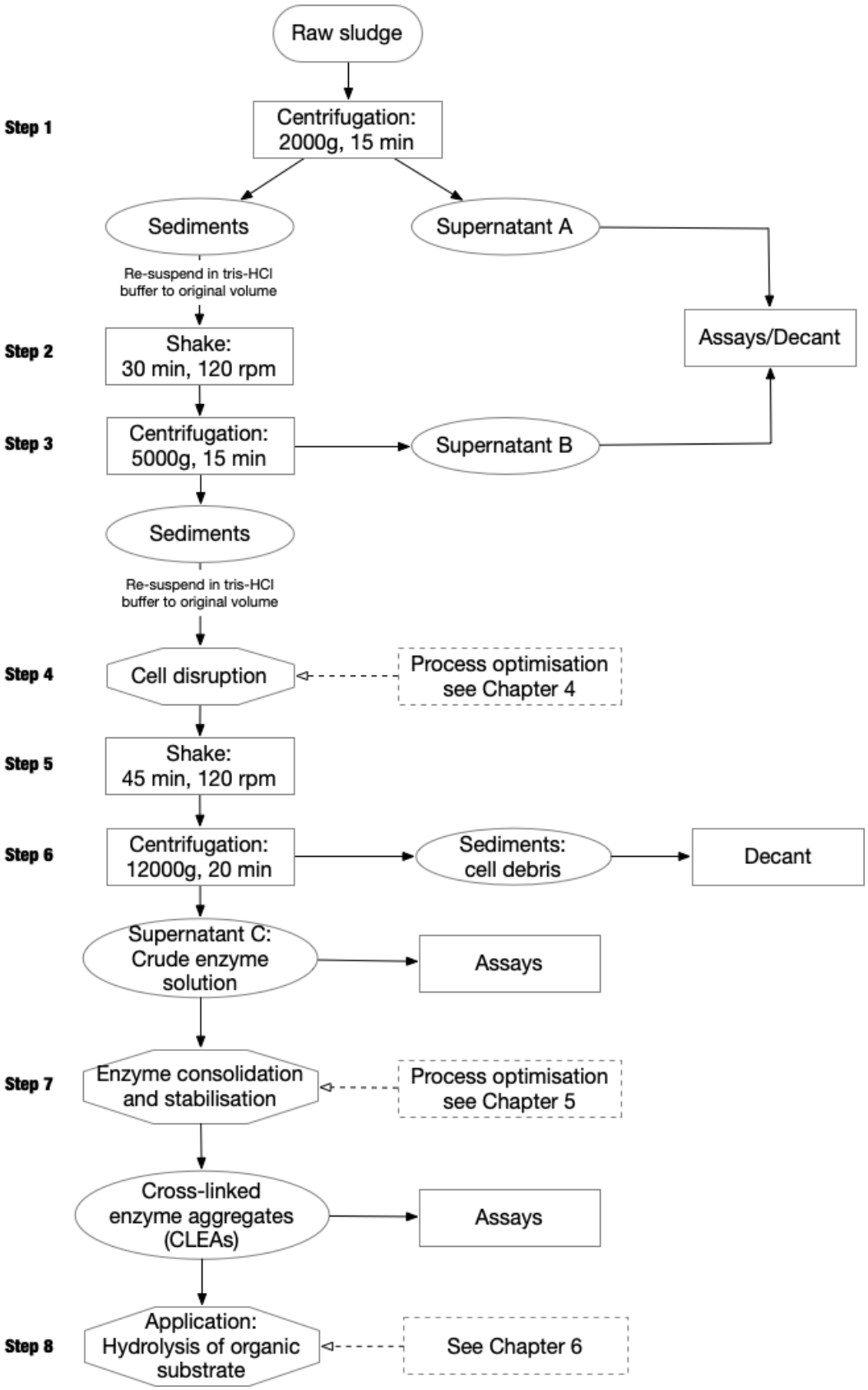

Figure 3-5 General procedures of enzyme extraction and recovery

3.5 Indicators of cell disruption

3.5.1 Protein

The Lowry method (Lowry et al., 1951) has been widely used for quantifying protein contents of biological samples (Winters and Minchin, 2005) and was selected in this study, due to: (1) sensitivity to low protein concentrations (0.01 mg protein/mL (Waterborg, 2009)), (2) specific reactivity towards tryptophan and tyrosine, which show little variation in AS microbial proteins (0.66-1.02% and 2.1-2.4% for tryptophan and tyrosine, respectively (Vriens et al., 1989)). However, the conventional method (Lowry et al., 1951) is susceptible to interference from external phenolic compounds (co-extracted from sludge matrix) and Tris buffer added to the samples (Potty, 1969; Rej and Richards, 1974), leading to over-estimation of the protein content. Thus, a modified method was used to measure the protein content of crude enzyme extracts following the procedure of Potty (1969), using BSA as the standard, to minimise potential interferences. The assay was performed by adding 5 mL of Reagent C, which was prepared fresh before use by mixing solution A (containing 20 g/L Na_2CO_3, 4 g/L NaOH and 0.5 g/L Rochelle salt) and solution B (5 g/L $CuSO_4 \cdot 5H_2O$) at a volume ratio equivalent to 50:1, to 1 mL of activated sludge extract (see Chapter 4). After mixing in a vortex and standing for 10 min at room temperature, 0.5 mL of Folin & Ciocalteu's Phenol Reagent (Sigma-Aldrich, diluted to 1 N (equivalent to 0.67 mol/L) before use) was added. The absorbance at 660 nm (Abs_{660}) of the samples was measured using a UV-Vis spectrophotometer (UV-2401PC, Shimadzu Corporation, UK) after 30 min. The calibration curve of protein content against Abs_{660} values was in the range from 50 to 250 µg BSA/mL ($y= 0.0024x$, $R^2 > 0.99$), with the standard BSA dissolved in 10 mM Tris-HCl (pH 7.0) buffer.

3.5.2 Deoxyribonucleic acid

The deoxyribonucleic acid (DNA) content provides an indicator of sludge floc disruption and the release of cellular substances, and was quantified by the diphenylamine method (Li et al., 2014) with minor modification. The assay was performed by adding 4 mL of freshly prepared diphenylamine reagent (aqueous acetaldehyde solution, 16 mg/mL) and solution D (1.5% diphenylamine, dissolved in acetic acid, with 1.5% w/v concentrated H_2SO_4 addition) combined at a volume ratio of 1:200), to 2 mL of sample. The mixture was heated to boiling temperature in a water bath for 15 min. The sample was cooled to room temperature and the absorbance at 595 nm (Abs_{595}) was measured against a blank. The calibration curve of DNA content against Abs_{595} values was in the range 40-200 µg/mL, using salmon sperm DNA as standard ($y = 0.0011x$, $R^2 > 0.99$).

3.6 Enzyme activity assays

3.6.1 Protease activity

Protease activity was measured using the Lowry method described by Nabarlatz et al. (2010) with casein as the substrate. Casein solution (3 mL of 0.65% w/v prepared in 50mM phosphate buffer, pH 7.5) was mixed with 1 mL of the enzyme solution and incubated for 10 min at 37 °C; 3 mL of 110 mM trichloroacetic acid (TCA) was added to stop the enzymatic reaction. Clear supernatant of the reaction mixture (2 mL), obtained after centrifugation at 10,000 g, was mixed with 5 mL of Na_2CO_3 (500 mM) and 1 mL of Folin & Ciocalteu's Phenol reagent (1N, equivalent to 0.67 mol/L). The absorbance of this solution (centrifuged if necessary) was measured at 660 nm (Abs_{660}) against a blank (without enzyme addition), after 30 min of incubation at 37 °C in a temperature-controlled water bath. The calibration curve was constructed ranging from 10 to 50 µg/mL with L-tyrosine as the standard (y=0.0168x, R^2 > 0.99). One protease activity unit was equivalent to the generation 1 µmol of L-tyrosine/min under the assay conditions.

3.6.2 Lipase activity

Lipase activity was determined using p-nitrophenol palmitate (pNPP) as substrate and the release of p-nitrophenol (pNP) was measured continuously by spectrophotometric determination (Pencreach and Baratti, 1996). The reaction was started by adding 0.3 mL of enzyme solution to 2.7 mL of working substrate solution (16.5 mM pNPP in iso-propanol mixed with 50 mM Tris-HCl buffer containing 0.4% w/v TX100 and 0.1% w/v arabic gum, pH 8.0, at a volume ratio = 1:9), which was pre-equilibrated at room temperature in a 1 mL cuvette. The variation of the absorbance at 410 nm (Abs_{410}) was monitored with a UV-vis spectrophotometer for 5 min. The concentration of pNP and corresponding lipase reaction rate was calculated from the slope of the Abs_{410}-time curve using an apparent molar extinction coefficient of 15.362 ×10^6 cm^2/mol for pNP obtained from a standard calibration curve with the pNP concentration ranging from 0.01 to 0.05 mmol/L (y = 15.362x, R^2 > 0.99). One lipase unit was equivalent to 1 µmol of pNP liberated per min under the assay conditions.

3.6.3 Amylase activity

Amylase activity was determined by the 3,5-dinitrosalicylic acid (DNS) method (Sahutoglu and Akgul, 2015), with starch as the substrate and glucose as the standard. Enzyme solution (1mL) was mixed with 1 mL of soluble starch (2% w/w, in 20 mM sodium phosphate buffer with 6.7 mM NaCl, pH 6.9), and incubated for 30 min at 50 °C in a water bath. The reaction was stopped by adding 3 mL of DNS reagent (containing 7.1 mg/mL DNS, 13.2 mg/mL NaOH, 204 mg/mL Rochelle salt, 5.4 mg/mL phenol and 5.5 mg/mL sodium metabisulphite), and boiling in a water bath for 5 min. The mixture was immediately cooled to room temperature with running tap

water and the absorbance of the solution was measured at 540 nm (Abs540) against a blank using a UV-Vis spectrophotometer. The effective working range of the calibration curve was from 40 to 120 μg/mL, with glucose as standard ($y = 7.1029x - 0.2616$, $R^2 > 0.99$). One unit of amylase activity released 1 μmol glucose under the assay conditions.

For measuring α-amylase (which is mentioned in Chapter 4), preheat treatment at 68 °C for 10 min was applied to the enzyme solution to inactivate β-amylase before the enzyme assay.

3.6.4 Cellulase activity

Cellulase activity was measured according to the carboxymethyl cellulose (CMC) method (Ghose, 1987) using CMC as the substrate and glucose was the standard. Enzyme solution (1 mL) was mixed with 1 mL of CMC solution (2% w/w, in 50 mM citrate buffer, pH 4.8). DNS reagent (3 mL) was added to stop the reaction after incubation for 30 min at 50°C in a temperature-controlled water bath, followed by boiling in a water bath for a further 5 min. The release of glucose was measured by the DNS method, as describe in Section 3.6.3. One cellulase activity unit was equivalent to 1 μmol of glucose liberated from cellulose per min under the assay conditions.

3.6.5 Dehydrogenase activity

Dehydrogenase activity was performed following the method of Yao et al. (2010) with minor modification, using 2,3,5-triphenyltetrazolium chloride (TTC) as the substrate. Tris-HCl buffer (0.2 M, pH 7.3, 1.5 mL), 0.5 mL of glucose solution (0.1 M), 0.5 mL of TTC solution (0.4% w/v) and 0.5 mL of Na_2SO_3 solution (0.36% w/v) was added sequentially into 2 mL of the enzyme sample. The mixture was incubated for 20 min at 37°C in a temperature-controlled water bath, and 100 μl of concentrated sulphuric acid was subsequently added to stop the deoxidization reaction of TTC. The formed triphenyl formazan (TF) was extracted by adding 5 mL of toluene and shaking at 200 rpm for 10 min, followed by centrifugation of the mixture at 4000 rpm for 5 min. The absorbance of the toluene extract (i.e. clear supernatant after centrifugation) was measured at 492 nm against a blank. The working range of the calibration curve was 10 to 60 μg/mL, using TTC as the standard ($y = 0.0149x$, $R^2 > 0.99$). One dehydrogenase activity unit was defined as the amount of enzyme that reduced 1 μmol of TTC per hour under the assay conditions.

3.7 Statistical analysis

Where applicable, data in figures are shown as mean of three replicates ± standard deviation (vertical bars). One-way analysis of variance (ANOVA) was used to determine statistical significance. Correlations were considered statistically significant at a 95% confidence interval (*P value* < 0.05) in this research. All statistical analyses were performed in Microsoft excel software unless stated.

4 Optimisation of crude enzyme extraction from activated sludge

4.1 Introduction

Activated sludge mainly consists of microbial biomass that degrades organic pollutants in wastewater by producing substantial quantities of hydrolytic enzymes. Thus, AS is potentially a cost-effective alternative raw material for hydrolytic enzyme extraction. Several hydrolytic enzymes (e.g., amylase, glucosidase, phosphatase, lipase, etc.) have been detected in AS flocs. Most of the hydrolytic enzymes are either adsorbed to the cell surface or embedded in the EPS of the cellular biomass in AS (summarised in Table 2-1). Enzyme extraction, following sludge floc disruption, has been demonstrated and is technically feasible in bench-scale experiments (Jung et al., 2002; Gessesse et al., 2003; Marin et al., 2018).

As is shown in Table 2-2, a wide range of techniques have been extensively reported for physical disruption of microbial cells, releasing intracellular substances and enzymes embedded in the sludge EPS matrix. Sonication treatment is considered as a viable technique for enzyme extraction because it provides advantages, including: reduced extraction time and solvent consumption, as well as higher extraction yields at lower operational temperatures, which is more suitable for thermolabile compounds, compared to other cell disruption methods, such as: maceration, freeze-thaw, and high-pressure homogenisation (Mittal et al., 2017; Pereira et al., 2020). Bead-milling is another technique that is widely used to disrupt microbial cells and harvest cellular products, via collision and gridding effects between the beads and cells. Chemical additives, such as surfactants (e.g. TX100) and cation removal agents (i.e. EDTA), have also been extensively used to enhance enzyme extraction efficiency.

However, no consistent, optimal approach is available for enzyme extraction from AS and the production of bio-enzymes from this biomass source can be affected by a range of factors, including the operational extraction parameters and upstream wastewater treatment conditions. Thus, it is difficult to determine the maximum potential enzyme recovery and activity for AS and the different conditions used provide a range of performances for comparison. For example, for bead milling, the collision frequency between agitated beads and cells has a profound influence on the efficacy of cell disruption, therefore bead size and its loading rate is a critical parameter (see Section 2.4.2.2.2). For sonication treatment, sonication conditions including ultrasound frequency, treatment duration, and energy level input need to be optimised to enhance cell lysis and maximise the enzyme release into the extractant (Section 2.4.2.1.2). When a chemical additive is applied, the concentration of the additive needs to be considered (Section 2.4.3). Moreover, hydrolytic enzymes are not uniformly distributed in AS flocs and are either located in the easily extracted LB-EPS fraction

or are closely attached to the microbial cell surface. The efficacy of extracting a certain enzyme type, therefore, largely depends on its location and abundance in AS flocs, which is significantly affected by the corresponding availability of organic substrates present in sewage effluent (see Section 2.4.4); however, there is no information regarding hydrolytic enzyme activities in the AS in the presence of varying levels of organic substrates. The aim of this chapter, therefore, is to develop a robust enzyme extraction protocol from waste AS and to identify the impacts of both internal and external factors on the process. The specific objectives are to:

- Determine the most effective techniques for sludge cell disruption among: stirring with chemical additives, bead milling, and sonication; the preferred method was selected on the basis of the maximum enzyme recovery rate under standardised experimental conditions, and was also assessed in terms of protein and DNA content in the crude extract, as indicators for cell disruption and cellular material release;
- Quantify the effects of operational sonication conditions on enzyme extraction, including ultrasound frequency, treatment duration, energy intensity, solids content of the material, and surfactant addition;
- Examine the effect of sample collection location on enzyme extraction from AS, including location across the AS reactor or from the thickening belt after secondary clarification, representing different sludge types with varying levels of organic substrate;
- Determine the enzyme activity recovery rate of the developed protocol.

4.2 Materials and methods

4.2.1 Sludge sampling

Thickened sludge samples from WWTP1 were used for the preliminary comparison of cell disruption methods and the optimisation process of the extraction protocol. Mixed liquor samples from WWTP2 were used to investigate the effects of AS sampling location on enzyme extraction. Details of sludge collection methods are described in Section 3.2.

4.2.2 Preliminary comparison of enzyme extraction methods

The general protocol for crude enzyme extraction from AS is illustrated in Figure 3-5 (Step 1-6). Five alternative techniques were examined to disrupt the resuspended sludge suspension (Step 4 in Figure 3-5), including: sonication treatment (by either a bath-type or a probe-type sonicator), bead milling, and chemical disruption with either EDTA or TX100. The extraction process was carried out at 0-4 ^{o}C, and the corresponding operational conditions are described as follows and are summarised in Table 4-1:

- Sonication:

The effects of two common types of sonication device for enzyme release were tested and included a probe sonicator and water-bath sonicator, to examine the effects of direct and indirect delivery of ultrasound energy for cell disruption, respectively. The methods thus differed in terms of the pattern of energy distribution and delivery to target particles, and also ultrasound frequency. Resuspended sludge suspension was therefore placed in a water-bath sonicator (PUL. 125, Kerry Ultrasonics Ltd, UK) (Figure 4-1(a)), or subjected to sonication treatment with an ultrasound processor (VCX130, Sonics & Materials Inc., UK) (Figure 4-1(b)) connected to a sonication probe of titanium alloy (tip diameter = 13 mm), for different time periods.

A 50mL glass beaker filled with 25 mL of the sludge samples was immersed in the water-bath sonicator tank (length × width × depth = 25 × 15.5 × 15 cm, filled with reverse-osmosis (RO) deionised water). The water bath was operated at an ultrasound power input of 120 W and ultrasound frequency of 40 kHz for 10 min, with an on-and-off pulse mode (1 min on followed by 1 min off).

Sludge samples (25 mL) were placed in a 50 ml conical polypropylene centrifuge tube (diameter = 3 cm), and the sonication probe was fitted into the sample tube with its tip dipped about halfway into the sludge suspension (to avoid injecting air into the sample, that may cause the sample to foam). The sample tube was immersed in an ice-water bath during the extraction to prevent heating of the biomass material. The probe-type processor delivered a constant amplitude (AMP) with a corresponding power input of 76 μm at 100% AMP (i.e. “amplitude controlled” as specified by the manufacturer), and was operated at an ultrasound power input equivalent to 130W, ultrasound frequency of 20kHz, 50% AMP, for 2 min and 4 min in pulsed on-and-off mode operation for 10 s/10 s.

- Bead milling:

The resuspended sludge suspension (25 mL) was mixed with glass beads (diameter = 0.5 mm) in a round-bottom centrifugation tube (diameter = 2.5 cm, capacity = 35 mL, with a liner-less screw top cap) (Figure 4-1(c)). The volume loading rate of glass beads was 40% v/v. The tube was placed on a Whirlimixer® cyclone vortex mixer (agitation speed: 200-2800 rpm, Fisons Plc, UK) and mixed at maximum speed for 5 min. The pulse mode of operation (1 min on and 1 min off) was adopted, and the tube was placed in an ice-water bath during the off-cycle, to avoid over-heating of the sample.

- Chemical extractants:

Chemical extractants, including EDTA or TX100, were mixed with 25 mL sludge suspension in a 50 mL glass beaker to achieve a final concentration of 2% w/w; the beaker was immersed in an ice-water bath and stirred by magnetic stirrer at 600 rpm for 1 h.

Protein and DNA contents in the crude enzyme extract was measured according to procedures described in Section 3.5, as indicators of cell disruption and release of intracellular materials. α-Amylase, protease, lipase and cellulase activity was measured to examine the effectiveness of the extraction protocol; the procedures for the activity assays are described in Section 3.6.

Table 4-1 Summary of the specific conditions for different enzyme extraction methods tested

Number	Treatment method	Condition code	Corresponding operational conditions
1	None	Control	No physical disruption or chemical additives applied
2	Stirring with TX100	TX	Concentration = 2% w/w Stirring speed = 1000rpm Duration = 1h
3	Stirring with EDTA	EDTA	Concentration = 2% w/w Stirring speed= 600rpm Duration = 1h
4	Bead milling	BM	Bead diameter = 0.5 mm loading rate = 40% v/v agitation speed = 2800pm Duration = 5 min (1 min on, 1 min off)
5	Sonication water bath	SWB	Ultrasound power = 120 W Ultrasound frequency = 40 kHz Duration = 10 min (1 min on, 1 min off)
6	Sonication probe 2 min	SP2	Ultrasound power = 130 W Ultrasound frequency = 20kHz Amplitude = 50% Duration = 2 min (10 s on, 10 s off)
7	Sonication probe 4 min	SP4	Ultrasound power = 130 W ultrasound frequency = 20kHz Amplitude = 50% Duration = 4 min (10 s on, 10 s off)

Note: the extraction process was carried out at 0-4 ^{o}C.

(a) (b) (c)

Figure 4-1 Apparatus used for activated sludge disruption: (a) water-bath type sonication, (b) probe-type sonication, and (c) bead milling

4.2.3 Optimising probe sonication for activated sludge disruption and enzyme extraction

4.2.3.1 Summary of experimental optimisation conditions

Following the preliminary assessment of enzyme extraction methods given in Table 4-1, probe-type sonication was selected for further detailed optimisation as the most effective sludge cell disruption method in this study (see Section 4.3.1). Thus, operational conditions including duration, energy level (by controlling the AMP of ultrasound), solids content (by diluting the sludge samples) and surfactant addition, were optimised through a series of experiments, shown in Table 4-2 and further details are described in following sections. α-Amylase, protease and cellulase activity in the crude extract were measured according to the procedure in Section 3.6, as indicators to show the effect of sonication condition on enzyme extraction efficiency.

Table 4-2 Summary of different experimental conditions for the optimisation of probe sonication extraction of enzymes from activated sludge

Experiment	Sonication duration	Sonication amplitude %	Solids dilution factor	Surfactant addition
1	2	40	5	-
2	5	40	5	-
3	10	40	5	-
4	15	40	5	-
5	10	20	5	-
6	10	60	5	-
7	10	80	5	-

8	10	40	2	-
9	10	40	3	-
10	10	40	5	-
11	10	40	5	1% v/v

Note: the sonication treatment process was carried out at 0-4 °C.

4.2.3.2 Effect of sonication duration and energy level

The impact of treatment duration was investigated by sonicating diluted sludge samples at 40% AMP for 2, 5, 10 and 15 min; the corresponding specific energy consumption was 10.7. 24.6, 49.3 and 74.0 kJ/g VS, respectively. The effect of energy level was examined by disrupting diluted sludge samples at 20, 40, 60 and 80% AMP for 10 min; the corresponding energy levels, expressed in power density (defined in Section 2.4.2.1.2), during each treatment were 343, 872, 1547 and 2312 W/L, respectively.

Sludge samples were diluted with Tris-HCl (10 mM, pH 7.0) buffer five times based on mass (see Section 4.2.3.3 for the explanation of the dilution factor (DF), which, in this case, was set to5) before ultrasound disruption; the final solids concentration was 10.6 g VS/L.

4.2.3.3 Effect of solids content

The crude sludge sample used for enzyme extraction had a solids content of 69.4 ± 0.42 g TS/L and 53.2 ± 0.10 g VS/L. The effect of solids content on enzyme extraction was tested by diluting the sludge sample with Tris-HCl buffer (10 mM pH 7.0), to achieve a DFs equivalent to 2, 3, 5 and 10 before sonication treatment. The sludge disruption was performed with the sonication probe set at 40% AMP for 10 min, providing a specific energy input (defined in Section 2.5.2.1.2) equivalent to 21.8, 30.4, 49.9 and 99.2 kJ/g VS, respectively. The optimal solids content of AS for disruption and enzyme extraction was determined from the relationship between the specific enzyme activity (U/g VS) and corresponding specific energy input (kJ/g VS).

The sludge dilution factor (DF) was defined as:

$$DF = \frac{mass\ of\ diluted\ mixture\ (g)}{mass\ of\ original\ sludge\ (g)} \quad \text{(Eq 4-1)}$$

4.2.3.4 Effect of surfactant addition

Sludge samples were diluted (DF = 5) with Tris-HCl buffer (10 mM, pH 7.0) containing 1% v/v TX100 and subjected to sonication disruption at 40% AMP for 10 min duration.

4.2.4 Effect of activated sludge sampling location on enzyme extraction

Enzyme types and activities may differ between the anoxic, anaerobic and aerobic zones of AS reactors, but the largest growth rates and, therefore, activities would be expected in the aerobic region (Petersen et al., 2003). Hence, mixed liquor samples from the aeration tank were collected to determine the impact of nutrient supply on enzyme extraction within a consistent aerobic environment, and AS samples from the thickening belt, at WWTP2 were used to investigate the patterns of enzyme activity and the viability of the sludge biomass (see Section 3.2). Sludge samples were diluted (DF = 5) before ultrasonic disruption (following the optimised enzyme extraction protocol determined from the results: 40% AMP for 10 min, 1% v/v TX100 addition, see Section 4.3.2). α-Amylase, protease and cellulase activity in the crude extract were measured (according to the procedure in Section 3.6). Dehydrogenase activity was used as an indicator of the general rate of microbial activity (the activity assay for dehydrogenase is described in Section 3.6).

4.2.5 Enzyme recovery rate

The recovery rate of α-amylase, protease and cellulase was measured to determine the efficiency of the extraction protocol, using a spike-and-recovery method (Stoeckel et al., 2009). Thickened sludge from WWTP1 was used and the re-suspended sludge obtained from Step 3 in Figure 3-5 was diluted to the optimum solids content according to the results from the optimisation experiments and spiked with commercial α-amylase, protease and cellulase (all in solid form, for product information see Section 3.1), to provide a final concentration equivalent to 1.2, 0.1 and 0.04 mg solid/mL diluted sludge, respectively. The enzyme-spiked sludge samples were extracted following to the optimised extraction protocol (see Section 4.3.2). The recovery rate (*R*) was calculated as follows:

$$R(\%) = \frac{Total\ enzyme\ activity - Background\ enzyme\ activity}{Spiked\ enzyme\ activity} \times 100 \qquad \text{(Eq 4-2)}$$

Where,

Total enzyme activity and Background enzyme activity refer to the activity of the crude products extracted from sludge samples (Supernatant C in Figure 3-5), with and without enzyme spike, respectively; *Spiked enzyme activity* refers to the activity of pure enzyme solution that has equivalent enzyme dose to the spiked enzymes (measured following the experimental conditions described in Section 3.6), which is equivalent to 0.16, 0.15 and 0.32 U/mL for α-amylase, protease and cellulase, respectively.

4.3 Results

4.3.1 Preliminary comparison of activated sludge disruption methods

Stirring with chemical additives, bead milling, and sonication have been widely applied in earlier studies of microbial cell disruption and enzyme extraction; the efficiency of these methods in cell disruption (measured by protein release) and enzyme extraction (measured by volumetric activity) was compared, relative to a control (see Table 4-1). No enzyme activity was found in the centrifugation supernatants obtained before cell disruption (supernatant A and B shown in Figure 3-5, which were therefore decanted in subsequent experiments), or in the control group, which did not receive a cell disruption treatment.

In general, sonication probe showed the highest overall levels of cell disruption and enzyme extraction efficiency. As is shown in Figure 4-2, 1523.8 μg/mL protein was released after sonication probe treatment for 2 min (SP2), and the volumetric activity of protease and lipase in the crude extract was 0.060 and 0.074 U/mL, respectively. α-amylase and cellulase activities in the crude extract were also measured (as specified in Section 4.2.2). However, the values were considered unreliable and were therefore not reported due to high background absorbance of the blank sample. Increasing the duration of sonication to 4 min (SP4) improved the extraction efficiency, and gave the best overall protein release, and protease and lipase activities, equivalent to 2089.3 μg/mL, 0.072 U/mL and 0.132 U/mL, respectively, compared to the other extraction conditions tested (Figure 4-2). Bead milling increased enzyme extraction compared to the control, but only modestly relative to sonication, and only 8-10% of the protease and lipase activity level was obtained in comparison to SP4. However, the lowest overall extraction efficiency was measured for the water-bath sonication treatment. In this case, protein release and protease activity were equivalent to approximately 2% of the SP4 group, and no lipase activity was detected in the crude extract after water-bath sonication. Based on these results, sonication probe was selected for physical disruption of AS cells in the subsequent enzyme extraction experiments.

The effectiveness of adding chemical extractants was also investigated. As shown in Figure 4-2, stirring the sludge matrix with 2% w/w TX100 for 1 h (without physical disruption of the sludge cells) released 266.0 μg/mL protein and extracted 0.036 and 0.065 U/mL protease and lipase. EDTA addition, under equivalent conditions, increased the release of protein by 2.7 times compared to TX100 to a value equivalent to 724.3 μg/mL. However, in contrast to TX100, no protease and lipase was detected in the crude extract with EDTA. This behaviour was consistent with the results reported by Gessesse et al. (2003), which showed that AS stirred with TX100 (dosage = 0.01-2%) and EDTA (10 mM), at 900 rpm for 1 h, alone or in combination, gave lipase and protease activities up to 320 and 4000 U/g VS with TX100,

respectively, whereas the maximum activities measured with EDTA extraction were reduced to 75 and 45% of the TX100 values, respectively. Ni et al. (2017) also extracted AS with 1% TX100 for 1 h (no agitation speed was given) and detected 5.1 U/g wet sludge of protease activity whereas the enzyme activity was reduced to 0.8 U/g wet sludge without TX100. Therefore, the chemical extractant, TX100, was adopted to enhance enzyme extraction from AS in further experiments. Gessesse et al. (2003) indicated that the interaction between chemical extractants and enzymes was responsible for the increased release, rather than this being attributed to physical disruption caused by shear forces induced during continuous stirring of the sludge matrix, since no enzyme activity was detected when AS was stirred with buffer alone.

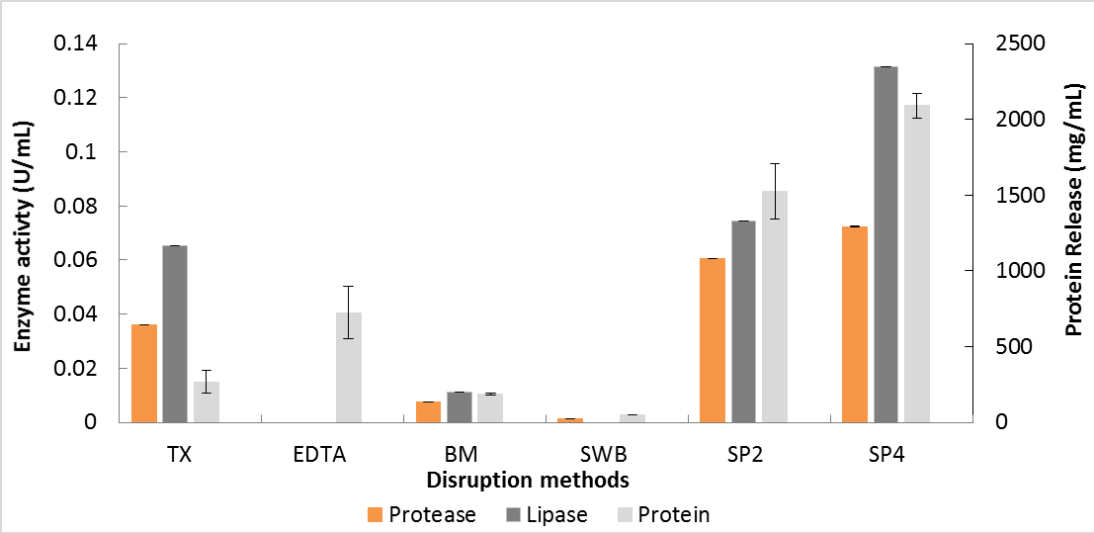

Figure 4-2 Volume activity of protease and lipase enzymes and protein content in the crude extracts from activated sludge extracted by different cell disruption methods (vertical bars represent the standard deviation, n=3; see Table 4-1 for explanation of disruption methods

4.3.2 Effect of Sonication conditions

4.3.2.1 Duration and energy level

Figure 4-3 shows the effect of different durations of sonication on protein and DNA release, which provide markers of the extent of cell disruption (see Section 3.5). Protein and DNA release increased with duration, but the magnitude of the response generally declined with increasing treatment time. A similar response was also observed with the enzyme recovery patterns, with maximum enzyme activities being observed at 15 min duration, shown in Figure 4-4. α-Amylase gave the largest overall enzyme activity in AS, followed by cellulase and protease, and the maximum enzyme activities detected were approximately: 25, 7.5 and 3.0 U/g VS, respectively.

The sonication probe used in this work was AMP controlled, thus, under certain amplitudes, the energy consumption was directly proportional to the processing time. Extending the processing time from 10 to 15 min, increased the specific energy consumption also by 50.1% (from 49.3 to 74.0 kJ/g VS, see Section 4.2.3.2). However, the activities of α-amylase, protease and cellulase were only modestly improved with increasing energy input, by approximately 17%, 10% and 9.0%, respectively. Therefore, 10 min was selected as the optimum duration for sonication treatment. This also offered practical advantages compared to the longer treatment periods, by reducing the sample processing time and the risk of heating the sample and enzyme denaturation (discussed in Section 2.5.2.1.2). The activities of α-amylase, protease and cellulase obtained under this regime were equivalent to 22.4, 2.7 and 6.8 U/g VS, respectively.

Figure 4-5 shows the extraction efficiency of sludge sonication treatment with increasing AMP and related power density for a duration of 10 min. The specific enzyme activity increased with power density and the maximum activity of α-amylase, protease and cellulase was 29.7 U/g VS at 2312 W/L (80% AMP), 2.71 U/g VS at 872 W/L (40% AMP) and 7.34 U/g VS at 1547 W/L (60% AMP), respectively. Amplitudes of 60% and 80% caused rapid heating of the samples, despite the measures adopted to control the sample temperature by completing the cellular disruption step in an iced-water bath (see Section 3.3). Reduced thermostability and damage to the chemical bonds that maintain enzyme structural conformation may account for the lower protease enzyme activity observed at the higher energy intensities (Nadar and Rathod, 2017), compared to α-amylase and cellulase. Therefore, 40% AMP (power density = 872 W/L) was selected as the optimum energy level for AS disruption in subsequent sonication experiments.

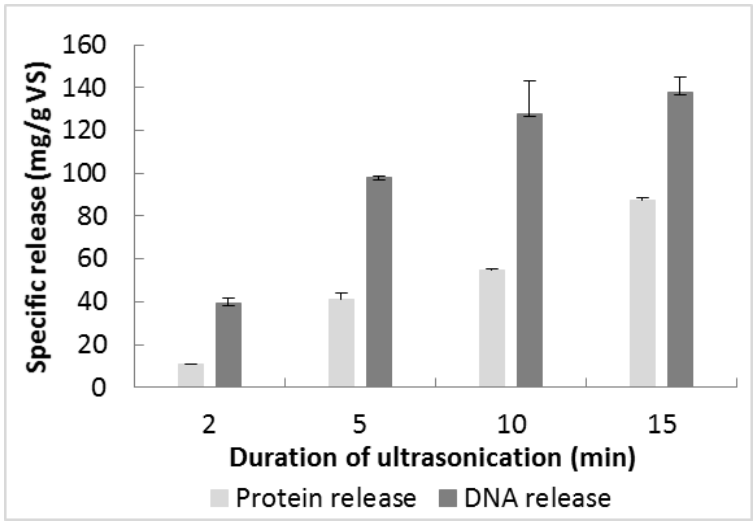

Figure 4-3 Effect of sonication duration (minutes) on protein and DNA release from activated sludge at 40% amplitude (vertical bars represent the standard deviation, n=3)

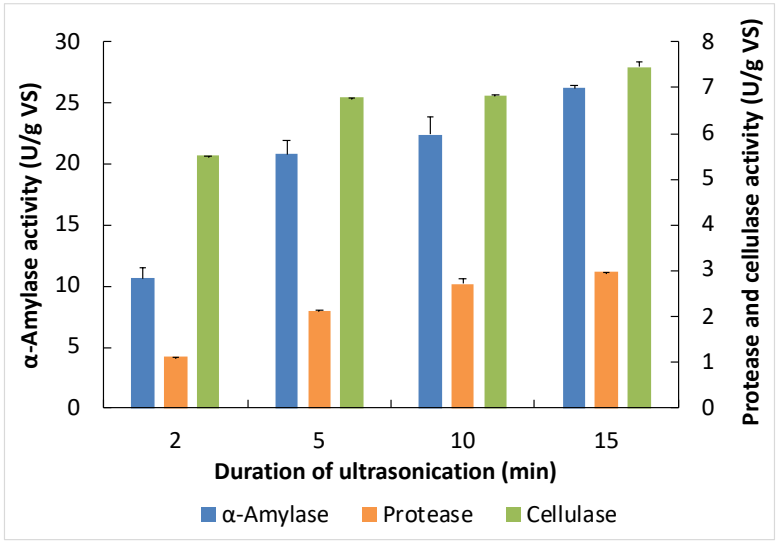

Figure 4-4 Effect of sonication duration (minutes) on specific enzyme activities at 40% amplitude (vertical bars represent the standard deviation, n=3)

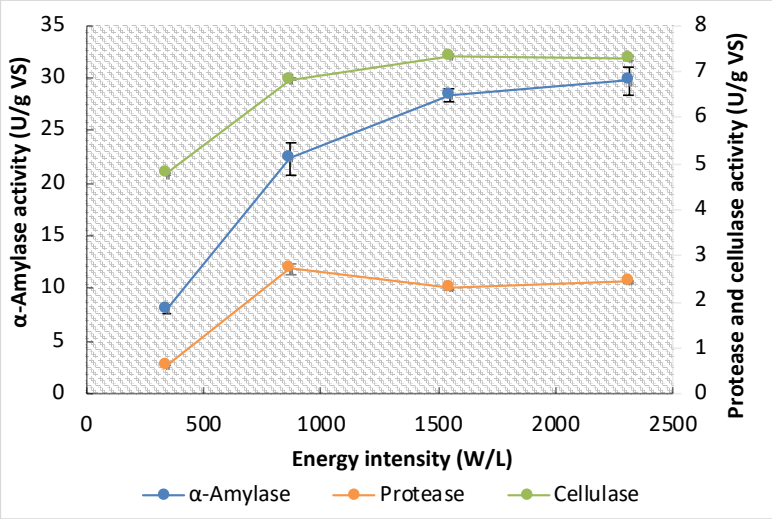

Figure 4-5 Effect of sonication power density (for 10 min duration) on specific enzyme activities (vertical bars represent the standard deviation, n=3)

4.3.2.2 Solids content

Figure 4-6 shows the effects of increasing sludge dilution on the enzyme activities of α-amylase, protease and cellulase. Maximum activities were obtained at DF = 5 and were equivalent to approximately 31, 3.0 and 10.4 U/g VS activity, respectively. Increasing the DF from 5 to 10 almost doubled the energy input from 49.9 kJ/g VS to 99.2 kJ/g VS (see Section 4.2.3.3), but had no effect on enzyme activity. Ni et al. (2017) observed a similar trend for protease activity extracted from AS (via stirring with 1% TX100), which increased to 20 U/g VS with decreasing solids content to an optimum solid/liquid ratio of 1:4 (DF equivalent to 5) at a, and subsequently remained relatively consistent with further dilution of the sludge to a minimum solid/liquid ratio applied equivalent of 1:6 (Ni et al., 2017). Therefore, the solids contents of sludge samples prepared for sonication were adjusted to the optimum ratio of approximately 10g VS/L (equivalent to DF = 5) in subsequent experiments.

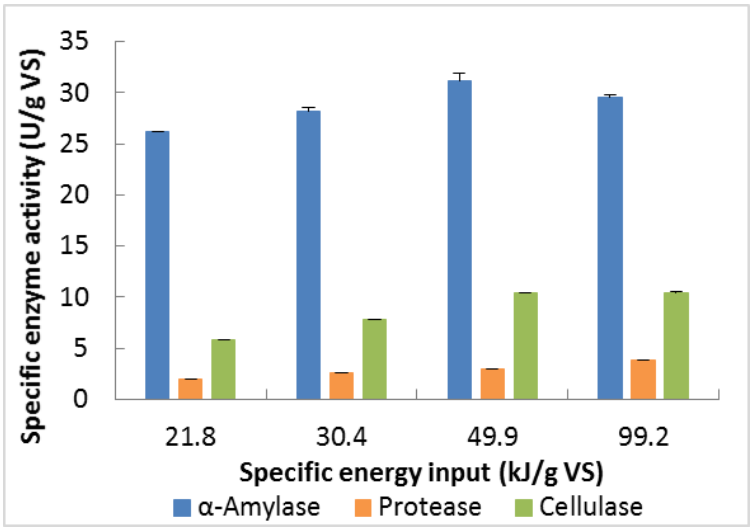

Figure 4-6 Effect of solids content on enzyme activity after sonication treatment for 10 min duration and 40% amplitude (vertical bars represent the standard deviation, n=3)

4.3.2.3 Surfactant addition

TX100 increased the release of extracellular proteins, mainly associated with the EPS fraction of the sludge flocs, by a factor of two compared to sonication treatment without surfactant addition (Table 4-3). However, no effect of TX100 was observed on DNA release or cell lysis. This behaviour was consistent with results reported by Glauche et al. (2017) showing the addition of TX100 (2% v/v) for cell disruption of *E. coli* increased the release of soluble proteins.

The results from the surfactant experiments (Table 4-3) showed that the addition of 1% (v/v) TX100 significantly improved protease release with sonication, almost doubling the activity of this enzyme, compared to the control (sonication treatment in buffer without extractant). Relative to protease, surfactant addition had a comparatively smaller effect on the activity of α-amylase and cellulase. Similar results have also been reported in the literature. For example, Gessesse et al. (2003) found that sonication treatment (power = 200W, frequency = 15 kHz , duration = 30 min in a pulse mode with 2min on and 5 min off) of AS in the presence of 0.1% TX100 increased lipase extraction by three times, to 335 U/g VS of lipase, compared to sonication under equivalent conditions without TX100.

Table 4-3 Effect of surfactant addition on activated sludge disruption and extracted enzyme activity

	α-Amylase (U/g VS)	Protease (U/g VS)	Cellulase (U/g VS)	Protein release (mg/g VS)	DNA release (mg/g VS)
Without TX	22.39±1.53	2.71±0.11	6.83±0.02	54.70±0.42	127.63±15.57
With 1% TX	24.64±0.59	5.62±0.04	7.72±0.25	128.66±8.22	126.43±8.82
Improvement	+10.0%	+107.6%	+13.1%	+135.2%	-0.94%

4.3.2.4 Summary of optimum sonication protocol for activated sludge disruption and enzyme extraction

Sonication was effective at disrupting AS flocs and releasing hydrolytic enzymes and the results demonstrated that the developed protocol was an effective approach to extracting enzymes from WAS. The optimum operational parameters were: 40% AMP (equivalent to a power density of 872 W/L) and 10 min duration. The solids content of sludge samples was also an important parameter influencing ultrasonic disruption and optimisation experiments indicated that a solids content of approximately 10 g VS/L provided the maximum enzyme activity. Surfactant addition (1% v/v TX100) also enhanced protein release as well as enzyme activity in the AS extract and also therefore incorporated into the standard enzyme extraction protocol for AS.

4.3.3 Effect of activated sludge sampling location on enzyme extraction

Specific enzyme activities measured at the different sampling points of the AS aeration tank at WWTP2 are shown in Figure 4-7. Microbial activity of AS was measured using dehydrogenase activity, which increased from the inlet of the aeration tank to the centre position (Point 3 in Figure 3-2), and the maximum rate was equivalent to 5 U/g VS. As may be expected, the rate of microbial activity decreased at the end of the aeration tank, by approximately 35%, reflecting substrate exhaustion. By contrast, hydrolytic enzyme activities in the AS extract did not follow the same patterns observed in dehydrogenase activity and were generally relatively consistent at the different sampling locations and there was no statistically significant correlation (*P* values of Pearson correlation coefficients for α-amylase, protease, and cellulase activity relative to dehydrogenase activity were 0.60, 0.34 and 0.26, respectively). The maximum activities of enzymes extracted from AS sampled directly from the aeration tank using the optimised sonication protocol (Section 4.3.2.4) were 52.2, 8.2 and 9.9 U/g VS for amylase, protease and cellulase, respectively, which were also comparable to those observed for sludge sampled directly from the thickening belt (Point 6 in Figure 4-7).

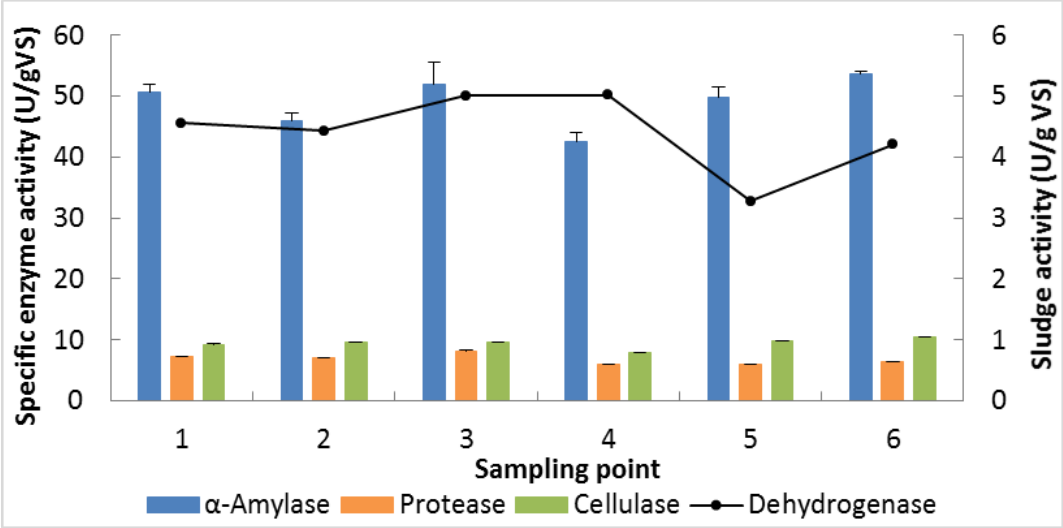

Figure 4-7 Hydrolytic enzyme activities (on left axis) and sludge microbial activity (on right axis) at different sampling points along the length of an activated sludge aeration reactor (point 1-5); sample point 6 was taken from the activated sludge thickening belt (vertical bars represent the standard deviation, n=3)

4.3.4 Enzyme recovery rate

Alpha-amylase, protease and cellulase were selected to examine the recovery rate of enzymes from sludge using the proposed protocol. The recovery rate for protease and cellulase was 63.1% and 115.3% respectively. Ni et al. (2017) reported a similar recovery rate (66.7% for protease, as the indicator) of hydrolytic enzymes from AS by stirring with TX100 for 60 min. Interestingly, the activity of cellulase in the sludge extract was apparently enhanced by addition of the commercial enzyme formulation (see Section 4.2.5), thus a recovery rate >100% was indicated by the cellulase activity assay. Indeed, sonication can induce the hyperactivation of enzymes by causing conformational changes of the enzyme structure under certain conditions (mentioned in Section 2.4.2.1.3). For instance, ultrasound treatment can cause the breakage of covalent bonds within the enzyme (Ladole et al., 2017), releasing more active sites from inside the protein structure, resulting in higher apparent enzymatic activity when exposed to the substrate (CMC in this case – see Section 3.6). Ladole et al. (2017) found the hyperactivation of cellulase by sonication was linked to significant changes in the α-helix and β-sheet ratio within the secondary protein structure of the enzyme. Ultrasound treatment can also improve the apparent enzyme activity by increasing mixing and diffusion of reactive components of both substrate and enzyme (Capelo et al., 2004).

As was the case with the other enzymes examined, α-amylase was also spiked into the sludge sample to measure the activity recovery rate (Section 4.2.5). However, significant interference in the colorimetric reaction (DNS assay for amylase, described in Section 3.6) was found and a recovery rate greater than 500% was obtained. This behaviour could be explained due to the reaction mechanism of the assay. The DNS assay quantifies reducing sugars by the

oxidation of free aldehyde (CHO) or ketone (C=O) groups present in certain carbohydrates (so-called “reducing sugars”) under alkaline conditions, reducing 3,5-dinitrosalicylic acid (yellow) to 3-amino-5-nitrosalicylic acid (orange red), which is measured at a wavelength of 540 nm (Hu et al., 2008; Deshavath et al., 2020). It is possible that the pure enzyme spiked into the sludge suspension reacted with the sludge matrix and/or other materials present in the commercial enzyme formulation, to produce other substances containing active carbonyl groups (e.g. various amino acids, as the reaction products of protease) which also reacted with DNS. A similar response of the DNS assay was reported by Teixeira et al. (2012): in the presence of 20 mM of either tryptophan, cysteine, histidine, tyrosine, or hydroxyproline, which overestimated the concentration of 3.7 mM glucose (which was the standard substance for the amylase assay also used here, see Section 3.6.3) by 76%, 50%, 35%, 18%, and 10%, respectively, thus, that apparent activity of xylanase and cellulase was increased by three and two times, respectively, due to presence of substances that react to the activity assay in a similar manner to reducing sugars.

4.3.5 Energy consumption

Erosion of the sonication probe is possible after prolonged periods of use, leading to the gradual loss of spherical particles which form and are stripped from the probe under the effect of intense cavitation and/or chemical reactions, forming erosion pits on the surface of the probe (Dong et al., 2016). For example. Tian et al. (2018) reported that the performance of a sonication probe (made of titanium alloys) in an ultrasound-assisted aluminium casting process (at temperature of 650 °C) was severely reduced after 36 h service time, and erosion pits appeared at various positions on the probe. This is a concern because the increased surface roughness may impede the transmission of ultrasound energy into the samples. Thus more energy would be required to maintain the same intensity of vibration in the sample. However, the specific energy supplied to sludge samples under optimal conditions showed no significant increase over time (P >0.1) after processing >30 batches of sludge (ranging from 52.0-76.2 kJ/g VS, see Appendix A-1), indicating that erosion of the probe was negligible during this period. In contrast to the damage observed by Tian et al. (2018), this operational stability was probably explained because: (1) the cell disruption process was carried out at a relatively low temperature (4 °C, compared to 650 °C by Tian et al. (2018)), minimising thermal damage to the probe material, and (2) the sonication probe was thoroughly cleaned and carefully polished with soft dry cloth as recommended by the manufacturer after each use, therefore severe corrosion by the chemical/electrochemical reactions was minimised.

4.3.6 Reproducibility of enzyme activities in different batches of activated sludge

The activities of four hydrolytic enzymes (amylase, protease, lipase, and cellulase), representing the enzymes responsible for hydrolysing the main organic constituents in urban

wastewater (protein, fat, starch and cellulose, respectively) were measured (methods see Section 3.6), using AS samples collected from the thickening belt at WWTP1 and/or WWTP2 (Section 3.2) following the optimum sonication extraction protocol (Section 4.3.2.4): 40% AMP, 10 min duration, DF = 5, 1% v/v TX100 addition). The activities of the extracted enzymes extracted from different batches of sludge are shown in Figure 4-8 (the date of sampling and the corresponding specific activities in the crude extracts was shown in Appendix A-1). The most abundant hydrolytic enzyme was amylase (ranging 179-412 U/g VS), which was 1-2 orders higher than the other target enzyme types, followed by cellulase, lipase and protease. The variation of enzyme activities within a certain range can be explained because the production of extracellular hydrolytic enzymes by microorganisms in AS flocs often dynamically changes according to the composition of sewage influent. This can be significantly affected by a range of factors including temperature, season, industry type, rainfall, etc. (Martin and Vanrolleghem, 2014; Rashid and Liu, 2020)), and the presence of certain substrates can induce the production/expression of the corresponding hydrolytic enzymes, as discussed in Section 2.4. The largest activities of amylase (393 and 412 U/g VS, which was excluded from the box diagram in Figure 4-8) could be explained, for instance, due to inputs of starch-rich wastewater into the sewage collection system, for example, from the brewery or bakery industries, although this was not verified.

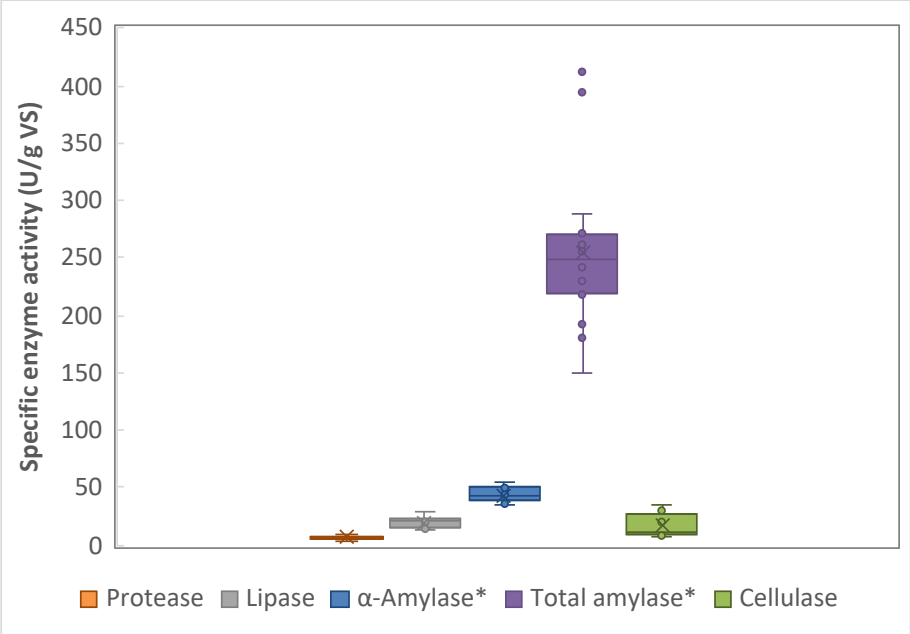

Figure 4-8 Activities of major hydrolytic enzymes extracted from different batches of activated sludge (see Appendix A-1) under optimal conditions (*Note: for measuring α-amylase only, preheat treatment was applied to inactivate the β-amylase contained in the crude enzyme solution, see Section 3.6.3)

4.4 Discussion

4.4.1 Comparison of cell disruption methods

4.4.1.1 Bead milling

Bead milling is a technique that is widely used to disrupt microbial cells and harvest cellular products. Microbial cell walls are disrupted during vigorous collisions between cells and beads that are rotating at high speed in the milling chamber. The grinding effect induced by layers of rolling beads moving at different speeds also contributes to cellular disruption (Section 2.4.2.2.1). Krah et al. (2016) reported that bead milling of AS at an agitation speed of 6 m/s for 45 s, using a commercial bead mixture containing 64% ZrO_2 beads (1.4 mm), 33% SiO_2 beads (0.2 mm) and one glass bead (4 mm), increased the extraction of phosphatase, galactosidase and glucuronidase by 15.1, 67.3 and 13%, respectively, to values of 43.5, 25.6 and 11.3 U/mg, compared to sonication treatment (frequency = 20 kHz, power density = 1 W/mL, 10 min).

However, in this study, bead milling was only moderately effective at extracting enzymes, compared to sonication probe treatment (Figure 4-2). This may be explained because the solids content (TS = 60-70 g/L) of the AS samples examined here was approximately 3-10 times larger compared to the conditions reported in previous investigations (Jung et al., 2001; Krah et al., 2016). This was purposefully done to allow comparison between different methods (e.g. sonication) under similar conditions, however, the TS was not specifically optimised for effective cell disruption. Indeed, the disruption efficacy obtained by bead milling could change with varying solids content. However, reducing the TS to the potentially optimal values reported previously (Jung et al., 2001; Krah et al., 2016) would itself reduce the concentration and activity of recovered enzymes. Postma et al. (2015) also reported that the soluble protein yield after disrupting microalgae cells of *Chlorella vulgaris* by a Dyno mill (1 mm ZrO_2 beads with 65% v/v loading rate) was significantly influenced by the concentration of biomass fed into the unit, regardless of the agitation speed (ranging from 6 to 12 m/s). They also found that the highest protein yield (42%) was obtained at the smallest biomass concentration (25 g TS/kg (as received)) and that it decreased by 25% as the biomass concentration increased to 145 g TS/kg (as received). The lower enzyme extraction efficiency by bead milling at high solids content can be explained by the formation of insoluble protein aggregates at high biomass densities due to increased local protein concentrations, shear forces and interactions with other cellular substances/components (Postma et al., 2015). Furthermore, microbial cell suspensions with high solids contents often show increased viscosity, and handling such material is practically more challenging due to greater biomass losses and reduced mixing properties, compared to a lower solids content. Thus, significant dilution of thickened AS collected from WWTP would be necessary if adopting a bead milling procedure for enzyme

extraction, which would increase the volume necessary for biomass disruption and also reduce the enzyme activity in the crude extract.

Furthermore, the temperature of the samples rapidly heated during the bead milling process, from the vigorous friction between particles within the chamber, which converts a significant portion of the available energy into heat (Günerken et al., 2015; Koubaa et al., 2020). This reduces the efficiency of energy transfer to individual cells for disruption and also requires an intensive, energy-demanding cooling system to protect the recovery of functionally fragile products, such as heat-sensitive enzymes, from thermal degradation. For example, Jung et al. (2001) found that the continuous disruption of AS in a Dyno mill (with 0.5 mm diameter beads, and a loading rate of 60% v/v) increased the temperature rapidly to 50 and 80 °C after 15 min milling at 3200 and 4200 rpm, respectively, despite the attachment of a cooling apparatus. Moreover, extra measures, such as sieving and centrifugation, to separate the beads from disrupted sludge, would be required for continuous mode operation, increasing the complexity and energy consumption of an industrial scale process for enzyme recovery from AS. Therefore, bead milling was not selected in the standard protocol for cell disruption of, and enzyme extraction from, AS and was unlikely to be suitable for up-scaling to an industrial level for the commercial treatment of AS for enzyme recovery.

4.4.1.2 Sonication

Sonication probe was considerably more effective at enzyme extraction from AS compared to the other techniques examined, and this was achieved with a shorter treatment time and power consumption. This behaviour was consistent with results reported by Nabarlatz et al. (2010), which showed that sonication treatment (power intensity = 3.9 W/cm^2, in the presence of 2% v/v TX100) extracted 52.9 U/g VS protease and 23.0 U/g VS lipase from AS in 10 and 20 min, respectively, whereas stirring with 2% v/v TX100 (stirring velocity = 500 rpm) for up to 1 h extracted a similar amount of protease, but lipase was reduced by 50%. Moreover, the power consumption by stirring was considerably greater, and up to six times larger at 50 x 10^{-3} kWh compared to 8.3-16.7 x 10^{-3} kWh for sonication (Nabarlatz et al., 2010).

Extracellular enzymes of bacteria are either accumulated in the gel-like EPS matrix, which has a three-dimensional structure with an extremely large surface area that holds microbial cells together to form the sludge floc, or they are tightly bound to cell membranes via hydrogen and/or ionic bonding (Yu et al., 2007; Lin et al., 2014). A possible hypothesis to explain the mechanism of enzyme release from AS by ultrasound treatment is that the cavitation generated by ultrasound disrupts the EPS matrix that acts as a protective layer for enzymes. Following disruption, the enzymes in EPS are exposed to the surrounding aqueous solution and are readily detached by shear forces induced through shaking within the solution (Wingender et al., 1999; Karn et al., 2013; Nadar and Rathod, 2017). Cavitation generated by

ultrasound also produces pores on the cell membrane, releasing periplasmic enzymes and cellular proteins (Loustau et al., 2018) (see Section 2.4.2.1.1). The results reported here (Figure 4-3) confirmed that sonication treatment released DNA into the crude extraction solution, which is mainly located in the nucleoid of bacteria, indicating that the disruption of cell membranes had occurred.

The preliminary experiment comparing different cell disruption techniques (Section 4.2.2 and Figure 4-2) was designed to examine the enzyme extraction performance under a standardised set of equivalent, representative conditions and showed that sonic probe treatment was by far the best approach, by up to an order of magnitude. Therefore, whilst the various techniques were not specifically optimised, given the large difference in performance, compared to bead milling, for instance, for conditions representative of a practical enzyme recovery system, sonication was selected as the preferred method for cell disruption and enzyme release.

4.4.2 Sonication device

Two types of sonication device were applied to disrupt AS cells: (1) probe sonicator and (2) water-bath sonicator. Sonication treatment by sonication probe produced the largest enzyme yield from AS disruption among all of the methods tested, whereas water-bath sonication exhibited only minimal enzyme extraction from sludge samples (Figure 4-2). The better performance of probe sonication is consistent with previous literature. For example, Liu et al. (2013) reported that sonication treatment by a probe-type sonicator (ultrasound frequency = 20 kHz) showed better performance in disrupting yeast *Saccharomyces cerevisiae* cells compared to a bath-type sonicator (ultrasound frequency = 25 kHz) and protein release was 0.55 and <0.1 mg/mL, respectively, under equivalent conditions (200 mL cell suspension with 1% w/w DS content, ultrasound power input = 600 W, total treatment duration = 21 min operated in on-and-off pulse cycle with a pulse duration period equivalent to 50% of the cycle time).

The higher efficiency by probe sonicator can be explained by several reasons discussed below:

1) Pattern of energy distribution and delivery to target particles

Probe sonication is a direct sonication method and is in direct contact with the sample. The sonication processor converts high frequency electrical energy (50/60 Hz and 240 V electricity supply) to mechanical vibrations, which are intensified by the probe and are transferred directly to the sample. The energy delivered by the probe, via expanding and imploding of cavitation bubbles (see Section 2.4.2.1.1), is highly localised and intensive (Dhanalakshmi and Nagarajan, 2011), which is highly efficient and effective at disrupting sludge cells directly surrounding the probe tip.

In contrast, water-bath sonication is an indirect sonication method where ultrasound energy is transmitted to water and through sample container, thus, the sample is not in direct contact with the energy source. The energy in a bath sonicator spreads diffusely, rather than being highly localised as is the case with the probe sonicator, and only a small fraction of the energy is imparted to each particle in the sample at a given energy input (Malaki et al., 2019). Therefore, a larger energy input is required due to the energy attenuation by water and sample container. Devadasu et al. (2020) reported that, for delignification of *Tectona grandis* saw dust, the specific energy consumption (12.6×10^7 kJ/kg biomass) by a bath-type sonicator (frequency = 22kHz) was almost double that required by a probe sonicator (frequency = 24 kHz) to obtain comparable lignin yields (82-85%) under equivalent condition (biomass loading = 10% w/w, constant treatment duration = 70 min, pulse cycle operation with 15 min on and 10 min off, ultrasound power = 150 W). This could explain why bath sonicators are more typically used for agitation/mixing, liquid degassing and cleaning purposes (Sandhya et al., 2021), rather than size-reduction of particles or microbial cells, which would require relatively long treatment compared to probe sonicators. Hu et al. (2016) compared the effectiveness of bath and probe sonicator on oil extraction and recovery from petroleum sludge in the presence of various organic solvents (including cyclohexane, ethyl acetate, and methyl ethyl ketone). The optimum solvent (cyclohexane) and solvent-to-sludge ratio (4:1 v/w) was similar for both devices. However, longer treatment duration (20 s by probe compared to 15 min by bath) and higher energy consumption (21 W by probe compared to 80 W by bath) was required by bath sonicator to achieve equivalent levels of oil recovery (59.8-62.6%).

A further issue with water-bath sonication is related to heterogeneity of the energy distribution, influencing the reproducibility of the process (Nascentes et al., 2001). Nascentes et al. (2001) indicated that parameters including: water volume, temperature, horizontal and vertical positions of the sample, number of tubes in the bath and sonication duration, impact the distribution of cavitation energy in water-bath sonicators. Thus, the operational conditions must be carefully optimised to ensure the repeatability of a water-bath sonicator. Feasibility of scaling-up the cell disruption process could be much lower compared to probe sonicator.

2) Ultrasound frequency

The ultrasound frequencies emitted by the probe and water bath were 20 and 40 kHz, respectively, and may also contribute to the observed different cell disruption efficiency. The better performance of the probe sonicator may also be explained because it emits a lower frequency ultrasound, which generates larger cavitation bubbles that produce stronger shear forces on implosion in the fluid that are more disruptive to microbial cells, compared to smaller cavitation bubbles formed at high frequencies (e.g. >200 kHz) (Tiehm et al., 2001) (see Section 2.4.2.1.2). Ultrasound frequencies above 30 kHz can also denature the protein

structure of enzymes, mainly because of the marked increase in local pressure and temperature changes caused by the intensive collapse of small cavity bubbles (Yasuda et al., 2010; Nadar and Rathod, 2017). Similar results were also observed by Yu et al. (2009) for ultrasound extraction of extraction of enzymes from AS at a frequency of 20 kHz, which gave yields of approximately 20, 11 and 5 U/g VS for amylase, alkaline phosphatase and acid phosphatase (specific power input =138 W/g TS, duration = 2 min). By contrast, sonication treatment with 40 kHz ultrasound reduced the amylase activity to 16 U/g VS and the other enzymes were not detected under these conditions. Indeed, most studies on enzyme recovery use an ultrasound frequency in the range 20-25 kHz (Nabarlatz et al., 2010; Nabarlatz et al., 2012; Krah et al., 2016).

Furthermore, the intensity of applied ultrasound, necessary to overcome the cohesive forces of the liquid media and achieve a given degree of cavitation to create voids, is correspondingly increased at higher frequencies (Sponer, 1990; Nguyen et al., 2017). This is explained because the cycle of compression and expansion caused by ultrasound is shorter at higher frequencies and, therefore, molecules of the liquid cannot effectively separate to form voids (Subhedar and Gogate, 2013). Consequently, the power requirement to initiate cavitation is much greater for high-frequency sonication (Subhedar and Gogate, 2013). Sponer (1990) proposed that the threshold acoustic intensity (I_t, in W/cm^2) required to initiate a cavitation event is linearly related to the frequency of the ultrasound (f, in MHz), and was expressed by $I_t = 0.9965f - 0.80$ (p-value <0.001, for f ranging from 0.5 to 10 MHz). Nguyen et al. (2017) similarly showed that the threshold pressure of cavitation (P_t, in kPa) was linearly related to the ultrasound frequency (f, in kHz), with $P_t = 0.1255f + 60.25$ (p value <0.001, for f ranging from 22 to 4800 kHz).

In summary, probe-type sonication treatment has several advantages over the bath-type regarding its intensive and localised ultrasonic intensity, and the direct delivery of the ultrasound energy to the samples. Applying a low-frequency probe-type ultrasound device for cell disruption in practice could therefore offer significant benefits by reducing power consumption and increasing the overall enzyme recovery rate, compared to water-bath sonication, which is less feasible for scaling-up the cell disruption process.

4.4.3 Effect of operational conditions on enzyme extraction efficiency by sonication probe

4.4.3.1 Duration, amplitude and energy level

It is necessary to provide suitable conditions that achieve the “lysis threshold” when using ultrasound for cell disruption, which is specific to the type of cells under investigation (Rubin et al., 2018). Optimising the energy level, in particular, is critical to maximise enzyme recovery, but also to minimise energy consumption and therefore cost. The results from the sonication extraction performance analysis (Figure 4-3, 4-4, and 4-5) showed that the optimum duration

was 10 min and power density was 872 W/L. In comparison, reduced durations (2 and 5 min) and power density = 343 W/L were less effective at cellular disruption and enzyme release. This behaviour may be explained because there was insufficient damage to cell membranes and, therefore, relatively poor release of cell membrane bounded enzymes (e.g. protease, see Section 2.3.1) into the extractant buffer solution was observed under these conditions.

Consistent exposure of the sludge cells to cavitation was provided through extended ultrasound treatment time (>=10 min) in this study. Several other studies also demonstrate effective cellular disruption and enzyme release by sonication requires a minimum treatment period >10 min. For example, Zhang et al. (2007) demonstrated effective AS cell lysis occurred after 10 min probe sonication treatment (25 kHz ultrasound, 0.5 W/mL ultrasonic power density, sludge suspension with 1% TS content). Monique et al. (2008) used a probe sonicator (0.75 W/mL power density, ultrasound frequency was not indicated) to recover proteins from AS, and found that protein release (measured by BSA equivalence) increased with ultrasound treatment time, from 100 mg /g VS after 2 min to 160 mg protein/g VS after 10 min.

The sonication probe used in this work was amplitude controlled in terms of the power input (as specified in Section 4.2.2), which means the energy consumption was directly proportional to the amplitude at constant sonication duration. Therefore, the enzyme activities at different amplitudes were standardised and shown in Figure 4-5 as “power density”, and effect of energy level (at corresponding amplitude) was discussed here.

Effect of sonication amplitude on sludge disruption and enzyme extraction was compared at duration = 10 min in Figure 4-5; the results showed that extracted enzyme activity generally increased with increased amplitude (with some inconsistency). The critical energy input level for maximum enzyme release was 872 W/L (with 40% AMP) and enzyme extraction was significantly reduced at energy inputs (343 W/L with 20% AMP) below this critical value (Figure 4-5). Han et al. (2013) also observed the occurrence of a critical energy level for the extraction of EPS by sonication from sewage sludge. In that study, sewage sludge was treated by a probe sonicator to extract LB-EPS (definition see Section 2.3.1), and the sonication treatment was operated at an ultrasound frequency = 25 kHz for 2 min duration, with varying ultrasound energy input (power density ranging 3.2-150 W/10mL sludge). LB-EPS release from AS cells was positively corelated with increased power density, however, significant cell lysis was only observed when the sonication power density was increased to >=35 W/10 mL. Under these conditions the DNA content in the extracted LB-EPS rapidly increased from <1 mg/g dry solid at lower power density (3.2-13 W/10mL sludge) to approximately 6 mg/g dry solid, indicating membrane disruption and release of cellular contents. Indeed, Yu et al. (2009) demonstrated that ultrasound intensity was more important than the duration for controlling the efficiency of enzyme extraction. Thus, the DNA content of crude enzyme extracts was small and <7 mg/g

VS at a fixed specific power input of 138 W/g TS, irrespective of the sonication duration (2 to 20 min). In contrast, at a fixed duration (10 min), the DNA content was significantly increased with increasing power input from 138 to 690 W/g TS, and the maximum DNA release (approximately 15 mg/g TS) was measured at 552 W/g TS.

The data presented in Figure 4-5 show the significant improvement in enzyme activities by 331.2%, 178.1%, 42.8% for protease, α-amylase and cellulase, respectively, with increasing power density from 343 to 872 W/L. However, raising the energy level further slightly improved α-amylase extraction, but had little or no effect on the activities of protease or cellulase. The results therefore showed that showed that enzymes embedded in the TB-EPS or closely attached to the cell surface (such as protease, see Section 2.3.1) can be effectively extracted by increasing the energy input level up to a critical value, and that the efficiency of extracting enzymes which typically locate in easily extracted LB-EPS fraction (such as amylase and cellulase) are also improved.

4.4.3.2 Solids content of sludge

As discussed in Section 2.4.2.1.2, the attenuation of ultrasound energy (and the corresponding vibration intensity) during the sonication treatment process largely depends on the characteristics of the target material, and especially on the solids content. The optimal solids content for disrupting AS determined in this study was approximately 10g VS/L (Figure 4-6), and this was obtained through a five times dilution factor of the AS suspension with buffer solution (i.e. DF = 5).

The decrease in enzyme extraction efficiency at solids concentrations above the optimum value (i.e. DF = 2 and 3) can be explained due to the increase in sludge viscosity (mentioned in Section 4.4.1.1) and, consequently, the greater attenuation of ultrasound energy by large amounts of particulate matter (Tytla and Zielewicz, 2016). Therefore, the optimum solids content and degree of cell disruption are often related to the energy consumption efficiency of the sonication treatment. The attenuation of ultrasound intensity (I) with distance (d) follows an exponential relationship, and can be described by the equation (Majumdar et al., 1998):

$$I = I_0 e^{-\alpha d} \quad \text{(Eq 4-3)}$$

$$\alpha = 8\mu\pi^2 f^2 3\rho C^3 \quad \text{(Eq 4-4)}$$

Where, I_0 is the ultrasound intensity at the tip of the ultrasound source; α is the attenuation coefficient for a given liquid, which depends on the physico-chemical properties of the target liquid (including the density ρ and viscosity μ) and also the characteristics of the ultrasound itself (i.e., the speed of ultrasound in the liquid C and the ultrasound frequency f).

Moreover, cavitation bubble formation within the sludge matrix requires sufficient liquid for vaporisation to take place and, consequently, the development and propagation of cavitation bubbles can be severely limited above the optimum solids content (Show et al., 2007).

On the other hand, solids concentrations below the optimum value may reduce the efficiency of energy utilisation and the economic feasibility of a scaling up the process. Indeed, increasing the DF from 5 to 10 approximately doubled the specific energy input required, from 49.9 to 99.2 kJ/g VS, to maintain a constant vibration amplitude (40% AMP as describe in Section 4.2.3.3), however, no significant increase in specific enzyme activities was observed (Figure 4-6).

4.4.3.3 Surfactant addition

Treatment of microbial cells by chelating agents (EDTA) or surfactants (TX100) disrupts the microenvironment outside the cell, releasing proteins from the EPS (which consists mainly of phospholipids, lipopolysachrides and proteins), and those bound to the cell-wall (e.g. for Gram negative bacteria (Desvaux et al., 2006)). The non-ionic surfactant, TX100, was more effective at enzyme extraction on its own and with sonication, compared to EDTA, which extracted proteins from sludge cells, but no enzyme activity was detected in the crude extract (Figure 4-2). This is probably explained because EDTA chelates with the cations that are involved in maintaining the structural stability of sludge EPS (via ionic bridges, discussed in Section 2.3.1), and also with essential cations of some metalloenzymes (i.e. the metal ion cofactor, see Section 2.2.1), such as Ca^{2+} of amylase, or Zn^{2+} of alcohol dehydrogenase. The simultaneous loss of metal cofactors during cell disruption therefore also leads to the inactivation of these enzymes.

In the optimisation experiments, TX100 showed significant increase in protease activity when combined with sonication, but only a moderate improvement was observed in amylase and cellulase extraction (Table 4-3). The different responses to TX100 addition may be related to the degree of cellular disruption achieved and the corresponding release of enzymes. Indeed, different enzymes are associated with LB- and TB-EPS fractions and this determines their ease of separation from sludge flocs (see Section 2.3.1). Thus, the majority of protease enzymes are tightly attached to the cell wall, whereas amylase and other, related, sugar-degrading enzymes are mainly located in the more easily extractable LB-EPS within the outer layer of EPS (Figure 2-1). Therefore, surfactant treatment increases protease extraction by removing the protective EPS layer, by contrast, amylase and cellulase are present in LB-EPS and are readily extracted directly without TX100 addition.

4.4.4 Effect of activated sludge sampling location on enzyme extraction

In the AS process (illustrated in Figure 2-1), settled sewage from primary wastewater sedimentation (combined with returned AS) is subjected to biological treatment in the bioreactor to remove the non-settleable, soluble and colloidal pollutants. Microbial activity increases and is typically ten times greater at the front of the plug-flow AS process in response to the availability of readily degradable substrates in the influent wastewater compared to the discharge point, where only biologically recalcitrant materials are present (Tchobanoglous et al., 2014). Dehydrogenase is an oxidoreductase that plays an important role in catalysing biochemical reactions for microbial dissimilation. Dehydrogenase is involved in transferring electrons from the substrate to an electron acceptor, usually NAD+/NADP+, in the cell, and its activity is indicative of the rate of electron transport when active microorganisms oxidise organic pollutants in wastewater. There is a strong correlation between dehydrogenase activity and microbial oxygen uptake rate (OUR) (Awong et al., 1985; Bohacz, 2018): increased OUR indicates higher rates of microbiological activity. Consequently, dehydrogenase is frequently used as an effective indicator of the activity of the microbial biomass in AS (Goel et al., 1998b; Feng et al., 2016; Robledo-Mahon et al., 2019). Indeed, the dehydrogenase activities reported here (Figure 4-7) were consistent with the microbial growth observed in plug flow, aerobic biological sewage treatment reactors (Tchobanoglous et al., 2014), where returned AS is activated when combined with the incoming substrate stream in settled sewage, and reduced microbial activity and growth rates are observed near the end of the process as substrates are exhausted and the microbial biomass enters a state of endogenous respiration.

The apparent consistent activities of protease, amylase and cellulase measured at different stages of the aerobic, plug flow sewage treatment reactor (Figure 4-7) indicated that hydrolytic enzymes can be maintained even under conditions of severe nutrient deprivation. This behaviour is explained by a microbial ecological strategy to survive extreme nutrient shortage. Indeed, Kovárová-Kovar and Egli (1998) showed that hydrolytic enzymes involved in bacteria carbon catabolism are active, not only when organic substrates are sufficient at the inlet to the AS process, but also when organic carbon sources are deficient. Thus, a relatively stable concentration of hydrolytic enzymes is maintained within the sludge flocs, mainly in the EPS fraction of the cell, to permit the rapid hydrolysis and assimilation of new substrates when they become available in the surrounding environment, without the need to divert resources to, or wait for, enzyme synthesis. This is also important from a practical perspective because the results demonstrated that AS collected after secondary sedimentation and mechanical thickening was also suitable for enzyme extraction recovery and is easy to sample and had a comparable enzyme activity to mixed liquor from the aeration tank.

4.4.5 Summary of crude enzyme extraction from sludge

Activated sludge contains a wide range of hydrolytic enzymes, and the results presented here showed that:

- Sonication was effective at disrupting AS flocs and releasing hydrolytic enzymes. The optimum operational parameters for AS floc disruption were: 40% AMP (equivalent to an energy intensity of 872W/L) and 10 min duration. The solids content of sludge samples was also an important parameter influencing ultrasonic disruption and optimisation experiments indicated that a solids content of approximately 10g VS/L (DF = 5) provided the maximum enzyme activity. Surfactant addition (1% v/v TX100) enhanced protein release as well as enzyme activity in the AS extract. Under optimum conditions, the recovery rates of protease and cellulase were 63.1% and ~100%, respectively.
- No correlation was found between sludge microbial activity and the activity of hydrolytic enzymes. Therefore, thickened WAS, collected directly following secondary clarification, is a viable and practical source of biomass for enzyme extraction.

5 Consolidation and stabilisation of crude enzymes by cross-linking

5.1 Introduction

Crude enzyme extracts from AS inevitably contain a large amount of water, and their stability in storage and for industrial application is relatively limited. The presence of inhibitory substances, co-extracted from the sludge biomass, can also reduce the activity of crude enzyme mixtures, although, as discussed below, purification treatment also causes performance losses to a certain extent. Nevertheless, the benefits of consolidating and purifying enzymes to upgrade crude AS extracts will enable the development of marketable, high value commercial products from this secondary biomass source. The basic consolidation and purification of enzyme extracts is possible by several chemical precipitation, dialysis, and ultrafiltration techniques, and higher degrees of purity can be achieved by chromatography, electrophoretic systems and gel separation (Sharma et al., 2001).

Free enzymes often show poor storage and operational stability, they are readily inactivated and are difficult to recycle and reuse, which limits their large-scale commercial application (Sahutoglu and Akgul, 2015). Immobilisation of free enzymes is a promising approach to overcome these drawbacks, by enhancing mechanical strength, increasing resistance to denaturation and facilitating recycling of the enzyme catalyst within a reaction system (Katchalskikatzir, 1993; Sheldon and van Pelt, 2013).

Conventional enzyme immobilisation is by chemical or physical binding to an inert carrier (e.g. sepharose, zeolites, silica, agarose, alginate, polyacrylamide, hollow fibres and acrylic resins) via adsorption, entrapment or encapsulation (Bisswanger, 2011b). However, the carrier introduces a large amount of non-catalytic material, typically representing 90 to 99% of the total mass of the enzyme product (Schoevaart et al., 2004), which significantly dilutes the enzyme activity. Cross-linked enzyme aggregates (CLEAs), on the other hand, enable carrier-free immobilisation, by intermolecular cross-linking between adjacent enzyme molecules (shown in Figure 2-8, providing an alternative method to conventional carrier-bound enzyme immobilisation (Cao et al., 2000; Cui et al., 2017; Asgher et al., 2018). CLEAs of protease (Asgher et al., 2018), lipase (Zhu et al., 2021), penicillin acylase (Shah et al., 2006; Wang et al., 2011), α-amylase (Torabizadeh et al., 2014), and laccase (Sinirlioglu et al., 2013) have been produced.

The general process of cross-linking involves aggregation of soluble enzymes through the mechanism of protein precipitation from an aqueous solution after adding an inorganic salt (e.g. $(NH_4)_2SO_4$), an organic solvent (e.g. acetone) or a non-ionic polymer (e.g. PEI), followed

by chemical cross-linking of the aggregated enzymes by a bifunctional reagent, i.e. the cross-linker (see Section 2.6.4). Glutaraldehyde, which contains two aldehyde residues, is one of the most widely used cross-linkers for preparing CLEAs, due to its strong reactivity towards protein moieties, such as amino and thiol groups (see Table 2-3). In some instances, glutaraldehyde cross-linking may lead to severe enzyme inactivation by altering the active centre of the enzyme (Amaral-Fonseca et al., 2018). Therefore, alternative, macromolecular cross-linkers (e.g. dextran aldehyde) have been proposed, which react less aggressively with and, thus, have less destructive effects on, the enzyme molecular structure compared to glutaraldehyde (see Section 2.6.4.2).

One of the advantages of the CLEA technique is that it combines consolidation and stabilisation into a single operation, which can be performed directly on both purified enzymes as well as crude enzyme extracts (Yamaguchi et al., 2018). For example, CLEAs have been successfully produced from crude enzyme solutions extracted from fermentation broths of microorganisms (Lai et al., 2012; Bashir et al., 2018), mung beans (Yu et al., 2013), and fresh fruit (Tandjaoui et al., 2015). Co-immobilisation of multiple enzymes to produce multi-CLEAs and combi-CLEAs (two types of co-immobilised enzyme products, defined in Section 2.6.6.1) have also been reported. For example, Ozacar et al. (2019) produced a multi-CLEA of protease, lipase, and catalase from sunflower seeds, via $(NH_4)_2SO_4$ precipitation (55% w/v), glutaraldehyde cross-linking (100 mM, 17 h at 4 °C) and starch addition (8 mg/mL); the activity recovery of protease, catalase, and lipase in the multi-CLEA was 87, 61, and 60%, respectively.

The consolidation and stabilisation of crude enzymes by cross-linking from AS, an alternative source of biomass rich in hydrolytic enzymes, has not been previously attempted, therefore this research is highly original and novel. Activated sludge is a highly complex matrix containing a wide range of enzyme types, as well as other cellular substances (e.g. proteins and polysaccharides etc) that could interfere with the enzyme cross-linking reaction. Therefore, optimisation of the operational conditions is necessary to maximise the recovery of AS enzymes in the CLEA. Furthermore, the efficiency of CLEA preparation also largely depends on the physicochemical properties of the target enzymes, especially the abundance of the reactive residues that can interact with the cross-linker. Insufficient reactive residues on the enzyme surface often leads to inadequate cross-linking and CLEA formation of low mechanical stability (Cui and Jia, 2015). In such cases the efficiency of cross-linking can be improved by co-aggregation of the enzyme with an inert additive that provides a large number of amino groups (such as BSA and PEI, see Section 2.6.5).

Protein products are formulated into either solid or liquid states for application in biological industries (Robinson, 2015). In general, however, solid-state preparations are preferred

because the absence of water reduces physical and chemical degradation, improving storage stability and shelf-life (Roy and Gupta, 2004), compared to liquid protein formulations. Freeze drying is one approach to concentrating and drying biologically active substances (such as enzymes, proteins and peptide-based drugs (Abdul-Fattah et al., 2007)), but it can also cause damage to the chemical structure due to stresses induced during the freeze-drying-thawing process (Piszkiewicz and Pielak, 2019). Alternatively, preservation of enzyme products is possible by formulating enzymes in a liquid state by suspension in buffer solution.

The aim of this chapter is to develop a protocol to consolidate and stabilise crude enzymes extracted from AS to produce a CLEA product with high catalytic activity. This was achieved through a step-by step procedure to examine the effects of external lysine additive, precipitant type and cross-linker type, and to enable the comparison of different reagents involved in cross-linking chemistry under equivalent conditions. The specific objectives are as follows:

- To select a suitable precipitant and cross-linker to immobilise AS extracted enzymes, and determine the optimum reagent concentrations and reaction duration.
- To determine the effects of additives (including BSA and PEI) on the efficiency of CLEA preparation.
- To determine the enzyme activity recovery rate after cross-linking compared to the original crude extract.
- To compare the effectiveness of preserving the produced CLEA in either solid state (after freeze drying) or liquid state (after suspending in buffer solution), and to examine the storage stability (shelf-life) of the CLEA product under the optimal preservation method.

5.2 Materials and methods

5.2.1 Enzyme preparation

Commercial protease (from *Aspergillus melleus*, activity ≥3 units/mg solid, Sigma-Aldrich) and α-amylase (from *Aspergillus oryzae*, activity up to 1.5 U/mg solid Sigma-Aldrich) solutions were prepared (concentration = 2 and 40 mg solid/mL, respectively) by stirring at room temperature with Tris-HCl buffer (10 mM, pH 7.0), to provide an average volume activity equivalent to 3.66 ± 0.0015 and 8.67 ± 0.012 U/mL (see Section 3.6 for methods and procedures). The enzyme solutions were used in preliminary cross-linking experiments. Subsequently, crude enzyme extract from thickened AS samples, collected from WWTP1 and prepared following procedures described in Chapter 4, was used to optimise the cross-linking of AS enzymes.

5.2.2 CLEA preparation methodology

5.2.2.1 General CLEA preparation process

The principle of CLEA preparation is illustrated in Figure 2-8. In general, the soluble enzyme solution was mixed with a lysine-rich additive (BSA or PEI), followed by a precipitant ($(NH_4)_2SO_4$ or acetone, see Section 5.2.2.2), and continuously stirred by magnetic stirrer for 30 min in an ice-water bath. Cross-linker (glutaraldehyde or dextran aldehyde, see preparation methods described in Section 5.2.2.3) was subsequently added in a drop-wise manner to the required concentration. The mixture was continuously stirred for 3.5 h at room temperature and centrifuged at 10,000g (10 min, 4°C). The sediment was washed three times and re-suspended in Tris-HCl buffer (10 mM, pH 7.0) to the original volume.

5.2.2.2 Chemical precipitation of soluble enzyme

Two contrasting protein precipitants were compared, representing the most widely used reagents for this purpose, including an inorganic salt, $(NH_4)_2SO_4$ (at 80% saturation, which has been frequently adopted in previous studies (e.g. (Yu et al., 2013; Zhou et al., 2017b; Zeinali and Lenjannezhadian, 2018)) for maximised protein/enzyme precipitation efficiency) and the organic solvent, acetone (Section 2.6.3). The detailed procedure for each precipitant is described as follows:

1) Ammonium sulphate

Solid $(NH_4)_2SO_4$ (oven-dried at 107 °C overnight and cooled in a desiccator) was slowly added into the enzyme solution to achieve 80% saturation; the weight of solid $(NH_4)_2SO_4$ required per L of solution was 516 g, which was calculated as follows (Wingfield, 2001):

$$Weight\ (g) = \frac{G_s(S_2 - S_1)}{1 - \frac{V \cdot G_S \cdot S_2}{1000}} \quad \text{(Eq 5-1)}$$

Where,

G_s is the mass of $(NH_4)_2SO_4$ in 1 L of a 100% saturated solution; S_1 and S_2 are the initial and the final saturation of the solution, respectively; V is the apparent specific volume of $(NH_4)_2SO_4$ in a saturated solution. G_s and $V \cdot G_s/1000$ are equivalent to: 515.35 and 0.722 at 0 °C, respectively (Wingfield, 2001).

$(NH_4)_2SO_4$ addition was carried out under continuous stirring in an ice-water bath, to avoid localised high concentrations, which potentially could cause enzyme denaturation (Morris, 2019).

2) Acetone

Cold acetone (analytical grade, Sigma-Aldrich, stored at -20 °C) was added to the enzyme solution at a volume ratio equivalent to 4:1 by continuous stirring for 30 min in an ice-water

bath. Mixing organic solvents into aqueous solutions is an exothermic process (Section 2.6.3.3), therefore, addition of cold acetone reduces potential heat generation and the risk of protein denaturation.

5.2.2.3 Cross-linking of the precipitated enzymes

The effectiveness of two chemical cross-linkers was quantified in different sets of experiments, including: (1) glutaraldehyde, prepared by diluting a proprietary chemical (50% w/v aqueous solution, Sigma-Aldrich) with RO water to 5% w/v; and (2) dextran aldehyde, which is a macromolecular polyaldehyde prepared from dextran via periodate oxidation, as described by Mateo et al. (2004). Dextran 1.65 g (average MW = 150000 Da) was dissolved in 50 mL of RO water and 3.85 g sodium metaperiodate was added. The solution was stirred at room temperature for 90 min, and purified by five dialysis cycles, each for 2 h, against 5 L RO water at room temperature using dialysis tubing (Sigma-Aldrich, MW cut-off = 12400 Da, average diameter = 20 mm, capacity = 100 mL/ft). The final volume of the dextran aldehyde was approximately 56 mL (exact volumes were measured in each case). The periodate oxidation process was performed in the dark to prevent the photolysis of periodate (Hermanson, 2013a).

5.2.3 Preliminary tests

5.2.3.1 Precipitation of AS enzymes by $(NH_4)_2SO_4$

Ammonium sulphate is frequently reported as the preferred precipitant for enzyme recovery, and was therefore selected to precipitate AS enzymes in the preliminary experiments. The crude AS enzyme solution was precipitated with 80% saturated $(NH_4)_2SO_4$ following the methods described in Section 5.2.2.2. The precipitate of AS enzymes was harvested by centrifugation (10000 g, at 4 °C for 15 min), and resuspended in Tris-HCl buffer (10 mM, pH 7.0) to the original volume.

The soluble protein contents in crude AS solutions and supernatants after centrifugation were measured by the Lowry method (Section 3.5.1). Precipitation efficiency (%) was quantified as the percentage of protein content in the enzyme precipitate relative to the total soluble protein content in the crude AS enzyme solution, as follows:

$$\frac{\text{Protein content in the crude AS enzyme solution - Protein content in supernatant}}{\text{Protein content in the crude AS enzyme solution}} \times 100\% \qquad \text{(Eq 5-2)}$$

Residual activity of α-amylase and protease was expressed as the percentage of the enzyme activities in the precipitate relative to the crude AS enzyme solution (the procedure is described in Section 3.6).

5.2.3.2 CLEA preparation from commercial protease with $(NH_4)_2SO_4$ precipitation

Commercial protease was used as the enzyme source to determine the optimal parameters in preliminary tests for CLEA preparation with 80% saturated $(NH_4)_2SO_4$ precipitation. The

solution of commercial protease enzyme was mixed with BSA or PEI and the CLEA was prepared following the procedures described in Section 5.2.2, and the experimental conditions are summarised in Table 5-1. Group 1 is the control group (without BSA or PEI addition to the enzyme solution). The volume activity of the CLEAs and washed supernatants after washing (three times) was measured, and the protease activity recovery rate after cross-linking, R_{CLEA} *(%)*, (expressed in the following equation) was compared.

$$R_{CLEA}\% = \frac{Activity\ in\ the\ CLEA}{Activity\ of\ the\ original\ enzyme\ solution} \times 100\% \quad \text{(Eq 5-3)}$$

Table 5-1 Summary of experimental conditions for CLEA preparation from commercial protease enzyme, with 80% saturated $(NH_4)_2SO_4$ as the precipitant and glutaraldehyde as the cross-linker

No.	Additive	Additive concentration (mg/mL)	glutaraldehyde concentration (w/v)	Cross-linking condition
1	None	None	0.20%	3.5 h, RT
2	BSA	0.55	0.20%	3.5 h, RT
3	PEI	0.65	0.20%	3.5 h, RT
4	BSA	0.55	0.50%	3.5 h, RT
5	PEI	0.65	0.50%	3.5 h, RT
6	BSA	2	0.20%	3.5 h, RT
7	BSA	5	0.20%	3.5 h, RT
8	BSA	10	0.20%	3.5 h, RT
9	BSA	2	0.20%	6 h, RT
10	BSA	5	0.20%	6 h, RT
11	BSA	10	0.20%	6 h, RT

Note: BSA, bovine serum albumin; PEI, polyethylenimine; RT, room temperature.

5.2.3.3 CLEA preparation from commercial amylase with acetone precipitation

Commercial amylase was used as the enzyme source to determine the optimal parameters for preliminary CLEA preparation with acetone precipitation. The commercial amylase solution was mixed with BSA (2 and 5 mg/mL) and precipitated by acetone (4:1 v/v, see Section 5.2.2.2), followed by cross-linking with 0.2% w/v glutaraldehyde for 3.5 h at room temperature. The volume activity of the CLEAs and washed supernatants after washing (three times) was

measured, and the amylase activity recovery rate (R_{CLEA}%, see Eq 5-3) after cross-linking was compared to the control group (without BSA addition). Precipitation efficiency of amylase by acetone in the control group (under equivalent conditions without BSA) was also measured according to Eq 5-2.

5.2.4 CLEA preparation from crude AS enzyme extracts

5.2.4.1 Enzyme cross-linking by glutaraldehyde

The crude, extracted AS enzyme solution was mixed with BSA (5 mg/mL) and subjected to the CLEA preparation process, by precipitation with 80% saturated $(NH_4)_2SO_4$ at 0 °C for 30 min and cross-linking with increasing concentrations of glutaraldehyde (from 0.005% to 2.0%) at room temperature for 3.5 h. The effect of glutaraldehyde concentration on CLEA preparation was quantified using amylase as an indicator, since the largest overall activity was detected for this enzyme in crude AS extracts (see Figure 4-8). The activities of amylase, and of the other main target enzyme types, including: protease, lipase and cellulase, were subsequently measured at the optimum concentration of glutaraldehyde determined from the amylase activity. Enzyme activity assays were performed following the procedures described in Section 3.6.

5.2.4.2 Enzyme cross-linking by dextran aldehyde

Crude, extracted AS enzyme solution was mixed with BSA (5 mg/mL). The precipitants, $(NH_4)_2SO_4$ and acetone, were used following the procedures described in Section 5.2.2.2 and cross-linking of the precipitated enzymes was performed with dextran aldehyde at room temperature for 3.5 h. The concentrations of dextran aldehyde were in the range: 0.01 to 0.28% w/v for $(NH_4)_2SO_4$ and 0.01 to 0.20% w/v in the case of and acetone. The activities of protease, lipase, amylase and cellulase were measured before and after cross-linking by dextran aldehyde. Enzyme activity assays were performed following the procedures described in Section 3.6.

5.2.5 Fourier-transform infrared spectroscopy

Fourier-transform infrared (FTIR) spectrophotometry (Magna 560, Nicolet Instrument Corporation, US) was used to examine: (1) the oxidation of dextran into dextran aldehyde (process illustrated in Figure 2.12) and (2) formation of new chemical bonds after cross-linking of the AS enzymes under the optimised preparation conditions.

The FTIR spectrum of freeze-dried dextran (before and after periodate oxidation) in comparison to glutaraldehyde is shown in Figure 5-1. Dextran prior to periodate oxidation showed characteristic bands at 912, 998, 1099 and 1151 cm^{-1}, representing stretching of C-N, C-C and C-O bonds within dextran α (1-6) glycosidic linkages (Ahmed et al., 2012). Dextran was chemically modified by periodate oxidation treatment by reducing the peak at 912 cm^{-1},

shifting the peak at 998 to 1016 cm^{-1}, and simultaneously increasing peaks at 2156, 2028 and 1976 cm^{-1}, which was probably explained by ketene C=C=O stretching (Sigma-Aldrich, 2020), compared to untreated dextran. The FTIR profile of oxidised dextran was similar to glutaraldehyde, indicating the successful oxidation of the α (1-6) glycosidic bonds and introduction of carbonyl groups into dextran molecules.

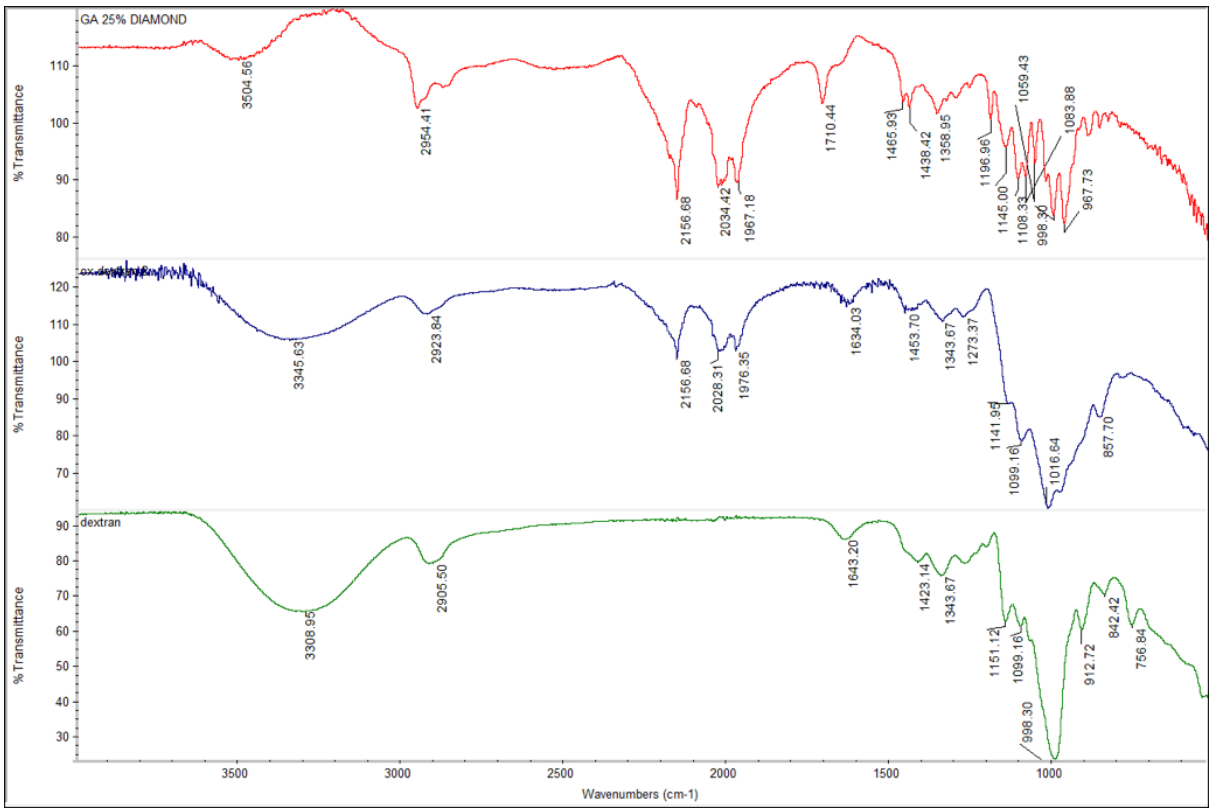

Figure 5-1 FTIR spectra in 4000–500 cm^{-1} region of glutaraldehyde (red line), periodate oxidised and dialysed dextran aldehyde (blue line), and untreated dextran (green line)

5.2.6 CLEA morphology

The morphology of the soluble enzyme and immobilised CLEA was examined by scanning electron microscopy (SEM; Sigma 500 VP Field Emission-Scanning Electron Microscope, Zeiss, Germany). The crude enzyme extract and the CLEA were produced under corresponding optimal conditions and were prepared for scanning by freeze drying.

5.2.7 Preservation of prepared CLEAs

CLEAs of AS enzymes were prepared following the optimised procedure (see Section 5.3.2.3). Two methods of preserving the CLEAs were compared and the residual enzyme activity of the CLEA (% relative to the activities of the fresh prepared CLEA suspension measured at Day 0) was measured after the storage time:

1) Suspension in buffer solution: CLEAs were resuspended in Tris-HCl buffer (10 mM, pH 7.0) to original volume (compared to the crude enzyme extract) and stored at 4 °C in a

fridge. The activity of protease, lipase, amylase and cellulase was measured after 12, 20 and 27 days of refrigerated storage.

2) Freeze-drying: CLEAs were dried for three consecutive days in a freeze dryer (Modulyo 4K; Edwards, UK) and the solid residue was stored in an air-tight container at -20 °C in a freezer. The CLEA powder was resuspend in Tris-HCl buffer (10 mM, pH 7.0) to original volume and the activities of protease, lipase, amylase and cellulase were determined immediately after freeze drying and after 40 days of storage in the freeze-dried condition.

5.3 Results

5.3.1 Preliminary tests

5.3.1.1 Precipitation of AS enzymes by $(NH_4)_2SO_4$

The precipitation efficiency of AS enzymes by 80% saturated $(NH_4)_2SO_4$, as well as residual amylase and protease activities in the precipitate, are shown in Table 5-2. More than 90% of soluble proteins, and 92.7% of protease activity, were recovered from the crude AS enzyme solutions by $(NH_4)_2SO_4$ precipitation. However, no α-amylase was detected in the precipitate.

Table 5-2 Precipitation efficiency and residual activity of protease and α-amylase in the precipitate

Crude AS enzyme extract		Precipitated AS enzymes	
Soluble protein content (μg/mL)	1337.50 ± 975.00	Precipitation efficiency (%)	92.9±0.00
Protease (U/mL)	0.053 ± 1.81 ×10^{-7}	Residual protease (%)	92.7±0.01
α-Amylase (U/mL)	0.291 ± 4.52×10^{-5}	Residual α-amylase (%)	Not detected

Note: values shown as mean values ± standard deviation of three replicated measurements.

5.3.1.2 CLEAs of commercial protease with $(NH_4)_2SO_4$ precipitation

As precipitation with $(NH_4)_2SO_4$ inactivated the amylase activity, commercial protease enzyme was used in preliminary investigations to determine the optimal parameters for CLEA preparation with 80% saturated $(NH_4)_2SO_4$ precipitation. These were also examined: (1) the effect of glutaraldehyde concentration (0.2 and 0.5% w/v) and duration (3.5 h and 6 h) on cross-linking and (2) the effects of additive compounds, BSA and PEI; the results are shown in Figure 5-2:

(1) Effect of additive:

The additive type and concentration had a profound influence on the enzyme activity recovery rate. Addition of PEI (0.65 mg/mL) into the enzyme solution at a glutaraldehyde cross-linker concentration of 0.2% w/v (Group 3, Figure 5-2) did not show a significant effect on the cross-

linking efficiency compared to the control (Group 1, Figure 5-2), and protease recovery in the CLEA fraction in these treatments was equivalent to 17.1 and 13.7%. Indeed, PEI addition apparently reduced the overall protease activity (sum of the activity in the CLEA and three washed supernatants, relative to the original enzyme solution) to 31.6%, which was approximately 50% of the value obtained for the control group (72.2%).

By contrast, BSA addition at 0.55 mg/mL (Group 2, Figure 5-2) increased the protease activity recovered in the CLEA (at 0.2 % glutaraldehyde) compared to the control by approximately 50%, but the majority of the enzyme activity (44.1% compared to the original enzyme solution) was detected in the first washed supernatant, indicating a relatively modest degree of cross-linking. Raising the BSA concentration to 2 mg/mL (Group 6, Figure 5-2) increased the cross-linking efficiency compared to the control by a factor of approximately four and, in this case, greater activity was retained in the CLEAs compared to the supernatant solutions after washing. Increasing the BSA concentration (Group 7 and 8, Figure 5-2) further had relatively little and no significant effect on the enzyme recovery in the CLEA compared to Group 6 ($P > 0.05$).

(2) Effect of cross-linker concentration:

Increasing glutaraldehyde concentration from 0.2% to 0.5% w/v with BSA addition reduced the total enzyme activity recovery and enzyme recovery in the CLEAs (R_{CLEA}%) from 75.8 to 40.2%, and 21.7 to 13.0%, respectively, relative to the crude enzyme solution (Group 2 and 4, Figure 5-2). A similar pattern was also observed between Group 3 and 5 with PEI addition (Figure 5-2) and, in this case, the total enzyme activity recovery and enzyme recovery in the CLEAs was reduced by approximately 58%.

(3) Effect of cross-linking reaction duration:

No significant effect ($P > 0.05$) of increasing the cross-linking reaction time from 3.5 to 6 h was detected on the enzyme activity recovery rate. Nevertheless, protease recovery in the CLEAs decreased to a small extent after 6 h, to a mean value of 51.8% (Group 9-11, Figure 5-2), compared to 55.9 % at 3.5 h (Group 6-8, Figure 5-2).

Amongst all the treatment conditions tested, the lowest total enzyme activity recovery (13.4%) and enzyme recovery in the CLEAs (7.5%) was obtained under the treatment conditions in Group 5. This behaviour could be explained by an interaction between the higher glutaraldehyde concentration (0.5% w/v) and PEI additive (0.65 mg/mL), compared to the other treatment groups. On the other hand, the highest overall cross-linking efficiency was obtained for CLEAs of protease prepared by cross-linking with 0.2% w/v glutaraldehyde (3.5 h, at room temperature) and 5 mg/mL BSA addition (Group 7, Figure 5-1), which gave, an enzyme activity recovery equivalent to 56.5% in the CLEA and relatively small recoveries of

3.54, 6.44, 6.79% in the first, second and third washing supernatant, respectively. The CLEA of commercial protease prepared under this condition had an orange-yellow colour and was readily separated from the buffer solution by gravity sedimentation or rapid centrifugation (shown in Figure 5-3).

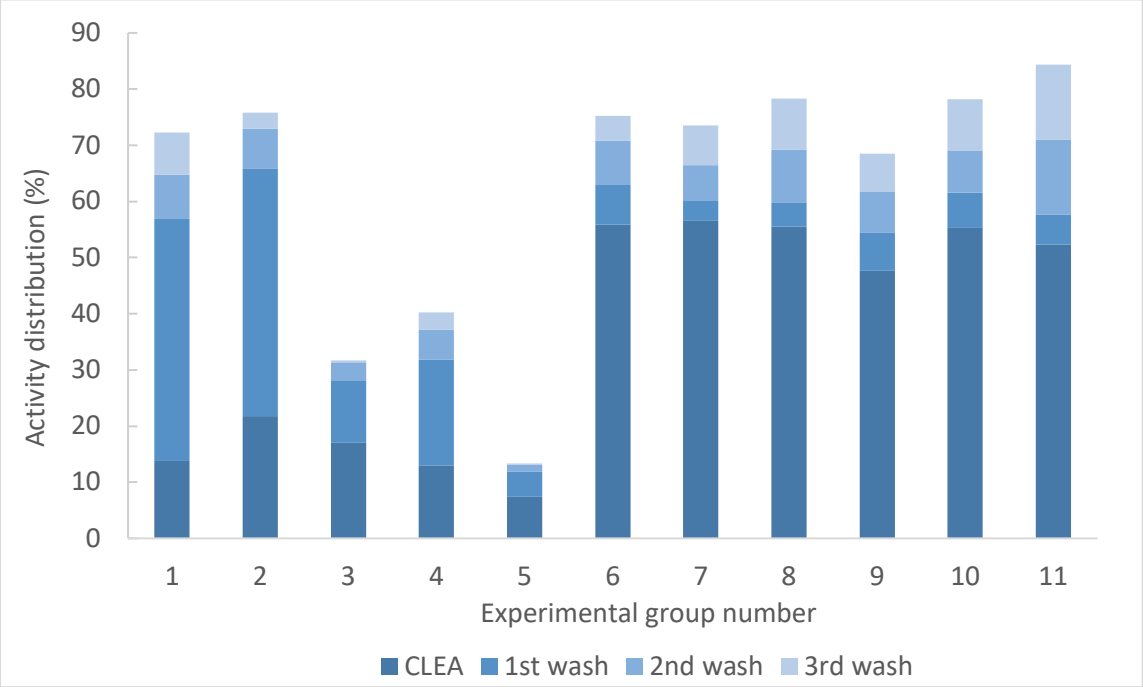

Figure 5-2 Distribution of protease activity in CLEA, and supernatants after the 1st, 2nd and 3rd wash (volume activity in original enzyme solution was set as 100%); group number corresponds to the experimental conditions shown in Table 5-1; mean values of two replicate measurements

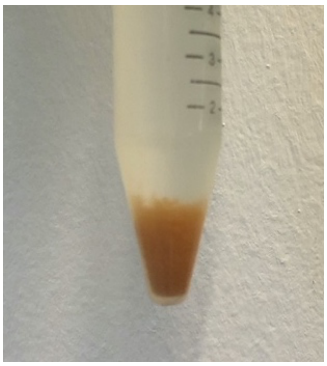

Figure 5-3 CLEA of commercial protease enzyme prepared with 5 mg/mL BSA addition, 80% saturated $(NH_4)_2SO_4$ precipitation, and 0.2% glutaraldehyde cross-linking for 3.5 h at room temperature

5.3.1.3 CLEAs of commercial amylase with acetone precipitation

Acetone was used as an alternative precipitant to prepare CLEAs of commercial amylase. Unlike $(NH_4)_2SO_4$, which inactivated the amylase enzyme (Section 5.3.1.1), acetone (4:1 v/v) precipitation recovered approximately 76.9% of the enzyme from solution without additives

(other experimental conditions were equivalent to Section 5.3.1.1). Torabizadeh et al. (2014) also reported the increased efficiency of organic solvents for enzyme precipitation compared to $(NH_4)_2SO_4$. Thus, ethanol, acetone, acetonitrile, isopropanol and tert-butanol (all at v/v of enzyme:solvent of 1:9) recovered 67-99% of free enzyme activity of thermostable α-amylase after precipitation at 0 °C for 20 min, and the highest overall precipitation efficiency was obtained for tert-butanol (Torabizadeh et al., 2014). By contrast, the recovery with saturated $(NH_4)_2SO_4$ under equivalent conditions was 56.1%.

The effect of BSA addition at 2 and 5 mg/mL on CLEA preparation with commercial amylase enzyme was also investigated and compared to the control group without BSA addition. No CLEA formation occurred in the control group in the absence of BSA. By contrast, increasing BSA concentration from 2 and 5 mg/mL significantly ($P < 0.05$) increased the recovery of amylase activity to 2.33% and 5.12% (relative to the initial enzyme solution), and no amylase activity was detected in the wash supernatants.

5.3.1.4 Summary of the preliminary experiments

Activities of protease and amylase, representing two major hydrolytic enzyme types in the crude AS solution (see Section 4.3), were measured as indicators for the preliminary optimisation of CLEA preparation from AS.

Additive type and concentration had a major influence on the recovery rate of the enzymes in the CLEAs. BSA was more effective for preparing CLEA of commercial protease (with $(NH_4)_2SO_4$ precipitation) compared to PEI, and approximately 56% of the protease activity was recovered in the CLEA at BSA concentration = 2 mg/mL. However, increasing the BSA concentration further to 5 and 10 mg/mL did not further or significantly ($P < 0.05$) improve protease activity recovery in the CLEA. Addition of lysine-rich BSA facilitated the formation of stable CLEAs of amylase, and increasing BSA addition from 2 to 5 mg/mL almost doubled amylase activity recovered in the CLEAs (with acetone precipitation). Therefore, BSA addition at 5 mg/mL was adopted in subsequent experiments.

Both $(NH_4)_2SO_4$ and acetone precipitants were used in the preparation of CLEAs from crude AS extracts. $(NH_4)_2SO_4$ precipitated >92% of the protease from the crude AS enzyme solution, but inactivated amylase in the absence of the BSA. However, the results showed that acetone can used as an effective, alternative precipitant for amylase CLEA, and >76% of amylase activity was preserved with this precipitant.

High glutaraldehyde concentrations (0.5% w/v) reduced the enzyme recovery rate in the CLEA compared to lower concentrations (0.2% w/v) and further work was undertaken to optimise the cross-linker concentration used in CLEA preparation of AS extracts. Increasing the cross-linking duration (6 h) had no effect on the enzyme activity recovery in the CLEA compared to

the shorter period of 3.5 h, which was therefore selected in subsequent experiments on CLEA preparation from AS.

5.3.2 CLEAs of AS extracted enzymes

5.3.2.1 Cross-linking with glutaraldehyde

The effect of glutaraldehyde concentration on CLEA preparation was investigated with BSA addition (5 mg/mL) and precipitation with 80% saturated $(NH_4)_2SO_4$ and the results are shown in Figure 5-4. Amylase was selected for investigating CLEA preparation from AS as this enzyme has the highest overall activity rate in AS extracts, compared to the other enzyme types examined (see Section 4.3.6). Amylase activity in the CLEA increased significantly with decreasing concentration of glutaraldehyde to 0.04% and remained relatively consistent as the concentration decreased further to a minimum value of 0.005% w/v glutaraldehyde (Figure 5-4). A slight improvement in activity, to a value equivalent to 19.0%, relative to the crude enzyme extract, was obtained at the smallest concentration of glutaraldehyde, but the overall mean activity in this range was equivalent to 17.6%. No amylase activity was detected in the CLEAs prepared using concentrations in the range 0.3-2.0% w/v, which may be explained because amylase was fully inactivated at these levels of glutaraldehyde. A linear relationship ($R^2 = 0.96$ and $P < 0.001$) was found between CLEA activity recovery rate (R_{CLEA}%, defined in Section 5.2.3) and glutaraldehyde concentration (C_{GA}): $R_{CLEA} = -64.37C_{GA} + 0.1847$, with $0.005\% \leq C_{GA} \leq 0.3\%$ w/v.

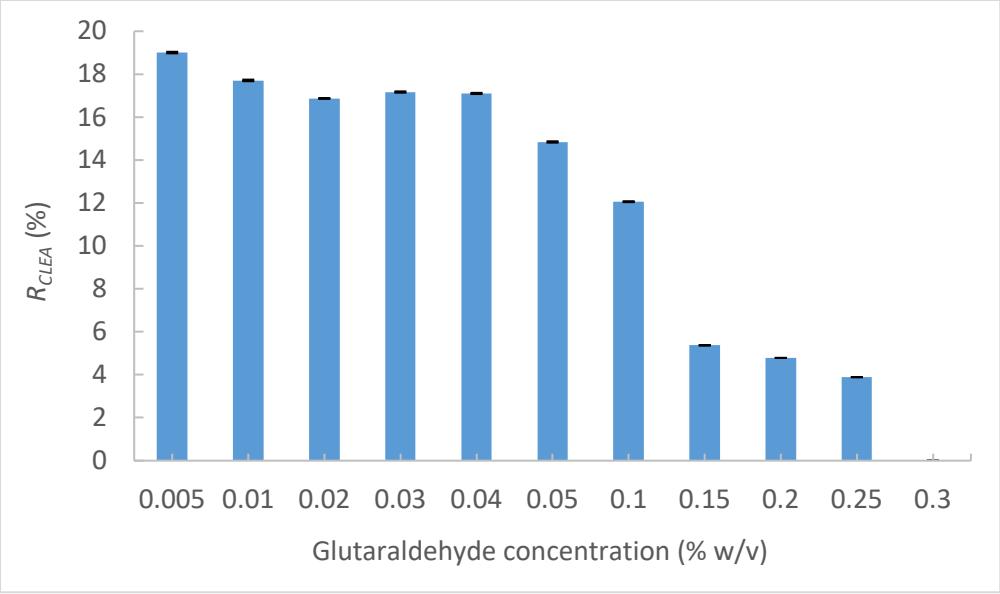

Figure 5-4 Effect of glutaraldehyde concentration on amylase activity of CLEA prepared from crude AS extracts with 5 mg/mL BSA addition and precipitation with 80% saturated $(NH_4)_2SO_4$ (R_{CLEA}: volume activity in original enzyme solution was set as 100%; error bars represent the standard deviation)

Solid-liquid separation of the CLEAs prepared with 0.05-0.3% w/v glutaraldehyde was observed after overnight storage in the fridge (Figure 5-5); however, greater settleability at higher glutaraldehyde concentrations corresponded with decreased enzyme activity recovery rate (Figure 5-4). Therefore, this observed behaviour suggested the formation of denser aggregates (with larger particle size) was associated with excessive cross-linking of the enzymes in the presence of increasing amounts of the cross-linker. Chaudhari and Singhal (2017) similarly observed the formation of denser CLEAs and corresponding reduced activity of cutinase (a hydrolytic enzyme that can hydrolyse a variety of xenobiotic synthetic polymer esters) at high levels of glutaraldehyde cross-linking.

By contrast, CLEAs produced at lower glutaraldehyde concentrations (<0.05% w/v) remained suspended to an extent in the buffer solution after overnight standing, indicating a relatively smaller particle size compared to concentrations ≥0.05% w/v. Therefore, a concentration of 0.04% w/v glutaraldehyde was selected as the optimal condition, as this provided amylase activity representative of the maximum range. Furthermore, whilst smaller concentrations of the cross-linker gave similar enzyme activities, 0.04% w/v was also selected to reduce the potential chemical instability of the CLEA and leaching of enzymes from the cross-linked aggregates, which may arise due to insufficient cross-linking at low levels of glutaraldehyde (Graebin et al., 2018). The activity recovery rate (relative to the crude enzyme extract, R_{CLEA}) of amylase, protease, lipase, and cellulase in the CLEAs at 0.04% w/v glutaraldehyde was measured and 17.5% and 23.6% of amylase and lipase was recovered, respectively, however, no protease or cellulase activity was detected in the CLEAs.

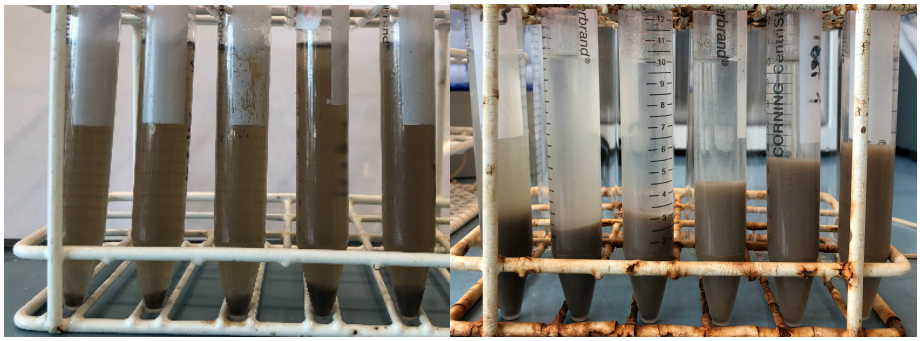

Figure 5-5 Effect of glutaraldehyde concentration on solid-liquid separation of CLEAs prepared from AS extracts with 5 mg/mL BSA addition and precipitation with 80% saturated $(NH_4)_2SO_4$. Glutaraldehyde concentrations (% w/v) (left to right): 0.005, 0.01, 0.02, 0.03, 0.04, 0.05, 0.1, 0.15, 0.2, 0.25 and 0.3.

5.3.2.2 Cross-linking with dextran aldehyde

5.3.2.2.1 Precipitation by 80% saturated $(NH_4)_2SO_4$

The effect of dextran aldehyde concentration on CLEA preparation in combination with enzyme precipitation with 80% saturated $(NH_4)_2SO_4$ precipitation and 5 mg/mL BSA addition

is shown in Figure 5-6(a). The highest amylase activity recovery (27.5% relative to the crude enzyme solution) was obtained at 0.08% w/v dextran aldehyde and increasing the concentration up to a maximum value equivalent to 0.28% w/v reduced the recovery rate to approximately 20.1%. The dextran aldehyde concentration had a more profound influence on activity of protease and lipase compared to amylase. Protease activity in the CLEAs was undetectable at dextran aldehyde concentrations of 0.01% and 0.04% w/v, and significantly increased to 20.4% and 25.7% with increasing concentration to 0.08% and 0.12% w/v, respectively. Protease activity was reduced by approximately 50% at the largest dextran aldehyde concentrations used (0.24 and 0.28% w/v) compared to the maximum rate of activity measured. A similar behaviour was also observed for lipase, which also showed the highest activity recovery rate (26.3%) at 0.12% w/v of dextran aldehyde.

5.3.2.2.2 Precipitation by 4:1 acetone

Effect of dextran aldehyde concentration on CLEA preparation with 4:1 acetone precipitation and 5 mg/mL BSA addition is shown in Figure 5-6(b). Amylase, protease and lipase activity in the CLEA increased to maximum values equivalent to 42.6%, 48.3% and 54.4%, respectively, with increasing dextran aldehyde concentration to 0.04% w/v. However, increasing the dextran aldehyde concentration to 0.2% w/v further decreased the activities of amylase, protease, and lipase, to varying degrees. Protease and amylase showed the most severe decline in activity (by 100%), compared to the maximum rate, whereas lipase activity was reduced by a smaller extent (by 68.9%). By contrast, the activity recovery of cellulase was not significantly affected by dextran aldehyde concentrations of 0.04% w/v and above (P > 0.05, except for the inconsistent response obtained at 0.16% w/v) and was in the range 31.0 to 35.1%.

The results also demonstrated that the activity recovery rate of amylase, protease and lipase in the CLEA prepared from AS extracted enzymes by precipitation with the organic solvent, acetone, was almost twice that compared to the inorganic salt, $(NH_4)_2SO_4$. Furthermore, no cellulase activity was detected with $(NH_4)_2SO_4$ precipitation, however, an activity recovery rate for cellulase equivalent to 31% was obtained with ≥0.04% dextran aldehyde concentration using acetone as the precipitant.

(a)

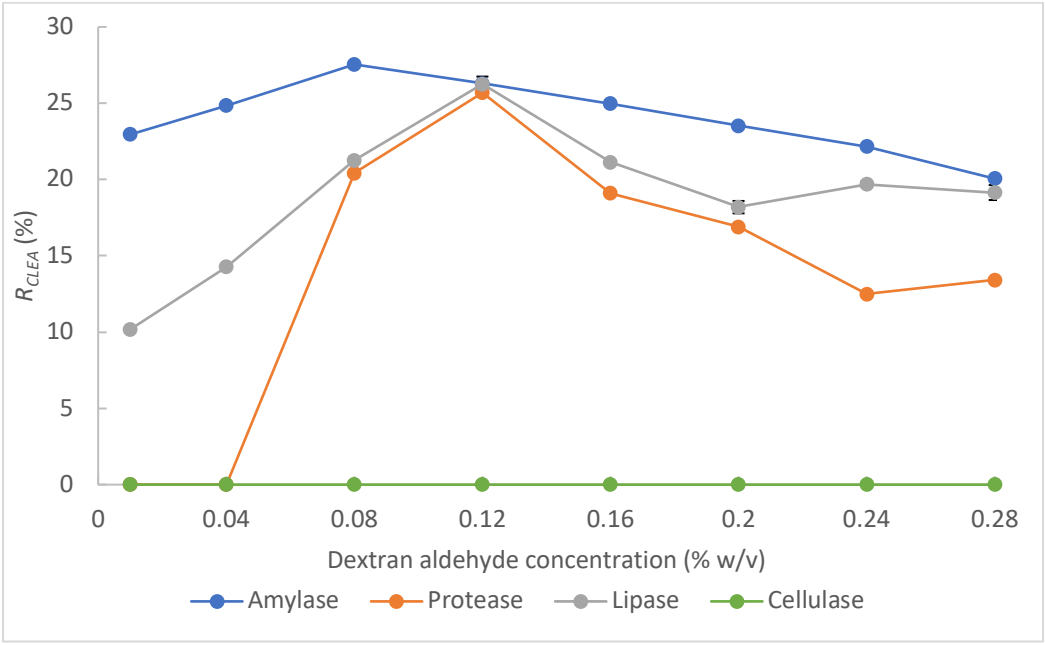

(b)

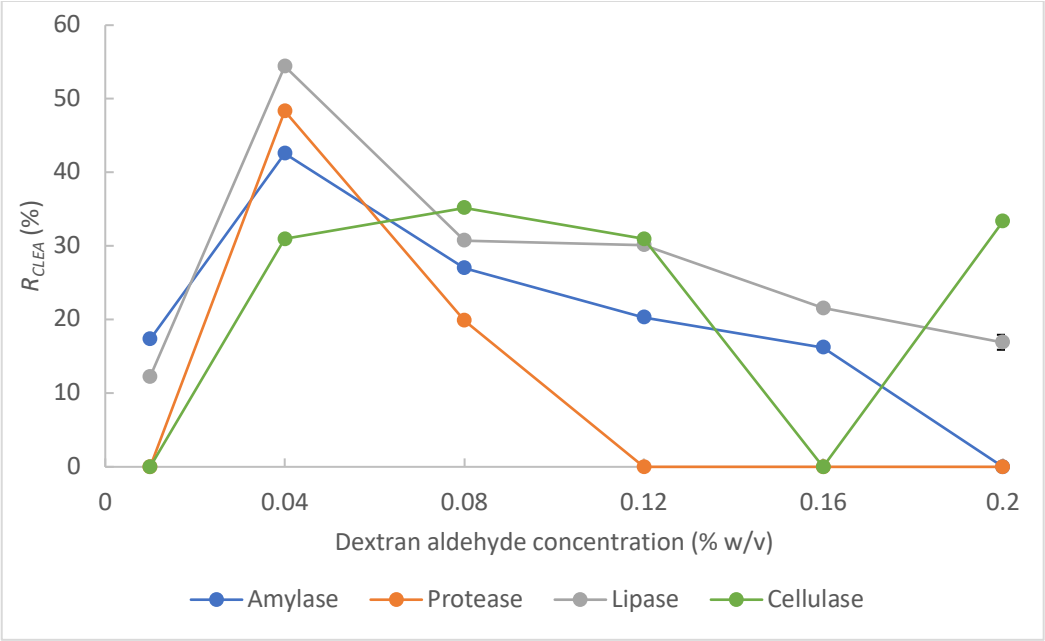

Figure 5-6 Effect of dextran aldehyde cross-linker concentration on activities of four different enzymes in CLEA prepared from AS extracts with 5 mg/mL BSA addition and precipitation with (a) 80% saturated $(NH_4)_2SO_4$ or (b) 4:1 acetone (R_{CLEA}: volume activity in original enzyme solution was set as 100%; error bars represent the standard deviation)

5.3.2.3 Summary of optimal conditions for CLEA preparation from crude enzyme extracts from AS

The largest overall enzyme activity recovery rates in CLEAS prepared from crude AS enzyme extracts (Figure 5-4, 5-6) were obtained with acetone precipitation (volume ratio = 4:1, 0.5 h at 0 °C), dextran aldehyde cross-linking (0.04% w/v, 3.5 h at room temperature), and 5 mg/mL BSA addition. These conditions were therefore selected to produce CLEAs of enzyme extracts from AS.

5.3.3 FTIR analysis

The FTIR spectra (Figure 5-7) showed notable conformational changes in the secondary structure of AS enzymes after CLEA preparation, confirming the occurrence of the cross-linking reaction. Presence of typical peaks for protein polypeptides (i.e. amides) were observed for both soluble enzymes and the CLEA, with their respective assignments listed in Table 5-3. In general, the multiple peaks between 1000 and 1700 cm^{-1} are recognised as different bending and stretching vibrations associated with C-O, C-C, C-N, C=O and N-H linkages of enzyme molecules (Chaudhari and Singhal, 2017). In particular, the peaks at 1628 cm^{-1} (which could be assigned to lysine NH^+ and/or NH_3^+ asymmetric bending (Kong and Yu, 2007)), 1505 cm^{-1} (which could be assigned to N-terminal, e.g. $-NH_2$ and $-NH_3^+$ (Kristoffersen et al., 2020)) decreased in the CLEA, compared to the crude AS enzyme extract. By contrast, the peak at 1634 cm^{-1} (imine C=N stretching) increased in the CLEA, confirming the formation of Schiff's base linkage between amino groups of the enzyme and the aldehyde groups of the cross-linker (see Figure 2-9).

The appearance of the peak at 1520 cm^{-1} (Figure 5-7) can be attributed to the formation of positively charged, quaternary-amino groups in the cross-linked enzymes (Li et al., 2013). Similarly, Hero et al. (2018) also observed the appearance of a peak at 1547 cm^{-1} in the CLEA of xylanase (produced by 60% saturated $(NH_4)_2SO_4$ precipitation and 0.5% glutaraldehyde cross-linking). The peak representing amide/amine C-N and N-H was shifted from 1245 cm^{-1} in the crude enzyme extract to 1235 cm^{-1} in the CLEA (Figure 5-7), probably due to the conformational sensitivity of these chemical bonds (Hero et al., 2018). Li et al. (2013) and Chaudhari and Singhal (2017) also observed shifts of amide bands in FTIR spectra of chitosan and cutinase cross-linked with glutaraldehyde, respectively.

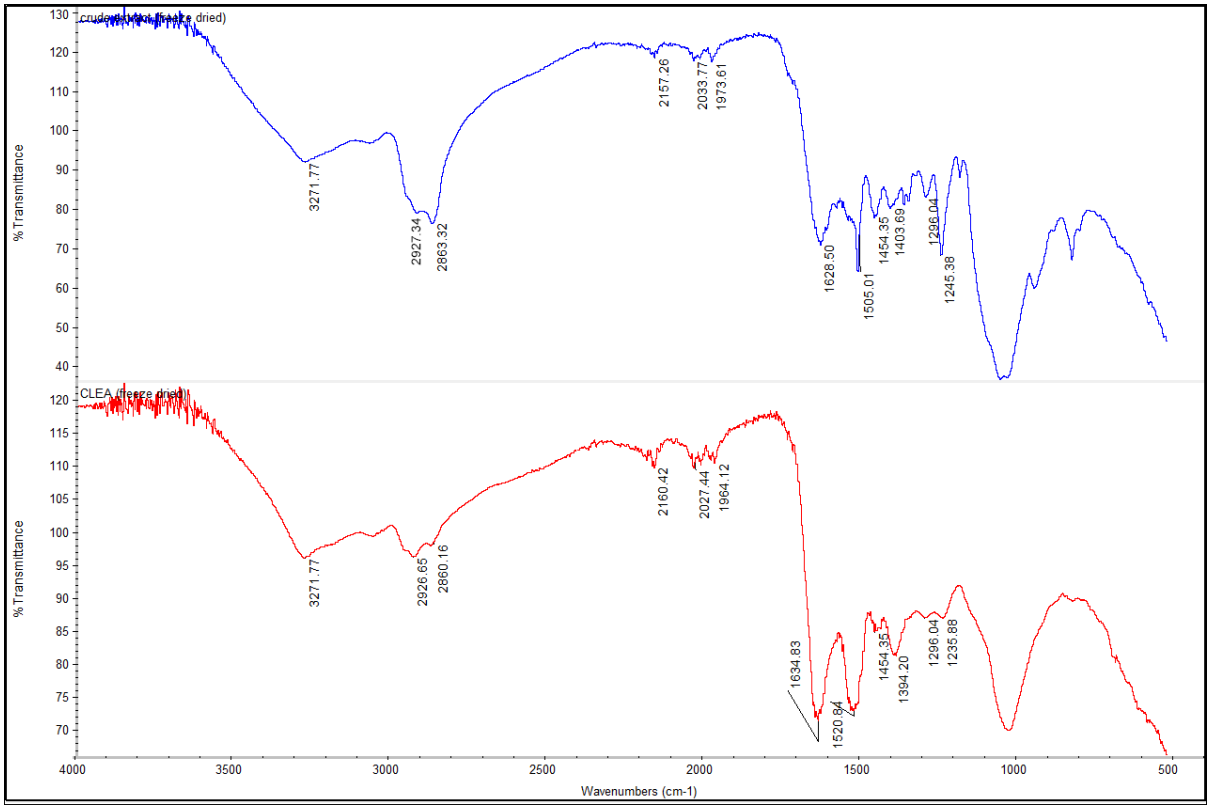

Figure 5-7 FTIR spectra in 4000–500 cm $^{-1}$ region of freeze-dried crude AS enzyme solution (blue line), and the CLEA prepared under optimal conditions (red line)

Table 5-3 FTIR peaks and bands relevant to the conformational changes after CLEA preparation of AS enzymes

Class and groups	Assignments	Band/peak position (wavenumber, cm^{-1})	
		Free enzyme	CLEA
Amide	N-H stretching	3271	3271
Aliphatic; amine salt	C-H stretching; N-H stretching	2863-2927	2860-2926
Amide	C=O stretching, N-H bending and C-N stretching	1628	1634
Imine (Schiff's Base)	C=N stretching	-	1634
Amide	N-H bending and C-N stretching	1505	1520
Amide/amine	N-H Bending and C-N stretching, along with C-H and N-H deformation	1245	1235

Note: the tentative assignments are based on literature values (Kong and Yu, 2007; Parida et al., 2011; Baldino et al., 2015; Chaudhari and Singhal, 2017; Hero et al., 2018; Kristoffersen et al., 2020; Sigma-Aldrich, 2020)

5.3.4 Morphology and micro-structure of AS CLEAs

The freeze-dried, crude enzyme extract from AS before CLEA preparation had a dispersed appearance and showed a net-like micro-structure in SEM images, with a pore size of approximately 0.5 μm (Figure 5-8(a)). Freeze dried CLEAs, on the other hand, had a very different micro-structure compared to crude enzyme extracts and demonstrated mixed types of aggregate shapes, including irregular spherical forms, with a diameter ranging from 0.5 to 1.5 μm (Figure 5-8(b)), as well as regions of amorphous bulky material (Figure 5-8(c)). The mixed types of micro-structure can be explained by the presence of different types of enzymes and proteins in crude AS extracts that vary in response to precipitation and cross-linking mechanisms during CLEA preparation.

Schoevaart et al. (2004) suggested that the physico-chemical properties of target enzymes can affect the CLEA structure. Thus, CLEAs prepared from *Candida antarctica* lipase B (a highly lypophilic and almost not glycosylated enzyme) by 10 mM glutaraldehyde cross-linking (3 h at room temperature), formed elastic ball-shaped aggregates of approximately 1 μm diameter, which was classified as a “type-1” structure. In contrast, CLEAs of *Candida rugosa* lipase (a hydrophilic enzyme with a highly glycosylated surface) exhibited a more amorphous structure with a particle size up to 100 μm, and was classified as a “type-2” shape). However, there is not necessarily a clear distinction between the two types of morphology, and CLEAs of some enzymes (e.g. formate dehydrogenase from *Candida boidinii* (Kim et al., 2013b)) can show a morphology intermediate between the two types.

(a)

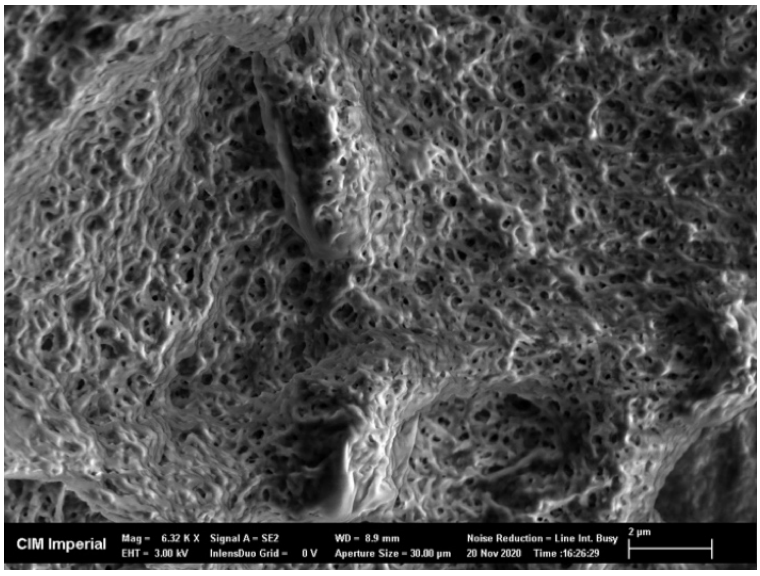

(b)

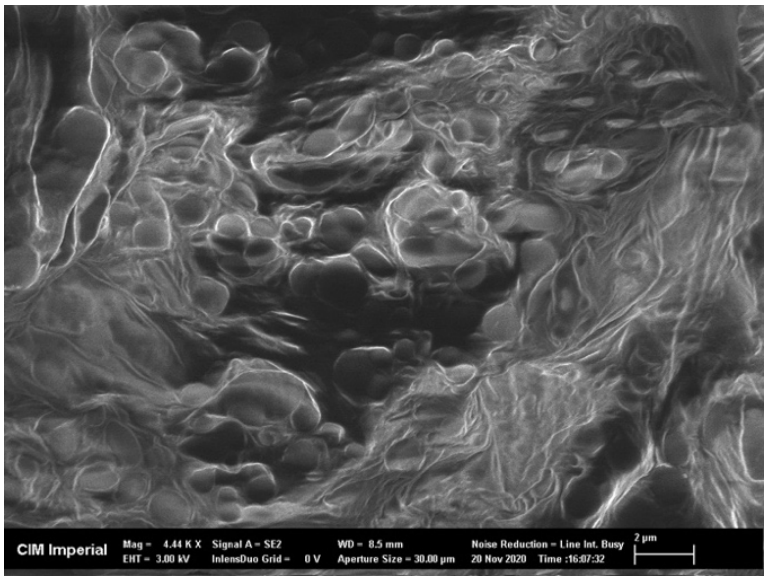

(c)

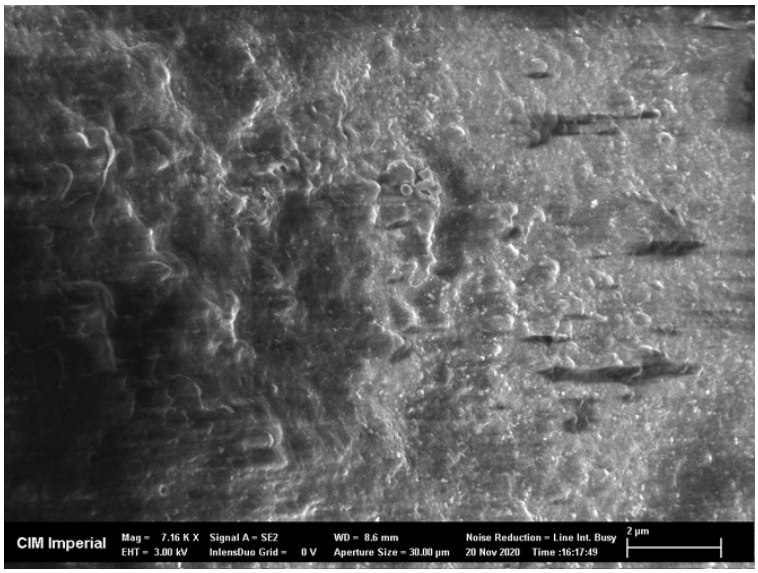

Figure 5-8 SEM images of: (a) freeze dried crude AS enzyme extract (magnification = 6320×); (b) CLEAs of AS extracted enzymes with irregular ball-shape structure (magnification = 4440×); (c) CLEAs of AS extracted enzymes with amorphous structure (magnification = 7160×)

5.3.5 Preservation of prepared CLEAs

Resuspension of the CLEAs in buffer solution and freeze-drying were compared as preservation techniques to assess the effects of different storage conditions on CLEA activity with time. The results showed there was no statistically significant differences ($P > 0.05$) observed in the activities of amylase, protease, lipase and cellulase enzymes with time, for CLEAs resuspended in buffer solution for a maximum storage period tested equivalent to 27 days (Figure 5-9). On the contrary, freeze-drying reduced the activities of amylase, protease

and lipase enzymes to 89.5%, 77.4% and 36.9%, respectively, immediately after drying process (Table 5-4). Interestingly, however, cellulase activity slightly increased to 111.2% compared to the original freshly prepared CLEA. After 40 days of storage of the freeze-dried CLEA, amylase and cellulase activity were severely reduced to 21% and 37% relative to fresh CLEAs, whereas the activities of lipase and protease were shown to increase to approximately 75% and more than 100%, respectively, compared to the original CLEA.

Similar results reported by Roy et al. (2020) showed that freeze-drying a crude extract from disrupting the microalgae *Dunaliella tertiolecta* cells using silica beads decreased the activity of cellular antioxidant enzymes, peroxidase and superoxide dismutase, by 26% and 42%, from 0.031 and 14.67 U/mg protein to 0.023 and 8.54 U/mg protein, respectively. However, enzymes may vary in response as cellular catalase activity showed no change in activity with freeze-drying (ranging 22-25 U/mg protein). Freeze-dried extracts stored at -20 °C for 30 days showed further reductions in catalase, peroxidase and superoxide dismutase activity by 31, 43 and 39%, respectively.

However, the hyperactivation of cellulase was also observed immediately after freeze drying. This behaviour can be explained due to the alteration of the enzyme protein structure when insufficient protective compounds are present. For example, Roy and Gupta (2004) found that freeze-drying altered the protein conformation, reducing the α-helix content and increasing the β-sheet content of the secondary protein structure. After resuspension in buffer solution, more active enzyme sites could thus be released from the interior part of the CLEA increasing exposure to substrate molecules and the apparent catalytic activity. The hyperactivation of enzymes by freeze-drying has also been reported in other media types. For example, Martysiak-Żurowska et al. (2020) found that freeze drying of human milk induced a small increase in lysozyme activity by approximately 9.8%. Lester et al. (2004) found that the activities of catalase, glutathione reductase, monodehydroascorbate reductase, and superoxide dismutase in freeze-dried whole spinach leaves were increased by 1.7, 1.1, 1.5, 2.75 times, respectively, compared to fresh spinach leaves.

The significant variation in enzyme activities observed with freeze-drying suggested that this was unsuitable as a preservation technique for extending the shelf-life of CLEAs produced from crude AS enzyme extracts. By contrast, the enzyme activities for CLEA preserved in buffer solution maintained relatively constant over a period of 27 days. Therefore, Tris-HCl buffer (10 mM, pH 7.0), which maintained the CLEA activity, was selected to preserve the CLEAs produced in further experiments.

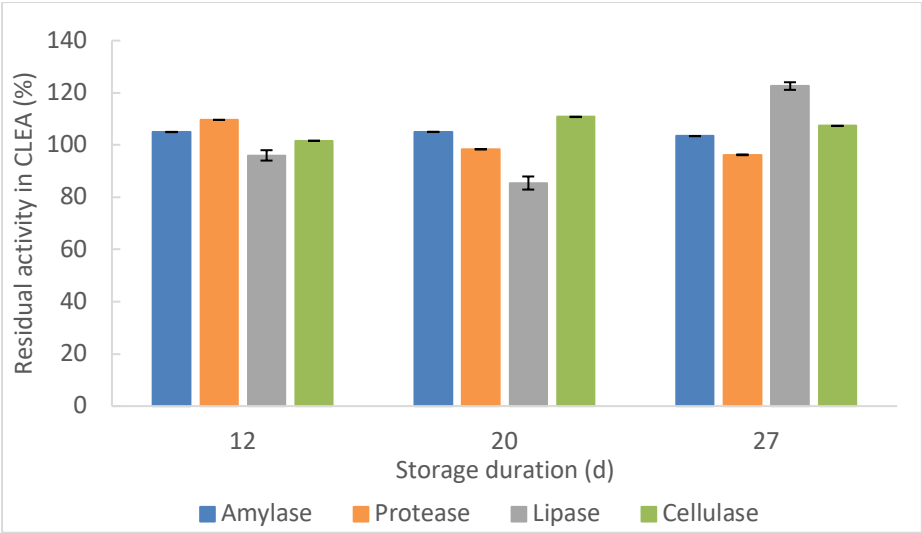

Figure 5-9 Residual enzyme activity in CLEA prepared from crude AS extracts and maintained in Tris-HCl buffer (10 mM, pH 7.0) for 12, 20 and 27 days (% relative to the activities of the fresh prepared CLEA suspension; error bar: standard deviation)

Table 5-4 Residual enzyme activity of freeze-dried CLEA prepared from crude AS extracts before and after storage at -20 °C (% relative to the fresh prepared CLEA suspension before freeze drying)

Enzyme	Amylase	Protease	Lipase	Cellulase
*Day 0	89.5	77.4	36.9	111.2
Day 40	21.5	105.6	74.7	37.5

Note:* activities on Day 0 were measured by re-suspending CLEAs in Tris-HCl buffer (10 mM, pH 7.0) immediately after freeze-drying

5.4 Discussion

5.4.1 Precipitants

The first stage in CLEA preparation, involves the aggregation and precipitation of soluble enzymes by the addition of a protein precipitant. Enzyme aggregation/precipitation is closely related to removal of the hydration layer (Section 2.6.3.1). Three types of precipitants are typically used for aggregation and precipitation of enzymes, including neutral salts, organic solvents and nonionic polymers, and the effectiveness of the different precipitant types varies depending on the protein conformation of the target enzyme, as well as the operational conditions. Large amounts of inhibitory materials potentially present in crude enzyme extracts, such as those obtained from complex matrices like AS, may also hinder the enzyme aggregation (Bashir et al., 2018). For example, Henríquez et al. (2020) indicated that natural polyphenols (including flavonoids and phenolic acids) can induce the disassembly of misfolded aggregated proteins (α-synuclein, a presynaptic neuronal protein) by blocking

specific amino acid regions that are prone to aggregation via intermolecular interactions. Therefore, precipitant selection is critical to optimise enzyme recovery in CLEA preparation.

Ammonium sulphate (80% saturation), a neutral salt, is frequently reported as the optimal precipitant with the greatest precipitation efficiency. Yu et al. (2013) found that 80% saturated $(NH_4)_2SO_4$ precipitated 95% of free epoxide hydrolase present in solution from a crude extract of Mung bean, compared to PEG, acetone, 2-propanol and 1-buty alcohol, which achieved precipitation rates of 27%, 28%, <5% and 60%, respectively. CLEA prepared by cross-linking the $(NH_4)_2SO_4$ precipitated enzyme with 20 mM glutaraldehyde at 4 °C for 12 h retained 92% of the free enzyme activity. Zeinali and Lenjannezhadian (2018) prepared gel-entrapped CLEAs from crude sword bean urease (protein content of 20% w/w) with either $(NH_4)_2SO_4$ (80% saturation) or acetone precipitation, followed by cross-linking with 7 mM glutaraldehyde at 4 °C for 4 h, and found the enzyme activity was approximately three times greater with $(NH_4)_2SO_4$ compared to acetone-precipitation. Zhou et al. (2017b) compared five precipitants (methanol, ethanol, acetone and isopropanol at 1:2 v/v, and saturated $(NH_4)_2SO_4$ solution) to prepare nitrile hydratase CLEAs. Aggregates produced by $(NH_4)_2SO_4$ precipitation gave the largest overall recovery of free enzyme activity, equivalent to 80%, compared to the other organic solvents, which were in the range 5-50%.

Here, however, enzyme activity recovery rates in CLEAs of AS extracted enzymes with $(NH_4)_2SO_4$ precipitation were smaller compared to acetone under equivalent conditions (see Section 5.3.2.2). This could be explained because $(NH_4)_2SO_4$ at 80% saturation may potentially introduce a high level of charged, ionic chemical species into the enzyme solution causing the excessive replacement of water and the loss of the essential hydration layer from enzyme molecules (see Section 2.6.3.2). The relationship between polar hydrophilic and non-polar hydrophobic regions of the protein molecular structure in maintaining the stability and biological activity of enzymes is shown in Figure 2-10. Essential hydrophobic, or at least non-hydrophilic, polypeptide chains may therefore become exposed to the surrounding water, which may lead to detrimental conformational changes of the enzyme protein structure. The loss of α-amylase activity after precipitation may be explained by the removal of Ca^{2+} ions (which are an essential cofactor of amylase (Section 2.6.5.5)) due to the high concentration of $(NH_4)_2SO_4$ and formation of insoluble calcium sulphate ($CaSO_4$).

Moreover, Perzon et al. (2017) reported the formation of an orange coloured ‘gel’ after the addition of glutaraldehyde to $(NH_4)_2SO_4$-precipitated cellulase, which was probably caused by an unknown reaction between the cross-linker and the $(NH_4)_2SO_4$ that was competing with the enzyme cross-linking mechanism. A similar orange colour was also observed here during CLEA preparation of commercial protease enzyme (Figure 5-3). Thus, entrapment of enzyme

molecules in the gel-like matrix could limit accessibility of substrates to enzyme active sites, reducing the apparent CLEA activity. Perzon et al. (2017) further indicated that CLEAs produced by $(NH_4)_2SO_4$ precipitation were also prone to clustering during centrifugation (discussed later in Section 7.2.3.3) that could also lead to gel formation and a CLEA activity loss.

5.4.2 Cross-linker

5.4.2.1 Glutaraldehyde

Cross-linker agents are aldehyde compounds that form covalent bonds between functional groups on the surface of aggregated enzymes, producing insoluble CLEAs (Figure 2-9). Glutaraldehyde is one of the most common choices of cross-linker for CLEA production, as it is relatively inexpensive and readily available (Sheldon and van Pelt, 2013). The recovered activity in the CLEAs prepared using glutaraldehyde depends on the target enzyme, due to the varying surface characteristics of different enzymes, and also on the concentration of glutaraldehyde.

Insufficient glutaraldehyde may lead to inadequate cross-linking reactions and reduced operational stability and reusability of the CLEA, due to leaching of free enzymes into the aqueous solution from loosely-structured aggregates (Graebin et al., 2018). In general, the enzyme activity recovery rate in the CLEA increases with glutaraldehyde concentration, up to a maximum value, which defines the optimum cross-linker concentration. For example, Chaudhari and Singhal (2017) found that the activity recovery rate of a CLEA prepared from *Fusarium sp.* ICT SAC1 cutinase increased with glutaraldehyde concentration up to 125 µmol, which gave a maximum recovery of 55.4%; higher glutaraldehyde concentration (250-750 µmol) led to reduced recovery rates (19-36%). A similar pattern of behaviour was also reported by Matijošytė et al. (2010) for CLEAs produced from laccase using dioxane, DME or 2-propanol as the precipitants and glutaraldehyde as the cross-linker. Chui and Wan (1997) found that small concentrations of glutaraldehyde (0.1 and 0.25% v/v) did not visibly precipitate the enzyme after 1 h reaction at room temperature, whilst insoluble enzymes appeared with higher concentrations (0.5-10% v/v).

Excessive amounts of glutaraldehyde, on the other hand, can inactivate CLEAs due to its high reactivity and small MW (100.11) compared to the average MW of an enzyme, which is typically in the range of 12000 to 300000 (Ogston, 1962)). Therefore, glutaraldehyde molecules can penetrate recessed parts of the enzyme structure where the active catalytic sites are located (Figure 2-2). Glutaraldehyde molecules may therefore bind with the functional groups essential for the enzyme catalytic activity (e.g. primary amino-, imidazole-, phenolic- and thiol-groups, see Table 2-3), reducing the affinity of the enzyme for its target substrate. Graebin et al. (2018) and Torabizadeh et al. (2014) indicated that excessive amounts of

glutaraldehyde can promote the rigidification of the CLEA structure and reduce the flexibility of the enzyme active sites (mentioned in Section 2.2.2) within the cross-linked aggregate, which subsequently leads to internal mass transfer limitations. Migneault et al. (2004) also indicated that, when there is insufficient enzyme available in the solution, glutaraldehyde molecules tend to react with the same enzyme molecule so that intramolecular (rather than intermolecular) cross-linking can occur (more discussion in Section 7.2.3.2), causing distortion of the protein structure, reducing or eliminating enzymatic activity in the CLEA.

Glutaraldehyde was effective at cross-linking a commercial protease enzyme (Figure 5-2) and amylase and lipase in a CLEA prepared from a crude enzyme from AS (Figure 5-4) and activity recovery rates of or up to 56.5, 17.5 and 23.6% were obtained, respectively. However, increasing glutaraldehyde concentrations reduced the activities of protease (at a concentration of 0.5% w/v, Figure 5-2) and amylase from AS (at concentrations >0.04% w/v, Figure 5-4). CLEAs formed with glutaraldehyde concentrations greater than 0.04% w/v also produced denser and larger particles (Figure 5-5). However, the cross-linking reaction varied depending on the enzyme type and biomass matrix and, in the case of protease and cellulase from crude AS extracts, no activity was detected in CLEAs prepared with glutaraldehyde (at 0.04% w/v).

In other examples, the activity recovery rate of a CLEA of *Penicillium notatum* lipase (using saturated $(NH_4)_2SO_4$ as the precipitant) increased to 64.3% with increasing glutaraldehyde concentration from 50 up to 200 mM, however, raising the cross-linker concentration further, to 250 and 300 mM, reduced the CLEA activity (Rehman et al., 2016). By contrast, Sahutoglu and Akgul (2015) reported no inverse proportionality between CLEA activity of *Aspergillus oryzae* α-amylase and *Aspergillus niger* glucoamylase (produced with 90% acetone and $(NH_4)_2SO_4$ precipitation, respectively, followed by glutaraldehyde cross-linking), which remained consistent (approximately 21% and 40%, respectively) with increasing glutaraldehyde concentrations above the optimal values (5 mM and 50 mM for the two enzymes, respectively). This behaviour was explained because the active site amino acids (asparagine and glutamic acid) of both enzymes apparently do not chemically react with glutaraldehyde.

Interestingly, exposure of CLEAs to excessive amounts of cross-linker may lead to hyperactivation of the enzyme in the CLEA under certain circumstances, probably due to structural modifications of the enzyme during cross-linking. For example, Aytar and Bakir (2008) found the activity recovery rate of tyrosinase in a CLEA (prepared using 60% saturated $(NH_4)_2SO_4$ precipitation, with 50 mg/ml BSA) increased to 112% compared to the enzyme without cross-linking at glutaraldehyde concentrations equivalent to 3% w/v. Schoevaart et al. (2004) produced CLEAs of *Candida antarctica* lipase by dimethoxyethane precipitation, followed by glutaraldehyde cross-linking, and found that the enzyme recovery rate was

relatively constant (at approximately 120%) with <10 mM of cross-linker, and increased to more than 140% with higher cross-linker concentrations up to 100 mM. Schoevaart et al. (2004) also found that the protein content of the soluble enzyme solution (measured as the volume activity) affected the extent to which lipase in CLEAs was hyperactivated. Thus, hyperactivation was observed using >10 U/mL lipase to produce CLEAs and reached a "tentative maximum" at approximately 25 U/mL, but further increases in lipase concentration reduced the CLEA activity.

5.4.2.2 Dextran aldehyde

Glutaraldehyde is widely used as a cross-linker for CLEA preparation, however, there are several disadvantages to cross-linking enzymes with this reagent, for example, it was found to inactivate cellulase and protease from AS extracts, it is highly reactive and can damage enzyme structures and the activity recovery rate is therefore sensitive to its concentration. Dextran aldehyde is a potential alternative cross-linking agent offering a number of advantages, for instance, it is a non-toxic, biodegradable, biocompatible, renewable polysaccharide based macromolecular polymer, with a higher MW (150,000 Da in this study) compared to glutaraldehyde.

The highest amylase activity recovery rate obtained for dextran-CLEAs (27.5% at 0.04% w/v dextran aldehyde) was approximately 45% higher compared to glutaraldehyde-CLEAs (19.0% at 0.005% w/v), produced under equivalent conditions (5 mg/mL BSA addition, 80% saturated $(NH_4)_2SO_4$ precipitation) (Figure 5-4 and 5-6). Increased enzyme recovery rates with dextran have been frequently reported compared to glutaraldehyde, and several examples are discussed in Section 2.6.4.2. Indeed, Nadar et al. (2016) found CLEAs of α-amylase produced with several macromolecular polyaldehyde cross-linkers (including: dextran, agar, chitosan, and gum arabic) all exhibited larger enzyme activity recovery rates compared to glutaraldehyde under equivalent conditions (80% saturated $(NH_4)_2SO_4$ precipitation for 30 min at 4 °C, cross-linking at 0.21 mol/L aldehyde content for 20 h at 30 °C). Dextran gave the highest overall enzyme activity recovery (91%), followed by chitosan (84%), agar (69%) and gum Arabic (60%), compared to glutaraldehyde, which produced the lowest overall activity recovery in the CLEAs, equivalent to 42%.

Furthermore, dextran aldehyde concentrations greater than the optimum value tend to have less severe impacts on enzyme activity, compared to glutaraldehyde under equivalent conditions. Kim et al. (2013b) prepared a CLEA of formate dehydrogenase from *Candida boidinii* via 90% saturated $(NH_4)_2SO_4$ precipitation (20 min at 4 °C) followed by glutaraldehyde (2–30 mM) or dextran aldehyde (6-150 μg/mL) cross-linking for 150 min at 4 °C. Enzyme recovery significantly decreased from 16% to <5% with increasing glutaraldehyde concentration from 6 to 8 mM, however, dextran aldehyde had relatively little effect on CLEA

activity (recovery rate = 10-15%) over a considerably wider concentration range of 6-150 μg/mL

The improved performance of dextran aldehyde cross-linking in CLEA preparation may be explained by the larger molecular size and presence of multiple aldehyde groups on the dextran molecular backbone, whereas there are only two aldehyde groups present in glutaraldehyde monomers, which reduces the possible penetration of the cross-linker into enzyme molecules and reaction with active sites or essential amino acid residues of the enzyme. Mateo et al. (2004) measured the recovery of active sites in a CLEA prepared with penicillin acylase, which has an N-terminal serine that can readily react with aldehyde groups, by titration with the enzyme inhibitor phenylmethylsulfonylfluoride (PMSF) before and after cross-linking. The amount of PMSF required for complete inactivation of the enzyme corresponded to the number of active sites. Twice the number of active sites, equivalent to a recovery of 92%, were preserved with dextran aldehyde cross-linking compared to glutaraldehyde, which recovered 48% of active sites. Therefore, dextran aldehyde can be regarded as a more moderate reagent for enzyme cross-linking compared to glutaraldehyde, and may be more suitable for enzymes that contain essential functional groups at the catalytic active centre that are susceptible to binding with a small-sized cross-linker molecule (see Table 2-3).

However, the moderate reactivity of dextran aldehyde could potentially reduce the structural stability of dextran-CLEAs relative to glutaraldehyde-CLEAS. For example, Valdes et al. (2011) reported that CLEAs of lipase formed by dextran aldehyde had lower thermal stability than glutaraldehyde and only 46.8% of the initial activity in the dextran-CLEA was retained after 50 h of incubation at 60 °C, compared to up to 70.2% activity retention for glutaraldehyde-CLEA. This can be explained because the enzymes not cross-linked as effectively with dextran aldehyde compared to glutaraldehyde and could detach from the aggregate and, consequently, re-suspended enzymes were readily inactivated when exposed to high temperature for prolonged periods. However, Kim et al. (2013b) found that the residual activity of dextran-CLEAs remained over 95% after 10 cycles of reuse, and the thermal stability of the CLEAs was increased by a factor of 3.6 compared to free enzyme.

In addition to the benefits of dextran aldehyde for CLEA preparation, the chemical also has environmental advantages over glutaraldehyde. For example, Akyon et al. (2019) reported that the abiotic properties of glutaraldehyde (50-300 mM) delayed the removal of a number of organic compounds (including acetate, guar gum, ethylene glycol, ethanol, and isopropanol at 50,000 mg/L) due to altered microbial activity in a biofilm treatment system compared to the control condition without glutaraldehyde.

5.4.3 Additives

Bovine serum albumin is an inert protein additive that provides a large number of lysine groups that form covalent bonds with aldehyde groups (see Section 2.6.5.1). BSA also serves as a bridging agent between proteins facilitating co-aggregation between adjacent protein molecules (see Figure 2-8(b)), which increases the precipitation efficiency in the enzyme solution (von Buelow et al., 2019). Moreover, BSA molecules surrounding the enzyme stabilise the protein structure and provide protection against external stresses. For example, this mechanism can offer protection from strong dipole forces that may be induced by acetone, which are capable of disrupting the enzyme protein structure, or the excessive loss of the essential hydration layer during the precipitation process (see Section 2.6.3), by forming hydrogen bonds with the functional groups on the enzyme surface as a "water replacement" (Carpenter et al., 1993; Schoevaart et al., 2004).

Adding BSA into the crude enzyme solution improved the activity recovery rate observed here (Section 5.3.1), and the dosage of BSA was critical for efficient CLEA formation to maximise enzyme activity. Indeed, if the supply of BSA is insufficient then enzymes may leach from the CLEA (Torabizadeh et al., 2014). Thus, at low levels of BSA addition (0.55 mg/mL), the majority of protease was released from the CLEA and was detected in the supernatant after washing (Figure 5-2). On the other hand, excess concentrations may increase the particle size of the CLEAs, reducing the surface-to-volume ratio and apparent activity of the CLEA (Chaudhari and Singhal, 2017), since a larger proportion of enzyme active sites in the interior of the CLEA are hindered by BSA and thus inaccessible to the substrate. Torabizadeh et al. (2014) suggested that higher BSA dosage than the optimum ratio may prevent necessary cross-linking of enzyme molecules, caused by competition between the free amino groups of BSA and those of the target enzyme. It may also In this study, however, increasing the amount of BSA (10 mg/mL) had no apparent effect on the cross-linking efficiency of commercial protease compared to 5 mg/mL (Figure 5-2). Kim et al. (2013b) observed a similar pattern of behaviour and found the highest activity recovery of a dehydrogenase-CLEA (18%, which was 1.3 times larger compared to the control without BSA) was obtained by dosing a mass ratio of BSA to enzyme equivalent to 0.5:1. Further increases in the amount of BSA supplied did not affect the activity recovery under equivalent conditions (90% saturated $(NH_4)_2SO_4$ precipitation, followed by 30 μg/mL dextran aldehyde cross-linking for 2.5 h at 4 °C).

5.4.4 Micro-structure/morphology of CLEAs and its enzyme activity

Although enzyme activity recoveries in CLEAs can be up to 100% under optimal conditions (Schoevaart et al., 2004), in general, CLEA activities tend to be lower compared to the original enzyme solution from which the CLEA was prepared. The maximum enzyme activity recovery rates for amylase, protease, lipase and cellulase measured in CLEAs prepared from crude AS

extracts under optimum conditions were 42.6, 48.3, 54.4, and 31.0%, respectively (see Section 5.3.2.3). The partial loss of enzyme activity can be explained by changes in the morphology and the available catalytically active sites of the CLEAs.

Two types of aggregate were found in CLEAs prepared from AS (Section 5.3.4, Figure 5-8), including irregular spherical shapes (type-1) and more amorphous features (type-2). Catalytically active sites buried in the interior region of both types of CLEA structure may be less accessible to substrate molecules, however, this is likely to affect amorphous forms to a greater extent. Indeed, spherical CLEA structures have elastic properties, improving the potential interaction between the aggregate and substrate molecules and the subsequent reaction catalysis (Schoevaart et al. (2004). The mechanism of fitting and binding of the enzyme and reaction with the substrate is shown in Figure 2-2. Yu et al. (2013) identified multiple active layers of enzymes in amorphous structures of Mung bean epoxide hydrolase CLEA, indicating that there are empty spaces between the layers providing sufficient active surface area for substrate attachment. Schoevaart et al. (2004), on the other hand, suggested that the space between the layers of type-2 CLEAs, prepared from *Candida rugosa* lipase, was filled with, possibly inert, proteins, which reduced access to the substrate and the apparent catalytic activity.

5.4.5 CLEA preservation

5.4.5.1 Buffer suspension

Preserving the CLEA activity by suspending in buffer solution showed superior performance compared to freeze drying into a solid state. The activities of amylase, protease, lipase and cellulase for CLEAs resuspended in buffer solution were maintained at approximately 100% (relative to the freshly prepared CLEA), for a maximum storage period tested equivalent to 27 days. This can be explained by the high hydration level of the suspended CLEAs.

The hydration layer of enzymes is critical to protein solubilisation and aggregation in aqueous solutions, and also to the conformational stability and bio-function of proteins (see Section 2.6.3.1). Thus, storing in buffer solution maintained full hydration of the enzyme protein structure, preserving the water bound to ionic or polar groups on the molecule surface (e.g. amino residuals), which is essential to maintain the catalytic function of enzymes (Rupley et al., 1983; Roy and Gupta, 2004).

5.4.5.2 Freeze drying

Freeze drying can remove both solvent and protein-bound water by sublimation and desorption. The freeze-drying process can be divided into three main stages and each stage can expose CLEAs to various physico-chemical stress conditions, which can lead to

conformational changes and possible inactivation of the immobilised enzymes (Arakawa et al., 2001; Roy and Gupta, 2004; Butreddy et al., 2021):

(1) Initial freezing involves the development of ice nuclei (i.e. small ice crystals) below 0 °C that form separately from the solute containing the soluble proteins. Separation of the solvent-water and formation of an ice-water interface increases the local protein concentration, resulting in a significant pH change and, consequently, protein denaturation.

(2) Primary drying is the stage where the solvent-water, separated from the solute, is removed by sublimation. To reduce protein denaturation, this stage should be performed at a suitable temperature to minimise unfolding of the protein molecule.

(3) Secondary drying occurs after the frozen water has sublimed and significantly affects the final water content and the enzyme catalytic activity of the dried CLEA, since the essential 'bound water' to the protein molecules is removed at this stage.

The amylase, protease and lipase activities were severely reduced immediately after freeze-drying to 89.5, 77.4 and 36.9% compared to fresh, unfrozen CLEA. After 40 days, amylase, cellulase and lipase activity of freeze-dried CLEA was 21, 37 and 75% relative to unfrozen CLEA (however, protease activity increased to >100%). Thus, the partial inactivation of enzymes in freeze-dried CLEA was probably explained by a combination of the above factors. In addition, CLEA enzymes may be susceptible to stress and denaturation induced during the freeze-drying process due to the removal of lyoprotectants and cryoprotectants (protective compounds against drying and freezing, respectively (Mohammadipanah et al., 2017)) that are naturally present in microbial cells (such as polysaccharides and phenolics (Roy et al., 2020)), by the cell disruption (see Chapter 4) and cross-linking process. Therefore, CLEA preservation by freeze-drying requires sophisticated freeze-drying apparatus and careful optimisation and control to avoid damage to the CLEA activity.

Dried CLEAs are unlikely to become fully rehydrated by resuspension after freeze-drying because the changes in microstructure of enzyme proteins after cross-linking (Figure 5-8) into irregular spheres and amorphous material may limit the ability of water molecules to access and re-hydrate enzymes located within the interior region of the aggregates. Furthermore, cross-linking can produce a surface that comprises only of an amide backbone without other ionised groups, reducing the condensation and binding of water vapour onto the enzyme surface and, consequently, rehydration of the CLEA (Rupley et al., 1983). Moreover, thawing of freeze-dried CLEAs by resuspending in buffer solution can also cause activity loss. For example, Arsiccio et al. (2020) found that the ice-water interface (formed during stage one of freeze drying) lowers the free-energy barrier for protein unfolding and adding liquid molecules

that react with enzyme functional groups of the CLEA can trigger protein unfolding and consequently enzyme inactivation.

5.4.5.3 Selection of preservation conditions

In summary, suspending the CLEA of AS enzyme in Tris-HCl buffer solution maintained enzyme activities (with little variance detected) for the storage period tested (27 days) and is more suitable for preserving and extending the shelf-life of CLEAs produced from crude AS enzyme extracts, compared to freeze drying.

It is not necessary to resuspend and preserve CLEAs to original volumes, which was necessary in the experimental research reported here to compare the enzyme activities under different conditions. Where CLEAs are used to accelerate a hydrolysis process, for example, smaller volumes of buffer solution can be used (for example, equivalent to 20% of the volume of the crude extract, see Chapter 6). This offers practical benefits by reducing the volumes of liquid materials.

5.4.6 Summary of CLEA preparation from AS

A major benefit of the CLEA technique is that it combines consolidation and stabilisation of enzymes into a single step, which can be performed directly on both purified enzymes and crude enzyme extracts. CLEAs and multi-CLEAs (defined in Section 2.6.6.1) have been produced from crude secondary materials (e.g. fermentation broths of microorganisms, mung beans and food waste), however, this study is the first time that CLEAs have been prepared from the biological AS generated during municipal wastewater treatment, which is a complex waste biomass containing a wide range of hydrolytic enzymes. Key outcomes from this chapter showed that:

- Optimisation of the operational conditions (including combinations and concentrations of additive, precipitant and cross-linker) is necessary to maximise the recovery of AS enzymes in the CLEA and have a profound influence on the morphology and the catalytic activity of the CLEA.
- Bovine serum albumin, an inert protein additive, stabilised the enzyme protein structure and supplied lysine groups, forming covalent bonds with the cross-linker, facilitating the enzyme aggregation and enhancing the enzyme activity recovery in the CLEA.
- Macromolecular cross-linker, dextran aldehyde, improved the enzyme activity recovery rate in the CLEA due to the moderate reactivity and larger molecular size, which reduces the possible penetration of the cross-linker into enzyme molecules and reaction with essential active sites of the enzyme, compared to glutaraldehyde.

- Acetone precipitation was more effective for enzyme cross-linking process, compared to $(NH_4)_2SO_4$, which can inactivate amylase in the absence of BSA.
- The conditions for CLEA preparation from crude AS enzyme extracts were optimised and were as follows: acetone precipitation (volume ratio = 4:1, 0.5 h at 0 °C), followed by dextran aldehyde cross-linking (0.04% w/v, 3.5 h at room temperature), with 5 mg/mL BSA addition. The highest enzyme recovery in the CLEA for amylase, protease, lipase and cellulase obtained following this procedure was 42.6%, 48.3%, 54.4% and 35.1%, respectively.
- Preserving the CLEA as a suspension in Tris-HCl buffer maintained the enzyme activity at an equivalent level to fresh CLEA and is recommended for storing the CLEA product, compared to freeze-drying, which significantly reduced catalytic activity.
- The results reported here demonstrate the feasibility of the CLEA technique for recovering valuable, industrial enzyme products from waste AS from biological wastewater treatment.

6 Substrate hydrolysis activity of CLEAs prepared from activated sludge

6.1 Introduction

Compared to inorganic chemical catalysts, enzymes exhibit higher substrate specificity and can catalyse reactions under milder conditions, with reduced by-product formation (see Section 1.1). The feasibility of the enzymatic conversion of complex organic materials (e.g. agricultural residues, municipal solid waste, wastewater with organic particulates and slaughterhouse waste) into fermentable structures, which can be further processed into value-added products, has been widely demonstrated (Wang et al., 2009; Teo and Wong, 2014; Arun and Sivashanmugam, 2015; Hero et al., 2018; Mlaik et al., 2019; Mirzaei Teshnizi et al., 2020).

One of the obstacles preventing the extensive use of enzymatic technology for conversion of organic materials is the high cost of commercial enzymes (Parawira, 2012). Moreover, free, soluble enzymes often exhibit low operational stability and reusability in continuous treatment processes (Section 2.5.2), further increasing the operational costs of applying enzymatic hydrolysis in practice. However, the drawbacks associated with soluble enzymes can be overcome by enzyme immobilisation. Immobilised enzymes are more resistant to changing conditions in operational environments (Section 2.5.2), and permit the efficient and effective recovery of both enzymes and products, rapid termination of reactions and reuse of enzymes for a prolonged time periods in continuous processes (Brena and Batista-Viera, 2006; Homaei et al., 2013).

Carrier-free immobilised enzymes, CLEAs, offer significant advantages for bioconversion of organic materials by consolidating and stabilising enzymes in a single step (Chapter 5). For example, Mahmod et al. (2015) prepared a multi-CLEA from crude enzyme solution of protease and lipase (extracted from fish viscera), via $(NH_4)_2SO_4$ precipitation, glutaraldehyde cross-linking with BSA addition, and the CLEA was used for biodiesel production from vegetable cooking oil at 40 °C with enzyme-to-oil ratio equivalent to 1:10. The multi-CLEA converted approximately 51.7% of free fatty acids into fatty acid ethyl esters after 5 h reaction, and the conversion rate was 3.5 times greater compared to mixed soluble enzymes under equivalent conditions. Yan et al. (2012) compared the hydrolysis of fish oil at 40 °C by a CLEA prepared from *Geotrichum sp.* lipase (by acetone precipitation, glutaraldehyde cross-linking, and with PEI addition) to the free enzyme. The CLEA achieved 42% hydrolysis, determined by the change in acidity of the fish oil, after a 10 h incubation period, compared to 12% by free enzyme. The significantly poorer performance of the free enzyme was explained because it is

more likely to form agglomeration pellets in an oil–water microemulsion compared to CLEAs, therefore reducing accessibility of the substrate.

Anaerobic digestion is widely used for the treatment of waste biomass, including sewage sludge, providing environmental benefits including solids reduction and pathogen control, reducing greenhouse gas emissions by diverting biodegradable waste from landfill disposal and minimising odour emissions (Khan and Ahring, 2021); it can also provide economic benefits by providing a renewable energy source and as an organic agricultural fertiliser (Smith, 2014). The process of AD is divided into four stages: hydrolysis, acidogenesis, acetogenesis, and methanogenesis; hydrolysis is often the rate-limiting step due to the presence of intact cells and other complex, slow-biodegradable organic polymers (e.g. cellulose, hemicellulose and lignin) in the waste biomass. Enzymatic pretreatment of waste biomass, as one of the biological pretreatment methods, is suggested as a possible approach to improve the performance of the AD process, by accelerating the hydrolysis stage, which could offer advantages over other mechanical, chemical and thermal methods because it requires less energy (Mishra et al., 2018).

Proteases (EC 3.4, enzymes acting on peptide bonds) and glycosidases (EC 3.2.1, enzymes acting on glycosidic bonds e.g. lysozymes, amylases) are the major enzyme candidates for hydrolysing waste biomass. Mallick et al. (2010) investigated the effects of enzymatic pretreatment on the mesophilic AD of yeast-cell-rich waste materials from the distillery industry (distillery spent wash and pot ale residues). More than 90% lysis of yeast cells was obtained after pretreatment with mixed β-glucanase and protease (dosage = 2.5 mL/g TS) for 24 h at 37 °C. Enzymatic pretreatment increased the COD removal of distillery spent wash and pot ale to >50% and 87%, respectively, by AD with a retention time of 10 day, compared to the controls (without enzyme addition), which showed negligible and 13% COD reduction, respectively, under equivalent conditions. Guo et al. (2014) showed that dosing AS with a multi-enzyme (commercial composite enzyme containing bromelain and lysozyme) at 2% v/v solubilised the sludge EPS fraction and increased the dissolved carbohydrate, protein and soluble chemical oxygen demand (sCOD) content in liquid phase of sludge by 1.1, 1.3 and 3.9 times after incubation for 5 h at 30 °C. Oszust et al. (2017) used lyophilisate of a crude multi-enzyme mixture (harvested from a culture filtrate of *Trichoderma atroviride* G79/11, with 22 U/mL cellulolytic activity) to pretreat mixed organic waste (containing fruit processing waste, dairy sewage sludge, corn silage, and grain broth) at dosage = 0.5 mg/g TS, prior to mesophilic AD (37 °C). The biogas production from pre-treated organic waste increased by 30%, compared to the control without the multi-enzyme.

Previous studies on the effects of enzymatic pretreatment of complex organic substrates (including waste AS) for AD have used commercial soluble enzyme products (e.g. (Guo et al.,

2014)). However, the application of immobilised enzymes, particularly in the form of CLEAs, for sewage sludge hydrolysis has not been previously explored. Sewage sludge is a highly complex substrate for enzymatic hydrolysis comprising of a mixture of microbial cells and EPS, as well as other inorganic and organic soluble and solid constituents with potential to cause inhibitory effects on the CLEA activity; the pH condition and ionic strength of the sludge matrix can also affect the CLEA reaction (Zhang et al., 2018). Therefore, it is important to understand the potential impacts of the sludge chemical environment on the potential hydrolysis of AS by the CLEA product. Furthermore, this study prepared CLEAs from AS enzymes for the first time and the use of AS CLEAs for hydrolysis applications of other organic materials has similarly not been investigated.

Therefore, the aim of the chapter is to examine the hydrolytic effects of the CLEAs prepared from AS on complex organic substrates, including waste AS from the biological wastewater treatment process, as a potential sludge pretreatment technique. Specific objectives are:

- To quantify the effectiveness of CLEA addition on the hydrolysis of wheat flour, as a representative, complex organic substrate source;
- To determine the impact of the sewage sludge matrix on the CLEA activity;
- To quantify the effects of CLEA addition on the enzymatic hydrolysis of whole AS;
- To compare the effects of different pretreatment methods, including: autoclaving, γ-radiation and sonication, on the hydrolysis of disrupted AS by the CLEA.

6.2 Materials and methods

6.2.1 Wheat flour and primary sludge

Wheat flour, is a complex organic matrix containing carbohydrates (mainly as starch), proteins and lipids, and has been widely used to quantify the hydrolytic activity of enzymatic reaction systems (e.g. (Zorov et al., 2006; Kagliwal et al., 2013; Wolter et al., 2013; Juhnevica-Radenkova et al., 2021)). Here, wheat flour was used as a surrogate complex organic material for sludge, but in the absence of active microbial cells, their metabolites and EPS, to preliminary examine the hydrolytic activity of the AS CLEA. Food grade white wheat flour was used in the experiments with the following composition: TS, 93.0%; VS, 92.0%, and the content of fat, carbohydrates, fibre and proteins was equivalent to 1.7, 71.7, 3.3, and 12.7% w/w (as received), respectively.

Primary sludge is mainly composed of the settleable solids in the sewage influent (Xu and Li, 2017). The constitution of the liquid fraction of primary sludge resembles that of the influent, with the presence of various dissolved organic substances, nutrients (N, P), and also heavy metals and hazardous pollutants (Svendby, 2019). Therefore, primary sludge supernatant was

used to examine the potential inhibitory effects of the sludge matrix on the CLEA. Primary sludge samples (TS = 1.26%, VS = 0.99%, pH = 6, conductivity = 1281 μS/cm at room temperature) were collected at the belt mouth of the thickening belt of WWTP1, after the lamella clarifier. The collected primary sludge was transported to the lab (procedures see Section 3.2) and centrifuged at 9000 g at 4 °C for 15 min (Sorvall RC6 Centrifuge, Rotor HS-4), followed by filtration through a cellulose filter paper (Whatman 1001-150, pore size = 11 μm) to remove residual particulates. The primary sludge supernatant was autoclaved at 121 °C for 15 min and stored in the fridge at 4 °C before use. Thickened AS samples from WWTP1 were collected following the procedures described in Section 3.2.

6.2.2 CLEA preparation

CLEAs were prepared using thickened AS sample from WWTP1 following the developed crude enzyme extraction method described in Section 4.3.2.4, and cross-linked by the optimised protocol in Section 5.3.2.3. The obtained CLEA CLEAs were re-suspended in Tris-HCl buffer (10 mM, pH 7.0) and stored in the fridge at 4 °C before use. The activity of the CLEA suspension was 3.024 ± 0.004 and 0.103 ± $4x10^{-5}$ U/mL for amylase and protease, respectively.

6.2.3 Substrate preparation

6.2.3.1 Wheat flour

The wheat flour was added into in RO water to prepare a mixture of 1.5% w/w TS content. The mixture was freshly prepared and continuously stirred at 100 rpm by a magnetic stirrer prior to the CLEA hydrolysis.

6.2.3.2 Sludge

Thickened AS samples from WWTP1 (TS content = 5-7%) were diluted 5 times (DF = 5, see Section 4.2.3.3) and were subjected to the following pretreatment methods, to disrupt the sludge flocs and the endogenous bio-activity of sludge cells before enzymatic hydrolysis:

(1) Autoclaving: diluted AS was placed in 500 mL Schott bottles and was treated by a steam autoclave (PS/RSC/EH230, Priorclave Ltd., UK) at 121 °C, 1.06 bar for 15 min;

(2) Sonication: diluted AS was treated by sonication probe (10 min duration at 0 °C, 40% AMP, pulse cycle mode with 1 min on followed by 1 min off), as described in Section 4.2.3;

(3) Gamma (γ) irradiation: diluted AS was treated by a caesium (Cs) 137 radiator (Gammacell 3000 ELAN, Best Theratronics Ltd, Canada). The AS suspension (450 mL) was placed in a 500 mL HDPE bottle and was exposed to the radiator for 10 h at room temperature; the total radiation dose was 1944 Gy at a dose rate of 3.24 Gy/min.

The diluted whole AS (without biomass disruption treatment), as well as the autoclaved, sonicated, and γ-irradiated AS were stored in a fridge at 4 °C and used as the substrates for CLEA hydrolysis on the following day.

6.2.4 Hydrolysis of organic materials

200 mL of the prepared substrates (wheat flour and AS, see above) was transferred to a 500 mL Schott bottle and pre-heated in a water bath at 40 °C for 10 min. CLEA suspension was added at a volume ratio of CLEA/substrate equivalent to 1:10 and 1:100 for flour hydrolysis, and 1:10 for AS hydrolysis. The mixture was stirred continuously at 120 rpm for 26 h. Similar flasks were prepared for the control, and in this case an equivalent volume of Tris-HCl buffer (10 mM pH 7.0) was added, in place of the CLEA suspension. Aliquots (20 mL) were collected from each bottle immediately and after 1, 2, 3.5, 4.5, 5.5, 6.5, 24 and 26 h (excepted for hydrolysis of autoclaved AS, with the aliquots collected immediately and after 1, 3, 5, 7, 24 and 26 h) and were heated in boiling water for 10 min to inactivate the CLEA. The boiled mixture was cooled immediately and centrifuged at 18000 rpm for 20 min. The supernatant was collected and filtered through a 0.45μm cellulose nitrate membrane to remove residual cell debris or particulate matter, and was stored in a freezer at -18 °C.

6.2.5 Inhibition of sludge matrix on CLEA activity

Under standard conditions, enzyme activities are determined using a pH-controlled buffer solution providing an optimum environment for enzymatic function. In practice, however, the enzyme interacts with the substrate matrix and the conditions may be suboptimal due to the presence of potentially inhibitory factors. Sewage sludge represents a complex substrate matrix, therefore, the potential for inhibitory effects of the sludge physico-chemical properties on CLEA activity was determined by measuring the CLEA activity for amylase, protease, lipase and cellulase in primary sludge supernatant (obtained from Section 6.2.1) compared to standard buffer solution. The activity in buffer solution was measured according to the standard procedures in Section 3.6 and was set at 100% and a similar approach was followed for the sludge supernatant, but with some modifications. In this case the specific substrates for each enzyme (starch, casein, pNPP, and CMC, respectively) were dissolved separately into the supernatant solution.

6.2.6 Sludge cell culture

The biological activity of the disrupted sludge samples was examined by a standard culturing method (de Farias et al., 2010). The culture medium was prepared by adding 39 g potato dextrose agar (PDA) to 1 L RO water. The mixture was boiled until the PDA completely dissolved and sterilised in by a steam autoclave at 121 °C, 1.06 bar for 15 min. The medium (15 mL) was transferred into sterile Petri dishes (diameter = 9 cm) and cooled at room temperature in a Class II microbiology cabinet. The pH value of the PDA was equivalent to 5.6

± 0.2 after autoclaving. Disrupted AS samples and diluted (DF=5), undisrupted control sludge were homogenised by thorough shaking and aseptically transferred to separate dishes (three replicate dishes for each sample) and maintained at 25 °C for 3 days in a temperature-controlled incubator (MIR 253, Sanyo, UK) in the dark.

6.2.7 Indicators of the progress of enzymatic hydrolysis

6.2.7.1 Soluble total organic carbon

The soluble total organic carbon (sTOC) concentration in the filtrates of the reaction mixture (see Section 6.2.4) was measured with a Shimadzu TOC-Vwp analyser (Shimadzu Corperation, UK), to provide a general indication of enzymatic solubilisation of particulate substrates in flour and AS.

Phosphoric acid reagent was prepared by diluting 100 mL of 85% reagent grade phosphoric acid with RO water to a total volume of 500 mL, and stored in the dark at 4 °C. Persulphate oxidiser was prepared by dissolving 50 g of sodium persulphate and 15 mL of 85% phosphoric acid in RO water to a final volume of 500 mL to provide final concentrations of each reagent of 10.5% and 3.8%, respectively; the solution was stored in the dark at 4 °C before use.

The sample was acidified by adding the phosphoric acid (final concentration = 3%), with the inorganic carbon in the sample converted to carbon dioxide (CO_2) which was eliminate by sparging the sample with nitrogen gas for 3 min. The persulphate oxidiser (1.5 mL) was mixed with the sparged sample and heated under UV illumination to convert the residual organic carbon in the sample to CO_2 which was passed through a dehumidifier and presented to the detector. The area of the CO_2 peak signal was measured and converted to total organic carbon concentration (C_{TOC}) using a pre-prepared calibration relationship, Area = $173.85C_{TOC}$ + 119.11 (R^2>0.99), with potassium hydrogen phthalate as the standard, in the range 0 to 10 mg/L.

6.2.7.2 Reducing sugar and tyrosine

Starch and proteins constitute the majority mass of flour (>80% w/w, see Section 6.2.1), therefore the hydrolysis products of amylase and protease in the CLEA, i.e. reducing sugar and tyrosine, were measured to show the effectiveness of CLEA in hydrolysing flour.

More than 60% of the TS content of AS is composed of various polysaccharides and proteins (Zhang et al., 2018). For hydrolysis of whole AS and autoclaved AS, reducing sugar accumulation was measured for as the indicator to examine the performance of polysaccharide-degrading enzymes in the CLEA (including amylase, which represents the most abundant hydrolytic enzymes in the CLEA, and also cellulase (see Chapter 5)). However, the reducing sugar content showed a slight increase and no significant change for whole AS and autoclaved AS, respectively (see Section 6.3.2). Therefore, in the following experiments

where γ-irradiated and sonicated AS was hydrolysed, both tyrosine and reducing sugar accumulation was measured, to expand the range of the CLEA enzyme types examined.

Reducing sugar was measured according to the 3,5-dinitrosalicylic acid (DNS) method (Miller, 1959). DNS reagent (3 mL, see Section 3.6.3 for preparation procedure) was added to 2 mL of filtrate of the reaction mixture (obtained in Section 6.2.4), followed by boiling in a water bath for 5 min. The mixture was immediately cooled to room temperature with running tap water and the absorbance of the solution was measured at 540 nm (Abs_{540}) against a blank using a UV-Vis spectrophotometer. Reducing sugar content (C_{RS}) was quantified using a pre-prepared calibration curve, Abs_{540} = 6.2843 C_{RS} - 0.2658 (R^2>0.99), with glucose as the standard, in the range 40 to 120 μg/mL.

Tyrosine was measured by the Lowry method (Lowry et al., 1951). Filtrate of the reaction mixture (2 mL), prepared following the procedure described in Section 6.2.5, was mixed with 5 mL of Na_2CO_3 (500 mM) and 1 mL of Folin & Ciocalteu's Phenol reagent (1N, equivalent to 0.67 M). The absorbance of the solution was measured at 660 nm (Abs_{660}) against a reagent blank after incubation for 30 min at 37 °C in a temperature-controlled water bath. Tyrosine concentration (C_T) was quantified using a pre-prepared calibration curve, Abs_{660} = 0.0173 C_T (R^2>0.99) with L-tyrosine as the standard, in the range 0 to 50 μg/mL.

The background concentration of sTOC, reducing sugar and tyrosine in the CLEA suspension was also measured and deducted from the result to normalise the data and avoid internal interferences.

6.2.8 Progress curve of enzymatic hydrolysis

A first-order reaction model was used to describe the kinetics of enzymatic hydrolysis by the CLEA, in which the concentration of the hydrolysis product initially increased rapidly, followed a decline in the accumulation rate to become asymptotic as the equilibrium concentration (i.e. the "plateau", see Section 2.2.3) was approached. The non-linear pattern of increasing hydrolysis reaction product concentrations was described as follows (Goñi et al., 1997; Butterworth et al., 2012):

$$C = C_0 + (C_\infty - C_0)(1 - e^{-kt}) \quad \text{(Eq 6-1)}$$

Where, C and C_0 are the concentration of the product at time t (h) and time zero, respectively, C_∞ is the equilibrium concentration of the product, and k denotes the solubilisation rate constant (h^{-1}). The parameters, C_0, C_∞ and k, for accumulated reducing sugar, tyrosine and sTOC were estimated by fitting the model to the experimental data using the Graphpad Prism 7.0 software; the best-fitting values for the parameters was determined by the software within 95% confidence intervals. The statistical validity of the relationships was defined by (Motulsky,

2016): (1) the R^2 values; (2) comparing the fitting of the non-linear model to a linear relationship (via hypothesis testing at 0.05 significance level); (3) visual examination of the residual plots: a randomly and evenly distributed residual point against X axis indicates good fitting of the model (with the "residual" defined as the vertical distance in Y axis of the experimental data point from the fit curve); (4) the scatter of points around the best-fit curve: the model fitting is valid if the scatter of points around the best fitting curve follows a Gaussian distribution. This was examined by carrying out a D'Agostino-Pearson normality test (alpha = 0.05) (D'Agostino, 1986) on the residuals: If the *P* value for the normality test is large, the residuals pass the normality test and the scatter is Gaussian; if *P* value < 0.05, the residuals fail the normality test, which means the data do not follows the regression curve (Motulsky, 2016).

The first order curves were used for indicative purposes to predict the maximum potential yield of sTOC, reducing sugar and tyrosine from the enzymatic hydrolysis of wheat flour, which was calculated as follows:

$$\text{Yield } (\%) = \frac{C_\infty - C_0}{C_{Total} - C_0} \times 100\% \quad \text{(Eq 6-2)}$$

Where, C_∞ and C_0 is the equilibrium and starting concentration for sTOC, reducing sugar and tyrosine products, and was estimated by their respective first-order reaction model parameters (results shown in Table 6-1); C_{Total} represents the total concentration of sTOC, reducing sugar or tyrosine in wheat flour, and was estimated as follows:

1) C_{Total} for sTOC was derived from the specific VS content of flour (0.989 g/g TS), based on the element carbon ratio of wheat flour (C:H:O:N:S = 1:2.004:0.625:0.249:0.01) reported by (Yao, 2014), and was equivalent to 0.568 g/g TS.
2) C_{Total} for reducing sugar was derived by dividing the total carbohydrate content in the flour (0.771 g/g TS, which was assumed to be in the form of starch) by the coefficient 0.9 (Deepa et al., 2010), and was equivalent to 0.857 g/g TS.
3) C_{Total} for tyrosine was estimated based on the reported values (which range from 1.54 to 5.6 mg/g TS (McDermott and Pace, 1957; Ranhotra et al., 1995; Hanft and Koehler, 2005; Jiang et al., 2008; Siddiqi et al., 2020)) and was assumed to be 5.6 mg/g TS of flour.

Eq 6-2 was also used to predict the maximum potential yield of tyrosine from the CLEA hydrolysis of sonicated and γ-irradiated AS. C_∞ and C_0 for tyrosine was estimated by their respective first-order reaction model parameters (results shown in Table 6-3). C_{Total} is the total concentration of tyrosine in AS, and was estimated based on the data reported by Vriens et al. (1989): tyrosine content of AS is equivalent to 2.4% of crude AS protein (N×6.25), where N

constitutes 9.6-11.2% w/w TS of AS. Thus, C_{Total} for tyrosine in AS was equivalent to 14.4-16.8 mg/g TS.

6.3 Results

6.3.1 Hydrolysis of flour

6.3.1.1 Accumulation of hydrolysis products

A general indication of the effects of CLEA addition on the hydrolysis of wheat flour was obtained by measuring the sTOC concentration of the reaction mixture for a 26 h incubation period at 40 °C and the results are shown in Figure 6-1. The sTOC concentration increased significantly with both rates of CLEA addition, and the largest release of sTOC was observed at the higher rate of CLEA input (1:10 v/v). The largest amounts of sTOC accumulated after 6.5 h and 5.5 h of incubation, equivalent to 36.8 and 56.9 mg/g TS for 1:100 and 1:10 v/v dose rates, were 1.8x and 2.8x larger than the control, respectively; the sTOC decreased to approximately 25 and 35 mg/g TS after 26 h reaction for 1:100 and 1:10 v/v dose rates, respectively. By contrast, the sTOC content in the control (without CLEA addition) increased to a small extent from approximately 12-15 to 20 mg/g TS within 0-2 h, and remained at a relatively constant level until the end of the incubation period (except for the data at 24 h in Figure 6-1(a)).

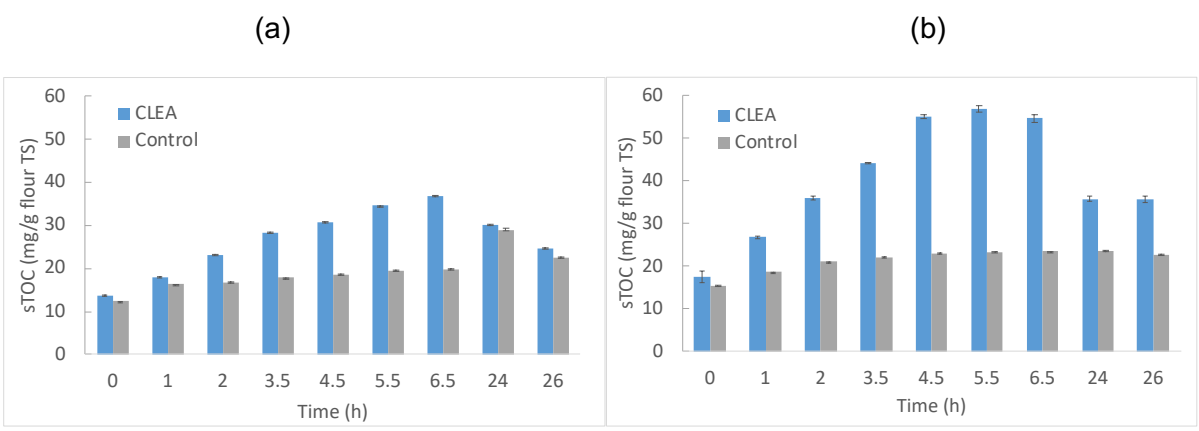

Figure 6-1 Effect of AS CLEA at rates of (a) 1:100 v/v and (b) 1:10 v/v on the accumulation of soluble total organic carbon (sTOC) from the hydrolysis of wheat flour incubated at 40 °C (error bars indicate the standard deviation)

Reducing sugar and tyrosine accumulation in the reaction mixture was also measured, representing the products of amylase and protease hydrolysis by the CLEA, respectively. Similar to sTOC, the CLEA significantly increased the reducing sugar concentration in the initial 6.5 h period ($P < 0.001$) compared to the control, but concentrations subsequently decreased after 24 h to small or undetectable values. The largest concentrations of reducing sugar were 22.2 and 32.1 mg/g TS with 1:100 and 1:10 v/v of CLEA input, respectively, which were 1.2x and 2.1x larger than the respective control treatments, without CLEA addition

(Figure 6-2). Reducing sugar in the control also increased in the initial 6.5 h, but to a smaller extent, to a maximum value of approximately 15-17 mg/g TS, which was probably explained by the solubilisation and degradation of non-starch carbohydrates by endogenous enzymes present in non-sterilise wheat flour. Arabinoxylan, for example, is a hemicellulose in cell walls of plants that is naturally present in wheat four, at approximately 1.5-2.5% w/w (Izydorczyk, 2009). Cleemput et al. (1997) reported that commercial wheat flour can exhibit enzymatic activity towards arabinoxylan, ranging from 0.275-0.588 nkat/g solids (equivalent to 0.016-0.035 U/g TS). (nkat refers to nanokatal, which is also an enzyme activity unit; one katal refers to an enzyme catalysing the reaction of one mole of substrate per second, i.e. 1 U = 1 µmol/min = 16.67 nkat.)

(a) (b)

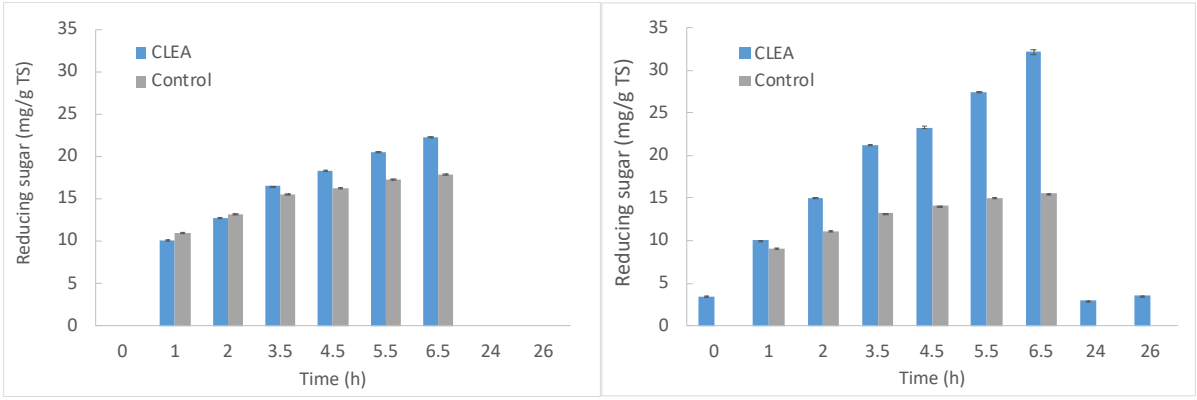

Figure 6-2 Effect of AS CLEA at rates of (a) 1:100 v/v and (b) 1:10 v/v on the accumulation of reducing sugar from the hydrolysis of wheat flour (error bars indicate the standard deviation)

Tyrosine accumulation generally showed a similar pattern to the release of reducing sugar during the hydrolysis of wheat flour by the CLEA and significantly increased above the control ($P < 0.001$). The tyrosine concentration in the control showed a small increase with incubation time and was in the range 1.0-1.5 mg/g TS. With 1:100 v/v CLEA addition, the tyrosine yield increased to a maximum value more than 2x the control, equivalent to 2.87 mg/g TS of flour after 6.5 h, and remained relatively constant for the duration of the incubation period (26 h) (Figure 6-3(a)). At the higher rate of CLEA (1:10 v/v), the maximum observed tyrosine yield was obtained after 5.5 h and was approximately 5x the control, equivalent to 5.0 mg/g TS, however, the response after 6.5 h was more variable and the tyrosine concentration declined and was significantly less than (0.1 mg/g TS) the control after 26 h (Figure 6-3(b) ($P < 0.001$). Indeed, formation of sediments was observed in the sample at 6.5 h (shown in Figure 6-4), probably due to self-aggregation of the proteins, or protein aggregation with other complex polymers in the wheat flour; the apparent decline in tyrosine may therefore be explained

because the Lowry method (specified in Section 6.2.7) only quantifies soluble products of protein hydrolysis.

(a) (b)

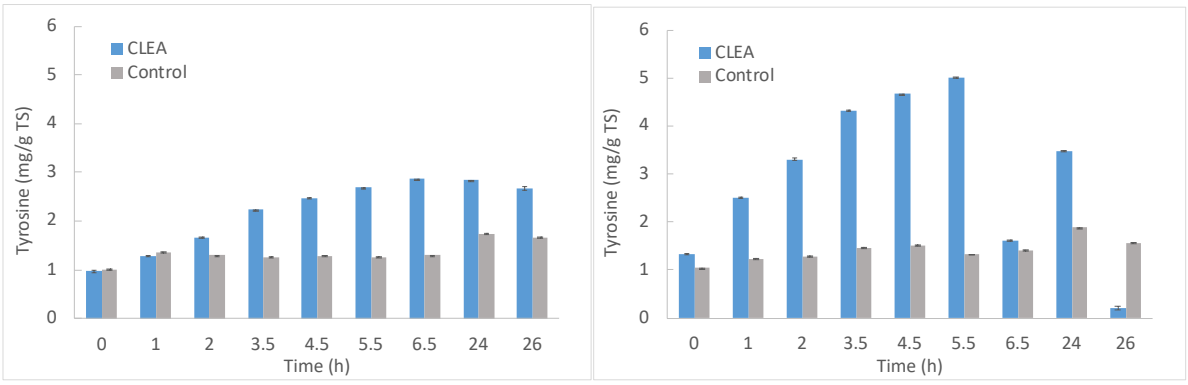

Figure 6-3 Effect of AS CLEA at rates of (a) 1:100 v/v and (b) 1:10 v/v on the accumulation of tyrosine from the hydrolysis of wheat flour (error bars indicate the standard deviation)

(a) (b)

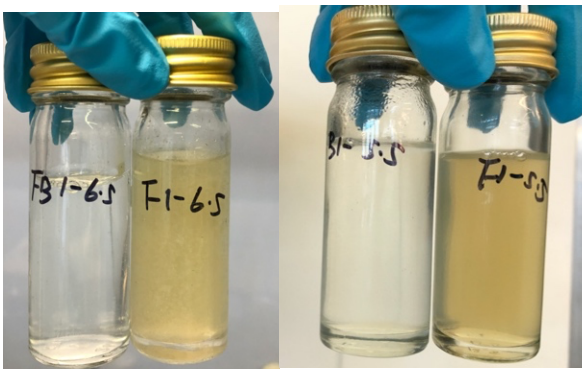

Figure 6-4(a) Sediments in the filtrate at 6.5h, compared to (b) the clear filtrate at 5.5h (the bottles with transparent filtrate were control groups at corresponding time)

6.3.1.2 Hydrolysis kinetics of wheat flour

A first-order relationship (Section 6.2.8) was used to describe the rate of the hydrolysis reaction, and to estimate the potential maximum yield of sTOC, reducing sugar and tyrosine. The hydrolysis of wheat flour and release of sTOC, reducing sugar and tyrosine by CLEA addition was described by the model during the initial 6.5 h incubation period with a high level of goodness of fit, with R^2 ranging from 0.96 to >0.99 in all cases; and the results from hypothesis test showed that the non-linear first order reaction model fits better than linear relationships, with $P < 0.001$ in all cases. The P values for D'Agostino-Pearson normality test were all >0.05, indicating the validity of the model fitting process (except for tyrosine with 1:100 v/v CLEA addition). The residual plots see Appendix (A-2).

The model coefficients are displayed in Table 6-1 and the relationships are shown in Figure 6-5. The enzymatic hydrolysis reaction velocity, indicated by *k*, increased in response to the rate of CLEA addition. Thus, the hydrolysis rate constants, *k*, of sTOC, and tyrosine were both 2.3x, and the value for reducing sugar was 1.2x, larger at the highest CLEA input,1:10 v/v, compared to the smaller rate of CLEA added,1:100 v/v. The maximum potential concentration of products is provided by C_∞ (Table 6-1) and, whilst this can only give a general indication of the total yield (due to the absence of experimental results in the asymptote region), the maximum yields of sTOC, reducing sugar and tyrosine CLEA rates of 1:100 and 1:10 v/v were, respectively, 8.0 and 9.3%, 4.1 and 6.5%, 75.9 and 108.7%. Butterworth et al. (2012) reported a similar reducing sugar yield (11.7%) when using commercial α-amylase (dosage = 0.33 U/mL) to hydrolyse wheat starch (5 g/L TS) at pH 7.3 and 37 °C for 2 h, and found that the hydrolysis process curve can be divided into two stages, with the hydrolysis rate constant (*k*) for reducing sugar reduced from 0.049 min^{-1} over the first 0.5 h to 0.008 min^{-1} (from 0.5 to 2 h). Hargono et al. (2020) used mixed commercial α-amylase and glucoamylase (mass ratio=1:1, dosage = 1.5% w/w) to hydrolyse Suweg starch (200 g/L TS) at pH 4.5 and 70 °C for 12 h; the hydrolysis rate constant (*k*) for reducing sugar was 0.4433 h^{-1} over the incubation period, which was 4 to 5 times higher than the results shown in Table 6-1. This can be explained by the high reaction temperature adopted by the author (70 °C), which accelerated the enzymatic reaction. A higher reducing sugar yield (47.7%) compared to the results obtained in this study was also reported by Hargono et al. (2020), probably because the substrate (Suweg starch, which contains only starch content) was more readily-hydrolysed than wheat flour (containing starch, proteins and lipids); impact of substrate composition on enzymatic hydrolysis of substrate is to be discussed in later sections.

As shown in Figure 6-5, 90 % of the equilibrium concentrations (C_∞) of the hydrolysis products may potentially be achieved over a period of 26 h at both CLEA rates. The reason that the experimental samples at 24 h and 26 h were far below the values predicted by the first order function (and were therefore not included in the model) may be explained due to interference from the consumption and breakdown of the products of enzymatic hydrolysis by other microbial reactions in the system.

Table 6-1 First order kinetic model of soluble total organic carbon (sTOC), reducing sugar and tyrosine accumulation from the enzymatic hydrolysis of wheat flour by AS CLEA at two addition rates and incubated at 40 °C for 6.5 h (best-fit coefficients in 95% confidence interval ± standard deviation)

Chemical parameter, model coefficient and statistics	CLEA dose rate (CLEA suspension : substrate)	
	1:100 v/v	1:10 v/v
sTOC:		
C_0 (mg/g TS)	13.6 ± 0.22	15.5 ±2.16
C_∞ (mg/g TS)	58.0 ±3.78	66.9 ± 5.08
k (h^{-1})	0.1137 ± 0.0137	0.2634 ± 0.0586
Equation	$C = 13.60 + 44.42 (1-e^{-0.1137t})$	$C = 15.51 + 51.39 (1-e^{-0.2634t})$
R^2	>0.99	0.96
P for normality test	>0.05	>0.05
Pass the test (alpha = 0.05)	Yes	Yes
Reducing sugar:		
C_0 (mg/g TS)	7.19 ± 0.12	4.05 ± 0.45
C_∞ (mg/g TS)	42.4 ± 2.31	59.9 ± 9.39
k (h^{-1})	0.0859 ± 0.0077	0.1022 ± 0.0236
Equation	$C = 7.19 + 35.24 (1-e^{-0.0859t})$ *	$C = 4.05 + 55.82 (1-e^{-0.1022t})$
R^2	>0.99	0.99
P for normality test	>0.05	>0.05
Pass the test (alpha = 0.05)	Yes	Yes
Tyrosine:		
C_0 (mg/g TS)	0.92 ± 0.02	1.34 ± 0.02
C_∞ (mg/g TS)	4.47 ± 0.34	5.97 ± 0.08

k (h^{-1})	0.1252 ± 0.0176	0.2873 ± 0.0099
Equation	$C = 0.92 + 3.55 (1-e^{-0.1252t})$	$C = 1.34 + 4.63 (1-e^{-0.2873t})$ **
R^2	>0.99	>0.99
P for normality test	<0.001	>0.05
Pass the test (alpha = 0.05)	No***	Yes

Note: * fitting of the model was based on data within 1-6.5 h since reducing sugar was not detected at t = 0; **fitting of the model was based on data within 0-5.5 h, and the data at 6.5 h was excluded due to the inconsistent response compared with other data (see Section 6.3.1.1); *** the residual did not pass the normality test; corresponding residual plot see Appendix A-2(e).

(a)

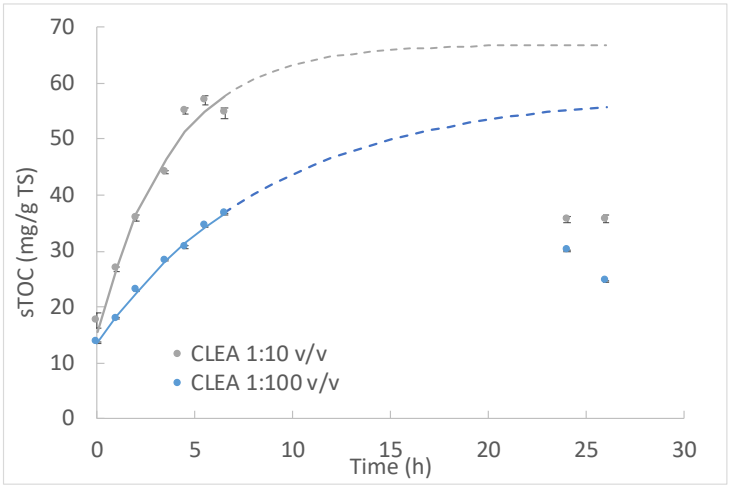

(b)

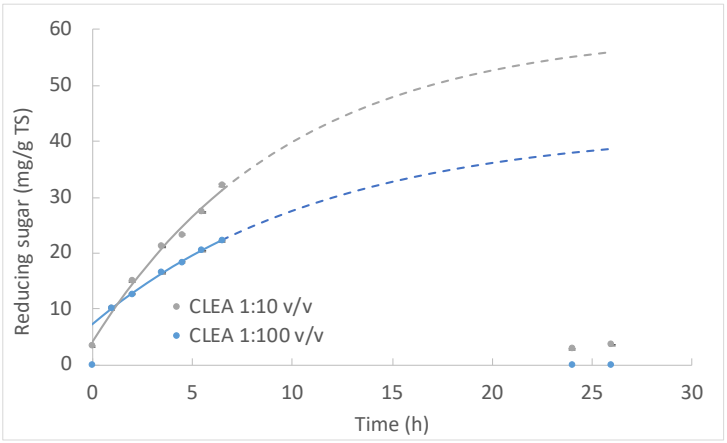

(c)

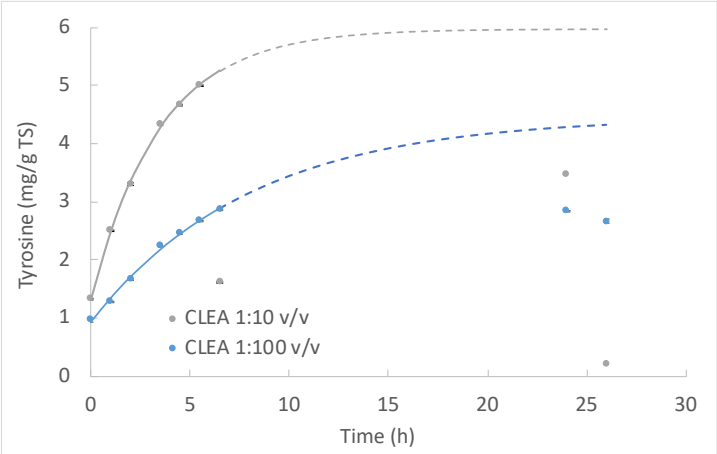

Figure 6-5 First order kinetic model of (a) sTOC, (b) reducing sugar and (c) tyrosine accumulation from the enzymatic hydrolysis of wheat flour by AS CLEA at two addition rates (1:100 and 1:10 v/v) and incubated at 40°C showing the maximum potential yield of each product (solid line: model prediction for the incubation period 0-6.5 h based on experimental data; dashed line: extrapolation beyond the available experimental data for the period 6.5-26 h; solid symbols: experimental data; error bars: standard deviation)

6.3.2 Hydrolysis of activated sludge

6.3.2.1 CLEA activity in sludge supernatant

The CLEA activity for cellulase and protease was not significantly (P > 0.05) affected by the sludge supernatant matrix; on the contrary, slightly increased and decreased activities of amylase and lipase were observed, respectively (Table 6-2). Overall, >83% of the original CLEA activity was detected in the sludge supernatant, suggesting that aqueous phase in sludge is unlikely to interfere with the hydrolysis behaviour of the CLEA suitable to be used in hydrolysing sludge.

Table 6-2 Average CLEA activities (%) in primary sludge supernatant compared to the activity in standard buffer solution, which was set as 100%

Enzyme	Amylase	Cellulase	Protease	Lipase
Relative activity (%)	109.2	96.2	92.5	83.6
P	0.012	>0.05	>0.05	0.003

Note: *P* value indicates the statistical significance of the enzyme activity in sludge supernatant compared to buffer solution.

6.3.2.2 Whole AS

The hydrolysis of whole AS was examined by measuring the soluble TOC and reducing sugar contents in the reaction mixture during the incubation period, up to a maximum duration of 26 h. The results for sTOC and reducing sugar showed generally similar patterns. No significant

effect ($P > 0.05$) of incubation time on sTOC concentration was observed for the control within the initial 6.5 h of incubation; however, a small, albeit statistically significant ($P = 0.003$), increase in sTOC (by 16.4%) was detected with CLEA addition after 5.5 h of incubation compared to the initial concentration (0 h). Reducing sugar concentrations were significantly increased with time, to a small extent, with both CLEA addition and in the control within 6.5 h of incubation, however, the magnitude of the response was slightly larger with the CLEA addition (15.6%), compared to the control (11.8%). sTOC subsequently decreased by approximately 30% to approximately 17 mg/g TS after 26 h in both treatments (Figure 6-6(a)). Reducing sugar concentration also decreased after 6.5 h to a similar extent in both treatments to approximately 6.0 mg/g TS (Figure 6-6(b)).

(a)

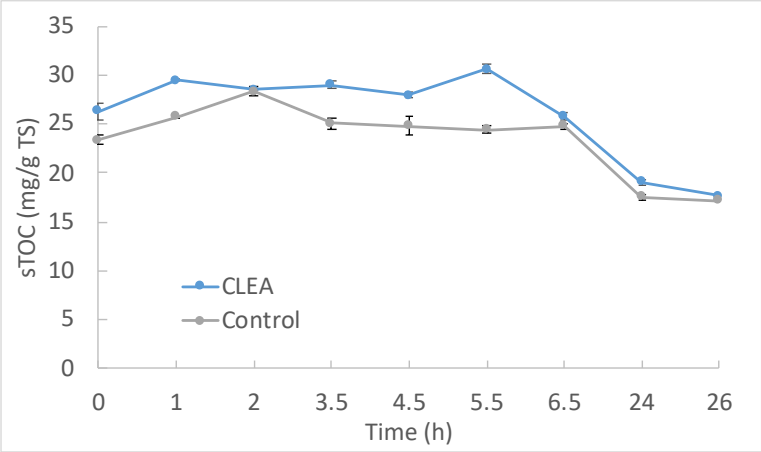

(b)

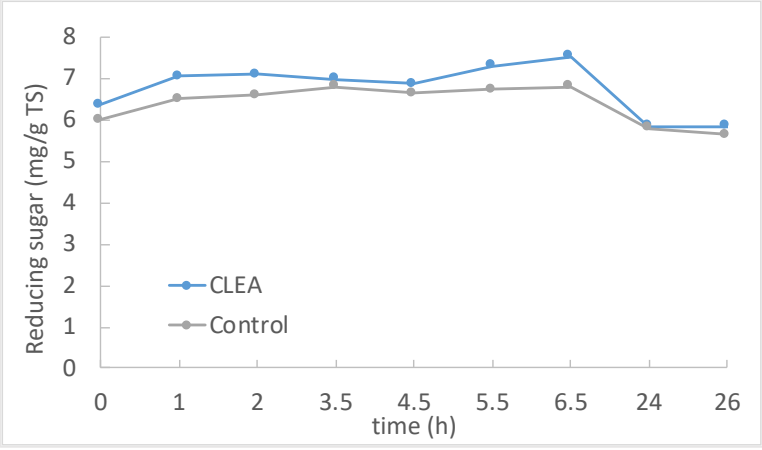

Figure 6-6 Effect of CLEA addition (1:10 v/v) on (a) sTOC and (b) reducing sugar release from the hydrolysis of whole AS (error bars indicate the standard deviation; reducing sugar content shown as average values of two replicate measurements)

6.3.2.3 Autoclaved AS

In general, no significant differences ($P > 0.05$) in sTOC content were observed for autoclaved AS with time over the duration of the incubation period (0-24 h), with CLEA addition to the autoclaved AS. For the control group, the sTOC concentration remained relatively constant during the initial 0-5 h incubation period, with a mean concentration equivalent to 56.4 mg/g TS, and subsequently increased after 7 h to a value larger than with CLEA (>86 mg/g TS). The reducing sugar content in the reaction mixture did not significantly change ($P > 0.05$) with time for both the control and with CLEA addition, and no significant difference ($P > 0.05$) in the reducing sugar content was observed treatments.

(a)

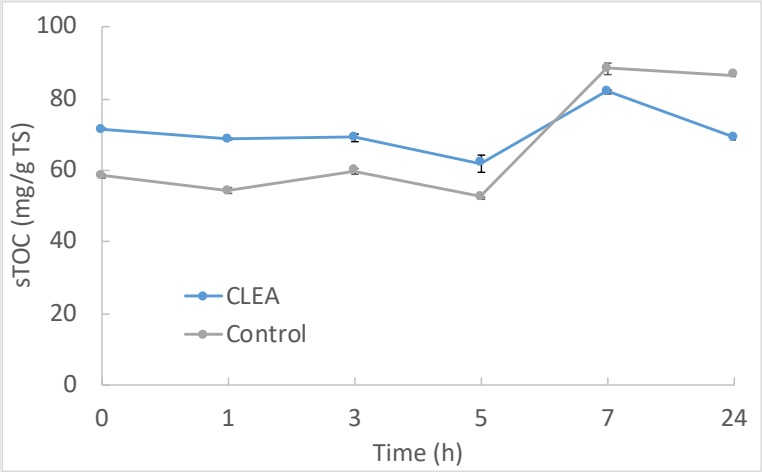

(b)

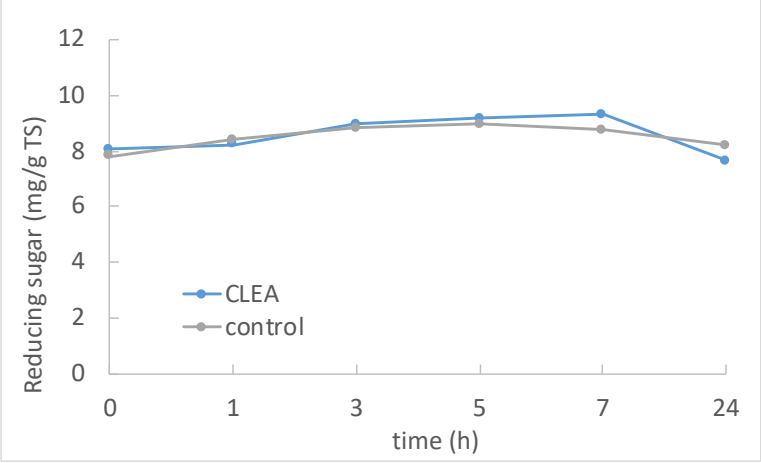

Figure 6-7 Effect of CLEA addition (1:10 v/v) on (a) sTOC and (b) reducing sugar release from the hydrolysis of autoclaved AS (error bars indicate the standard deviation; reducing sugar content shown as average values of two replicate measurements)

6.3.2.4 γ-Irradiated AS

The AS matrix mainly consists of microbial cells, and contains polysaccharide and proteins. Quantification of enzymatic hydrolysis reactions was extended to include monitoring the accumulation of tyrosine from protein degradation as well as the hydrolysis of starch in γ-irradiated AS.

No evidence of sTOC or reducing sugar accumulation was found, and both showed a significant ($P < 0.001$ and $P = 0.006$, respectively) decrease in concentration by the end of the incubation period (Figure 6-8(a, b)). The significant increase in sTOC and reducing sugar concentration with CLEA addition compared to the control, which was consistently observed at the beginning of the incubation period, was probably due to release of sTOC and reducing sugar from the complex AS CLEA matrix. By contrast tyrosine release from γ-irradiated AS showed a clear pattern of accumulation with incubation time (Figure 6-8(c)). Thus, tyrosine increased significantly ($P < 0.001$) after 3.5 h of incubation, compared to the initial concentration (0 h) to a maximum value equivalent to 8.1 mg/g TS. Tyrosine concentrations varied to some extent over the following 4.5 h, but generally remained consistent over this period followed by a significant ($P < 0.001$) decline equivalent to 44% to ⩽ 4.5 mg/g TS after 24 h. By contrast no significant ($P > 0.05$) change in tyrosine was detected for the control during the first 3.5 h period, and the mean concentration was equivalent to 5.6 mg/g TS. Similar to CLEA addition, the tyrosine content in the control also decreased significantly ($P < 0.001$) after 6.5 h by approximately 41% after 24 h of incubation.

(a)

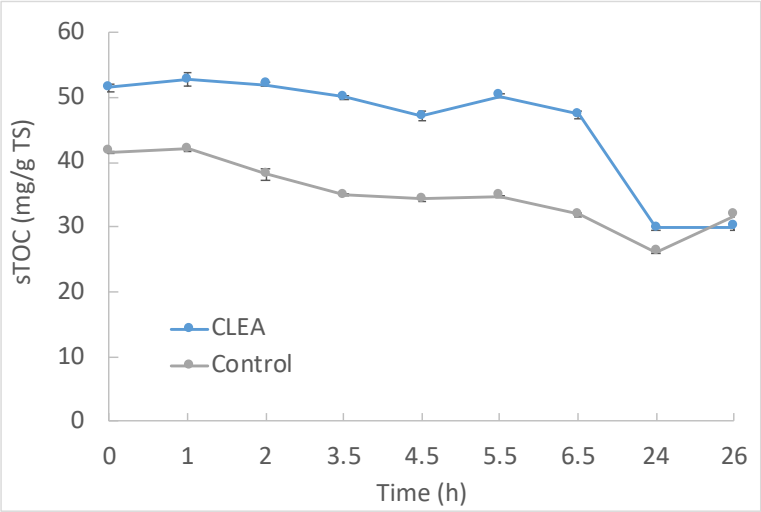

(b)

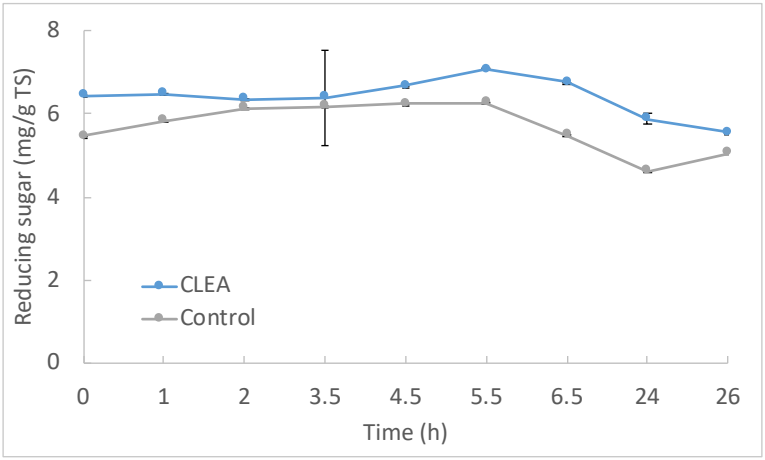

(c)

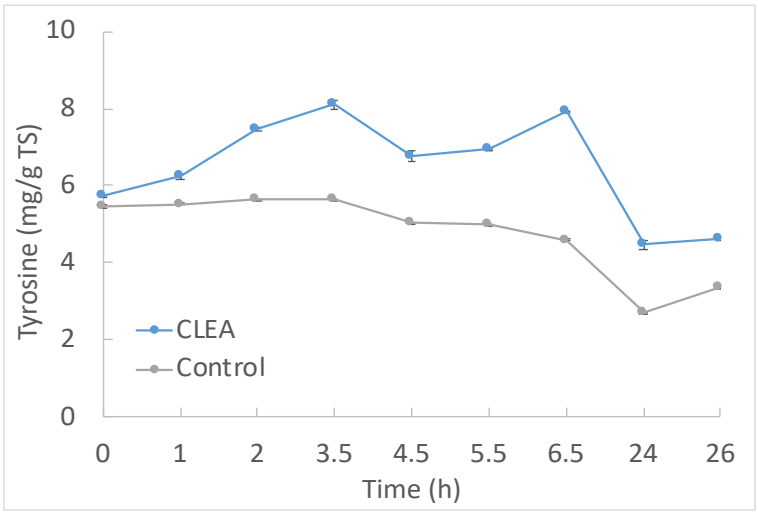

Figure 6-8 Effect of CLEA addition (1:10 v/v) on (a) sTOC, (b) reducing sugar and (c) tyrosine release from the hydrolysis of γ-irradiated AS (error bars indicate the standard deviation)

6.3.2.5 Sonicated AS

Soluble TOC content, accumulated reducing sugar and tyrosine were measure in the reaction mixture to determine the effects of CLEA on the hydrolysis of sonicated AS. No evidence of sTOC or reducing sugar accumulation compared to the control was found. sTOC showed a significant decrease ($P < 0.001$) by the end of the incubation period (Figure 6-9(a)). The reducing sugar content with CLEA addition to the sonicated AS remained relatively constant for the initial 6.5 h, and decreased by 7.4% of the initial content at the end of the incubation Figure 6-9(b). The reducing sugar content showed a similar pattern for the control group, with the concentration maintained relatively constant within 0-6.5 h ($P > 0.05$) and dropped by a larger ratio compared with CLEA addition (35.6% of the initial concentration) after 24 h.

The tyrosine content in the reaction mixture with CLEA addition (Figure 6-9(c)) showed a consistently increasing response equivalent to 39% compared to the initial value (0 h) from 7.1 mg/g TS to 9.9 mg/g TS after 6.5 h (except 5.5 h). After 24 h incubation, however, a decrease equivalent to 43% compared to 6.5 h was obtained and the final concentration of tyrosine was equivalent to 4.2 mg/g TS after 26 h. Tyrosine content varied between 6.9 and 8.0 mg/g TS in the control, but generally did not change significantly within 0-6.5 h ($P > 0.05$); after 24 h reaction, the tyrosine content in control group also decreased, to approximately 2.6 mg/g TS.

(a)

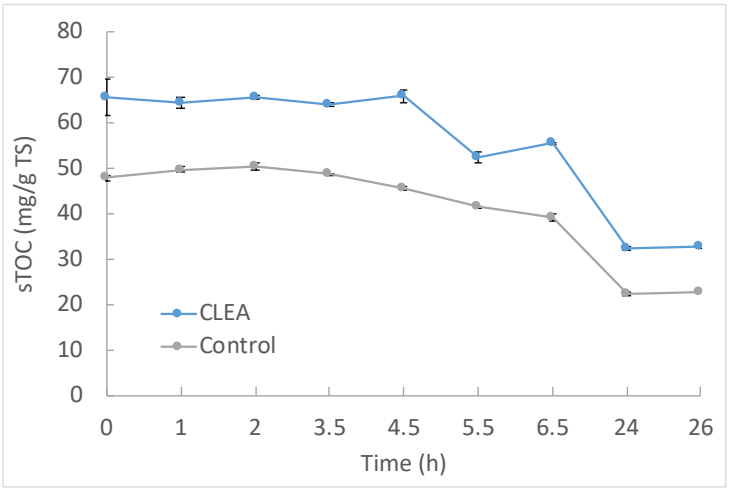

(b)

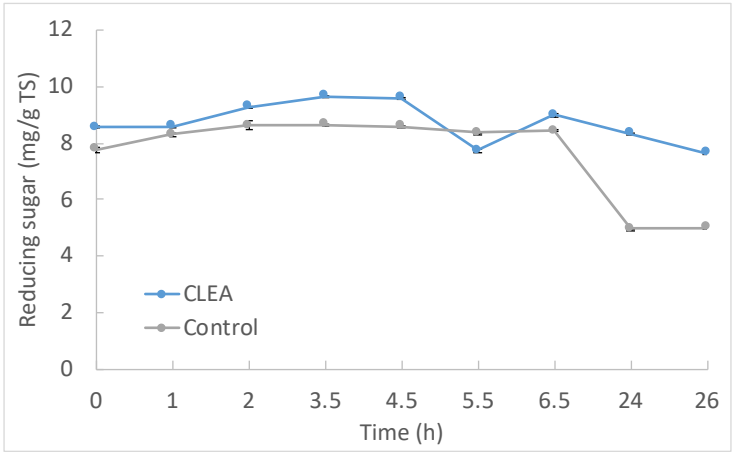

(c)

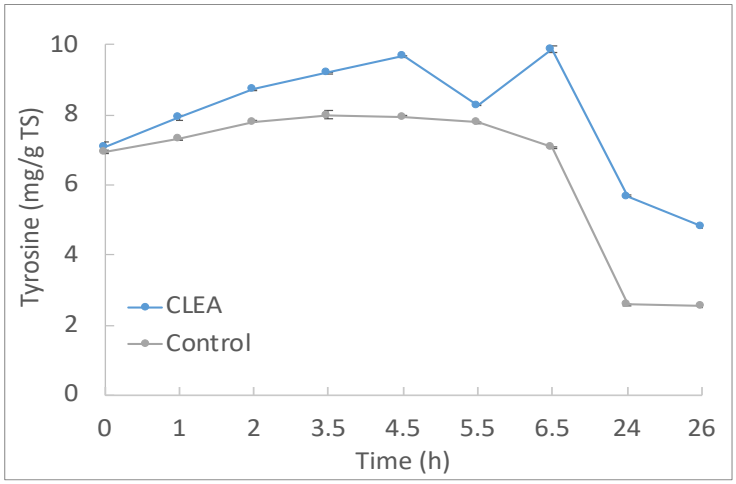

Figure 6-9 Effect of CLEA addition (1:10 v/v) on (a) sTOC, (b) reducing sugar and (c) tyrosine release from the hydrolysis of sonicated AS (error bars indicate the standard deviation)

6.3.2.6 Sludge cell culture

The concentrations of sTOC, reducing sugar, and tyrosine decreased in the experiments with AS after incubation for 24 h (Figure 6-7, 6-8 and 6-9). This suggested possible competition reactions were apparent between the enzyme hydrolysis and utilisation of the soluble product by the microbial population present in the sludge, which was examined by culturing sludge samples on microbial media.

Microbial growth was observed for both γ-irradiated and sonication-disrupted sludge, although less extensively compared to the control group (no pretreatment) (Figure 6-10). This indicated that γ-irradiation and sonication were only moderately effective at inactivating AS microbes.

(a) (b) (c)

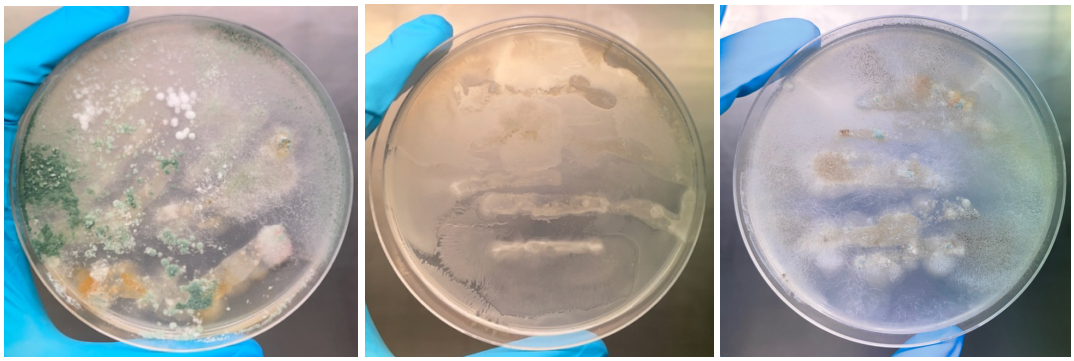

Figure 6-10 Microbial cultures of (a) whole AS, (b) by γ-irradiated AS and (c) sonicated AS

6.3.2.7 Hydrolysis kinetics of γ-irradiated AS and sonicated AS

The first-order relationship (Eq 6-1) was also used to estimate the potential maximum yield of tyrosine from γ-irradiated and sonicated AS. The tyrosine release during the initial 6.5 h incubation period by CLEA hydrolysis of the two AS types fitted well to the model, with R^2 ranging from 0.91 to >0.99 in all cases; and the results from hypothesis test showed that the non-linear first order reaction model fits better than linear relationships, with $P < 0.001$ in all cases. The residual plots see Appendix (A-3).

The model coefficients are displayed in Table 6-3 and the relationships are shown in Figure 6-11. The maximum potential yield of tyrosine from γ-irradiated AS and sonicated AS is calculated by Eq 6-2, and was equivalent to 23.2-29.6% and 32.8-43.5%, respectively. It should be noted that, this can only give a general indication of the total yield of tyrosine, as is specified in Section 6.2.8.

Table 6-3 First order kinetic model of tyrosine accumulation from the enzymatic hydrolysis of γ-irradiated AS and sonicated AS by CLEA at 1:10 v/v dosage rate and incubated at 40 °C for 6.5 h (best-fit coefficients in 95% confidence interval ± standard deviation)

Sludge type	γ-irradiated AS	Sonicated AS
C_0 (mg/g TS)	5.61 ±0.18	7.08 ±0.06
C_∞ (mg/g TS)	8.21 ± 0.23	10.27 ±0.12
k (h^{-1})	0.5212 ±0.1309	0.3422 ±0.0312
Equation	$C = 5.61 + 2.60\ (1-e^{-0.5212t})$ *	$C = 7.08 + 3.19\ (1-e^{-0.3422t})$ **
R^2	0.91	>0.99
P for normality test	>0.05	>0.05
Pass the test (alpha=0.05)	Yes	Yes

Note:* model fitting based on data obtained within 0 ≤ t ≤ 3.5h and t = 6.5 h; ** model fitting based on data obtained within 0≤ t ≤ 6.5h, excluding data at t = 5.5 h.

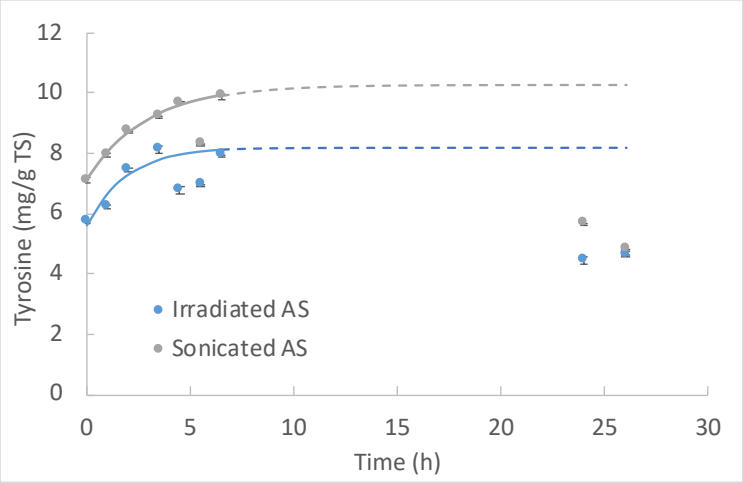

Figure 6-11 Predicted data by first order reaction model and its comparison to the experimental data (solid lines-predicted data within 0-6.5 h; dash lines: predicted data within 6.5-26 h; solid dots: experimental data; error bars: standard deviation)

6.4 Discussion

6.4.1 Quantifying the kinetics of enzymatic hydrolysis reactions

The kinetics of enzymatic reactions are usually quantified by either: (1) steady-state kinetics based on Michaelis–Menten model (Eq 2-1), or (2) time-course kinetics based on the reaction progress curve. The Michaelis-Menten model determines the initial velocity (V_0) of the reaction, which represents the amount of product produced per unit time at the start of the reaction, measured at varying substrate concentrations (S). This is obtained from the relationship between $1/V_0$ and $1/S$ (Eq 6-3, derived from Eq 2-1), and the kinetic parameters, V_{max} and K_m (definition see Section 2.2.3), are determined from the x- and y-intercept. As for the full time-course progress curve approach, the enzymatic reaction (Section 2.2.3) is monitored under each condition (for example, varying substrate concentrations, but can also include other factors, such as temperature), and is not limited to only measuring the initial rate of the reaction.

$$\frac{1}{V_0} = \frac{K_m}{V_{max}} \cdot \frac{1}{S} + \frac{1}{V_{max}} \qquad \text{(Eq 6-3)}$$

Both approaches are valid for assessing the kinetics characteristics of enzymes, although most studies (e.g. (Mafra et al., 2018)) have tended to apply initial rate measurements to obtain V_{max} and K_m values. However, other studies have also used the full time-course progress method (e.g. (Pleiss, 2018; Buchholz et al., 2019)).

The time-course kinetic method was used here to assess the effectiveness of the produced CLEA on hydrolysing complex organic materials. The progress curve of the CLEA hydrolysis reactions was monitored and the progress curve was described using a first-order reaction model, which is an exponential function showing the changing pattern of the hydrolysis product accumulation against time (see Section 6.2.8), to predict the maximum product yield. The

rationale of using progress curve analysis, rather than the steady-state kinetic methods, is because the latter has two major limitations under the experimental condition:

Firstly, the Michaelis–Menten equation is only suitable to describe the steady-state stage of an enzyme reaction (Section 2.2.3), during which the product increases linearly with time. The initial velocity is therefore defined as the reaction rate at the substrate concentration that exactly equates to is the amount that was initially added. Therefore, enzyme activity assays must be performed over very short time scales (representing only seconds or mins of the overall reaction, see Section 2.2.3) to accurately measure the kinetic parameters. However, in practice, the substrate concentration inevitably varies, declining as the reaction proceeds, which may affect the measured initial rate values.

Secondly, the Michaelis–Menten equation (Eq 2-1) is often used to examine simple, single-substrate reactions (Pleiss, 2018), rather than multi-substrate reaction systems. In a multi-substrate reaction system, competitive and/or non-competitive inhibition of the enzyme by different constitutions in the substrate and or by products from other enzymes may occur, thus, the initial rate of multi-CLEA hydrolysis does not depend solely upon the variations in substrate concentration. Here, two multi-substrate systems were used to assess the effectiveness of the AS CLEA: wheat flour, which mainly consists of non-bioactive carbohydrates and proteins, and AS, which contains a large number of rigid microbial cells and microbial metabolites. The multi-CLEA is capable of hydrolysing different substrates simultaneously, however, a wide range of interacting factors can significantly influence the CLEA catalytic activity (to be discussed in the following sections).

Therefore, the time-course analysis of the progress curve is more suitable and appropriate to determine the kinetic characteristics of CLEA hydrolysis reactions. Furthermore, analysing the kinetic properties of CLEA hydrolysis by the reaction progress approach can also provide a more quantitative description of the full enzymatic reaction, compared to the steady-state kinetic analysis. Using a time-dependent numerical function to describe either substrate depletion or product formation with time may also provide additional, valuable information about the process that may be difficult to observe experimentally during the initial phase of the reaction, such as variation of the reaction velocity against time, reversibility of the reaction, product/substrate inhibition and enzyme inactivation over prolonged reaction periods (Buchholz et al., 2019; Meraz et al., 2020). Specifically, the reaction progress method was used to provide an indicative estimate of the maximum product yield (as Specified in Section 6.2.8).

6.4.2 Hydrolysis of wheat flour

6.4.2.1 Factors influencing the CLEA hydrolysis of wheat flour

Starch is the predominant carbohydrate in wheat flour, ranging from 73% to 80% of flour TS (Yuan et al., 2021; Zhang et al., 2021); non-starch carbohydrates in wheat flour include cellulose (fibre), hemicellulose and free sugars, which are derived from wheat cell walls (D'Appolonia and Rayas-Duarte, 1994; Garofalo et al., 2011). Hydrolysis of the complex carbohydrates in flour releases reducing sugars, such as sucrose, maltose and glucose. Here, the effects of the hydrolysis activity of AS CLEA on carbohydrates in wheat flour was determined based on the accumulation of reducing sugars, specifically glucose, as the hydrolysis product of starch. Protein (gluten) in wheat flour contains different amino acids including glutamic acid, proline, isoleucine, leucine, lysine, cystine, and tyrosine (McDermott and Pace, 1957)) and enzymatic treatment cleaves the peptide bonds, releasing soluble, free amino acids as hydrolysate. The activity of the CLEA towards proteins in the flour was therefore quantified by measuring the accumulation of tyrosine as a major product of protein hydrolysis (Yang et al., 2010).

The accumulation of reducing sugar demonstrated the effective hydrolysis of starch in wheat flour by the AS CLEA. Maximum yields of reducing sugar of approximately 4.1% and 6.5% at CLEA addition rates of 1:100 and 1:10, respectively, were predicted by the first-order kinetic model (Eq 6-1). Thus, reducing sugar yield by CLEA hydrolysis was relatively moderate compared to other studies. For example, Dojnov et al. (2015) used crude *Aspergillus niger* amylase (produced from solid fermentation), as well as a commercial enzyme product (a mixture of protease, α-amylase, and amyloglucosidase) to hydrolyse wheat flour (2% TS content suspension in acetate buffer, pH 5.0) at 50 °C. The conversion rate of starch to glucose by the crude amylase and the commercial enzyme product was equivalent to 72.6% and 74.4%, respectively, at an equivalent amylase dose rate of 106.3 U/mL. Ba et al. (2013) applied crude sorghum malt extracted amylase (containing α-amylase 312.6 U/g, β-amylase 62.7 U/g, and pullulanase 1.3 U/g) for hydrolysis of wheat flour (a suspension of 30 % w/v TS content) at 65 °C and pH 5.5. The reducing sugar yield after 6 h was approximately 13, 25 and 30%, at dose rates of 0.03, 0.05 and 0.07 % (w/w) of the crude enzyme mixture, respectively.

The following factors have a major influence on the reducing sugar yield from CLEA hydrolysis of wheat flour:

(1) Starch-protein interactions in the flour suspension

Wheat flour contains a significant amount of protein, which physically adsorb onto starch granules in a flour suspension, thus, restricting the access of amylase to the starch substrate.

Eliasson and Tjerneld (1990) reported that the amount of glutenin (an extensively branched, multi-chained polypeptide present in wheat flour) adsorbed onto starch granules was approximately 5-6 mg/g starch when starch granules were incubated at 40 °C (equivalent to the temperature conditions applied here), and that adsorption increased with temperature, up to >12 mg/g at 80 °C. Furthermore, wheat gluten proteins can form a cross-linked network in flour suspensions (Mohamed and Rayas-Duarte, 2003; Ma et al., 2011), coating starch granules and consequently hindering enzymatic cleavage of the starch-glycosidic bonds.

The hydrolysis products from wheat flour starch can also interact with proteins, inhibiting the further hydrolysis of starch by amylase. Hill et al. (1997) reported that α-amylose hydrolysis of starch granules (30 g/L, at 45 °C) was subjected to inhibition by its hydrolysis product, glucose, and the enzyme activity exponentially decreased with increased glucose concentration present in the reaction system (up to 400 g/L). Hill et al. (1997) suggested that this inhibition was probably due to the glucose molecules directly binding to the active or other sites on the α-amylase protein structure, forming a complex that could hinder further hydrolysis. de la Rosa-Millan et al. (2020) used a commercial α-amylase (activity = 13 U/mL) to pretreat chickpea flour at 35 °C for 12 h; the α-amylase pretreated flour was further subjected to an *in vitro* enzymatic digestion process (by commercial mixed digestive enzymes) at 37 °C for 180 min. Rapid release of reducing sugar (measured as glucose) occurred in the first 20 min of the digestion, but, subsequently glucose accumulated at a comparable rate to raw flour (without amylase pre-treatment). This was explained because: the α-amylase cleaves the and α 1-4 glycosidic linkages of starch molecules during the pretreatment, producing smaller molecules (e.g. dextrin, as a partial hydrolysis product of starch) with higher susceptibility to the digestive enzyme attack; the rapid release of reducing sugar observed in the initial 20 min was due to further hydrolysis of these low MW molecules. However, the non-hydrolysed starch residues, mainly as linear-chained glucans gradually accumulated as the reaction proceeded, becoming inter-tangled with adjacent glucans, protein and fibre in the flour, hindering the enzymatic digestion reaction (de la Rosa-Millan et al., 2020).

Takeuchi (1969) indicated that starch-protein interactions occur in complex organic matrices, such as flour, due to electrostatic attraction between protein and starch molecules. Ryan and Brewer (2007) suggested that hydrophobic interactions between unfolded polypeptides chains and the hydrophobic region on the surface of starch granules, as well as hydrogen bonding, are also involved. The step-wise addition of protease followed by α-amylase enzymes can avoid potential protein-starch interactions and enable the enzymes to hydrolyse starch at the maximum rate (Goñi et al., 1997; Sun et al., 2019). The AS multi-CLEA supplied both protease and amylase enzymes simultaneously and therefore step-wise enzymatic treatment was not possible. Nevertheless, the results showed that the CLEA demonstrated hydrolytic activity

towards wheat flour and, whilst the reaction was potentially influenced by various protective and inhibitory mechanisms, the partial hydrolysis of starch in a complex substrate was achieved.

Starch-protein interactions may also explain the high tyrosine yield (approximately 76-100%) from the hydrolysis of flour by the CLEA (Section 6.3.1.2), compared to reducing sugar. Indeed, protein molecules are located on the outside of the starch granules, due to the starch-protein interactions, and are therefore more accessible and susceptible to protease attack (Ryan and Brewer, 2007).

(2) Physical and chemical structure of the substrate

The physical and chemical properties of wheat flour at both the molecular and granular levels influence the susceptibility to enzyme attack and hydrolysis efficiency (Sakintuna et al., 2003; Butterworth et al., 2012) and may explain the differences in behaviour measured here compared to the literature. Milling of wheat, for example, can influence the size distribution and shape of the flour particles. Ma et al. (2011) reported that the starch granules in a wheat flour showed varying shapes from ovoid to spherical, with heterogeneous sizes ranging from 19 to 35 μm in length and from 14 to 22 μm in width. The protein fragments attached to or located between the starch granules also varied in terms of both the amount and fragment shape. Ma et al. (2020) reported a wider range of particle sizes, from 17 to 358 μm, for a milled wheat flour, and found that the digestible starch content increased with decreasing particle size. Ma et al. (2020) explained that the shearing forces acting at the starch-protein interface caused crystallite slippage within the starch granule, leading to non-uniform distribution of digestible starch. Manelius et al. (1997) used α-amylase solution (0.002 U/ml) to hydrolyse 25 g wheat starch granules (with varying particle sizes) in a continuous reaction, with the amylase solution pumped at a rate of 0.33 mL/min. It was found that small wheat starch granules (diameter = 2.5 μm) were more readily attacked by α-amylase than larger granules (10 μm diameter), with the solubilisation rate (measured as carbohydrate content in the hydrolysate, relative to the total carbohydrate of starch) equivalent to 15% and 8%, respectively, during a 25 d reaction period at 25 °C.

The overall content and amounts of resistant types of starch in flour can also influence the degree of hydrolysis and susceptibility to enzymatic attack (Goñi et al., 1997). Amylose, a linear polysaccharide formed of α-D-glucose units, is an example of a resistant type of starch in wheat flour. MacGregor et al. (2002) applied a mixture of α-amylase, β-amylase and limit-extrinase (i.e. isoamylase) to hydrolyse several types of commercial barley starch containing 0 to 35% of amylose at 48-72 °C. The results showed that the reducing sugar yield from high-

amylose starch was reduced by approximately 1/3 to 1/4 compared to starch with lower amylose contents under equivalent conditions.

(3) Enzyme formulation

Immobilised enzymes present in CLEAs are carried within a granular, supramolecular structure (shown in Section 5.3.4) and, consequently, steric hindrance can limit the diffusion of macromolecular substrates, such as starch, into the interior of the CLEA, reducing accessibility to reaction sites and thus the reaction rate, which may have also been partially responsible for the relatively low yield of reducing sugars, compared to the results in previous literatures where soluble enzymes were used (see above). For instance, da Costa Luchiari et al. (2021) observed mass transfer limits when hydrolysing a 1% w/v starch suspension with immobilised enzyme; the conversion rate of starch into glucose by glucoamylase immobilised onto corncob powder (16%) was reduced by 80% compared to soluble glucoamylase (which gave a conversion rate of starch to glucose of 75%) at equivalent enzymatic load (30 U/g TS of starch) after 12 h reaction at 50 °C. However, the observed rapid and extensive hydrolysis of protein to tyrosine suggested that protein-starch chemistry was probably more important than mass transfer factors in limiting the overall hydrolysis of starch in wheat flour by the CLEA.

6.4.2.2 Competitive reactions to CLEA hydrolysis

The CLEA hydrolysis experiments included treatments with incubation periods extending to 26 h with the intention to obtain sufficient data for asymptotic model fitting. However, following the initial increase, when detected, or, indeed if concentrations remained relatively consistent initially, after 24h of incubation, the hydrolysis products decreased to small or undetectable amounts. This behaviour suggested a possible microbial interaction, which could be originated from the CLEA, and the utilisation of hydrolysis products interfered with the apparent accumulation of soluble hydrolysis products (Figure 6-6, 6-7, 6-8 and 6-9).

6.4.3 Effect of sludge chemical environment on CLEA hydrolysis activity

Activated sludge is generated in the biological wastewater treatment process and is therefore less likely to be affected by the raw wastewater influent properties compared to primary sludge. However, AS provides a matrix for heavy metal and organic pollutant sorption (Zhang et al., 2018) and the properties of the solute environment in sludge, including the pH and concentrations of inorganic ions, could be potentially inhibitory and influence enzymatic reactions of the CLEA, compared to measuring activity in standard laboratory conditions in a controlled buffer solution. Potentially inhibitory properties of sludge include:

(1) Organic pollutants:

Pharmaceuticals, cosmeceutical, biomedical, personal care products and flame-retardants are widely found in sewage influent. Conventional wastewater treatment is designed to

remove readily-biodegradable organic matter, nutrient substances and pathogens from raw sewage, but not specifically to degrade persistent emerging pollutants. The majority of organic pollutants have hydrophobic properties and transfer to the solid phase during wastewater treatment (Moayed et al., 2020; Tasselli et al., 2021). The concentrations of these pollutants in primary sludge and secondary AS can be up to 10^3-10^4 ng/g TS (Verlicchi and Zambello, 2015).

Inhibitory effects of organic pollutants on hydrolytic enzyme activities have been reported, for example, phenolic compounds, can inhibit activity by non-covalently binding with enzymes (Rawel et al., 2005). Bwanganga Tawaba et al. (2015) used a crude amylase solution (containing α- and β-amylase extracted from red sorghum malt) to hydrolyse sorghum malt flour (5% w/v solids content) at 40°C. The rate of glucose release was negatively related to the concentration of phenolic compound addition in the reaction system (ranging 0-100 mg as gallic acid equivalent per 0.2mL substrate). Amariei et al. (2017) found that esterase activity of AS (125 mg/L solids content) was reduced by 50% by ibuprofen (a widely used analgesic drug) and triclosan (an antimicrobial agent) supplied at concentrations of 633 and 1.94 mg/L, respectively, for 1 h at 20 °C. By comparison, concentrations of organic pollutants in sludge are much smaller and are therefore unlikely to be inhibitory to enzymatic hydrolysis reactions.

(2) Heavy metals:

Heavy metals are also an important group of pollutants in wastewater; up to 80-90% of the heavy metals in wastewater can adsorb to the biological sludge, depending on the sludge redox potential, surface molecular structure, and charge density (Li et al., 2016; Agoro et al., 2020). Trace amounts of certain heavy metals are required for the activation and/or functioning of many hydrolytic enzymes (as a cofactor, see Section 2.2.1). However, at relatively high concentrations, metal ions can disrupt enzyme function and structure by binding with thiol and other groups on protein molecules, or by replacing naturally occurring metals in enzyme prosthetic groups, altering the performance of the biological processes (Mudhoo and Kumar, 2013). For example, Zohra et al. (2016) reported that mercury and copper (Hg^{2+} and Cu^{2+}) can reduce the α-amylase activity (towards starch measured at 50°C) by approximately 100% and 60% at 10 mM, respectively. However, by comparison, concentrations of soluble metals ions are much smaller in sludge (based on date reported by Tytła (2019)) and are unlikely to be inhibitory to enzymatic hydrolysis reactions.

(3) General chemical conditions of the sludge liquid fraction: pH and ionic strength

Each enzyme has an optimum pH range, beyond the limit of which the enzyme activity will be inhibited. The optimum pH for amylases, cellulases and lipase is typically 4.6-7.0, 4.2-5.2 and 8, respectively (Worthington et al., 2019). Proteases have a wider optimum pH range, and

acidic, neutral and alkaline proteases from various microbes have been identified (Rao et al., 1998). Indeed, most of the enzyme activity assays are carried out within their optimum pH range (see Section 3.6). Changes in pH condition affects the polar and non-polar intramolecular attractive and repulsive interactions between the acidic and basic groups on the enzyme surface (and interior in the protein molecule), which could alter the shape and active site of the enzyme and consequently reduce the affinity to the substrate molecules (Zinchenko, 2012). Ionic strength of sludge matrix can affect the enzyme activity, mainly due to the neutralising effect by the counterion of the salts on the electrostatic interactions required for substrate binding (Eun, 1996); increased ionic strength often leads to reduced effective binding affinity (SchÄGger, 2003). The ionic strength may also affect the enzymatic reaction by changing the stability and solubilities of the enzyme as well as those of the substrates (Eun, 1996).

Here, a primary sludge supernatant, which contains most of the soluble substances present in raw sewage influent that may transferred to AS, was used in place of the standard buffer solution to quantify the potential effects of the sludge matrix on the CLEA activity. The CLEA protease and cellulase activity was not significantly affected ($P > 0.05$) by the primary sludge supernatant, compared to measurements using standard buffer conditions (Table 6-2). Lipase activity decreased by 16.4% compared to the standard condition, which could be explained because lipase favours a weak alkaline condition (pH 8) whereas the sludge supernatant presented a slightly acidic condition (pH 6, see Section 6.2.1). CLEA amylase activity slightly increased by 9.2% probably because the presence of sodium and calcium ions (Na^+ and Ca^{2+}), which are cofactors of amylase, in the primary sludge supernatant stimulated the enzyme (Zohra et al., 2016).

Furthermore, it should be noted that the CLEA activity assays (Section 3.6) carried out with either standard buffer solutions or primary sludge supernatant are essentially simplified hydrolysis reactions, during which a simple substrate with a single component is exposed to the specific enzyme (e.g. casein and starch for protease and amylase, respectively), for a short period of time (5-30 min). Therefore, the results in Table 6-2 also showed that the AS CLEA has equivalent hydrolysis activity towards various substrates in single-substrate systems and was not affected by the sludge matrix.

However, in the subsequent sludge hydrolysis experiments, moderate degradation of complex cellular substances was observed, with the tyrosine content gradually increased by approximately 30-40% (compared to the control group) over a 6.5 h reaction period for γ-irradiated and sonicated AS; solubilisation of TOC and polysaccharides was not detected for all types of AS. This suggests that: under the experimental conditions applied in this study, the performance of the CLEA in hydrolysing the AS was not closely related to the chemical

inhibitors in the sludge matrix; other factors, particularly the physicochemical and biological properties of the AS substrate, may have a greater impact on the hydrolysis process and is discussed in the following section.

6.4.4 Hydrolysis of activated sludge

6.4.4.1 Whole sludge

The CLEA was effective at the hydrolysis of protein and carbohydrate in wheat flour, however, whole AS was relatively resistant to hydrolytic attack by the AS CLEA and only a small, albeit statistically significant, release of reducing sugar was observed after 5.5 h compared to the initial concentration and relative to the control (Section 6.3.2.2). This may be explained due to the protective layer of EPS surrounding intact cells and the protection to hydrolytic conditions provided by microbial cell walls (Wang et al., 2014). Activated sludge flocs from biological wastewater treatment represent agglomerations of microbial cells, predominantly bacterial, which are enveloped by a protective cell wall. The cell wall is constructed from peptidoglycan, a polysaccharide of two glucose derivatives, N-acetylglucosamine and N-acetylmuramic acid, alternating in long chains (Dörr et al., 2019). The chains are cross-linked by stretchable tetrapeptides (including L-alanine, D-glutamine, L-lysine and D-alanine), forming an elastic and mesh-like structure around the cell, which is essential for maintaining the shape and structural integrity of the cell, and also protects the cell from lysis (Huang et al., 2008; Bruslind, 2020). Floc forming cells also produce large amounts of EPS, which mainly consists of protein and polysaccharides (Section 2.4.1). The EPS fraction in AS flocs is substantial and represents approximately 60-80% of the mass of the sludge (Jafari et al., 2020). The gel-like, 3D structured EPS matrix is located outside of the cell with adhesive properties that are important in the formation of sludge flocs and provide a protective layer against environmental stress (Section 2.3.1), thus protecting the AS biomass from hydrolytic enzyme attack by the CLEA.

Moreover, both sTOC and reducing sugar decreased after 24 h, which could be due to the metabolism of CLEA hydrolysis products by the active microorganisms in the whole AS, as a nutrient and energy source for cell synthesis. The reducing sugar (glucose), for example, can be readily taken up by the microorganisms and directly utilised in the glycolytic pathway (Erni, 1989).

The results from the experiments with whole AS indicated that: (1) the rigid microbial cell structure exhibited high resistance to the CLEA attack, and (2) microbial activity could potentially utilise the released soluble products of hydrolysis. Therefore, several pretreatment methods were applied to alter the sludge floc structure and to disrupt microbial activity in the sludge matrix. The potential impact of the pretreatment methods on the availability of different cellular components for hydrolysis by the CLEAs was compared.

6.4.4.2 Autoclaved AS

Thermal treatment by autoclaving uses high-pressure steam to break down cell structures and release cellular materials (including EPS and intracellular substances) into the liquid phase (Weemaes and Verstraete, 1998). It has been widely used to sterilise sludge (Wang et al., 2017) and to pre-solubilise polymers in sludge and consequently enhance the sludge digestibility in AD reactors (Aravinthan et al., 2001). However, no accumulation of sTOC, as well as reducing sugars from polysaccharides hydrolysis, was detected for autoclaved AS with CLEA addition. This may be explained because the majority of the complex cellular polymers were degraded to soluble and lower MW substances by the aggressive conditions experienced during autoclaving (Weemaes and Verstraete, 1998). Consequently, no apparent hydrolytic response to CLEA addition was observed. Indeed, the sTOC content in autoclaved AS with CLEA addition (approximately 70 mg/g TS, Figure 6-7(a)) was 2.5 times that for whole AS (Figure 6-6(a)). Similar solubilisation effect by autoclaving was previously reported. Kim et al. (2013a) showed that the soluble carbohydrate content in the thickened sludge (with 2% TS content) increased by 4.4 times, from 59 mg/L (raw sludge) to 257 mg/L after autoclave treatment at 121 °C 1.2 atm for 15 min. Xiao and Liu (2009) also found that sterilising AS at 121 °C, 1.5 atm for 30 min significantly increased the sCOD and soluble carbohydrate concentration from 177.3 and 8.1 mg/L (raw sludge, with 14 g/L TS content) to 2824.8 and 583.1 mg/L respectively.

The sTOC content in the control group increased after 7 h incubation (Figure 6-7 (a)), which was probably due to self-fermentation of the autoclaved sludge. The autoclave treatment was operated following a standard condition (at 121 °C for 15 min) for sterilising waste biomass, rigid bacteria spores may survive (O'Sullivan et al., 2015) and over the extended period of incubation during CLEA hydrolysis experiment, spore-forming bacteria could potentially proliferate and utilise the available organic substances in the sludge matrix for cell metabolism (Cabrol et al., 2017). Indeed, Xiao and Liu (2009) reported that autoclaved sludge can be used for hydrogen production in an anaerobic self-fermentation process (at 37 °C) without adding extra inoculum into the digester. The sCOD in the liquid phase increased from approximately 2800 to >3600 mg/L after 22 h reaction because of hydrolysis of the autoclaved sludge by the microorganisms, and a hydrogen yield of 16.26 mL/g VS was obtained, compared to 0.35mL/g VS for the non-sterilised sludge. The sTOC content in the group with CLEA addition did not significantly change over 24 h, probably because addition of the CLEA induced some microbial interactions (mentioned in Section 6.4.2.2) that could inhibit the self-fermentation of the sludge.

6.4.4.3 Gamma-irradiated AS

The use of γ irradiation for microbial inactivation and pathogen reduction of sludge has been widely reported (Xiang et al., 2016b; Asgari Lajayer et al., 2019; Asgari Lajayer et al., 2020).

The mechanism of γ irradiation generally falls into two categories: (1) direct radio-lytic cleavage of essential cellular structures (cell walls and organelles), as well as cross-linking of genetic material; (2) indirect generation of oxidising (i.e. hydroxyl radicals, OH·) and reducing species (e.g. hydrated electrons and hydrogen atoms (H·), as a result of radio-lytic cleavage of water molecules. These highly reactive species can penetrate cell membranes, react with bacteria nucleic acids as well as cellular proteins, disrupting the replication of nucleic acids and normal microbial activities (Hume et al., 2016; Wu et al., 2017).

Using a carefully controlled dosage, γ irradiation can be applied to inactivate microorganisms whilst preserving cellular integrity. For example, Correa et al. (2019) used γ irradiation to treat bacteria *Salmonella enterica* R60 at a dose rate of 5.5 Gy/min for different durations, and found that dosages at 600 Gy (and above) achieved almost 100% inactivation of bacteria. However, low doses of radiation (400-1000 Gy) had no impact on cell integrity and maintained the cell membrane lipid content, although a slight increase in the surface roughness of the bacteria (compared to untreated cells) was observed. Destruction of bacteria cells was obtained at doses ⩾ 2000 Gy (up to 8000 Gy). Similarly, Xiang et al. (2016a) used γ irradiation to disintegrate AS (1% w/w TS) at a dose rate of 0-20000 Gy, and found that high dose rates (⩾10000 Gy) were necessary for significant destruction of sludge cells.

Here, partial inactivation of the sludge cells after γ irradiation was observed (Figure 6-10(b)). A full-range UV scanning (wavelength = 190 to 800 nm) was carried out for AS with and without γ-irradiation treatment. Only a slight increase in absorbance was observed for the γ-irradiated AS, compared to the untreated AS (see Appendix A-4), suggesting preservation of the sludge cell integrity and a low level of cellular substance release. Therefore, indirect effects of γ irradiation may explain the partial inactivation of sludge cells. Preservation of the sludge cell integrity after γ irradiation treatment also suggested that the microbial cells were potentially protected from CLEA attack by the EPS fraction, and that tyrosine accumulation increased by approximately 30% of the initial content within the first 3.5 h with CLEA addition to the γ-irradiated AS (compared to the control which remained relatively constant, Figure 6-8(c)) resulted from the CLEA interacting with the sludge EPS fraction.

6.4.4.4 Sonicated AS

Sonication treatment disintegrates the sludge cell flocs and releases various cellular substances from the damaged cell structure by continuous acoustic vibrations and generated shear forces (see Section 2.4.2.1). Enhanced biodegradability of the sludge and methane production in AD process after sonication pretreatment has been previously reported (e.g. (Bougrier et al., 2005; Davidsson and la Cour Jansen, 2006)).

Sonication treatment facilitates the hydrolysis of sludge in AD process mainly by reducing the particle size and increasing the surface area accessible to subsequent enzymatic attack (Li et al., 2019). However, the disintegration degree of the sludge cells depends on the sonication parameters and on sludge characteristics (Pilli et al., 2011). For example, Salsabil et al. (2009a) investigated the effect of sonication treatment (20 kHz ultrasound) on the sludge digestibility, at varying energy input levels (3.6, 31.5, or 108 kJ/g TS), and found that the cell disintegration degree (as ratio of solubilised COD content after sonication to the total sCOD content of the sludge) increased with energy level, reaching the maximum of 47% at 108 kJ/g TS energy input; the solubilisation rate of N and P was at a moderate level under such condition, equivalent to 19.6% and 12%, respectively. Moreover, the concentration of intact cells in the sludge remained approximately constant at all energy input levels. The increase of soluble forms of COD, N and P was largely attributed to disruption of the EPS structure, which facilitated the extracellular proteins and polysaccharides shifting from the inner layer of the sludge flocs to the outer, rather than cell lysis. Weemaes and Verstraete (1998) showed that complete sludge cell disintegration can be obtained by sonication treatment at high specific energy input (of the order of 200 kJ/g TS).

In this study, the sonication pre-treatment of AS was carried at an energy level of 49 kJ/g VS (which is equivalent to 70 kJ/g TS, see Section 4.2.3), and the sonicated-AS was probably partially disintegrated and may contain intact sludge cells, which was confirmed by the observed microbial growth in the petri dish (Figure 6-10(c)). The whole sonication-disrupted sludge was used as the substrate, without solid-liquid separation prior to the CLEA hydrolysis, thus, providing a mixture of detached EPS, cell debris and intact cells. Similar with the case for γ-irradiated AS, the increase of the tyrosine content with CLEA addition during the first 6.5 h (Figure 6-9(c)) can be mainly attributed to the CLEA interacting with the EPS proteins, since EPS have higher solubility than insoluble cell debris (Jafari et al., 2020) and is therefore more mobile and able to diffuse to the catalytic site of the CLEA; degradation of the cell debris by the CLEA may also occur, although to a limited extent.

6.4.5 Summary

The results obtained from the CLEA hydrolysis experiments showed that:

- Compared to CLEAs of a single enzyme, multi-CLEAs include a variety of enzyme activities capable of numerous catalytic functions during bioconversion of heterogeneous organic substrates.
- There are many interacting factors affecting the hydrolysis of complex organic materials (e.g. flour or sludge) by the CLEA, and the hydrolysis performance depends not only on

the activity of the CLEA, but also on the physical, chemical and biological characteristics of the substrate.

- No evidence was found for the chemical inhibition of CLEA hydrolytic activity by the sludge matrix.
- However, enzymatic treatment of intact or partially disrupted sludge by the CLEA only showed a slight increase in reducing sugar release from hydrolysis of polysaccharide components of the AS substrate, which could be explained due to the protection of microbial cells by the gel-like EPS fraction and the rigid cell wall, the susceptibility of these structures to amylase attack and/or the rapid removal and assimilation of hydrolysis products by the active microbial biomass.
- CLEA proteases were more effective at hydrolysing wheat flour and AS compared to amylases. This may be explained by substrate (starch-protein) interactions, which reduces accessibility of starch to reaction sites on the enzyme, and also the apparently greater susceptibility of proteins to enzymatic hydrolysis in wheat flour, AS EPS and possibly cellular components by the CLEA.
- The results show that AS CLEAs are effective for the hydrolysis of specific complex organic materials containing polysaccharides and proteins such as wheat flour and AS. However, the presence of active microorganisms, rigid cell walls or EPS in the substrate, may influence the extent of the enzymatic reaction and release of soluble hydrolysis products. The amylase in the AS CLEA is more susceptible to these factors compared to protease.

7 General discussion

7.1 Multi-CLEA preparation from crude activated sludge enzyme extracts

7.1.1 Enzyme activity in AS CLEA

The hydrolytic enzymes in AS were extracted, and consolidated and stabilised into a solid CLEA product. As an insoluble biocatalyst, the specific activity (i.e. the number of units per mg of protein or solids) of the CLEA provides a more precise indicator of the catalytic efficacy, compared to volumetric activities, since insoluble CLEA products can be prepared into suspension at different concentrations, thus varying the volumetric activity. Table 7-1 summaries the CLEA preparation from AS in this study compared to other enzyme sources reported in the literature. Only a few published studies could be found that provide a direct comparison to the specific activities of AS CLEAs, and the reported values were calculated by different methods. Based on the available information shown in Table 7-1, the specific activities of CLEA prepared from commercial enzyme sources are generally larger than those obtained from crude sources. The specific activity of the AS CLEA in this study was comparable level to Yu et al. (2013), for a CLEA prepared from crude mung bean extract, which had an activity value equivalent to 0.067 U/mg solid and the CLEA prepared from crude maize flour extract by Bayraktar and Onal (2019) with an activity of 0.044 U/mg protein. Zhu et al. (2021) reported a higher specific activity (6.5 U/mg protein) for a CLEA produced from *Aspergillus niger* GZUF36, however, in this case, the crude fermentation broth was partially purified by reverse micelle extraction combined with acetone precipitation before cross-linking.

The enzyme recovery rate in the CLEA (relative to the original enzyme solution) demonstrates the performance/efficiency of the CLEA preparation protocol. Moderate degrees of cross-linking reaction during CLEA preparation should not cause severe activity loss or denaturation of the protein structure since lysine residues that are mainly involved in cross-linking reactions are usually not associated with the catalytic site of an enzyme (Migneault et al., 2004). As shown in Table 7-1, activity recovery rates equivalent to almost 100% are possible, however, reduced activity of cross-linked enzymes was observed in most cases, with the typical activity recovery rate ranging from 23% to <90% for both crude and commercial enzyme sources. Here, the maximum enzyme activity recovery rate of AS CLEAs (relative to soluble enzymes in the crude AS extract) for amylase, protease, lipase and cellulase was equivalent to 42.6%, 48.3%, 54.4% and 35.1%, respectively, under optimum preparation conditions (see Section 5.3.2.3), which falls within the typical reported range (Table 7-1).

The wide range of specific activities and activity recovery rates observed for CLEA products (Table 7-1) suggests that multiple factors can influence CLEA preparation and properties. In addition to preparation conditions (optimised in Chapter 5), these factors include the

characteristics of the enzyme and the chemical reactions involved in the cross-linking process. The factors influencing the enzyme cross-linking and CLEA behaviour are discussed in the following sections.

Table 7-1 Comparison of enzyme activities and recovery rate in carrier-free CLEAs (% of original soluble enzymes) at optimum conditions

Enzyme	Enzyme source	Enzyme source concentration (mean values of the volumetric activity)	Precipitation	Cross-linking	Additive	Recovery rate (mean values)	CLEA specific activity (mean values)	Reference
Crude enzyme sources:								
Amylase, protease, lipase, cellulase **	Crude activated sludge extract	2.209 U/mL, 0.073 U/mL, 0.273 U/mL, 0.332 U/mL	Acetone 1:4 v/v 30 min at 0 °C	Dextran aldehyde MW = 150 kDa 0.04% w/v 3.5 h at RT	BSA 5 mg/mL	42.6%, 48.3%, 54.4%, 35.1%	0.0895, 0.0034, 0.0257, 0.0314 U/mg freeze dried CLEA solids	This study
Amylase, protease, lipase, cellulase **	Crude activated sludge extract	2.209 U/mL, 0.073 U/mL, 0.273 U/mL, 0.332 U/mL	Acetone 1:4 v/v 30 min at 0 °C	Dextran aldehyde MW = 150 kDa 0.04% w/v 3.5 h at RT	BSA 5 mg/mL	42.6%, 48.3%, 54.4%, 35.1%	0.941, 0.035, 0.149, 0.113 U/mg protein	This study
Protease, catalase, lipase **	Crude sunflower seed extract	320 U/mL, 348 U/mL, 46 U/mL	$(NH_4)_2SO_4$ 55% saturated	Glutaraldehyde 100 mM *17 h, temperature not specified	Starch 8 mg/mL	87%, 61%, 60%	-	Ozacar et al. (2019)
Epoxide hydrolases	Crude mung bean extract	-	$(NH_4)_2SO_4$ 80% saturated 30 min at 4 °C	Glutaraldehyde 20 mM 12 h at 4 °C	Sugar (not specified)	92%	0.067 U/mg solid	Yu et al. (2013)
Alkaline protease	Fermentation broth of *Bacillus licheniformis*	148.9 U/mL	$(NH_4)_2SO_4$ 80% saturated	Glutaraldehyde 65 mM *16 h at room temperature	BSA 0.11 mM	39.8%	-	Bashir et al. (2018)

Tyrosinases	Crude mushroom (*Agaricus bisporus*) extract	-	$(NH_4)_2SO_4$ 60% saturated 5 min at 4 °C	Glutaraldehyde 2% v/v 3 h at RT	-	~100%	-	Aytar and Bakir (2008)
Proteases	Fermentation broth of *Aspergillus*	98.5 U/mL	$(NH_4)_2SO_4$ 80% saturated	Glutaraldehyde 65 mM *16 h at room temperature	BSA 0.15 mM	37.5%		Asgher et al. (2018)
α-Galactosidase	Crude maize flour extract	1.69 U mL−1, 26.4 mg mL−1, 0.064 U mg −1 1.69 U/mL	$(NH_4)_2SO_4$ 90% w/v	Glutaraldehyde 0.1% v/v *6 h at 4 °C	-	47%	0.044 U/mg protein –	Bayraktar and Onal (2019)
β-galactosidase	Fermentation broth of *Lactobacillus leichmannii* 313	236.6 U/mL	$(NH_4)_2SO_4$ 80% saturated 30 min at 4 °C	Glutaraldehyde 23.5 mM 3.4 h at 25°C	-	37.7%	-	Xu et al. (2020)
α-galactosidase	Fermentation broth of *Aspergillus niger* L63	0.55 U/mL	$(NH_4)_2SO_4$ 90% saturated 1 h at 4 °C	Glutaraldehyde 36.43 mM 1.71 h at 4 °C	-	90.9%	-	Liu et al. (2021)
Laccases	Crude culture supernatant of *Trametes versicolor* and *Fomes fomentarius*	Concentration not mentioned	$(NH_4)_2SO_4$ saturated 30 min at 4 °C	Glutaraldehyde 50 mM 1 h at 4 °C	-	Not reported	358.3 U/mg protein, and 255.7 U/mg protein	Vršanská et al. (2017)
Lipase	Partially purified fermentation broth of	15.84 U/mL	Tert-butanol 80% v/v Chilled, time not specified	Glutaraldehyde 30 mM 1.5 h at 25 °C	-	99.7%	6.5 U/mg protein	Zhu et al. (2021)

	Aspergillus niger GZUF36							
Commercial enzyme sources:								
Enoate reductases (ERs), glucose dehydrogenase (GDH) **	Commercial enzymes solids	7.33 U/mL and 33.3 U/mL	$(NH_4)_2SO_4$ 4.0 mol/L 60 min at 4 °C	Dextran aldehyde MW = 70 kDa 15% v/v 3 h at 4 °C	BSA 20 mg per 21.2 mg reductases and 0.3 mg glucose dehydrogenase	44.1% and 18.8%	-	Li et al. (2018)
Cellulase	Commercial enzyme mix liquid	Total cellulase activity = 7.0 U/ml	$(NH_4)_2SO_4$ 90% saturated 30 min at 4°C	Glutaraldehyde 0.87% w/v 6.8 h at 4°C	BSA 94.0 mg/mL	89.7%	-	Shuddhodana et al. (2018)
Tyrosinase	Commercial enzyme solid	1000 U/ml	$(NH_4)_2SO_4$ 60% saturated 5 min at 4 °C	Glutaraldehyde 2% v/v 3 h at RT	BSA 50 mg/ml	~100 %	-	Aytar and Bakir (2008)
Cellulase	Commercial enzyme liquid	63 U/mL	PEG 50% w/v 30 min at room temperature	Glutaraldehyde 30 mmol/L 2 h at room temperature	-	29%	-	Perzon et al. (2017)
Penicillin G acylase	Commercial enzyme solid	1060 U/mL	Acetone 3:5 v/v 30 min at 4 °C	Glutaraldehyde 0.37 w/v 2 h at 4 °C	Trehalose 20% w/v	79.3%	123.71 U/mg solids	Wang et al. (2011)
α-Amylase	Commercial enzyme solid	0.96 mg/mL enzyme =0.1296 U/mL	Tert-butanol 1:9 v/v 20 min in ice	Glutaraldehyde 5 mM 12 h at 2-3 °C	BSA 1:2 w/w (enzyme/BSA); Ca^{2+} 1200 mg/L; Na^{+} 400 mg/L	90.2%	1.99 U/mg protein	Torabizadeh et al. (2014)
Aminoacylase	Commercial enzyme solid	100 mg solids/mL	Tert-butyl alcohol solution	Glutaraldehyde 0.75 v/v	BSA	82%	900 U/gcat =0.9U/mg	Dong et al. (2010)

		Activity not mentioned	1:9 v/v 30 min at 4 °C	4 h at ambient temperature	10 mg per 100 mg enzyme		solids	
Lipase	Commercial enzyme solid	50mg solids/mL Activity not mentioned	Acetone 1:4 v/v 30 min at 4 °C	Glutaraldehyde 25 mM 4 °C for 3 h	BSA 5 mg/50 mg enzyme	100%,	-	Shah et al. (2006)
Penicillin acylase	Commercial enzyme liquid	Activity not mentioned	Dimethoxyethane ~1:3 v/v 30 min at 4 °C	Glutaraldehyde 25 mM 4 °C for 3 h	BSA 5 mg/125 μL enzyme	86%	-	Shah et al. (2006)
α-Amylase	Commercial enzyme liquid	4 mg/mL protein with total 356U activity	$(NH_4)_2SO_4$ 80% saturated 30 min at 4 °C	Dextran aldehyde MW = 60–90 kDa 0.21mol/L aldehyde content 20 h at 30 °C	-	91%	108 U/mg aggregate	Nadar et al. (2016)
Nitrile hydratase	Commercial enzyme liquid	0.4 mg pr/mL Activity not mentioned	$(NH_4)_2SO_4$ saturated 30 min at 4 °C	Dextran aldehyde MW = 500 kDa 2.5 mg/mL 4 h at 4 °C	Egg white 100 μL/mL enzyme	49.6%	-	Zhou et al. (2017b)
Urease, glucose oxidase, peroxidase	Commercial enzyme solids	4 mg solids/L Activity not mentioned	-	Glutaraldehyde 2% v/v 2 h at 25 °C	BSA 5 mg per 0.8 mL enzyme solution	74.6%, 94.8%, 90.0%	-	Ayhan et al. (2012)
α-Amylase	Commercial enzyme solid	5 mg solids /mL Activity not mentioned	$(NH_4)_2SO_4$ saturated 30 min at 4 °C	Glutaraldehyde 40 mM 3 h at 30 °C		45%	20 U/mg wet derivative of the CLEA	Talekar et al. (2012)

Lipase	Commercial enzyme solid	5 mg solids/ml Activity not mentioned	1 h at 4 °C	Glutaraldehyde 14 mM 30 min at 25 °C	BSA 5 mg/mL and PEI 3 g/L	15%	-	Velasco-Lozano et al. (2016)

Note: * donates that a simplified procedure (mentioned in Section 2.6.2) was adopted to produce CLEAs, by simultaneously adding the precipitating agent, cross-linker and additive to the enzyme solution; ** donates co-immobilised enzymes, including multi-CLEAs, and combi-CLEAs (definition see Section2.7); RT: room temperature; $(NH_4)_2SO_4$: ammonium sulphate; BSA: bovine casein albumin; PEG: polyethylene glycol.

7.1.2 Impact of enzyme characteristics on CLEA activity

7.1.2.1 Physical and chemical features

As shown in Table 7-1, various types of enzymes have been used to prepare CLEAs and the unique physical and chemical features of each enzyme type potentially has a profound influence on the activity recovered in the CLEA, including:

(1) *Availability of surface lysine residues*: the abundance of surface lysine residues varies among enzymes types and directly affects the number of covalent bonds (Schiff bases, see Section 2.6.2) formed after adding a cross-linker, and thus the morphology, conformational stability and catalytic activity of the final CLEA (Dubey and Tripathi, 2021). For enzymes lack of lysine residue, addition of BSA, a lysine rich protein, can effectively enhance the CLEA preparation (see Section 2.6.5.1 and Section 5.4.3).

(2) *Sensitivity of the enzyme catalytic site*: some enzymes may contain functional groups that react with the cross-linker at their catalytic site, e.g. aspartic acid, histidine and serine at the active site of serine proteases (Ruiz-Perez and Nataro, 2014), and are therefore incompatible with the cross-linking chemistry. This is particularly the case when a small MW cross-linker (e.g. glutaraldehyde) is used, as the cross-linker can penetrate into the catalytic site and inactivate the enzyme (see Section 5.4.2).

(3) *Rigidity of the enzyme protein structure*: enzyme precipitation and chemical cross-linking alters the enzyme surface charge and hydrophobicity, due to removal of the essential water layer and formation of covalent bonds between the charge groups (lysine residues) and cross-linker (see Section 2.6). Therefore, potential unfolding of the enzyme protein structure and, consequently, inactivation of the enzyme could occur during CLEA preparation (Faccio, 2018). Faccio (2018) suggested that enzymes that contain multiple disulphide bonds in their protein structure (e.g. lysozyme with 4 disulphide bonds) are less structurally affected by external environmental conditions, compared to enzymes with fewer disulphide bonds. In this study, the crude AS enzyme extract containing a wide range of hydrolytic enzymes from various microorganism including protease, lipase, amylase and cellulase (see Chapter 4), and disulphide bonds in their respective molecular structure showed a wide range (0-4) according to previous reports (Rao et al., 1998; Siddiqui et al., 2005; Bashirova et al., 2019; Gihaz et al., 2020). The wide range of conformational stability of the target enzymes can contribute the varying activity loss shown in Table 7-1.

Unlike single enzyme CLEAs that have been frequently reported by researchers (examples in Table 7-1), a multi-CLEA is produced here (definition see Section 2.6.6.1), with a wide range of hydrolytic enzymes produced by the sludge microorganisms co-immobilised together,

including but not limited to protease, lipase, amylase and cellulase. Optimising multi-CLEA production may be more challenging compared to CLEAs of single enzymes because the activity recovery rates of different enzymes will depend on the specific conditions and may therefore vary (for example, see data shown in Figure 5-6(a)).

7.1.2.2 Enzyme source

A major advantage of immobilising enzymes by cross-linking is that highly purified enzyme sources are not required for CLEA preparation (see Section 2.6). However, most of the reports relating to CLEA preparation (e.g. (Torabizadeh et al., 2014; Velasco-Lozano et al., 2016; Zhou et al., 2017b)) follow simplified systems using single, purified, commercial enzyme sources and only a limited number of examples prepare CLEAs from crude enzyme sources (e.g. (Yu et al., 2013; Bashir et al., 2018; Ozacar et al., 2019)). Here, a crude enzyme extract was obtained by physically disrupting AS cells by sonication treatment (with addition of a chemical additive, surfactant TX100), followed by centrifugation to remove the disrupted cell debris (see Chapter 4). The obtained AS enzyme solution is a highly complex mixture containing various hydrolytic enzymes produced by the sludge microbial cells as well as a wide range of cellular polysaccharides, lipids, proteins, and DNA etc (concentration shown in Figure 4-3); mechanisms of microbial cells disruption by sonication and simultaneous release of intra- and extra-cellular materials was shown in Figure 2-5. These co-extracted cellular materials could interfere with chemical stability of the hydrolytic enzymes and also subsequent CLEA preparation; in particular, non-enzymic cellular proteins and peptides can co-precipitate with enzymes by the same precipitation mechanism (Section 2.6.3) and/or active functional groups (including lysine, arginine, histidine, cysteine, etc., see Table 2-3) on these molecules can react with the cross-linker, which may explain the lower specific enzyme activities of AS CLEA measured here (ranging 35-54%) compared to CLEAS produced from purified enzyme sources (up to 100%, Table 7-1).

7.1.2.3 Summary

Enzyme characteristics directly influence the cross-linking reaction involved in the enzyme immobilisation process. This is dependent upon the enzyme protein structure, amino acid composition and surface properties and information on these properties can inform the cross-linking strategy, however, collecting this data is an involved and extensive process, particularly for CLEA (or multi-CLEA) production from crude enzyme sources (e.g. AS) (Faccio, 2018). Since the crude AS enzyme solutions inevitably contain a large amount of co-extracted cellular materials such as various types of proteins, polysaccharides, and DNA etc (shown in Figure 4-3), high-level purification of the crude AS enzyme solutions via chromatographic techniques (examples see Section 2.5.1) prior to the enzyme characterisation process is necessary to minimise the interference from these co-extracted materials. In practice, therefore, a thorough

optimisation of the CLEA preparation conditions (as described in Chapter 5) is necessary to maximise activities of target enzymes in the CLEA product.

7.1.3 Factors influencing cross-linking chemistry and CLEA properties

7.1.3.1 Random binding sites and enzyme orientation

The active site of an enzyme is usually located in the interior part within the enzyme structure (see Figure 2-2) and is connected to the external environment by a "substrate tunnel" (Kokkonen et al., 2019). Interaction between enzyme and substrate can be strengthened by a suitable orientation of the enzyme active site and the tunnel towards the substrate (Vršanská et al., 2017). However, lysine residues often spread over the surface of the enzyme in a carrier-free CLEA (Butterfield et al., 2002) and covalent bonds form at random sites on the enzyme surface. Immobilised enzymes in the CLEA also have varying orientations (see Figure 7-1(a)) and, together, these properties influence the overall activity of the CLEA.

Wu et al. (2015) investigated the impact of covalent binding site on the activity loss of the immobilised enzyme, lysozyme. The enzyme was covalently immobilised onto superparamagnetic beads at six amino acid residues, which were specifically chosen and located throughout the enzyme surface. Immobilisation at distant locations from the active site caused the least activity loss among all groups (19-26%); whereas higher activity loss (44%) occurred by immobilisation in proximity of the enzyme active site. This is explained because formation of covalent bonds may induce amino acid mutation effects near the active site and thus inhibit the catalytic activity of the enzyme (Wu et al., 2015).

Uncontrolled orientation of immobilised enzyme molecules in the CLEA can reduce active-site accessibility, and hinder the transfer of substrates, cofactors, solvents, and products to and from the active site, leading to mass transfer limitations that reduce the apparent enzyme activity of the CLEA, compared to soluble enzyme (Kokkonen et al., 2019; Wahab et al., 2020). Velasco-Lozano et al. (2016) prepared a CLEA of *Candida rugosa* lipase (50 mg/mL) by acetonitrile precipitation (60 min at 4 °C) followed by glutaraldehyde cross-linking (14 mM, 30 min at 25 °C), with addition of both PEI (3 g/L) and BSA (mass ratio of BSA/lipase = 1:10) and the CLEA activity recovery rate was compared to orientated, carrier-bound immobilised lipase (onto agarose functionalised with octyl-groups via hydrophobic adsorption). The activity recovery measured for the CLEA was equivalent to 15%, however, the activity of carrier-bound lipase increased to 53%. The improvement in performance was explained because octyl-activated agarose orientates lipase through its hydrophobic area site due to the interaction between the hydrophobic residues in the vicinity of the catalytic site and the alkyl chain on the carrier surface, resembling an oil-water interface, which facilitates lipase catalysis.

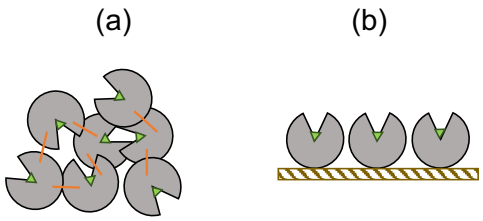

Figure 7-1 (a) Random orientation of enzymes in carrier-free CLEAs; (b) directed orientation of carrier-bound enzymes using a functionalised solid carrier (orange lines: cross-linker; green triangles: active catalytic site)

7.1.3.2 Intramolecular cross-linking

Intramolecular cross-linking can occur during CLEA preparation (Figure 7-2), with two-point covalent attachment formed between two vicinal aldehyde groups and two vicinal lysine groups on the surface of one enzyme molecule (Orrego et al., 2018). On one hand, formation of both inter-molecular bonds between adjacent enzymes and intra-molecular bonds within the enzyme aggregate can reinforce the rigidity of the three-dimensional arrangement of enzymes in the CLEA and thus prevent enzyme conformational changes under extreme conditions (Sangeetha and Emilia Abraham, 2008; Ahumada et al., 2015; Xu et al., 2018). On the other hand, however, formation of an excessive number of intramolecular covalent bonds potentially tightens the structure of the CLEA by excluding essential water molecules from the immobilised enzymes, consequently inactivating the enzyme (Migneault et al., 2004). The critical importance and role of the essential water content of proteins is discussed in more detail in Section 2.6.3.

The chemical characteristics of the cross-linker can affect the formation of intramolecular covalent bonds, contributing to the varying activities apparent in CLEA enzymes. Glutaraldehyde and dextran aldehyde with WM ranging from 10 to 500 kDa are mainly used as cross-linking agents for CLEA formation (Table 7-1). Salem et al. (2010) indicated that cross-linkers with shorter backbone chains (e.g. glutaraldehyde) tend to favour intramolecular cross-linking, whereas longer chains (macromolecular cross-linkers) tend to promote intermolecular cross-linking. Similarly, Orrego et al. (2018) reported that the use of smaller dextran molecules (e.g. MW = 1500 Da) favour intense intramolecular cross-linking, compared to larger dextran polymers (e.g. MW = 25000 Da), which tend to form intermolecular bonds at the enzyme surface.

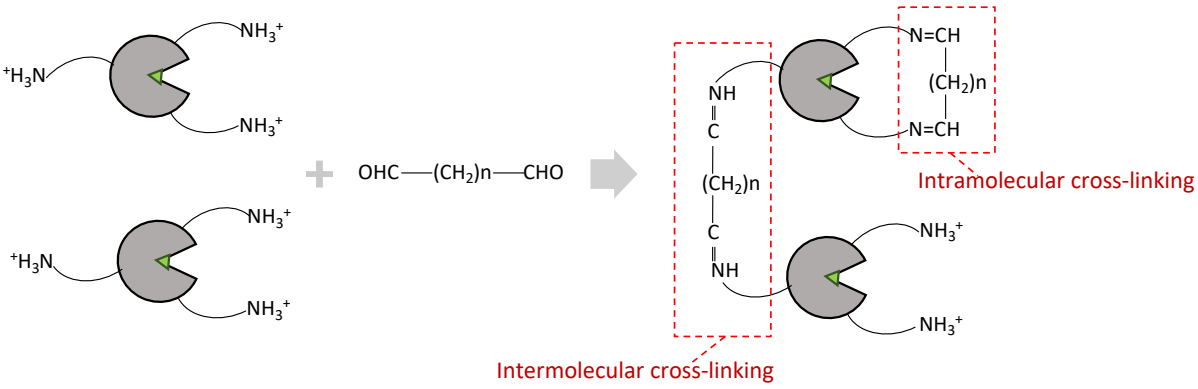

Figure 7-2 Intramolecular and intermolecular cross-linking of enzymes by a di-aldehyde cross-linker (adapted from (Ayhan et al., 2012))

7.1.3.3 Centrifugation and mass transfer limitations

Centrifugation is commonly used for rapid separation of insoluble CLEAs from the liquid phase. On one hand, the recovered enzyme activity depends on the amount of CLEA that is harvested after immobilisation. The optimum centrifugal speed maximises the yield of CLEA particles, whereas, as would be expected, CLEAs particles may remain suspended in the supernatant at slower speeds, reducing the overall yield (Li et al., 2015). On the other hand, centrifuge operation can affect the CLEA morphology and consequently the mass transfer processes within CLEA. Excessive centrifugation speeds can markedly increase the local protein concentration and compress the CLEAs together. As the distance between individual CLEAs shortens, large clusters can form due to intermolecular electrostatistic attraction, as well as hydrophobic interactions and van der Waals forces (Stradner et al., 2004; Soraruf et al., 2014; von Buelow et al., 2019). Schoevaart et al. (2004) found that the size of clusters of type-1 CLEAs (approximately 1 µm diameter as observed in this study, see Section 5.3.4) can increase up to 100 µm. Krishna and Ramachandran (1975) indicated that mass-transfer limitations on the enzymatic reaction velocity are inversely related to the particle size of the immobilised enzyme. Thus, mass-transfer, and therefore CLEA activity, may decline with increasing particle size, due to the heterogeneous distribution of enzymes within larger clusters.

In this study when preparing CLEA from commercial protease, protease activity was measured in the washed supernatants, but at a much lower level compared to the activity in the CLEA (see Figure 5-2 in Section 5.3.1.2), suggesting that the centrifugation speed applied here (10000 g, see Section 5.2.2.1) is adequate to harvest the majority of the active enzyme aggregates. Indeed, Xu et al. (2020) investigated the effect of centrifugation speeds during washing process on the final enzyme activity recovery rate of CLEAs. CLEAs of β-galactosidase were prepared using three different precipitants ($(NH_4)_2SO_4$, acetone and isopropanol) followed by glutaraldehyde cross-linking. The highest recovery rate (~100%) was

observed at 10000 g for CLEA with $(NH_4)_2SO_4$ precipitation and at 8000 g for acetone and isopropanol; faster (12000 g) or slower (4000 and 60000 g) centrifugation speeds reduced the activities of the CLEAs prepared with all of the precipitants.

7.1.3.4 Summary

The results demonstrate that carrier-free CLEAs are an effective approach to immobilise and stabilise enzymes released in crude biomass extracts, including AS. The immobilisation and stabilisation of enzymes by cross-linking potentially reduces the enzymatic activity relative to the crude extract (see Table 7-1) for a number of fundamental reasons relating to the cross-linking reaction, including, the enzyme orientation, covalent bond formation and mass transfer limitation. Nevertheless, the levels of enzymatic activity are sufficient as effective industrial catalysts (Sheldon, 2011b) and are potentially greater than alternative immobilised enzymes, which contain a large proportion of diluent solid support media (typically 95% w/w (Brask et al., n.d.)). Furthermore, CLEA preparation is considerably simpler and more cost effective compared to carrier-bound immobilisation as this requires the synthesis of a polymer with the required properties and functional groups, which is a time-consuming and costly process (Zdarta et al., 2018). Consequently, the CLEA technique offers a practical and economical approach for manufacturing industrial enzyme products and the results presented here show it can be used to develop high value enzyme products from complex, waste biomass materials including AS generated during the biological treatment of municipal wastewater.

7.2 Hydrolysis of complex organic substrates by AS CLEA

7.2.1 Wheat flour and activated sludge hydrolysis

7.2.1.1 Pattern of enzymatic hydrolysis product yield

The catalytic interaction between an enzyme and substrate depends on the bio-catalyst characteristics, and also on the physical, chemical and biological properties of the substrate, and this was highly evident from the results presented in Chapter 6 on hydrolysis of wheat flour and AS by the CLEA.

Starch and proteins (gluten) are the predominant organic components of wheat flour. A moderate degree of starch hydrolysis was observed with CLEA addition to flour whereas protein was more effectively hydrolysed at CLEA doses of 1:100 and 1:10 v/v. Thus, maximum yields of reducing sugar were equivalent to 4.1 and 6.5%, and, for tyrosine, yields were equivalent to 75.9 and 108.7%, at these CLEA dose rates, respectively (see Section 6.3.1.2). A similar pattern of hydrolysis product release was also generally observed for the enzymatic degradation of whole and pre-disrupted AS, at a CLEA/sludge volume ratio of 10% (see Section 6.3.2). A small, albeit significant, increase in reducing sugar was observed with CLEA addition to whole AS after 5.5 h of incubation (Figure 6-6(b)) although no accumulation of

reducing sugar was detected for autoclaved, γ-irradiated and sonicated AS with CLEA addition. By contrast, tyrosine accumulation significantly increased, when measured, for γ-irradiated AS and sonicated AS in the first 6.5 hours of the reaction, compared to the control (which remained relatively constant), and the maximum yield of tyrosine was equivalent to 23.2-29.6% and 32.8-43.5%, respectively (Section 6.3.2.7); the observed release of tyrosine from AS was probably explained by the CLEA interaction with sludge EPS fraction.

7.2.1.2 Factors influencing CLEA hydrolysis of complex organic matrices

The different hydrolysis yield of reducing sugar and tyrosine from wheat flour and AS suggests that the protease in the CLEA was more effective in hydrolysing complex organic substrates compared to the polysaccharide-degrading enzymes in CLEA (mainly amylase, cellulase. Similarly, Molobela et al. (2010) reported that protease was generally more effective than amylases at degrading the EPS fraction of biofilms formed by *Pseudomonas fluorescens* at 26 °C, with the hydrolysis rates of EPS protein and carbohydrate ranging from 36 to 75%, and from 9 to 28%, respectively. The lower effectiveness of CLEA polysaccharide-degrading enzymes compared to protease for sludge EPS may be explained because:

(1) Proteins may bind to polysaccharides which facilitating protein hydrolysis whilst hindering polysaccharide attack by hydrolytic enzymes (discussed in Section 6.4.2.1).

(2) The polysaccharide structural components of the sludge EPS may resist hydrolysis by polysaccharide-degrading enzymes in CLEA. Activated sludge EPS may contain a wide variety of polysaccharides produced by different bacteria species, including homopolysachharides, which are composed of one monosaccharide type, and heteoropolysaccharides, which consist of different forms of monosaccharides (including D-glucose, D-galactose, L-fructose, L-rhamnose, etc.) (Czaczyk and Myszka, 2007). Thus, amylase and cellulase (and other polysaccharide-degrading enzymes) in the CLEA may be unable to break down the wide range of glycosidic linkages and the complex molecular structures of the polysaccharides (linear and branched), which are responsible for the physical structure of the EPS (Molobela et al., 2010) (illustrated in Figure 2-3).

(3) Activated sludge has a larger protein content (Sponza, 2002; Xavier et al., 2007) which may increase the efficiency of tyrosine release, compared to reducing sugar. For example, Yu et al. (2008) reported that the protein and polysaccharide contents in sludge EPS for 14 full-scale WWTPs ranged from 66.6 to 902 mg/g VS and from 11.8 to 42.6 mg/g VS, respectively.

7.2.1.3 Feasibility of CLEA pretreatment of sludge

Enzymatic pretreatment by CLEA is a potentially feasible alternative approach to physical and chemical methods to increase anaerobic digestibility of sewage. The sTOC increased by 16.4%

after incubating the CLEA with whole AS for 5.5 h at 40 °C, compared to the initial sTOC content at 0 h (Section 6.3.2.2), at a dose rate of 1:10 v/v CLEA/sludge (providing a specific dose equivalent to approximately 8.8 and 259 U/g sludge TS for protease and amylase, respectively); no significant increase in sTOC was observed in the control group.

A similar degree of enzymatic hydrolysis efficiency of whole AS was reported by Yang et al. (2010). A mixture of soluble commercial protease and α-amylase enzymes (specific activity = 5000 and 6000 U/g, respectively, with a ratio of 1:3 w/w) was used to hydrolyse raw sludge under anaerobic conditions at a dose rate of 3-18% w/w (enzyme/TS). The hydrolysis efficiency of the sludge (measured as VS reduction) increased with the enzyme dose and reached the maximum value, equivalent to 29%, at 6% enzyme addition (specific dosage = 75 and 270 U/g sludge TS for protease and amylase, respectively). By contrast, the control group (without enzyme addition) showed a <5% VS reduction under equivalent conditions (at 40 °C for 4 h). Increasing the operational temperature from 40 to 50 °C also improved the VS reduction from 25.6% to 58% (Yang et al., 2010).

A potential advantage of CLEA pretreatment is that it can be operated under mild conditions (e.g. moderate temperature and pH) and requires less energy input for enzyme hydrolysis activities compared to physical and chemical methods, which atypically require extreme conditions (such as high temperature and extreme pH) with high energy input, or additional chemical costs.

Nevertheless, the results here showed that sludge hydrolysis efficiency is influenced by the protective effect of the EPS fraction of AS microbial cells and flocs, as well as the rigid cell wall structure (see Section 6.4.4). Therefore, an optimal approach may be to apply CLEA enzymes as a pretreatment in combination with, and following, other chemical/physical pretreatment methods (e.g. sonication) to remove the protective layer of the sludge prior to enzymatic treatment.

For example, Jafari et al. (2020) reported improved sludge digestibility in mesophilic AD (37 °C) by combined thermal and enzymatic pretreatment, compared to enzymatic pretreatment alone. The sludge (MLSS = 5000-10000 mg/L) was heated at 80 °C for 60 min followed by centrifugation at 6000 rpm for 15 min to separate LB-EPS from the sludge matrix. Commercial lysozyme was added into the LB-EPS-extracted sludge at varying doses of 100, 2550, 3040, and 5000 mg/L, and the mixture was incubated at 28°C for 3 h under continuous stirring. Sludge disintegration (measured as sCOD yield) increased to > 60% at lysozyme doses ≥2550 mg/L for all sludge concentrations. The combined pretreatment method improved the sludge AD process, increasing the COD removal and VS reduction after 20 d from 81% and 31% (for sludge with thermal pretreatment alone) to 95% and 41% in combination with enzyme

conditioning, respectively. The average daily biogas production over 20 days was also 1.14 times larger for the combined pretreatment compared to thermal pretreatment alone.

7.2.2 Feasibility of CLEA hydrolysis of complex organic waste materials into valuable commodities and products

The multi-CLEA produced from AS demonstrated high potential to be used, alone or in combination with other pretreatment methods, for hydrolysing and bioconversion of complex organic substances. Other examples showing the potential value of CLEAs, and the possible application of the AS CLEA for the hydrolysis of organic waste residues to produce valuable materials, include:

(1) Food waste:

Food-processing waste represents a substantial ecological burden due to the rapid growing population worldwide (Bilal and Iqbal, 2019). These waste streams are rich in carbohydrates (cellulose, starch, and monosaccharides), proteins, and lipids, and thus have significant potential for enzymatic transformation into an array of high-value products.

Kaushik et al. (2014) showed multi-enzyme pretreatment of canteen food waste can effectively improve the production of hydrochars and bio-oil from food waste in a hydrothermal carbonisation process. Mixed soluble commercial enzymes (carbohydrase 100 U/g, protease ≥ 2.4 U/g, and lipase ≥ 100000 U/g, in a ratio of 1:2:1) were added to food waste at doses of 6% and 12% w/w and the pretreatment was carried out at 35 °C for 12 h. The carbon contents and calorific values ranged from 43.7 to 65.4% and 17.4 to 26.9 MJ/kg for the hydrochars obtained with the enzymatic pre-treatment, respectively, compared to 38.2 to 53.5% and 15.0 to 21.7 MJ/kg, respectively, for the hydrochars without pre-treatment. In addition, the enzymatic pre-treatment also facilitated the formation of a bio-oil with a narrow distribution of organic compounds compared to the control group.

Bayraktar and Onal (2019) produced CLEA of α-galactosidase from a crude extract of maize flour; and the CLEA was used to hydrolyse raffinose-type oligosaccharides in soymilk (e.g. raffinose and stachyose). The α-galactosidase CLEAs catalysed the hydrolysis of the raffinose-type oligosaccharides present in soy milk as efficiently as soluble enzymes, with hydrolysis rate reaching 85% and 89%, respectively, after 24 h reaction under equivalent conditions (at 50 °C, with 1 U of α-galactosidase activity added per 10 mL of soymilk).

Guimaraes et al. (2021) evaluated the performance of a magnetic CLEA (definition in Section 2.6.6.2) of lipase (prepared from a commercial lipase product using octyl groups functionalised magnetic nanoparticles) in the enzymatic synthesis of bio-lubricants by transesterification of waste cooking oil (WCO) with isoamyl alcohol at 40 °C. The maximum yield of isoamyl ester (approximately 90% w/w) was obtained after 72 h at an enzyme load equivalent to 12

esterification units/g oil and a WCO/alcohol molar ratio of 1:6. By contrast, soluble lipase showed a maximum ester yield of 34% under equivalent conditions. The better performance of magnetic CLEA was explained because the magnetic nanoparticles functionalized with octyl groups favoured the transport of hydrophobic substrates from the bulk to the enzyme active sites.

(2) Lignocellulosic materials

Lignocelluloses are complex heterogeneous natural composites that comprise of three main biopolymers, including: lignin, celluloses, and hemicelluloses, and can be converted into valuable bioproducts such as rare sugars, surfactants, and biofuels by multi-enzymatic treatment (Periyasamy et al., 2016; Bilal and Iqbal, 2019). Holm et al. (2013) extracted the cellulose fraction from the primary sludge of a chemical pulping mill, using an ionic liquid (1-allyl-3-methylimidazolium chloride) to dissolve the sludge followed by addition of hot distilled water to precipitate the cellulose fraction. The cellulose fraction was treated with commercial cellulase and β-glucosidase enzymes and the total reducing sugar yield was equivalent to 96% w/w after 5 h reaction at pH 5.5 and 50 °C. The enzymatic treatment was significantly more effective than chemical hydrolysis with sulphuric acid at 50 °C for 2 h which produced a lower yield equivalent to 34% (Holm et al., 2012).

Periyasamy et al. (2016) produced a combi-CLEA of cellulose, xylanase, and β-1,3-glucanase from the crude supernatant of solid-state fermentation of *Trichoderma citrinoviride*, with a specific activity equivalent to approximately 120, 800 and 550 U/mg aggregate, respectively. The CLEA was used to convert sugarcane bagasse (a lignocellulosic biomass, delignified with liquid ammonia and milled) to fermentable sugars (including xylose and glucose) at 50 °C, compared to 77% by free enzyme under equivalent conditions.

Shuddhodana et al. (2018) used multi-CLEAs of endoglucanase, β-glucosidase and xylanase to convert the lignocellulosic content of alkaline-pretreated wheat straw (TS = 10% w/v) into fermentable sugars at pH 4.8 and 70 °C. A similar maximum saccharification yield (measured as reducing sugar yield from the total biomass cellulosic content) of 32.9% and 31.8% was obtained by the CLEA compared to the soluble enzymes, respectively, after continuous hydrolysis for up to 120 h. However, following repeated batch hydrolysis after five consecutive cycles of 24 h each (total hydrolysis time of 120 h), the overall saccharification yield with the CLEAs increase to 43.3%.

(3) Others

The multi-CLEA of AS enzymes also exhibits potential to be used for detergent reformulation (Vasconcelos et al., 2006), decolourisation of dyes (Sinirlioglu et al., 2013), dehairing of leather goods (Asgher et al., 2018), etc. More examples are shown in Table 7-2.

7.2.3 Operational attributes and advantages of CLEAs for industrial application

A key feature of immobilised CLEAs is that they can be separated from the product/substrate mixture and recycled multiple times without substantial loss of activity, which increases the economic feasibility of industrial scale enzymatic treatment processes, compared to soluble enzymes, which are more difficult to recover (Mahmod et al., 2015). The reusability of CLEAs has been mainly completed in lab-scale experiments, shown in Table 7-2. A loss of enzyme activity may occur through repeated washing with buffer solution and also centrifugation procedures for CLEA recovery and preparation for reuse (see Section 7.2.3.3). Uneven dispersion of clustered CLEAs in the reaction mixture could also contribute to the difficulty of recovering the CLEA aggregates (Bayraktar and Onal, 2019). Therefore, in addition to enzyme activity and recovery, CLEA preparation conditions should consider factors including operational stability, reusability and storage stability. Furthermore, the methods required to recycle CLEAs at larger scales, as well as the interaction with substrate properties (e.g. viscosity) that influence the recycling efficiency of immobilised enzymes, are also evaluated research priority.

In this study, the produced CLEA was preserved in buffer solution as a suspension, and the enzyme activities of the CLEA suspension maintained relatively stable for a period of 27 days (Section 5.3.5). Indeed, most of the researchers listed in Table 7-1 used buffer solution to preserve the CLEA products and reported similar storage stability. For example, Aytar and Bakir (2008) stored the CLEA of tyrosinase in sodium phosphate buffer (0.1 M, pH 7.0), and showed that CLEAs retained 87 % of its initial activity after 24 days of storage at room temperature and at 4 °C. van Pelt et al. (2008) prepared CLEA of nitrile hydratase from crude microbial cell extract (a haloalkaliphilic actinobacterium strain), and found that the CLEA maintained approximately 100% of the initial activity after 4 months of storage in Tris-HCl buffer (0.01 M, pH 8) at 21 °C; on the contrary, free nitrile hydratase in the crude extract lost all activity after 17 days under equivalent conditions. The enhanced storage stability of CLEAs compared to soluble enzymes could be beneficial in practice in terms of extended shelf-life of the CLEAs products.

The CLEAs show improved thermal and mechanical stability compared to soluble enzymes (examples mentioned in Section 2.6 and Section 5.4), enabling them to be applied in harsh reaction condition (e.g. high temperature, prolonged reaction period, and in the presence of organic solvent). It should be noted that enzymes co-immobilised in multi-CLEAs will exhibit the highest catalytic activity towards a specific substrate at their respective optimum pH and temperature conditions. Therefore, the operational conditions for CLEA hydrolysis should be carefully selected based on the specific enzymatic and substrate interaction and hydrolysis required. For example, Wang et al. (2009) used a crude enzyme mixture (produced from solid-

state fermentation of wheat pieces, containing various proteolytic enzymes including glucoamylase, protease, etc) to hydrolyse the protein and starch content in wheat flour at different temperatures (25, 55 and 68 °C). Starch hydrolysis was most effective at 68 °C and the starch substrate was almost completely hydrolysed after 10 h. By contrast, only limited protein hydrolysis was observed due to severe protease denaturation at this temperature. The optimum protease activity was observed at 55 °C and hydrolysed 21% of the flour protein after 78 h. However, the hydrolysis velocity for starch was reduced to <15% after a reaction period of 10 h. Wang et al. (2009) indicated that reduced energy consumption at lower reaction temperatures was attractive for large scale processes, although considerably longer reaction time would be required to achieve complete starch hydrolysis. Furthermore, performing enzymatic reactions at lower temperatures could lead to microbial contamination over prolonged reaction times (Wang et al., 2009). Indeed, the results presented here (Section 6.3) showed that competing microbial activity was probably responsible for the decline in reducing sugars and tyrosine from hydrolysis of flour and AS after 24 h reaction.

Table 7-2 Recyclability of various CLEAs in bioconversion processes

Enzymes	Recyclability of CLEAs:		Bioconversion	Conversion rate/efficiency:		Reference
	Numbers of cycles	Residual activity		Free enzyme	CLEA	
Lipase	5	72%	Hydrolysis of fish oil for enrichment of polyunsaturated fatty acids, 40 °C ,14h	12%	42%	Yan et al. (2012)
Laccases	4	50%	Aerobic oxidation of long chain alcohols (1-octanol) in buffer,8h	5%	45%	Matijošytė et al. (2010)
Cellulolytic enzymes (endoglucanase and xylanase)	5	77-86%	Hydrolysing alkali-pretreated wheat straw at 70 °C, 24h	31.8%	32.9%	Shuddhodana et al. (2018)
Laccase	5	60%	Decolorization activity on malachite green dye at room temperature ,24h	~90%	~90%	Sinirlioglu et al. (2013)
Proteases	10	66.5%	Removing a gelatinous layer from waste X-ray film at ph 8.0 and 37 °C, 50 min	~100%	~100%	Asgher et al. (2018)
Proteases	10	66.5%	Dehairing of goat hides, 12 h at 37 °C.	100%	100%	Asgher et al. (2018)

Magnetic CLEA: pectinase	7	87%	Clarification of apple juices (turbidity removal) 150 min at 50 °C	30%	26%	Sojitra et al. (2017)
Lipase-magnetic CLEA	5	68%	Biodiesel production from sunflower oil (vegetable oils), 2 h at 40 °C	42.8%	67.9%	Mehde et al. (2018b)
Gel entrapped CLEA: urease	15	90%	-	-	-	Zeinali and Lenjannezhadian (2018)
α - Galactosidase	6	22%	Hydrolysis of oligosaccharides in soymilk 24 h at 50 °C	89%	85%	Bayraktar and Onal (2019)

7.3 High-value enzyme product recovery from biological wastewater treatment

Circular economy based is recognised as having a central role in sustainable development in the global agenda (Bilal and Iqbal, 2019). Waste minimisation and valorisation, as well as resource recovery and recycling represent central attributes in circular economy. Waste biomass, in the form of sewage sludge generated by the Water Industry has high organic content and is in constant supply and provides significant opportunities to implement various resource recovery strategies to produce useful materials and commodities (Bora et al., 2020) (Section 2.1.2). However, whilst resource recovery is technically possible and can lead to marketable products and is well founded in the principles of sustainability, the operational costs often exceed the potential income, limiting the economic feasibility in practice. For example, P is an important, finite resource (Scholz et al., 2013) and struvite precipitations proven and technically feasible for P recovery from sludge dewatering liquors or wastewater in full-scale WWTPs, and the product is an effective agricultural fertiliser (Shaddel et al., 2019). However, the low market price of struvite fertilisers (approximately €55 per t (de Vries et al., 2016)), challenges the economic viability of the recovery process.

Recovery of high-value enzyme products, on the other hands, represents a unique technological approach for the valuable utilisation of waste sludge and to enhance the economic and environmental sustainability of the Water industry. The global industrial enzymes market has expanded rapidly in the last decade and is expected to increase from about $5.5 billion in 2018 to $7.0 billion by 2023 representing a compound annual growth rate of 4.9% (BCC Research, 2018) (Section 1.1). The typical market prices for enzyme products range from 3 $/kg up to 200-2000 $/kg (Sóti et al., 2018), which is considerably larger than other sludge-recovered, marketable products.

This study demonstrates the technical feasibility of producing a partially purified, carrier-free, immobilised hydrolytic enzyme product (i.e. CLEA) from biological wastewater treatment. Waste AS was used as the raw enzyme source, reducing the cost for the biomass culture media in conventional enzyme production process, which represents a significant component (30-40% (Tyagi and Lo, 2013)) of the total cost of producing enzyme products. Soluble hydrolytic enzymes can be effectively extracted directly from waste AS, without specific modifications to standard wastewater treatment processes. Consolidation and immobilisation of enzymes by the CLEA technique greatly expands the industrial application and increases the economic value and marketability of enzyme products extracted from AS. The CLEA fulfils many requirements as an immobilised biocatalyst, including improved operational stability compared to soluble biocatalysts, ease of separation and recycling, and reusability for repeated operational treatment process cycles. The AS CLEA also showed high potential to be employed for the hydrolysis and bioconversion of complex organic materials (e.g. food and agricultural products) under mild operating conditions, minimising energy requirements, and avoiding the use of corrosive, hazardous and expensive chemicals, such as acids or alkali.

Furthermore, the chemical requirements for CLEA preparation from AS are inexpensive, biodegradable (and can therefore be co-digested to recover valuable biogas by AD with sewage sludge) and are readily available from the market (e.g. surfactant TX100, organic solvent acetone and bio-renewable material dextran). The apparatus required for CLEA production from AS is also widely used in and is familiar to the Water Industry (e.g. sonication processer and centrifuge). Thus, emissions of hazardous pollutants are avoided. With further development to scale up the process, the CLEA production technology therefore offers significant technical, sustainability and commercial opportunities from integrating enzyme recovery into biological wastewater treatment and sludge management strategies.

8 Conclusions and recommendations for future research

The major conclusions from this study are as follows:

- Waste activated sludge, a by-product generated from conventional WWTPs, contains a wide range of hydrolytic enzymes which can be extracted and recovered as a high-value and marketable industrial product.
- Sonication was effective at disrupting AS flocs and releasing hydrolytic enzymes and the results demonstrated that the developed extraction protocol produced a mixture of enzymes (including but not limited to amylase, protease, lipase, cellulase) capable of hydrolysing a range of different substrates including starch, proteins, lipids and cellulose. The optimum operational parameters for AS floc disruption were: 40% AMP (equivalent to an energy intensity of 872W/L) and 10 min duration. The solids content of sludge samples was also an important parameter influencing ultrasonic disruption and optimisation experiments indicated that a solids content of approximately 10g VS/L (DF=5) provided the maximum enzyme activity. Surfactant addition (1% v/v TX100) enhanced protein release as well as enzyme activity in the AS extract. Under optimum conditions, the recovery rates of protease and cellulase were 63.1% and ~100%, respectively.
- The apparent activities of protease, amylase and cellulase maintained relatively stable at different stages of the aerobic, plug flow sewage treatment reactor, even under conditions of severe nutrient deprivation, and no correlation was found between sludge microbial activity and the activity of hydrolytic enzymes. Therefore, thickened WAS, collected directly following secondary clarification, is a viable and practical source of biomass for enzyme extraction.
- This study is the first time that CLEAs have been prepared from the biological AS generated during municipal wastewater treatment, which is a complex waste biomass containing a wide range of hydrolytic enzymes. The CLEA technique involves precipitation of soluble enzymes and chemical cross-linking of the precipitated enzymes, combining consolidation and stabilisation of crude AS enzymes into a single step. Optimisation of the operational conditions (including combinations and concentrations of additive, precipitant and cross-linker) is necessary to maximise the recovery of AS enzymes in the CLEA and has a profound influence on the morphology and the catalytic activity of the CLEA.
- Bovine serum albumin, an inert protein additive, stabilised the enzyme protein structure and supplied lysine groups, forming covalent bonds with the cross-linker, facilitating the enzyme aggregation and enhancing the enzyme activity recovery in the CLEA. Acetone precipitation was more effective for enzyme cross-linking, compared to $(NH_4)_2SO_4$, which

can inactivate amylase in the absence of BSA. The macromolecular cross-linker, dextran aldehyde, improved the enzyme activity recovery rate in the CLEA due to the moderate reactivity and larger molecular size, which reduces the possible penetration of the cross-linker into enzyme molecules and reaction with essential active sites of the enzyme, compared to glutaraldehyde.

- The conditions for CLEA preparation from crude AS enzyme extracts were optimised and were as follows: acetone precipitation (volume ratio = 4:1, 0.5 h at 0 °C), followed by dextran aldehyde cross-linking (0.04% w/v, 3.5 h at room temperature), with 5 mg/mL BSA addition. The highest enzyme recoveries in the CLEA for amylase, protease, lipase and cellulase obtained following this procedure were: 42.6%, 48.3%, 54.4% and 35.1%, respectively.
- The storage stability of the AS CLEA directly affects the shelf life of the CLEA, as a marketable end-product. Preserving the CLEA as a suspension in Tris-HCl buffer maintained the enzyme activity at an equivalent level to fresh CLEA and is recommended for storing the CLEA product, compared to freeze-drying, which significantly reduced catalytic activity.
- The produced AS CLEA contains a variety of hydrolytic enzymes, i.e a multi-CLEA, and demonstrated potential for hydrolysing complex organic materials including wheat flour and AS. The hydrolysis of complex substrate is influenced many interacting factors, including the activity of the CLEA, but also on the physical, chemical and biological characteristics of the substrate.
- The AS CLEA was effective at hydrolysing wheat flour, which mainly contains carbohydrates, proteins and lipids, and the hydrolysis efficiency showed a dose-dependent relationship. The maximum yields of reducing sugar and tyrosine, representing the products of amylase and protease hydrolysis by the CLEA, from wheat flour hydrolysis were: 5.0 and 7.0%, and 79.8 and 106.6% at 40 °C with CLEA dose rates = 1:100 and 1:10 v/v, respectively. The higher yield of tyrosine than reducing sugar may be explained by substrate (starch-protein) interactions that reduce accessibility of starch to reaction sites on the enzyme, and also the apparently greater susceptibility of proteins to enzymatic hydrolysis in wheat flour.
- Activated sludge is a highly complex organic substrate comprising of active microbial cells, as well as other inorganic and organic soluble and solid constituents. No evidence was found for the chemical inhibition of CLEA hydrolytic activity by the sludge matrix. However, enzymatic treatment of intact or partially disrupted sludge by the CLEA only showed a slight increase in reducing sugar from hydrolysis of the complex polysaccharide content in

AS. This could be explained due to the protection of microbial cells to amylase attack by the gel-like EPS fraction and the rigid cell wall, and the susceptibility of these structures to CLEA attack. However, greater tyrosine release from hydrolysis of protein components of the AS substrate was observed compared to polysaccharides, probably because of the polysaccharide-protein interaction (similar with starch-protein interaction) facilitating the CLEA protease attack, the resistance of the sludge polysaccharide structure to the polysaccharide-degrading enzymes in the CLEA, and dominance of protein content in the AS matrix. After 24 h incubation, however, concentrations of hydrolysis products declined probably due to rapid removal and assimilation by the active microbial biomass present in these non-sterile systems.

Based on the results obtained here, further research is required to develop the CLEA production technology from AS generated by biological wastewater treatment, including:

- Quantify the impact of different types of reactor (e.g. plug flow and continuously stirred-tank reactor, etc.), dissolved oxygen level (aerobic, anoxic and anaerobic), and solids retention time in the AS process on the efficacy of enzyme extraction and recovery by the developed protocol.
- Exploring the protein structure (including molecule shape, ammonia acid sequences, etc.) of enzymes extracted from AS, to further optimise CLEA preparation and understand the mechanisms controlling CLEA activity and behaviour; techniques such as FTIR and proteomic analysis can be applied to quantify the enzyme structure.
- Investigating the physical and chemical properties of the AS CLEA, including kinetic parameters (e.g. substrate affinity), mechanical stability, pH and thermal stability, reusability, etc., which can be used as indicators for further assessing the feasibility of using the CLEA for bioconversion of complex organic materials.
- Exploring the technical and economic feasibility of scaling up the AS enzyme recovery and AS CLEA production. For example, research is required to determine the effect of increasing scale on the efficiency of sludge cell disruption by sonication, and the enzyme recovery rate by the cross-linking technique; capital and operational costs (including for the sonication processor and centrifuge) to produce CLEA are required and an assessment of the projected market uptake of the CLEA product completed.
- Exploring the potential industrial application of the AS CLEA for the hydrolysis and pretreatment of different organic materials (e.g. food waste), identifying potential inhibition factors (e.g. production inhibition, substrate inhibition, shielding of the enzyme catalytic

site, etc.) to the CLEA hydrolysis efficacy via a data-modelling approach, and optimising the CLEA hydrolysis conditions of the target industrial process.

- Maximising the hydrolysis efficacy of the CLEA on the sludge (and other potential complex organic materials), via optimising the operational conditions of the hydrolysis reactions; development of an immobilised reactor system to retain the CLEA in the system is also necessary for continuous flow operation.
- Investigating the effect of using CLEA as a pretreatment unit on sludge AD, measuring the solids reduction in the AD reactor and biogas yield from the CLEA-pretreated sludge; the effect of combined enzyme and other chemical/physical pretreatment methods on sludge is also worth investigation.
- Explore potential applications of the AS CLEA in other areas, such as ethanol production, long chain elongation for fatty acids, reformulation laundry product, etc.

9 References

ABBASI, M., DEHGHANI, M., MOUSSAVI, G. & AZHDARPOOR, A. 2015. Degradation of organic matter of municipal sewage sludge using ultrasound treatment in Shiraz wastewater treatment plant. *Health Scope,* 4**,** e23507.

ABDUL-FATTAH, A. M., KALONIA, D. S. & PIKAL, M. J. 2007. The challenge of drying method selection for protein pharmaceuticals: Product quality implications. *Journal of Pharmaceutical Sciences,* 96**,** 1886-1916.

ABERER, W., HAHN, M., KLADE, M., SEEBACHER, U., SPOK, A., WALLNER, K. & WITZANI, H. 2002. Collection of information on enzymes. Luxembourg: European Communities.

ABRAMOV, O. V. 1999. Low-amplitude vibrations and waves. *High-Intensity Ultrasonics: Theory and Industrial Applications.* 1st ed. London: CRC Press.

ABU YAZID, N., BARRENA, R. & SANCHEZ, A. 2016. Assessment of protease activity in hydrolysed extracts from SSF of hair waste by and indigenous consortium of microorganisms. *Waste Management,* 49**,** 420-426.

AGORO, M. A., ADENIJI, A. O., ADEFISOYE, M. A. & OKOH, O. O. 2020. Heavy Metals in Wastewater and Sewage Sludge from Selected Municipal Treatment Plants in Eastern Cape Province, South Africa. *Water,* 12**,** 19.

AHMED, R. Z., SIDDIQUI, K., ARMAN, M. & AHMED, N. 2012. Characterization of high molecular weight dextran produced by Weissella cibaria CMGDEX3. *Carbohydrate Polymers,* 90**,** 441-446.

AHUMADA, K., URRUTIA, P., ILLANES, A. & WILSON, L. 2015. Production of combi-CLEAs of glycosidases utilized for aroma enhancement in wine. *Food and Bioproducts Processing,* 94**,** 555-560.

AKYON, B., LIPUS, D. & BIBBY, K. 2019. Glutaraldehyde inhibits biological treatment of organic additives in hydraulic fracturing produced water. *Science of the Total Environment,* 666**,** 1161-1168.

AL SHIKH, A. & MILOSEVIC, A. 2020. Effectiveness of Alcohol and Aldehyde Spray Disinfectants on Dental Impressions. *Clinical Cosmetic and Investigational Dentistry,* 12**,** 25-30.

ALASONAT, E. & SLAVEYKOVA, V. L. 2012. Effects of extraction methods on the composition and molar mass distributions of exopolymeric substances of the bacterium Sinorhizobium meliloti. *Bioresource Technology,* 114**,** 603-609.

AMARAL-FONSECA, M., KOPP, W., GIORDANO, R. D. C., FERNANDEZ-LAFUENTE, R. & TARDIOLI, P. W. 2018. Preparation of Magnetic Cross-Linked Amyloglucosidase Aggregates: Solving Some Activity Problems. *Catalysts,* 8.

AMARIEI, G., BOLTES, K., ROSAL, R. & LETÓN, P. 2017. Toxicological interactions of ibuprofen and triclosan on biological activity of activated sludge. *Journal of Hazardous Materials,* 334**,** 193-200.

ANBAZHAGAN, S. & PALANI, S. 2018. Extraction of consortium of hydrolytic enzymes from waste activated sludge using ultrasonication and stirring with surfactants. *Ultrasonics Sonochemistry,* 40**,** 874-880.

APHA 2017a. 2540 SOLIDS. *Standard Methods For the Examination of Water and Wastewater.* American Public Health Association.

APHA 2017b. 4500 pH VALUE. *Standard Methods For the Examination of Water and Wastewater.* American Public Health Association.

ARAGON-BRICENO, C. I., ROSS, A. B. & CAMARGO-VALERO, M. A. 2021. Mass and energy integration study of hydrothermal carbonization with anaerobic digestion of sewage sludge. *Renewable Energy,* 167**,** 473-483.

ARAKAWA, T., PRESTRELSKI, S. J., KENNEY, W. C. & CARPENTER, J. F. 2001. Factors affecting short-term and long-term stabilities of proteins. *Advanced Drug Delivery Reviews,* 46**,** 307-326.

ARAVINTHAN, V., MINO, T., TAKIZAWA, S., SATOH, H. & MATSUO, T. 2001. Sludge hydrolysate as a carbon source for denitrification. *Water Science and Technology,* 43**,** 191-199.

ARSICCIO, A., MCCARTY, J., PISANO, R. & SHEA, J.-E. 2020. Heightened Cold-Denaturation of Proteins at the Ice–Water Interface. *Journal of the American Chemical Society,* 142**,** 5722-5730.

ARUN, C. & SIVASHANMUGAM, P. 2015. Solubilization of waste activated sludge using a garbage enzyme produced from different pre-consumer organic waste. *RSC Advances,* 5**,** 51421-51427.

ARUN, C. & SIVASHANMUGAM, P. 2017. Study on optimization of process parameters for enhancing the multi-hydrolytic enzyme activity in garbage enzyme produced from preconsumer organic waste. *Bioresource Technology,* 226**,** 200-210.

ASGARI LAJAYER, B., NAJAFI, N., MOGHISEH, E., MOSAFERI, M. & HADIAN, J. 2019. Effects of Gamma Irradiated and Non-Irradiated Sewage Sludge on Growth Characteristics, Leaf Chlorophyll Index, and Macronutrients Concentrations in Basil. *Journal of Soil Science and Plant Nutrition,* 19**,** 580-591.

ASGARI LAJAYER, B., NAJAFI, N., MOGHISEH, E., MOSAFERI, M. & HADIAN, J. 2020. Effects of gamma irradiation on physicochemical and biological characteristics of wastewater effluent and sludge. *International Journal of Environmental Science and Technology,* 17**,** 1021-1034.

ASGHER, M., BASHIR, F. & IQBAL, H. M. N. 2018. Protease-based cross-linked enzyme aggregates with improved catalytic stability, silver removal, and dehairing potentials. *International Journal of Biological Macromolecules,* 118**,** 1247-1256.

ATAY, S. & AKBAL, F. 2016. Classification and effects of sludge disintegration technologies integrated into sludge handling units: An overview. *Clean-Soil Air Water,* 44**,** 1198-1213.

ATHA, D. H. & INGHAM, K. C. 1981. Mechanism of precipitation of proteins by polyethylene glycols - analysis in terms of excluded volume. *Journal of Biological Chemistry,* 256**,** 2108-2117.

AVVARU, B. & PANDIT, A. B. 2009. Oscillating bubble concentration and its size distribution using acoustic emission spectra. *Ultrasonics Sonochemistry,* 16**,** 105-115.

AWONG, J., BITTON, G. & KOOPMAN, B. 1985. ATP, oxygen-uptake rate and INT-dehydrogenase activity of actinomycete foams. *Water Research,* 19**,** 917-921.

AYHAN, H., AYHAN, F. & GULSU, A. 2012. Highly biocompatible enzyme aggregates crosslinked by L-lysine. *Turkish Journal of Biochemistry-Turk Biyokimya Dergisi,* 37**,** 14-20.

AYTAR, B. S. & BAKIR, U. 2008. Preparation of cross-linked tyrosinase aggregates. *Process Biochemistry,* 43**,** 125-131.

BA, K., AGUEDO, M., TINE, E., PAQUOT, M., DESTAIN, J. & THONART, P. 2013. Hydrolysis of starches and flours by sorghum malt amylases for dextrins production. *European Food Research and Technology,* 236**,** 905-918.

BAHREINI, G., NAZARI, L., HO, D., FLANNERY, C. C., ELBESHBISHY, E., SANTORO, D. & NAKHLA, G. 2020. Enzymatic pre-treatment for enhancement of primary sludge fermentation. *Bioresource Technology,* 305**,** 123071.

BAI, N. L., WANG, S., ABUDUAINI, R., ZHU, X. F. & ZHAO, Y. H. 2016. Isolation and characterization of Sphingomonas sp Y2 capable of high-efficiency degradation of nonylphenol polyethoxylates in wastewater. *Environmental Science and Pollution Research,* 23**,** 12019-12029.

BAIER, U. & SCHMIDHEINY, P. 1997. Enhanced anaerobic degradation of mechanically disintegrated sludge. *Water Science and Technology,* 36**,** 137-143.

BALASUNDARAM, B. & HARRISON, S. T. L. 2006. Study of physical and biological factors involved in the disruption of E. coli by hydrodynamic cavitation. *Biotechnology Progress,* 22**,** 907-913.

BALDINO, L., CONCILIO, S., CARDEA, S., DE MARCO, I. & REVERCHON, E. 2015. Complete glutaraldehyde elimination during chitosan hydrogel drying by SC-CO2 processing. *The Journal of Supercritical Fluids,* 103**,** 70-76.

BARBER, E. A., LIU, Z. & SMITH, S. R. 2020. Organic contaminant biodegradation by oxidoreductase enzymes in wastewater treatment. *Microorganisms,* 8.

BARBOSA, O., ORTIZ, C., BERENGUER-MURCIA, A., TORRES, R., RODRIGUES, R. C. & FERNANDEZ-LAFUENTE, R. 2014. Glutaraldehyde in bio-catalysts design: a useful crosslinker and a versatile tool in enzyme immobilization. *Rsc Advances,* 4**,** 1583-1600.

BASHIR, F., ASGHER, M., HUSSAIN, F. & RANDHAWA, M. A. 2018. Development and characterization of cross-linked enzyme aggregates of thermotolerant alkaline protease from Bacillus licheniformis. *International Journal of Biological Macromolecules,* 113**,** 944-951.

BASHIROVA, A., PRAMANIK, S., VOLKOV, P., ROZHKOVA, A., NEMASHKALOV, V., ZOROV, I., GUSAKOV, A., SINITSYN, A., SCHWANEBERG, U. & DAVARI, M. D. 2019. Disulfide Bond Engineering of an Endoglucanase from Penicillium verruculosum to Improve Its Thermostability. *International journal of molecular sciences,* 20**,** 1602.

BATISTA, J. M. S., BRANDAO-COSTA, R. M. P., DA CUNHA, M. N. C., RODRIGUES, H. O. S. & PORTO, A. L. F. 2020. Purification and biochemical characterization of an extracellular fructosyltransferase-rich extract produced by Aspergillus tamarii Kita UCP1279. *Biocatalysis and Agricultural Biotechnology,* 26.

BAUER, D. 2014. The Water-Energy Nexus: Challenges and Opportunities. *U.S. Department of Energy*.

BAYNE, S. J. & OTTESEN, M. 1976. Enzymatically Active, Cross-Linked Pig Heart Lactate-Dehydrogenase Crystals. *Carlsberg Research Communications,* 41**,** 211-216.

BAYRAKTAR, H. & ONAL, S. 2019. Cross-linked alpha-galactosidase aggregates: optimization, characterization and application in the hydrolysis of raffinose-type oligosaccharides in soymilk. *Journal of the Science of Food and Agriculture,* 99**,** 4748-4760.

BCC RESEARCH. 2018. *Global Markets for Enzymes in Industrial Applications* [Online]. Massachusetts, USA: BCC Publishing. Available: https://www.bccresearch.com/market-research/biotechnology/global-markets-for-enzymes-in-industrial-applications-bio030k.html [Accessed].

BERG, J. M., TYMOCZKO, J. L. & STRYER, L. 2002. *Biochemistry,* New York, W. H. Freeman.

BILAL, M. & IQBAL, H. M. N. 2019. Sustainable bioconversion of food waste into high-value products by immobilized enzymes to meet bio-economy challenges and opportunities – A review. *Food Research International,* 123**,** 226-240.

BISSWANGER, H. 2011a. Enzyme assays. *Practical Enzymology.* Weinheim: Wiley-VCH Verlag GmbH & Co. KGaA.

BISSWANGER, H. 2011b. Enzymes in technical applications. *Practical Enzymology.* Weinheim: Wiley-VCH Verlag GmbH & Co. KGaA.

BISSWANGER, H. 2011c. General aspects of enzyme analysis. *Practical Enzymology.* Weinheim: Wiley-VCH Verlag GmbH & Co. KGaA.

BISSWANGER, H. 2011d. Introduction. *Practical Enzymology.* Weinheim: Wiley-VCH Verlag GmbH & Co. KGaA.

BOCZAR, B. A., BEGLEY, W. M. & LARSON, R. J. 1992. Characterization of enzyme activity in activated sludge using rapid analyses for specific hydrolases. *Water Environment Research,* 64**,** 792-797.

BOHACZ, J. 2018. Microbial strategies and biochemical activity during lignocellulosic waste composting in relation to the occurring biothermal phases. *Journal of Environmental Management,* 206**,** 1052-1062.

BOLIVAR, J. M., ROCHA-MARTIN, J., MATEO, C., CAVA, F., BERENGUER, J., FERNANDEZ-LAFUENTE, R. & GUISAN, J. M. 2009. Coating of Soluble and Immobilized Enzymes with Ionic Polymers: Full Stabilization of the Quaternary Structure of Multimeric Enzymes. *Biomacromolecules,* 10**,** 742-747.

BONILLA, S., CHOOLAEI, Z., MEYER, T., EDWARDS, E. A., YAKUNIN, A. F. & ALLEN, D. G. 2018. Evaluating the effect of enzymatic pretreatment on the anaerobic digestibility of pulp and paper biosludge. *Biotechnology Reports,* 17**,** 77-85.

BORA, R. R., RICHARDSON, R. E. & YOU, F. 2020. Resource recovery and waste-to-energy from wastewater sludge via thermochemical conversion technologies in support of circular economy: a comprehensive review. *BMC Chemical Engineering,* 2**,** 8.

BOUGRIER, C., CARRÈRE, H. & DELGENÈS, J. P. 2005. Solubilisation of waste-activated sludge by ultrasonic treatment. *Chemical Engineering Journal,* 106**,** 163-169.

BOWES, J. H. & CATER, C. W. 1966. The reaction of glutaraldehyde with proteins and other biological materials*. *Journal of the Royal Microscopical Society,* 85**,** 193-200.

BRASK, J., FUGLSANG, C. C. & KIRK, O. n.d. . *General information relating to the cost of enzymes* [Online]. Novozymes A/S. Available: https://studylib.net/doc/7258453/cost-of-enzymes [Accessed 2021].

BRENA, B. M. & BATISTA-VIERA, F. 2006. Immobilization of Enzymes. *In:* GUISAN, J. M. (ed.) *Immobilization of Enzymes and Cells.* Totowa, NJ: Humana Press.

BRUFAU, J., FRANCESCH, M. & PEREZ-VENDRELL, A. M. 2006. The use of enzymes to improve cereal diets for animal feeding. *Journal of the Science of Food and Agriculture,* 86**,** 1705-1713.

BRUSLIND, L. 2020. Bacteria: Cell Walls. *General Microbiology.* Oregon, US: Oregon State University.

BUCHHOLZ, P. C. F., OHS, R., SPIESS, A. C. & PLEISS, J. 2019. Progress Curve Analysis Within BioCatNet: Comparing Kinetic Models for Enzyme-Catalyzed Self-Ligation. *Biotechnology Journal,* 14**,** 1800183.

BUGG, T. D. H. 2012. *Introduction to Enzyme and Coenzyme Chemistry,* West Sussex, John Wiley & Sons.

BUKRINSKY, J. T., BJERRUM, M. J. & KADZIOLA, A. 1998. Native Carboxypeptidase A in a New Crystal Environment Reveals a Different Conformation of the Important Tyrosine 248. *Biochemistry,* 37**,** 16555-16564.

BURGESS, R. R. 2009. Protein Precipitation Techniques. *In:* BURGESS, R. R. & DEUTSCHER, M. P. (eds.) *Guide to Protein Purification, Second Edition.*

BUSTO, M. D., ORTEGA, N. & PEREZMATEOS, M. 1997. Stabilisation of cellulases by cross-linking with glutaraldehyde and soil humates. *Bioresource Technology,* 60**,** 27-33.

BUTREDDY, A., JANGA, K. Y., AJJARAPU, S., SARABU, S. & DUDHIPALA, N. 2021. Instability of therapeutic proteins — An overview of stresses, stabilization mechanisms and analytical techniques involved in lyophilized proteins. *International Journal of Biological Macromolecules,* 167**,** 309-325.

BUTTERFIELD, D. A., COLVIN, J., LIU, J., WANG, J., BACHAS, L. & BHATTACHARRYA, D. 2002. Electron paramagnetic resonance spin label titration: a novel method to investigate random and site-specific immobilization of enzymes onto polymeric membranes with different properties. *Analytica Chimica Acta,* 470**,** 29-36.

BUTTERWORTH, P. J., WARREN, F. J., GRASSBY, T., PATEL, H. & ELLIS, P. R. 2012. Analysis of starch amylolysis using plots for first-order kinetics. *Carbohydrate Polymers,* 87**,** 2189-2197.

BWANGANGA TAWABA, J.-C., TSHIALA, H., KIBAL, I., BUETUSIWA, T. & DE DIEU MINENGU, J. 2015. Effects of phenolic compounds on the hydrolysis of red sorghum starch by extracted red sorghum malt α- and β-amylases. *Starch - Stärke,* 67**,** 854-859.

CABROL, L., MARONE, A., TAPIA-VENEGAS, E., STEYER, J.-P., RUIZ-FILIPPI, G. & TRABLY, E. 2017. Microbial ecology of fermentative hydrogen producing bioprocesses: useful insights for driving the ecosystem function. *FEMS Microbiology Reviews,* 41**,** 158-181.

CADORET, A., CONRAD, A. & BLOCK, J. C. 2002. Availability of low and high molecular weight substrates to extracellular enzymes in whole and dispersed activated sludges. *Enzyme and Microbial Technology,* 31**,** 179-186.

CAMISASCA, G., IORIO, A., DE MARZIO, M. & GALLO, P. 2018. Structure and slow dynamics of protein hydration water. *Journal of Molecular Liquids,* 268**,** 903-910.

CAMPBELL, G. L. & BEDFORD, M. R. 1992. Enzyme applications for monogastric feeds-A review. *Canadian Journal of Animal Science,* 72**,** 449-466.

CAO, L. Q., VAN LANGEN, L. & SHELDON, R. A. 2003. Immobilised enzymes: carrier-bound or carrier-free? *Current Opinion in Biotechnology,* 14**,** 387-394.

CAO, L. Q., VAN RANTWIJK, F. & SHELDON, R. A. 2000. Cross-linked enzyme aggregates: A simple and effective method for the immobilization of penicillin acylase. *Organic Letters,* 2**,** 1361-1364.

CAPELO, J. L., XIMENEZ-EMBUN, P., MADRID-ALBARRAN, Y. & CAMARA, C. 2004. Enzymatic probe sonication: Enhancement of protease-catalyzed hydrolysis of selenium bound to proteins in yeast. *Analytical Chemistry,* 76**,** 233-237.

CARPENTER, J. F., PRESTRELSKI, S. J. & ARAKAWA, T. 1993. Separation of Freezing- and Drying-Induced Denaturation of Lyophilized Proteins Using Stress-Specific Stabilization: I. Enzyme Activity and Calorimetric Studies. *Archives of Biochemistry and Biophysics,* 303**,** 456-464.

CHANG, B. S. & MAHONEY, R. R. 1995. Enzyme thermostabilization by bovine serum albumin and other proteins: evidence for hydrophobic interactions. *Biotechnology and Applied Biochemistry,* 22**,** 203-214.

CHATTERJEE, P., GHANGREKAR, M. M. & RAO, S. 2019. Biogas production from partially digested septic tank sludge and its kinetics. *Waste and Biomass Valorization,* 10**,** 387-398.

CHAUDHARI, S. A. & SINGHAL, R. S. 2017. A strategic approach for direct recovery and stabilization of Fusarium sp. ICT SAC1 cutinase from solid state fermented broth by carrier free cross-linked enzyme aggregates. *International Journal of Biological Macromolecules,* 98**,** 610-621.

CHEN, J. H., LIU, S. H., WANG, Y. M., HUANG, W. & ZHOU, J. 2018. Effect of different hydrolytic enzymes pretreatment for improving the hydrolysis and biodegradability of waste activated sludge. *Water Science and Technology***,** 592-602.

CHROST, R. J. 1991. Environmental-control of the synthesis and activity of aquatic microbial ectoenzymes. *In:* CHROST, R. J. (ed.) *Microbial Enzymes in Aquatic Environments.* New York: Springer-Verlag.

CHUI, W. K. & WAN, L. S. C. 1997. Prolonged retention of cross-linked trypsin in calcium alginate microspheres. *Journal of Microencapsulation,* 14**,** 51-61.

CLARA, M., KREUZINGER, N., STRENN, B., GANS, O. & KROISS, H. 2005. The solids retention time—a suitable design parameter to evaluate the capacity of wastewater treatment plants to remove micropollutants. *Water Research,* 39**,** 97-106.

CLAVIJO RIVERA, E., MONTALESCOT, V., VIAU, M., DROUIN, D., BOURSEAU, P., FRAPPART, M., MONTEUX, C. & COUALLIER, E. 2018. Mechanical cell disruption of Parachlorella kessleri microalgae: Impact on lipid fraction composition. *Bioresource Technology,* 256**,** 77-85.

CLEEMPUT, G., BOOIJ, C., HESSING, M., GRUPPEN, H. & DELCOUR, J. A. 1997. Solubilisation and changes in molecular weight distribution of arabinoxylans and

protein in wheat flours during bread-making, and the effects of endogenous arabinoxylan hydrolysing enzymes. *Journal of Cereal Science,* 26**,** 55-66.

COMTE, S., GUIBAUD, G. & BAUDU, M. 2006. Relations between extraction protocols for activated sludge extracellular polymeric substances (EPS) and EPS complexation properties: Part I. Comparison of the efficiency of eight EPS extraction methods. *Enzyme and Microbial Technology,* 38**,** 237-245.

CONFER, D. R. & LOGAN, B. E. 1998. Location of protein and polysaccharide hydrolytic activity in suspended and biofilm wastewater cultures. *Water Research,* 32**,** 31-38.

CORNISH-BOWDEN, A. 2012. *Fundamentals of Enzyme Kinetics,* Weinheim, Wiley-Blackwell.

CORREA, W., BRANDENBURG, J., BEHRENDS, J., HEINBOCKEL, L., REILING, N., PAULOWSKI, L., SCHWUDKE, D., STEPHAN, K., MARTINEZ-DE-TEJADA, G., BRANDENBURG, K. & GUTSMANN, T. 2019. Inactivation of Bacteria by γ-Irradiation to Investigate the Interaction with Antimicrobial Peptides. *Biophysical Journal,* 117**,** 1805-1819.

COSKUN, O. 2016. Separation techniques: Chromatography. *Northern clinics of Istanbul,* 3**,** 156-160.

COUSSIOS, GT, C, C., FARNY, C. H., TER HAAR, G. & ROY, R. A. 2007. Role of acoustic cavitation in the delivery and monitoring of cancer treatment by high-intensity focused ultrasound (HIFU). *International Journal of Hyperthermia,* 23**,** 105-120.

CUI, J., LIN, T., FENG, Y., TAN, Z. & JIA, S. 2017. Preparation of spherical cross-linked lipase aggregates with improved activity, stability and reusability characteristic in water-in-ionic liquid microemulsion. *Journal of Chemical Technology & Biotechnology,* 92**,** 1785-1793.

CUI, J. D. & JIA, S. R. 2015. Optimization protocols and improved strategies of cross-linked enzyme aggregates technology: current development and future challenges. *Critical Reviews in Biotechnology,* 35**,** 15-28.

CURRIE, J. A., DUNNILL, P. & LILLY, M. D. 1972. Release of protein from bakers-yeast (saccharomyces-cerevisiae) by disruption in an industrial agitator mill. *Biotechnology and Bioengineering,* 14**,** 725-&.

CZACZYK, K. & MYSZKA, K. 2007. Biosynthesis of extracellular polymeric substances (EPS) and its role in microbial biofilm formation. *Polish Journal of Environmental Studies,* 16**,** 799-806.

D'AGOSTINO, R. B. 1986. Tests for normal distribution. *In:* D'AGOSTINO, R. B. & STEPHENS, M. A. (eds.) *Goodness-of-fit Techniques.* New York: Marcel Dekker.

D'SOUZA, D. H., BHATTACHARYA, S. & DAS, A. 2020. Fibrinolytic protease from Bacillus cereus S46: Purification, characterization, and evaluation of its in vitro thrombolytic potential. *Journal of Basic Microbiology,* 60**,** 661-668.

D'APPOLONIA, B. L. & RAYAS-DUARTE, P. 1994. Wheat carbohydrates: structure and functionality. *In:* BUSHUK, W. & RASPER, V. F. (eds.) *Wheat: Production, Properties and Quality.* Boston, MA: Springer US.

DA COSTA LUCHIARI, I., CEDENO, F. R. P., DE MACÊDO FARIAS, T. A., PICHELI, F. P., DE PAULA, A. V., MONTI, R. & MASARIN, F. 2021. Glucoamylase Immobilization in Corncob Powder: Assessment of Enzymatic Hydrolysis of Starch in the Production of Glucose. *Waste and Biomass Valorization*.

DAHANAYAKE, J. N. & MITCHELL-KOCH, K. R. 2018. Entropy connects water structure and dynamics in protein hydration layer. *Physical Chemistry Chemical Physics,* 20**,** 14765-14777.

DAHANAYAKE, J. N., SHAHRYARI, E., ROBERTS, K. M., HEIKES, M. E., KASIREDDY, C. & MITCHELL-KOCH, K. R. 2019. Protein Solvent Shell Structure Provides Rapid Analysis of Hydration Dynamics. *Journal of Chemical Information and Modeling,* 59**,** 2407-2422.

DAL MAGRO, L., HERTZ, P. F., FERNANDEZ-LAFUENTE, R., KLEIN, M. P. & RODRIGUES, R. C. 2016. Preparation and characterization of a Combi-CLEAs from pectinases and cellulases: a potential biocatalyst for grape juice clarification. *Rsc Advances,* 6**,** 27242-27251.

DALL'OGLIO, F., AMICO, V. D., NASCA, M. R. & MICALI, G. 2012. Treatment of Cutaneous Warts An Evidence-Based Review. *American Journal of Clinical Dermatology,* 13**,** 73-96.

DAMASCENO, F. R. C., FREIRE, D. M. G. & CAMMAROTA, M. C. 2008. Impact of the addition of an enzyme pool on an activated sludge system treating dairy wastewater under fat shock loads. *Journal of Chemical Technology and Biotechnology,* 83**,** 730-738.

DAVIDSSON, Å. & LA COUR JANSEN, J. 2006. Pre-treatment of wastewater sludge before anaerobic digestion - hygienisation, ultrasonic treatment and enzyme dosing. *Vatten: tidskrift för vattenvård /Journal of Water Management and research,* 62**,** 335-340.

DE FARIAS, V. L., MONTEIRO, K. X., RODRIGUES, S., NARCISO FERNANDES, F. A. & SAAVEDRA PINTO, G. A. 2010. Comparison of Aspergillus niger spore production on Potato Dextrose Agar (PDA) and crushed corncob medium. *Journal of General and Applied Microbiology,* 56**,** 399-402.

DE LA ROSA-MILLAN, J., ORONA-PADILLA, J. L., FLORES-MORENO, V. M. & SERNA-SALDIVAR, S. O. 2020. Effect of jet-cooking and hydrolyses with amylases on the

physicochemical and in vitro digestion performance of whole chickpea flours. *International Journal of Food Science and Technology,* 55**,** 690-701.

DE ROSE, S. A., NOVAK, H., DOWD, A., SINGH, S., LANG, D. A. & LITTLECHILD, J. 2017. Stabilization of a Lipolytic Enzyme for Commercial Application. *Catalysts,* 7.

DE VRIES, S., POSTMA, R., VAN SCHOLL, L., BLOM-ZANDSTRA, G., VERHAGEN, J. & HARMS, I. 2016. Economic feasibility and climate benefits of using struvite from the Netherlands as a phosphate (P) fertilizer in West Africa. *Wageningen Plant Research report,* No. 673**,** 47.

DEEPA, G., SINGH, V. & NAIDU, K. A. 2010. A comparative study on starch digestibility, glycemic index and resistant starch of pigmented ('Njavara' and 'Jyothi') and a non-pigmented ('IR 64') rice varieties. *Journal of Food Science and Technology,* 47**,** 644-649.

DESHAVATH, N. N., MUKHERJEE, G., GOUD, V. V., VEERANKI, V. D. & SASTRI, C. V. 2020. Pitfalls in the 3, 5-dinitrosalicylic acid (DNS) assay for the reducing sugars: Interference of furfural and 5-hydroxymethylfurfural. *International Journal of Biological Macromolecules,* 156**,** 180-185.

DESVAUX, M., DUMAS, E., CHAFSEY, I. & HÉBRAUD, M. 2006. Protein cell surface display in Gram-positive bacteria: from single protein to macromolecular protein structure. *FEMS Microbiology Letters,* 256**,** 1-15.

DEVADASU, S., JOSHI, S. M., GOGATE, P. R., SONAWANE, S. H. & SURANANI, S. 2020. Intensification of delignification of Tectona grandis saw dust as sustainable biomass using acoustic cavitational devices. *Ultrasonics Sonochemistry,* 63**,** 104914.

DEWIL, R., BAEYENS, J. & GOUTVRIND, R. 2006. Ultrasonic treatment of waste activated sludge. *Environmental Progress,* 25**,** 121-128.

DHANALAKSHMI, N. P. & NAGARAJAN, R. 2011. Ultrasonic intensification of the chemical degradation of methyl violet: an experimental study. *International Journal of Chemical and Molecular Engineering,* 5**,** 1019-1024.

DOJNOV, B., GRUJIC, M. & VUJCIC, Z. 2015. Highly efficient production of Aspergillus niger amylase cocktail by solid-state fermentation using triticale grains as a well-balanced substrate. *Journal of the Serbian Chemical Society,* 80**,** 1375-1390.

DOLD, P. L., FLEIT, E., HAN, J. & COPP, J. B. 1995. Assay for determination of α-amylase activity in activated sludge mixed bacterial communities. *Environmental Technology,* 16**,** 181-188.

DONG, F., LI, X., ZHANG, L., MA, L. & LI, R. 2016. Cavitation erosion mechanism of titanium alloy radiation rods in aluminum melt. *Ultrasonics Sonochemistry,* 31**,** 150-156.

DONG, T., ZHAO, L., HUANG, Y. & TAN, X. 2010. Preparation of cross-linked aggregates of aminoacylase from Aspergillus melleus by using bovine serum albumin as an inert additive. *Bioresource Technology,* 101**,** 6569-6571.

DONOSO-BRAVO, A., RETAMAL, C., CARBALLA, M., RUIZ-FILIPPI, G. & CHAMY, R. 2009. Influence of temperature on the hydrolysis, acidogenesis and methanogenesis in mesophilic anaerobic digestion: parameter identification and modeling application. *Water Science and Technology,* 60**,** 9-17.

DÖRR, T., MOYNIHAN, P. J. & MAYER, C. 2019. Editorial: Bacterial Cell Wall Structure and Dynamics. *Frontiers in Microbiology,* 10.

DROBCHENKO, S. N., ISAEVAIVANOVA, L. S., KLEINER, A. R., LOMAKIN, A. V., KOLKER, A. R. & NOSKIN, V. A. 1993. An Investigation of The Structure of Periodate-Oxidized Dextran. *Carbohydrate Research,* 241**,** 189-199.

DUBEY, N. C. & TRIPATHI, B. P. 2021. Nature Inspired Multienzyme Immobilization: Strategies and Concepts. *ACS Applied Bio Materials,* 4**,** 1077-1114.

DURDEVIC, D., TRSTENJAK, M. & HULENIC, I. 2020. Sewage Sludge Thermal Treatment Technology Selection by Utilizing the Analytical Hierarchy Process. *Water,* 12.

E. POLIFKA, J. & HABERMANN, J. 2015. 2.9 - Anticoagulants, thrombocyte aggregation inhibitors, fibrinolytics and volume replacement agents. *In:* SCHAEFER, C., PETERS, P. & MILLER, R. K. (eds.) *Drugs During Pregnancy and Lactation (Third Edition).* San Diego: Academic Press.

EL HADJ-ALI, N., AGREBI, R., GHORBEL-FRIKHA, B., SELLAMI-KAMOUN, A., KANOUN, S. & NASRI, M. 2007. Biochemical and molecular characterization of a detergent stable alkaline serine-protease from a newly isolated Bacillus licheniformis NH1. *Enzyme and Microbial Technology,* 40**,** 515-523.

ELIASSON, A.-C. & TJERNELD, E. 1990. Adsorption of wheat proteins on wheat starch granules. *Cereal chemistry,* 67**,** 366-372.

ENVIRONMENT AGENCY. 2020. *Environment Agency strategy for safe and sustainable sludge use* [Online]. UK. Available: https://www.gov.uk/government/publications/environment-agency-strategy-for-safe-and-sustainable-sludge-use/environment-agency-strategy-for-safe-and-sustainable-sludge-use#contents [Accessed 26 May 2021].

ERAT, M., DEMIR, H. & ŠAKIROGLU, H. 2005. Purification of glutathione reductase from chicken liver and investigation of kinetic properties. *Applied Biochemistry and Biotechnology,* 125**,** 127-138.

ERIKSSON, L., STEEN, I. & TENDAJ, M. 1992. Evaluation of sludge properties at an activated-sludge plant. *Water Science and Technology,* 25**,** 251-265.

ERNI, B. 1989. GLUCOSE-TRANSPORT IN ESCHERICHIA-COLI. *Fems Microbiology Letters,* 63**,** 13-23.

EUN, H.-M. 1996. 1 - Enzymes and Nucleic Acids: General Principles. *In:* EUN, H.-M. (ed.) *Enzymology Primer for Recombinant DNA Technology.* San Diego: Academic Press.

EUROPEAN COUNCIL 2009. Urban Waste Water Treatment Directive (91/271/EEC). The Council of The European Communities.

EUROPEAN PARLIAMENT AND COUNCIL OF THE EUROPEAN UNION 2003. Regulation (EC) No 1831/2003 of the European Parliament and of the Council of 22 September 2003 on additives for use in animal nutrition. *Official Journal of the European Union,* L 268**,** 29-43.

EUROSTAT. 2021. *Sewage sludge production and disposal from urban wastewater (in dry substance (d.s))* [Online]. Luxembourg: Eurostat. Available: https://ec.europa.eu/eurostat/databrowser/view/ten00030/default/table?lang=en [Accessed 2006].

FACCIO, G. 2018. From Protein Features to Sensing Surfaces. *Sensors (Basel),* 18.

FELZ, S., AL-ZUHAIRY, S., AARSTAD, O. A., VAN LOOSDRECHT, M. C. M. & LIN, Y. M. 2016. Extraction of structural extracellular polymeric substances from aerobic granular sludge. *Jove-Journal of Visualized Experiments*.

FENG, Q., TAI, X. R., SUN, Y. Q. & LI, M. 2019. Influence of turbulent mixing on the composition of extracellular polymeric substances (EPS) and aggregate size of aerated activated sludge. *Chemical Engineering Journal,* 378.

FENG, Q., XIAO, Y. B., LI, X. C., XUE, Z. X., FANG, F., CAO, J. S., OLEYIBLO, J. O. & HU, Z. R. 2016. Using the dehydrogenase activity for alert of activated sludge system under different copper concentrations. *Desalination and Water Treatment,* 57**,** 17836-17843.

FERNANDEZ-LAFUENTE, R., ROSELL, C. M., RODRIGUEZ, V. & GUISAN, J. M. 1995. Strategies for enzyme stabilization by intramolecular crosslinking with bifunctional reagents. *Enzyme and Microbial Technology,* 17**,** 517-523.

FERNANDEZ-LORENTE, G., PALOMO, J. M., MATEO, C., MUNILLA, R., ORTIZ, C., CABRERA, Z., GUISAN, J. M. & FERNANDEZ-LAFUENTE, R. 2006. Glutaraldehyde cross-linking of lipases adsorbed on aminated supports in the presence of detergents leads to improved performance. *Biomacromolecules,* 7**,** 2610-2615.

FRANZ, A. W., KRONEMAYER, H., PFEIFFER, D., PILZ, R. D., REUSS, G., DISTELDORF, W., GAMER, A. O. & HILT, A. 2016. Formaldehyde. *Ullmann's Encyclopedia of Industrial Chemistry.* Berlin: Wiley-VCH Verlag GmbH & Co. KGaA.

FROLUND, B., GRIEBE, T. & NIELSEN, P. H. 1995. Enzymatic-activity in the activated-sludge floc matrix. *Applied Microbiology and Biotechnology,* 43**,** 755-761.

GARCIA, J., FERNANDEZ, S., MIRADA, F. J. & LOPEZ, F. 1997. Determination of the protease activity in activated sludges by gelatin hydrolysis. *Journal of Environmental Science and Health Part a-Toxic/Hazardous Substances & Environmental Engineering,* 32**,** 2537-2551.

GARCIA-GALAN, C., BARBOSA, O. & FERNANDEZ-LAFUENTE, R. 2013. Stabilization of the hexameric glutamate dehydrogenase from Escherichia coli by cations and polyethyleneimine. *Enzyme and Microbial Technology,* 52**,** 211-217.

GAROFALO, L., VAZQUEZ, D., FERREIRA, F. & SOULE, S. 2011. Wheat flour non-starch polysaccharides and their effect on dough rheological properties. *Industrial Crops and Products,* 34**,** 1327-1331.

GECIOVA, J., BURY, D. & JELEN, P. 2002. Methods for disruption of microbial cells for potential use in the dairy industry - a review. *International Dairy Journal,* 12**,** 541-553.

GESSESSE, A., DUEHOLM, T., PETERSEN, S. B. & NIELSEN, P. H. 2003. Lipase and protease extraction from activated sludge. *Water Research,* 37**,** 3652-3657.

GHERGHEL, A., TEODOSIU, C. & DE GISI, S. 2019. A review on wastewater sludge valorisation and its challenges in the context of circular economy. *Journal of Cleaner Production,* 228**,** 244-263.

GHOSE, T. K. 1987. Measurement of cellulase activities. *Pure and Applied Chemistry,* 59**,** 257-268.

GIBSON, W. & KOCH, C. 2019. *Biotechnology and Genetic Engineering,* Essex, ED-Tech Press.

GIHAZ, S., BASH, Y., RUSH, I., SHAHAR, A., PAZY, Y. & FISHMAN, A. 2020. Bridges to Stability: Engineering Disulfide Bonds Towards Enhanced Lipase Biodiesel Synthesis. *ChemCatChem,* 12**,** 181-192.

GILLETT, R. & GULL, K. 1972. Glutaraldehyde - its purity and stability. *Histochemie,* 30**,** 162-+.

GLAUCHE, F., PILAREK, M., BOURNAZOU, M. N. C., GRUNZEL, P. & NEUBAUER, P. 2017. Design of experiments-based high-throughput strategy for development and optimization of efficient cell disruption protocols. *Engineering in Life Sciences,* 17**,** 1166-1172.

GOEL, R., MINO, T., SATOH, H. & MATSUO, T. 1998a. Comparison of hydrolytic enzyme systems in pure culture and activated sludge under different electron acceptor conditions. *Water Science and Technology,* 37**,** 335-343.

GOEL, R., MINO, T., SATOH, H. & MATSUO, T. 1998b. Enzyme activities under anaerobic and aerobic conditions inactivated sludge sequencing batch reactor. *Water Research,* 32**,** 2081-2088.

GOÑI, I., GARCIA-ALONSO, A. & SAURA-CALIXTO, F. 1997. A starch hydrolysis procedure to estimate glycemic index. *Nutrition Research,* 17**,** 427-437.

GORISSEN, S. H. M., CROMBAG, J. J. R., SENDEN, J. M. G., WATERVAL, W. A. H., BIERAU, J., VERDIJK, L. B. & VAN LOON, L. J. C. 2018. Protein content and amino acid composition of commercially available plant-based protein isolates. *Amino Acids,* 50**,** 1685-1695.

GRAEBIN, N. G., DE ANDRADES, D., BARSE, L. Q., RODRIGUES, R. C. & AYUB, M. A. Z. 2018. Preparation and characterization of cross-linked enzyme aggregates of dextransucrase from Leuconostoc mesenteroides B-512F. *Process Biochemistry,* 71**,** 101-108.

GUELLIL, A., BOUALAM, M., QUIQUAMPOIX, H., GINESTET, P., AUDIC, J. M. & BLOCK, J. C. 2001. Hydrolysis of wastewater colloidal organic matter by extracellular enzymes extracted from activated sludge flocs. *Water Science and Technology,* 43**,** 33-40.

GUIMARAES, J. R., MIRANDA, L. P., FERNANDEZ-LAFUENTE, R. & TARDIOLI, P. W. 2021. Immobilization of Eversa(R) Transform via CLEA Technology Converts It in a Suitable Biocatalyst for Biolubricant Production Using Waste Cooking Oil. *Molecules,* 26.

GÜNERKEN, E., D'HONDT, E., EPPINK, M. H. M., GARCIA-GONZALEZ, L., ELST, K. & WIJFFELS, R. H. 2015. Cell disruption for microalgae biorefineries. *Biotechnology Advances,* 33**,** 243-260.

GUO, L., LU, M., LI, Q., ZHANG, J., ZONG, Y. & SHE, Z. 2014. Three-dimensional fluorescence excitation–emission matrix (EEM) spectroscopy with regional integration analysis for assessing waste sludge hydrolysis treated with multi-enzyme and thermophilic bacteria. *Bioresource Technology,* 171**,** 22-28.

GUPTA, P., DUTT, K., MISRA, S., RAGHUWANSHI, S. & SAXENA, R. K. 2009. Characterization of cross-linked immobilized lipase from thermophilic mould Thermomyces lanuginosa using glutaraldehyde. *Bioresource Technology,* 100**,** 4074-4076.

HABEEB, A. F. S. A. & HIRAMOTO, R. 1968. Reaction of proteins with glutaraldehyde. *Archives of Biochemistry and Biophysics,* 126**,** 16-26.

HAKI, G. D. & RAKSHIT, S. K. 2003. Developments in industrially important thermostable enzymes: a review. *Bioresource Technology,* 89**,** 17-34.

HAN, D., LEE, C. Y., CHANG, S. W. & KIM, D. J. 2017. Enhanced methane production and wastewater sludge stabilization of a continuous full scale thermal pretreatment and thermophilic anaerobic digestion. *Bioresource Technology,* 245**,** 1162-1167.

HANFT, F. & KOEHLER, P. 2005. Quantitation of dityrosine in wheat flour and dough by liquid chromatography-tandem mass spectrometry. *J Agric Food Chem,* 53**,** 2418-23.

HAO, Z. & JAHNG, D. 2019. Variations of organic matters and extracellular enzyme activities during biodrying of dewatered sludge with different bulking agents. *Biochemical Engineering Journal,* 147**,** 126-135.

HARGONO, H., JOS, B., BUDIYONO, B., SUMARDIONO, S., PRIYANTO, S., HARYANI, K. & ZAKARIA, M. F. 2020. Hydrolysis kinetic of suweg (Amorphophalluscampanulatus B) starch using a mixture of alpha amylase and glucoamylase. *AIP Conference Proceedings,* 2197**,** 120001.

HARING, D. & SCHREIER, P. 1999. Cross-linked enzyme crystals. *Current Opinion in Chemical Biology,* 3**,** 35-38.

HASAN, F., SHAH, A. A., JAVED, S. & HAMEED, A. 2010. Enzymes used in detergents: Lipases. *African Journal of Biotechnology,* 9**,** 4836-4844.

HASSARD, F., BIDDLE, J., HARNETT, R. & STEPHENSON, T. 2018. Microbial extracellular enzyme activity affects performance in a full-scale modified activated sludge process. *Science of the Total Environment,* 625**,** 1527-1534.

HE, Q. L., ZHANG, J., GAO, S. X., CHEN, L., LYU, W. L., ZHANG, W., SONG, J. Y., HU, X. L., CHEN, R. F., WANG, H. Y. & YU, J. 2019. A comprehensive comparison between non-bulking and bulking aerobic granular sludge in microbial communities. *Bioresource Technology,* 294.

HENRIQUES, R. O., BORK, J. A., FERNANDEZ-LORENTE, G., GUISAN, J. M., FURIGO, A., DE OLIVEIRA, D. & PESSELA, B. C. 2018. Co-immobilization of lipases and β-d-galactosidase onto magnetic nanoparticle supports: Biochemical characterization. *Molecular Catalysis,* 453**,** 12-21.

HENRÍQUEZ, G., GOMEZ, A., GUERRERO, E. & NARAYAN, M. 2020. Potential Role of Natural Polyphenols against Protein Aggregation Toxicity: In Vitro, In Vivo, and Clinical Studies. *ACS Chemical Neuroscience,* 11**,** 2915-2934.

HERMANSON, G. T. 2013a. Antibody Modification and Conjugation. *In:* HERMANSON, G. T. (ed.) *Bioconjugate Techniques.* Third ed. Boston: Academic Press.

HERMANSON, G. T. 2013b. Enzyme Modification and Conjugation. *In:* HERMANSON, G. T. (ed.) *Bioconjugate Techniques.* Third ed. Boston: Academic Press.

HERMES, J. D., BLACKLOW, S. C. & KNOWLES, J. R. 1987. The development of enzyme catalytic efficiency - An experimental approach. *Cold Spring Harbor Symposia on Quantitative Biology,* 52**,** 597-602.

HERO, J. S., ROMERO, C. M., PISA, J. H., PEROTTI, N. I., OLIVARO, C. & MARTINEZ, M. A. 2018. Designing cross-linked xylanase aggregates for bioconversion of agroindustrial waste biomass towards potential production of nutraceuticals. *International Journal of Biological Macromolecules,* 111**,** 229-236.

HILL, G. A., MACDONALD, D. G. & LANG, X. 1997. a-Amylase inhibition and inactivation in barley malt during cold starch hydrolysis. *Biotechnology Letters,* 19**,** 1139-1141.

HMIDET, N., BAYOUDH, A., BERRIN, J. G., KANOUN, S., JUGE, N. & NASRI, M. 2008. Purification and biochemical characterization of a novel alpha-amylase from Bacillus licheniformis NH1 - Cloning, nucleotide sequence and expression of amyN gene in Escherichia coli. *Process Biochemistry,* 43**,** 499-510.

HOLM, J., LASSI, U., ROMAR, H., LAHTI, R., KÄRKKÄINEN, J. & LAJUNEN, M. 2012. Pretreatment of fibre sludge in ionic liquids followed by enzyme and acid catalysed hydrolysis. *Catalysis Today,* 196**,** 11-15.

HOLM, J., ZINCHENKO, G., LASSI, U., HERNOUX-VILLIÈRE, A. & KÄRKKÄINEN, J. 2013. Enzyme-catalyzed hydrolysis of fibre sludge into reducing sugars. *Biomass Conversion and Biorefinery,* 3**,** 353-359.

HOMAEI, A. A., SARIRI, R., VIANELLO, F. & STEVANATO, R. 2013. Enzyme immobilization: an update. *Journal of chemical biology,* 6**,** 185-205.

HONG, P. N., HONDA, R., NOGUCHI, M. & ITO, T. 2017. Optimum selection of extraction methods of extracellular polymeric substances in activated sludge for effective extraction of the target components. *Biochemical Engineering Journal,* 127**,** 136-146.

HONIG, W. & KULA, M. R. 1976. Selectivity of Protein Precipitation with Polyethylene-Glycol Fractions of Various Molecular Weights. *Analytical Biochemistry,* 72**,** 502-512.

HOPPE, H.-G., KIM, S.-J. & GOCKE, K. 1988. Microbial decomposition in aquatic environments: combined process of extracellular enzyme activity and substrate uptake. *Applied and Environmental Microbiology,* 54**,** 784-790.

HOPPE, W., LOHMANN, W., MARKL, H. & ZIEGLER, H. 1983. *Biophysics,* Berlin-Heidelberg-New York-Tokyo, Springer Verlag.

HOU, X., LIU, S. & ZHANG, Z. 2015. Role of extracellular polymeric substance in determining the high aggregation ability of anammox sludge. *Water Research,* 75**,** 51-62.

HSIU, J., FISCHER, E. H. & STEIN, E. A. 1964. Alpha-Amylases as Calcium-Metalloenzymes. II. Calcium and the Catalytic Activity*. *Biochemistry,* 3**,** 61-66.

HU, G., LI, J., HUANG, S. & LI, Y. 2016. Oil recovery from petroleum sludge through ultrasonic assisted solvent extraction. *Journal of Environmental Science and Health, Part A,* 51**,** 921-929.

HU, R. F., LIN, L., LIU, T. J., OUYANG, P., HE, B. H. & LIU, S. J. 2008. Reducing sugar content in hemicellulose hydrolysate by DNS method: A revisit. *Journal of Biobased Materials and Bioenergy,* 2**,** 156-161.

HUANG, G., CHEN, S., DAI, C., SUN, L., SUN, W., TANG, Y., XIONG, F., HE, R. & MA, H. 2017. Effects of ultrasound on microbial growth and enzyme activity. *Ultrasonics Sonochemistry,* 37**,** 144-149.

HUANG, K. C., MUKHOPADHYAY, R., WEN, B., GITAI, Z. & WINGREEN, N. S. 2008. Cell shape and cell-wall organization in Gram-negative bacteria. *Proceedings of the National Academy of Sciences,* 105**,** 19282-19287.

HUME, A. J., AMES, J., RENNICK, L. J., DUPREX, W. P., MARZI, A., TONKISS, J. & MÜHLBERGER, E. 2016. Inactivation of RNA Viruses by Gamma Irradiation: A Study on Mitigating Factors. *Viruses,* 8**,** 204.

INGHAM, K. C. 1984. [20] Protein precipitation with polyethylene glycol. *Methods in Enzymology.* Academic Press.

IRITANI, E., KATAGIRI, N., YAMADA, M., HWANG, K. J. & CHENG, T. W. 2016. Ultrahigh-pressure expression of activated sludge assisted with self-flocculation caused by ultrasonication. *Chemical Engineering Research and Design,* 112**,** 16-23.

IZYDORCZYK, M. S. 2009. 23 - Arabinoxylans. *In:* PHILLIPS, G. O. & WILLIAMS, P. A. (eds.) *Handbook of Hydrocolloids (Second Edition).* Woodhead Publishing.

JAEGER, K. E. & EGGERT, T. 2004. Enantioselective biocatalysis optimized by directed evolution. *Current Opinion in Biotechnology,* 15**,** 305-313.

JAFARI, S., SALEHIZIRI, M., FOROOZESH, E., BARDI, M. J. & RAD, H. A. 2020. An evaluation of lysozyme enzyme and thermal pretreatments on dairy sludge digestion and gas production. *Water Science and Technology,* 81**,** 1052-1062.

JANNAT, M. & YANG, K. L. 2018. Immobilization of enzymes on flexible tubing surfaces for continuous bioassays. *Langmuir,* 34**,** 14226-14233.

JIANG, X. L., HAO, Z. & TIAN, J. C. 2008. Variations in amino acid and protein contents of wheat during milling and northern-style steamed breadmaking. *Cereal Chemistry,* 85**,** 504-508.

JUHNEVICA-RADENKOVA, K., KVIESIS, J., MORENO, D. A., SEGLINA, D., VALLEJO, F., VALDOVSKA, A. & RADENKOVS, V. 2021. Highly-Efficient Release of Ferulic Acid from Agro-Industrial By-Products via Enzymatic Hydrolysis with Cellulose-Degrading Enzymes: Part I-The Superiority of Hydrolytic Enzymes Versus Conventional Hydrolysis. *Foods (Basel, Switzerland),* 10.

JUNG, J., XING, X. H. & MATSUMOTO, K. 2001. Kinetic analysis of disruption of excess activated sludge by Dyno Mill and characteristics of protein release for recovery of useful materials. *Biochemical Engineering Journal,* 8**,** 1-7.

JUNG, J., XING, X. H. & MATSUMOTO, K. 2002. Recoverability of protease released from disrupted excess sludge and its potential application to enhanced hydrolysis of proteins in wastewater. *Biochemical Engineering Journal,* 10**,** 67-72.

KAGLIWAL, L. D., SURVASE, S. A., SINGHAL, R. S. & GRANSTRÖM, T. 2013. Wheat flour based propionic acid fermentation: An economic approach. *Bioresource Technology,* 129**,** 694-699.

KALMENDAL, R. & TAUSON, R. 2012. Effects of a xylanase and protease, individually or in combination, and an ionophore coccidiostat on performance, nutrient utilization, and intestinal morphology in broiler chickens fed a wheat-soybean meal-based diet. *Poultry Science,* 91**,** 1387-1393.

KARN, S. K. & KUMAR, A. 2019. Protease, lipase, and amylase extraction and optimization from activated sludge of pulp and paper industry. *Indian Journal of Experimental Biology,* 57**,** 201-205.

KARN, S. K., KUMAR, P. & PAN, X. L. 2013. Extraction of lipase and protease and characterization of activated sludge from pulp and paper industry. *Preparative Biochemistry & Biotechnology,* 43**,** 152-162.

KATCHALSKIKATZIR, E. 1993. Immobilized enzymes - Learning from past successes and failures. *Trends in Biotechnology,* 11**,** 471-478.

KAUSHIK, R., PARSHETTI, G. K., LIU, Z. & BALASUBRAMANIAN, R. 2014. Enzyme-assisted hydrothermal treatment of food waste for co-production of hydrochar and bio-oil. *Bioresource Technology,* 168**,** 267-274.

KAWAHARA, J., OHMORI, T., OHKUBO, T., HATTORI, S. & KAWAMURA, M. 1992. The structure of glutaraldehyde in aqueous solution determined by ultraviolet absorption and light scattering. *Analytical Biochemistry,* 201**,** 94-98.

KEHREIN, P., VAN LOOSDRECHT, M., OSSEWEIJER, P., GARFI, M., DEWULF, J. & POSADA, J. 2020. A critical review of resource recovery from municipal wastewater treatment plants - market supply potentials, technologies and bottlenecks. *Environmental Science-Water Research & Technology,* 6**,** 877-910.

KHAN, I., GANESAN, R. & DUTTA, J. R. 2019. Probiotic lipase derived from Lactobacillus plantarum and Lactobacillus brevis for biodiesel production from waste cooking olive oil: an alternative feedstock. *International Journal of Green Energy*.

KHAN, M. U. & AHRING, B. K. 2021. Improving the biogas yield of manure: Effect of pretreatment on anaerobic digestion of the recalcitrant fraction of manure. *Bioresource Technology,* 321**,** 124427.

KHOIRUNNISA, W., PUSPITARINI, S., ROHMAWATI, S. A., ELTAVIA, F., RAHAYU, R. P., UTOMO, D. H. & PERMATASARI, G. W. 2016. Molecular mechanism of formaldehyde and protein interaction in human cancer cell. *Trends in Bioinformatics,* 9**,** 30-34.

KHOSROSHAHI, M. E. & GHAZANFARI, L. 2010. Preparation and characterization of silica-coated iron-oxide bionanoparticles under N2 gas. *Physica E: Low-dimensional Systems and Nanostructures,* 42**,** 1824-1829.

KIM, M., OH, S., RAKWAL, R., LIU, C. & ZHANG, Z. 2013a. Biohydrogen production from sterilized sewage sludge as a substrate using mixed cultures. *International*

Proceedings of Chemical, Biological and Environmental Engineering (IPCBEE), 51**,** 87-93.

KIM, M. H., PARK, S., KIM, Y. H., WON, K. & LEE, S. H. 2013b. Immobilization of formate dehydrogenase from Candida boidinii through cross-linked enzyme aggregates. *Journal of Molecular Catalysis B: Enzymatic,* 97**,** 209-214.

KLOEKE, F. V. & GEESEY, G. G. 1999. Localization and identification of populations of phosphatase-active bacterial cells associated with activated sludge flocs. *Microbial Ecology,* 38**,** 201-214.

KOKKONEN, P., BEDNAR, D., PINTO, G., PROKOP, Z. & DAMBORSKY, J. 2019. Engineering enzyme access tunnels. *Biotechnology Advances,* 37**,** 107386.

KOLEY, D. & BARD, A. J. 2010. Triton X-100 concentration effects on membrane permeability of a single HeLa cell by scanning electrochemical microscopy (SECM). *Proceedings of the National Academy of Sciences of the United States of America,* 107**,** 16783-16787.

KONG, J. & YU, S. 2007. Fourier transform infrared spectroscopic analysis of protein secondary structures. *Acta Biochim Biophys Sin (Shanghai),* 39**,** 549-59.

KOUBAA, M., IMATOUKENE, N., DRÉVILLON, L. & VOROBIEV, E. 2020. Current insights in yeast cell disruption technologies for oil recovery: A review. *Chemical Engineering and Processing - Process Intensification,* 150**,** 107868.

KOVÁROVÁ-KOVAR, K. & EGLI, T. 1998. Growth kinetics of suspended microbial cells: from single-substrate-controlled growth to mixed-substrate kinetics. *Microbiology and Molecular Biology Reviews: MMBR,* 62**,** 646-666.

KRAH, D., GHATTAS, A. K., WICK, A., BRÖDER, K. & TERNES, T. A. 2016. Micropollutant degradation via extracted native enzymes from activated sludge. *Water Research,* 95**,** 348-360.

KRISHNA, R. & RAMACHANDRAN, P. A. 1975. Analysis of diffusional effects in immobilised two-enzyme systems. *Journal of Applied Chemistry and Biotechnology,* 25**,** 623-640.

KRISTOFFERSEN, K. A., VAN AMERONGEN, A., BÖCKER, U., LINDBERG, D., WUBSHET, S. G., DE VOGEL-VAN DEN BOSCH, H., HORN, S. J. & AFSETH, N. K. 2020. Fourier-transform infrared spectroscopy for monitoring proteolytic reactions using dry-films treated with trifluoroacetic acid. *Scientific Reports,* 10**,** 7844.

KUROWSKA, K., MARKS-BIELSKA, R., BIELSKI, S., KRYSZK, H. & JASINSKAS, A. 2020. Food Security in the Context of Liquid Biofuels Production. *Energies,* 13**,** 6247.

LAAGE, D., ELSAESSER, T. & HYNES, J. T. 2017. Water Dynamics in the Hydration Shells of Biomolecules. *Chemical Reviews,* 117**,** 10694-10725.

LADOLE, M. R., MEVADA, J. S. & PANDIT, A. B. 2017. Ultrasonic hyperactivation of cellulase immobilized on magnetic nanoparticles. *Bioresource Technology,* 239**,** 117-126.

LAI, J. Q., HU, Z. L., SHELDON, R. A. & YANG, Z. 2012. Catalytic performance of cross-linked enzyme aggregates of Penicillium expansum lipase and their use as catalyst for biodiesel production. *Process Biochemistry,* 47**,** 2058-2063.

LEE, J. 2016. Importance of Sonication and Solution Conditions on the Acoustic Cavitation Activity. *Handbook of Ultrasonics and Sonochemistry.* Singapore: Springer Singapore.

LEE, R. A. & LAVOIE, J.-M. 2013. From first- to third-generation biofuels: Challenges of producing a commodity from a biomass of increasing complexity. *Animal Frontiers,* 3**,** 6-11.

LEHNE, G., MULLER, A. & SCHWEDES, J. 2001. Mechanical disintegration of sewage sludge. *Water Science and Technology,* 43**,** 19-26.

LESTER, G. E., HODGES, D. M., MEYER, R. D. & MUNRO, K. D. 2004. Pre-extraction preparation (fresh, frozen, freeze-dried, or acetone powdered) and long-term storage of fruit and vegetable tissues: Effects on antioxidant enzyme activity. *Journal of Agricultural and Food Chemistry,* 52**,** 2167-2173.

LEVINE, A. D., TCHOBANOGLOUS, G. & ASANO, T. 1985. Characterization of the size distribution of contaminants in wastewater: Treatment and reuse implications. *Journal (Water Pollution Control Federation),* 57**,** 805-816.

LEVINE, A. D., TCHOBANOGLOUS, G. & ASANO, T. 1991. Size distributions of particulate contaminants in wastewater and their impact on treatability. *Water Research,* 25**,** 911-922.

LI, A.-J., LI, X.-Y. & YU, H.-Q. 2011. Effect of the food-to-microorganism (F/M) ratio on the formation and size of aerobic sludge granules. *Process Biochemistry,* 46**,** 2269-2276.

LI, B., SHAN, C.-L., ZHOU, Q., FANG, Y., WANG, Y.-L., XU, F., HAN, L.-R., IBRAHIM, M., GUO, L.-B., XIE, G.-L. & SUN, G.-C. 2013. Synthesis, Characterization, and Antibacterial Activity of Cross-Linked Chitosan-Glutaraldehyde. *Marine Drugs,* 11**,** 1534-1552.

LI, D. X. & XI, H. L. 2019. Layered extraction and adsorption performance of extracellular polymeric substances from activated sludge in the enhanced biological phosphorus removal process. *Molecules,* 24.

LI, H., XIAO, W. H., XIE, P. P. & ZHENG, L. Y. 2018. Co-immobilization of enoate reductase with a cofactor-recycling partner enzyme. *Enzyme and Microbial Technology,* 109**,** 66-73.

LI, L., LI, G., CAO, L.-C., REN, G.-H., KONG, W., WANG, S.-D., GUO, G.-S. & LIU, Y.-H. 2015. Characterization of the Cross-Linked Enzyme Aggregates of a Novel β-Galactosidase, a Potential Catalyst for the Synthesis of Galacto-Oligosaccharides. *Journal of Agricultural and Food Chemistry,* 63**,** 894-901.

LI, N. & ZONG, M.-H. 2010. Lipases from the genus Penicillium: Production, purification, characterization and applications. *Journal of Molecular Catalysis B: Enzymatic,* 66**,** 43-54.

LI, X., METTU, S., MARTIN, G. J. O., ASHOKKUMAR, M. & LIN, C. S. K. 2019. Ultrasonic pretreatment of food waste to accelerate enzymatic hydrolysis for glucose production. *Ultrasonics Sonochemistry,* 53**,** 77-82.

LI, X., WU, Y., ZHANG, L., CAO, Y., LI, Y., LI, J., ZHU, L. & WU, G. 2014. Comparison of three common DNA concentration measurement methods. *Analytical Biochemistry,* 451**,** 18-24.

LI, X. Y. & YANG, S. F. 2007. Influence of loosely bound extracellular polymeric substances (EPS) on the flocculation, sedimentation and dewaterability of activated sludge. *Water Research,* 41**,** 1022-1030.

LI, Y. & CHROST, R. J. 2006a. Enzymatic activities in petroleum wastewater purification system by an activated sludge process. *Journal of Microbiology and Biotechnology,* 16**,** 200-204.

LI, Y. & CHROST, R. J. 2006b. Microbial enzymatic activities in aerobic activated sludge model reactors. *Enzyme and Microbial Technology,* 39**,** 568-572.

LI, Y., XUE, F., LI, J., XU, S. H. & LI, D. 2016. Migration and transformation rule of heavy metals in sludge during hydrolysis for protein extraction. *Environmental Science and Pollution Research,* 23**,** 5352-5360.

LI, Z. & STENSTROM, M. K. 2018. Impacts of SRT on particle size distribution and reactor performance in activated sludge processes. *Water Environment Research,* 90**,** 48-56.

LIN, H., ZHANG, M., WANG, F., MENG, F., LIAO, B.-Q., HONG, H., CHEN, J. & GAO, W. 2014. A critical review of extracellular polymeric substances (EPSs) in membrane bioreactors: Characteristics, roles in membrane fouling and control strategies. *Journal of Membrane Science,* 460**,** 110-125.

LINDEBOOM, R. E. F., DING, L., WEIJMA, J., PLUGGE, C. M. & VAN LIER, J. B. 2014. Starch hydrolysis in autogenerative high pressure digestion: Gelatinisation and saccharification as rate limiting steps. *Biomass & Bioenergy,* 71**,** 256-265.

LIU, C.-Z., WANG, F., STILES, A. R. & GUO, C. 2012. Ionic liquids for biofuel production: Opportunities and challenges. *Applied Energy,* 92**,** 406-414.

LIU, D., ZENG, X. A., SUN, D. W. & HAN, Z. 2013. Disruption and protein release by ultrasonication of yeast cells. *Innovative Food Science & Emerging Technologies,* 18**,** 132-137.

LIU, Y. & FANG, H. H. P. 2003. Influences of extracellular polymeric substances (EPS) on flocculation, settling, and dewatering of activated sludge. *Critical Reviews in Environmental Science and Technology,* 33**,** 237-273.

LIU, Y., YANG, H., TAKATSUKI, H. & SAKANISHI, A. 2006. Effect of ultrasonic exposure on Ca2+-ATPase activity in plasma membrane from Aloe arborescens callus cells. *Ultrasonics Sonochemistry,* 13**,** 232-236.

LIU, Y., YANG, J., WANG, K., DUAN, F. & LU, L. 2021. Carrier-Free Immobilization of α-Galactosidase as Nano-Biocatalysts for Synthesizing Prebiotic α-Galacto-Oligosaccharides. *Molecules (Basel, Switzerland),* 26**,** 1248.

LIU, Z. & SMITH, S. R. 2020a. Enzyme activity of waste activated sludge extracts. *Water Science and Technology*.

LIU, Z. & SMITH, S. R. 2020b. Enzyme Recovery from Biological Wastewater Treatment. *Waste and Biomass Valorization*.

LIU, Z., YANG, H., HUANG, Z., ZHOU, P. & LIU, S. J. 2002. Degradation of aniline by newly isolated, extremely aniline-tolerant Delftia sp AN3. *Applied Microbiology and Biotechnology,* 58**,** 679-682.

LOHRI, C. R., DIENER, S., ZABALETA, I., MERTENAT, A. & ZURBRÜGG, C. 2017. Treatment technologies for urban solid biowaste to create value products: a review with focus on low- and middle-income settings. *Reviews in Environmental Science and Bio/Technology,* 16**,** 81-130.

LOPEZ-GALLEGO, F., BETANCOR, L., HIDALGO, A., ALONSO, N., FERNANDEZ-LAFUENTE, R. & GUISAN, J. M. 2005. Co-aggregation of enzymes and polyethyleneimine: A simple method to prepare stable and immobilized derivatives of glutaryl acylase. *Biomacromolecules,* 6**,** 1839-1842.

LOPEZ-SERRANO, P., CAO, L., VAN RANTWIJK, F. & SHELDON, R. A. 2002. Cross-linked enzyme aggregates with enhanced activity: application to lipases. *Biotechnology Letters,* 24**,** 1379-1383.

LOUPASAKI, E. & DIAMADOPOULOS, E. 2013. Attached growth systems for wastewater treatment in small and rural communities: a review. *Journal of Chemical Technology and Biotechnology,* 88**,** 190-204.

LOUSTAU, E., ROLS, J. L., LEFLAIVE, J., MARCATO-ROMAIN, C. E. & GIRBAL-NEUHAUSER, E. 2018. Comparison of extraction methods for the characterization of extracellular polymeric substances from aggregates of three biofilm-forming phototrophic microorganisms. *Canadian Journal of Microbiology,* 64**,** 887-899.

LOVRIEN, R. E. & MATULIS, D. 1997. Selective Precipitation of Proteins. *Current Protocols in Protein Science,* 7**,** 4.5.1-4.5.36.

LOWRY, O. H., ROSEBROUGH, N. J., FARR, A. L. & RANDALL, R. J. 1951. Protein measurement with the Folin phenol reagent. *The Journal of Biological Chemistry,* 193**,** 265-275.

LU, Q., CHANG, M., YU, Z. & ZHOU, S. G. 2015. The effects of three commonly used extraction methods on the redox properties of extracellular polymeric substances from activated sludge. *Environmental Technology,* 36**,** 2884-2891.

LV, J. P., ZHAO, F., FENG, J., LIU, Q., NAN, F. R. & XIE, S. L. 2019. Extraction of extracellular polymeric substances (EPS) from a newly isolated self-flocculating microalga Neocystis mucosa SX with different methods. *Algal Research-Biomass Biofuels and Bioproducts,* 40.

MA, S., WANG, C., LI, L. & WANG, X. 2020. Effects of particle size on the quality attributes of wheat flour made by the milling process. *Cereal Chemistry,* 97**,** 172-182.

MA, Z., BOYE, J. I., SIMPSON, B. K., PRASHER, S. O., MONPETIT, D. & MALCOLMSON, L. 2011. Thermal processing effects on the functional properties and microstructure of lentil, chickpea, and pea flours. *Food Research International,* 44**,** 2534-2544.

MACGREGOR, A. W., BAZIN, S. L. & IZYDORCZYK, M. S. 2002. Gelatinisation characteristics and enzyme susceptibility of different types of barley starch in the temperature range 48-72 degrees C. *Journal of the Institute of Brewing,* 108**,** 43-47.

MACKUL'AK, T., BODIK, I., SMOLINSKA, M., TAKACOVA, A., DRTIL, M., GAL, M. & FABEROVA, M. 2016. Automotive industry wastewater treatment by mixture of enzymes. *Monatshefte Fur Chemie,* 147**,** 159-164.

MAFRA, A. C. O., BELTRAME, M. B., ULRICH, L. G., GIORDANO, R. D. L. C., RIBEIRO, M. P. D. A. & TARDIOLI, P. W. 2018. Combined CLEAs of invertase and soy protein for economically feasible conversion of sucrose in a fed-batch reactor. *Food and Bioproducts Processing,* 110**,** 145-157.

MAHMOD, S. S., YUSOF, F., JAMI, M. S., KHANAHMADI, S. & SHAH, H. 2015. Development of an immobilized biocatalyst with lipase and protease activities as a multipurpose cross-linked enzyme aggregate (multi-CLEA). *Process Biochemistry,* 50**,** 2144-2157.

MAJUMDAR, S., KUMAR, P. S. & PANDIT, A. B. 1998. Effect of liquid-phase properties on ultrasound intensity and cavitational activity. *Ultrasonics Sonochemistry,* 5**,** 113-118.

MALAKI, M., MALEKI, A. & VARMA, R. S. 2019. MXenes and ultrasonication. *Journal of Materials Chemistry A,* 7**,** 10843-10857.

MALLICK, P., AKUNNA, J. C. & WALKER, G. M. 2010. Anaerobic digestion of distillery spent wash: Influence of enzymatic pre-treatment of intact yeast cells. *Bioresource Technology,* 101**,** 1681-1685.

MAÑAS, P., MUÑOZ, B., SANZ, D. & CONDÓN, S. 2006. Inactivation of lysozyme by ultrasonic waves under pressure at different temperatures. *Enzyme and Microbial Technology,* 39**,** 1177-1182.

MANELIUS, R., QIN, Z., ÅVALL, A.-K., ANDTFOLK, H. & BERTOFT, E. 1997. The mode of action on Granular Wheat Starch by Bacterial α-Amylase. *Starch - Stärke,* 49**,** 142-147.

MARIN, M., ARTOLA, A. & SANCHEZ, A. 2018. Production of proteases from organic wastes by solid-state fermentation: downstream and zero waste strategies. *3 Biotech,* 8**,** 205-220.

MARTIN, C. & VANROLLEGHEM, P. A. 2014. Analysing, completing, and generating influent data for WWTP modelling: A critical review. *Environmental Modelling & Software,* 60**,** 188-201.

MARTIN, M. A., GONZALEZ, I., SERRANO, A. & SILES, J. A. 2015. Evaluation of the improvement of sonication pre-treatment in the anaerobic digestion of sewage sludge. *Journal of Environmental Management,* 147**,** 330-337.

MARTYSIAK-ŻUROWSKA, D., ROŻEK, P. & PUTA, M. 2020. The effect of freeze-drying and storage on lysozyme activity, lactoferrin content, superoxide dismutase activity, total antioxidant capacity and fatty acid profile of freeze-dried human milk. *Drying Technology***,** 1-11.

MATEO, C., ABIAN, O., ERNEDO, M. B., CUENCA, E., FUENTES, M., FERNANDEZ-LORENTE, G., PALOMO, J. M., GRAZU, V., PESSELA, B. C. C., GIACOMINI, C., IRAZOQUI, G., VILLARINO, A., OVSEJEVI, K., BATISTA-VIERA, F., FERNANDEZ-LAFUENTE, R. & GUISAN, J. M. 2005. Some special features of glyoxyl supports to immobilize proteins. *Enzyme and Microbial Technology,* 37**,** 456-462.

MATEO, C., PALOMO, J. M., VAN LANGEN, L. M., VAN RANTWIJK, F. & SHELDON, R. A. 2004. A new, mild cross-linking methodology to prepare cross-linked enzyme aggregates. *Biotechnology and Bioengineering,* 86**,** 273-276.

MATIJOŠYTĖ, I., ARENDS, I. W. C. E., DE VRIES, S. & SHELDON, R. A. 2010. Preparation and use of cross-linked enzyme aggregates (CLEAs) of laccases. *Journal of Molecular Catalysis B: Enzymatic,* 62**,** 142-148.

MAWSON, R., GAMAGE, M., TEREFE, N. S. & KNOERZER, K. 2011. Ultrasound in Enzyme Activation and Inactivation. *In:* FENG, H., BARBOSA-CANOVAS, G. & WEISS, J. (eds.) *Ultrasound Technologies for Food and Bioprocessing.* New York, NY: Springer New York.

MCDERMOTT, E. E. & PACE, J. 1957. The content of amino-acids in white flour and bread. *British Journal of Nutrition,* 11**,** 446-452.

MEHDE, A. A., MEHDI, W. A., OZACAR, M. & OZACAR, Z. Z. 2018a. Evaluation of different saccharides and chitin as eco-friendly additive to improve the magnetic cross-linked enzyme aggregates (CLEAs) activities. *International Journal of Biological Macromolecules,* 118**,** 2040-2050.

MEHDE, A. A., MEHDI, W. A., SEVERGUN, O., CAKAR, S. & OZACAR, M. 2018b. Lipase-based on starch material as a development matrix with magnetite cross-linked enzyme

aggregates and its application. *International Journal of Biological Macromolecules,* 120**,** 1533-1543.

MELENDRES, A. V., HONDA, H., SHIRAGAMI, N. & UNNO, H. 1991. A kinetic analysis of cell disruption by bead mill. The influence of bead loading, bead size and agitator speed. *Bioseparation,* 2**,** 231-236.

MERAZ, M., ALVAREZ-RAMIREZ, J., VERNON-CARTER, E. J., REYES, I., HERNANDEZ-JAIMES, C. & MARTINEZ-MARTINEZ, F. 2020. A Two Competing Substrates Michaelis–Menten Kinetics Scheme for the Analysis of In Vitro Starch Digestograms. *Starch - Stärke,* 72**,** 1900170.

MERRYLIN, J., KALIAPPAN, S., KUMAR, S. A., YEOM, I. T. & RAJESH, B. J. 2013. Effect of extracellular polymeric substances on sludge reduction potential of Bacillus licheniformis. *International Journal of Environmental Science and Technology,* 10**,** 85-92.

MIDDELBERG, A. P. 1995. Process-scale disruption of microorganisms. *Biotechnology Advances,* 13**,** 491-551.

MIGNEAULT, I., DARTIGUENAVE, C., BERTRAND, M. J. & WALDRON, K. C. 2004. Glutaraldehyde: behavior in aqueous solution, reaction with proteins, and application to enzyme crosslinking. *Biotechniques,* 37**,** 790-+.

MILLER, G. L. 1959. Use of Dinitrosalicylic Acid Reagent for Determination of Reducing Sugar. *Analytical chemistry,* 31**,** 426-428.

MIRZAEI TESHNIZI, Z., ROBATJAZI, S. M. & MOHAMMADIAN MOSAABADI, J. 2020. Optimization of the Enzymatic Hydrolysis of Poultry Slaughterhouse Wastes using Alcalase Enzyme for the Preparation of Protein Hydrolysates. *Applied Food Biotechnology,* 7**,** 153-160.

MISHRA, S., SINGH, P. K., DASH, S. & PATTNAIK, R. 2018. Microbial pretreatment of lignocellulosic biomass for enhanced biomethanation and waste management. *3 Biotech,* 8**,** 458.

MITTAL, R., TAVANANDI, H. A., MANTRI, V. A. & RAGHAVARAO, K. S. M. S. 2017. Ultrasound assisted methods for enhanced extraction of phycobiliproteins from marine macro-algae, Gelidium pusillum (Rhodophyta). *Ultrasonics Sonochemistry,* 38**,** 92-103.

MLAIK, N., KHOUFI, S., HAMZA, M., MASMOUDI, M. A. & SAYADI, S. 2019. Enzymatic pre-hydrolysis of organic fraction of municipal solid waste to enhance anaerobic digestion. *Biomass and Bioenergy,* 127**,** 105286.

MOAYED, H. K., PANAHI, M., GHAZIZADE, M. J., ABEDI, Z. & GHAFFARZADEH, H. 2020. Removal of PAH compounds from refinery industrial sludge as hazardous environmental contaminants through anaerobic digestion. *International Journal of Environmental Science and Technology***,** 10.

MOBARAK-QAMSARI, E., KASRA-KERMANSHAHI, R., NOSRATI, M. & AMANI, T. 2012. Enzymatic pre-hydrolysis of high fat content dairy wastewater as a pretreatment for anaerobic digestion. *International Journal of Environmental Research,* 6**,** 475-480.

MOHAMED, A. A. & RAYAS-DUARTE, P. 2003. The effect of mixing and wheat protein/gluten on the gelatinization of wheat starch. *Food Chemistry,* 81**,** 533-545.

MOHAMMADIPANAH, F., PARVIZI, L., HAMEDI, J. & AZIZMOHSENI, F. 2017. Protective Effects of Cryoprotectants and Lyoprotectants on the Survival of Persipeptide Producing Streptomyces zagrosensis UTMC 1154. *Biopreserv Biobank,* 15**,** 451-456.

MOLOBELA, I. P., CLOETE, T. E. & BEUKES, M. 2010. Protease and amylase enzymes for biofilm removal and degradation of extracellular polymeric substances (EPS) produced by Pseudomonas fluorescens bacteria. *African Journal of Microbiology Research,* 4**,** 1515-1524.

MONIQUE, R., ELISABETH, G. N., ETIENNE, P. & DOMINIQUE, L. 2008. A high yield multi-method extraction protocol for protein quantification in activated sludge. *Bioresource Technology,* 99**,** 7464-7471.

MONTALESCOT, V., RINALDI, T., TOUCHARD, R., JUBEAU, S., FRAPPART, M., JAOUEN, P., BOURSEAU, P. & MARCHAL, L. 2015. Optimization of bead milling parameters for the cell disruption of microalgae: Process modeling and application to Porphyridium cruentum and Nannochloropsis oculata. *Bioresource Technology,* 196**,** 339-346.

MONTOYA-MEJÍA, M., HERNÁNDEZ-LLAMAS, A., GARCÍA-ULLOA, M., NOLASCO-SORIA, H., GUTIERREZ-DORADO, R. & RODRÍGUEZ-GONZÁLEZ, H. 2016. Apparent digestibility coefficient of chickpea, maize, high-quality protein maize, and beans diets in juvenile and adult Nile tilapia (Oreochromis niloticus). *Revista Brasileira de Zootecnia,* 45**,** 427-432.

MORRIS, C. W. 2019. *Protein Precipitation for the Purification of Therapeutic Proteins.* Thesis for Doctor of Engineering, The Department of Biochemical Engineering, UCL.

MOTULSKY, H. J. 2016. *Confidence intervals of parameters* [Online]. Available: https://www.graphpad.com/guides/prism/7/curve-fitting/reg_analysischeck_nonlin_completed.htm [Accessed 5 March 2016].

MUDHOO, A. & KUMAR, S. 2013. Effects of heavy metals as stress factors on anaerobic digestion processes and biogas production from biomass. *International Journal of Environmental Science and Technology,* 10**,** 1383-1398.

MULLER-STOVER, D., THOMPSON, R., LU, C. Y., THOMSEN, T. P., GLAESNER, N. & BRUUN, S. 2021. Increasing plant phosphorus availability in thermally treated sewage sludge by post-process oxidation and particle size management. *Waste Management,* 120**,** 716-724.

NABARLATZ, D., STUBER, F., FONT, J., FORTUNY, A., FABREGAT, A. & BENGOA, C. 2012. Extraction and purification of hydrolytic enzymes from activated sludge. *Resources Conservation and Recycling,* 59**,** 9-13.

NABARLATZ, D., VONDRYSOVA, J., JENICEK, P., STUBER, F., FONT, J., FORTUNY, A., FABREGAT, A. & BENGOA, C. 2010. Hydrolytic enzymes in activated sludge: extraction of protease and lipase by stirring and ultrasonication. *Ultrasonics Sonochemistry,* 17**,** 923-931.

NADAR, S. S., MULEY, A. B., LADOLE, M. R. & JOSHI, P. U. 2016. Macromolecular cross-linked enzyme aggregates (M-CLEAs) of α-amylase. *International Journal of Biological Macromolecules,* 84**,** 69-78.

NADAR, S. S. & RATHOD, V. K. 2016. Magnetic macromolecular cross linked enzyme aggregates (CLEAs) of glucoamylase. *Enzyme and Microbial Technology,* 83**,** 78-87.

NADAR, S. S. & RATHOD, V. K. 2017. Ultrasound assisted intensification of enzyme activity and its properties: a mini-review. *World Journal of Microbiology & Biotechnology,* 33.

NADEEM, F., MEHMOOD, T., NAVEED, M., SHAMAS, S., SAMAN, T. & ANWAR, Z. 2019. Protease production from Cheotomium globusum through central composite design using agricultural wastes and its immobilization for industrial exploitation. *Waste and Biomass Valorization*.

NASCENTES, C. C., KORN, M., SOUSA, C. S. & ARRUDA, M. A. Z. 2001. Use of ultrasonic baths for analytical applications: A new approach for optimisation conditions. *Journal of the Brazilian Chemical Society,* 12**,** 57-63.

NEPPIRAS, E. A. 1984. Acoustic cavitation series: part one: Acoustic cavitation: an introduction. *Ultrasonics,* 22**,** 25-28.

NGUYEN, T. T., ASAKURA, Y., KODA, S. & YASUDA, K. 2017. Dependence of cavitation, chemical effect, and mechanical effect thresholds on ultrasonic frequency. *Ultrasonics Sonochemistry,* 39**,** 301-306.

NI, H., FAN, X. M., GUO, H. N., LIANG, J. H., LI, Q. R., YANG, L., LI, H. & LI, H. H. 2017. Comprehensive utilization of activated sludge for the preparation of hydrolytic enzymes, polyhydroxyalkanoates, and water-retaining organic fertilizer. *Preparative Biochemistry & Biotechnology,* 47**,** 611-618.

NIE, L. J., ZHANG, H., WU, Z. K., WANG, Y. B., LIU, H., WU, X. L. & WANG, W. 2018. Modified TCA/acetone precipitation of plant proteins for proteomic analysis. *Plos One,* 13.

NIYONZIMA, F. N. 2019. Detergent-compatible bacterial cellulases. *Journal of Basic Microbiology,* 59**,** 134-147.

NYBROE, O., JORGENSEN, P. E. & HENZE, M. 1992. Enzyme activities in waste water and activated sludge. *Water Research,* 26**,** 579-584.

O'SULLIVAN, L. A., ROUSSEL, E. G., WEIGHTMAN, A. J., WEBSTER, G., HUBERT, C. R. J., BELL, E., HEAD, I., SASS, H. & PARKES, R. J. 2015. Survival of Desulfotomaculum spores from estuarine sediments after serial autoclaving and high-temperature exposure. *The ISME journal,* 9**,** 922-933.

OGSTON, A. G. 1962. Molecular Weights of Enzymes. *Nature,* 196**,** 171-172.

OJHA, B. K., SINGH, P. K. & SHRIVASTAVA, N. 2019. Enzymes in the animal feed industry. *In:* KUDDUS, M. (ed.) *Enzymes in Food Biotechnology: Production, Applications, and Future Prospects.* Cambridge, US: Academic Press.

OKUDA, K., URABE, I., YAMADA, Y. & OKADA, H. 1991. Reaction of Glutaraldehyde with Amino and Thiol Compounds. *Journal of Fermentation and Bioengineering,* 71**,** 100-105.

ONYECHE, T. I., SCHLÄFER, O., BORMANN, H., SCHRÖDER, C. & SIEVERS, M. 2002. Ultrasonic cell disruption of stabilised sludge with subsequent anaerobic digestion. *Ultrasonics,* 40**,** 31-35.

ORREGO, A. H., GHOBADI, R., MORENO-PEREZ, S., MENDOZA, A. J., FERNANDEZ-LORENTE, G., GUISAN, J. M. & ROCHA-MARTIN, J. 2018. Stabilization of Immobilized Lipases by Intense Intramolecular Cross-Linking of Their Surfaces by Using Aldehyde-Dextran Polymers. *Int J Mol Sci,* 19.

OSZUST, K., PAWLIK, A., JANUSZ, G., ZIEMINSKI, K., CYRAN, M., SICZEK, A., GRYTA, A., BILINSKA-WIELGUS, N. & FRAC, M. 2017. Characterization and Influence of a Multi-enzymatic Biopreparation for Biogas Yield Enhancement. *Bioresources,* 12**,** 6187-6206.

OZACAR, M., MEHDE, A. A., MEHDI, W. A., OZACAR, Z. Z. & SEVERGUN, O. 2019. The novel multi cross-linked enzyme aggregates of protease, lipase, and catalase production from the sunflower seeds, characterization and application. *Colloids and Surfaces B-Biointerfaces,* 173**,** 58-68.

PAN, Y.-R., WANG, X., REN, Z. J., HU, C., LIU, J. & BUTLER, D. 2019. Characterization of implementation limits and identification of optimization strategies for sustainable water resource recovery through life cycle impact analysis. *Environment International,* 133.

PARAWIRA, W. 2012. Enzyme research and applications in biotechnological intensification of biogas production. *Critical Reviews in Biotechnology,* 32**,** 172-186.

PARIDA, U. K., NAYAK, A. K., BINHANI, B. K. & NAYAK, P. L. 2011. Synthesis and Characterization of Chitosan-Polyvinyl Alcohol Blended with Cloisite 30B for Controlled Release of the Anticancer Drug Curcumin. *Journal of Biomaterials and Nanobiotechnology,* Vol.02No.04**,** 12.

PARK, C., NOVAK, J. T., HELM, R. F., AHN, Y. O. & ESEN, A. 2008. Evaluation of the extracellular proteins in full-scale activated sludges. *Water Research,* 42**,** 3879-3889.

PELMENSCHIKOV, V., BLOMBERG, M. R. & SIEGBAHN, P. E. 2002. A theoretical study of the mechanism for peptide hydrolysis by thermolysin. *JBIC Journal of Biological Inorganic Chemistry,* 7**,** 284-298.

PENCREACH, G. & BARATTI, J. C. 1996. Hydrolysis of p-nitrophenyl palmitate in n-heptane by the Pseudomonas cepacia lipase: A simple test for the determination of lipase activity in organic media. *Enzyme and Microbial Technology,* 18**,** 417-422.

PEREIRA, T., BARROSO, S., MENDES, S., AMARAL, R. A., DIAS, J. R., BAPTISTA, T., SARAIVA, J. A., ALVES, N. M. & GIL, M. M. 2020. Optimization of phycobiliprotein pigments extraction from red algae Gracilaria gracilis for substitution of synthetic food colorants. *Food Chemistry,* 321**,** 126688.

PERIYASAMY, K., SANTHALEMBI, L., MORTHA, G., AUROUSSEAU, M. & SUBRAMANIAN, S. 2016. Carrier-free co-immobilization of xylanase, cellulase and β-1,3-glucanase as combined cross-linked enzyme aggregates (combi-CLEAs) for one-pot saccharification of sugarcane bagasse. *RSC Advances,* 6**,** 32849-32857.

PERZON, A., DICKO, C., COBANOGLU, O., YUKSELEN, O., ERYILMAZ, J. & DEY, E. S. 2017. Cellulase cross-linked enzyme aggregates (CLEA) activities can be modulated and enhanced by precipitant selection. *Journal of Chemical Technology and Biotechnology,* 92**,** 1645-1649.

PETERS, K. & RICHARDS, F. M. 1977. Chemical cross-linking: reagents and problems in studies of membrane structure. *Annu Rev Biochem,* 46**,** 523-51.

PETERSEN, B., GERNAEY, K., HENZE, M. & VANROLLEGHEM, P. 2003. Calibration of activated sludge models: A critical review of experimental designs. *In: Biotechnology for the Environment: Wastewater Treatment and Modelling. Waste Gas Handling***,** 102-186.

PILLI, S., BHUNIA, P., YAN, S., LEBLANC, R. J., TYAGI, R. D. & SURAMPALLI, R. Y. 2011. Ultrasonic pretreatment of sludge: A review. *Ultrasonics Sonochemistry,* 18**,** 1-18.

PLEISS, J. 2018. Thermodynamic Activity-Based Progress Curve Analysis in Enzyme Kinetics. *Trends in Biotechnology,* 36**,** 234-238.

POSTMA, P. R., MIRON, T. L., OLIVIERI, G., BARBOSA, M. J., WIJFFELS, R. H. & EPPINK, M. H. M. 2015. Mild disintegration of the green microalgae Chlorella vulgaris using bead milling. *Bioresource Technology,* 184**,** 297-304.

POTTY, V. H. 1969. Determination of proteins in the presence of phenols and pectins. *Analytical Biochemistry,* 29**,** 535-539.

PRICE, N. & STEVENS, L. 1999. *Fundamentals of Enzymology,* Oxford, Oxford University Press.

QIN, Y., FU, Y., LI, Q., LUO, F. & HE, H. 2020. Purification and Enzymatic Properties of a Difunctional Glycoside Hydrolase from Aspergillus oryzae HML366. *Indian Journal of Microbiology*, 10.

QUIOCHO, F. A. & RICHARDS, F. M. 1964. Intermolecular Cross Linking of A Protein In The Crystalline State: Carboxypeptidase-A. *Proceedings of the National Academy of Sciences of the United States of America,* 52, 833-9.

RACHMAWATI, L. & ANGGRIYANI, E. 2018. The Use of Glutaraldehyde Tanning Materials for Goat Skin Tanning. *2018,* 42.

RAI, C. L., MUELLER, J., STRUENKMANN, G. & RAO, P. G. 2008. Microbial growth reduction in sewage sludge by stirred ball mill disintegration and estimation by respirometry. *Journal of Chemical Technology and Biotechnology,* 83, 269-278.

RAMOS, O. S. & MALCATA, F. X. 2011. Food-Grade Enzymes. *In:* MOO-YOUNG, M. (ed.) *Comprehensive Biotechnology* Second ed. Burlington: Academic Press.

RANHOTRA, G. S., GELROTH, J. A., GLASER, B. K. & LORENZ, K. J. 1995. Baking and nutritional qualities of a spelt wheat sample. *LWT - Food Science and Technology,* 28, 118-122.

RAO, M. B., TANKSALE, A. M., GHATGE, M. S. & DESHPANDE, V. V. 1998. Molecular and biotechnological aspects of microbial proteases. *Microbiology and molecular biology reviews : MMBR,* 62, 597-635.

RASHID, S. S. & LIU, Y.-Q. 2020. Assessing environmental impacts of large centralized wastewater treatment plants with combined or separate sewer systems in dry/wet seasons by using LCA. *Environmental science and pollution research international,* 27, 15674-15690.

RASMUSSEN, K. E. & ALBRECHTSEN, J. 1974. Glutaraldehyde. The influence of pH, temperature, and buffering on the polymerization rate. *Histochemistry,* 38, 19-26.

RAWEL, H. M., MEIDTNER, K. & KROLL, J. 2005. Binding of Selected Phenolic Compounds to Proteins. *Journal of Agricultural and Food Chemistry,* 53, 4228-4235.

REHMAN, S., BHATTI, H. N., BILAL, M. & ASGHER, M. 2016. Cross-linked enzyme aggregates (CLEAs) of Pencilluim notatum lipase enzyme with improved activity, stability and reusability characteristics. *International Journal of Biological Macromolecules,* 91, 1161-1169.

REJ, R. & RICHARDS, A. H. 1974. Interference by Tris buffer in the estimation of protein by the Lowry procedure. *Analytical Biochemistry,* 62, 240-247.

REZA, R., MARTÍNEZ PÉREZ, C., RODRÍGUEZ GONZÁLEZ, C., ROMERO, H. & GARCÍA CASILLAS, P. 2010. Effect of the polymeric coating over Fe3O4 particles used for magnetic separation. *Open Chemistry.*

RICHARD, M. T. 2003. Activated sludge microbiology problems and their control. *20th Annual USEPA National Operator Trainers Conference.* Buffalo, New York.

RIGBY, H., CLARKE, B. O., PRITCHARD, D. L., MEEHAN, B., BESHAH, F., SMITH, S. R. & PORTER, N. A. 2016. A critical review of nitrogen mineralization in biosolids-amended soil, the associated fertilizer value for crop production and potential for emissions to the environment. *Science of The Total Environment,* 541**,** 1310-1338.

ROBINSON, P. K. 2015. Enzymes: principles and biotechnological applications. *Essays in Biochemistry,* 59**,** 1-41.

ROBLEDO-MAHON, T., MARTIN, M. A., GUTIERREZ, M. C., TOLEDO, M., GONZALEZ, I., ARANDA, E., CHICA, A. F. & CALVO, C. 2019. Sewage sludge composting under semi-permeable film at full-scale: Evaluation of odour emissions and relationships between microbiological activities and physico-chemical variables. *Environmental Research,* 177.

ROY, I. & GUPTA, M. N. 2004. Freeze-drying of proteins: some emerging concerns. *Biotechnology and Applied Biochemistry,* 39**,** 165-177.

ROY, U. K., NIELSEN, B. V. & MILLEDGE, J. J. 2020. Effect of post-harvest conditions on antioxidant enzyme activity in Dunaliella tertiolecta biomass. *Biocatalysis and Agricultural Biotechnology,* 27.

RUBIN, D. M., ANDERTON, N., SMALBERGER, C., POLLIACK, J., NATHAN, M. & POSTEMA, M. 2018. On the behaviour of living cells under the influence of ultrasound. *Fluids,* 3.

RUIJGROK, J. M., BOON, M. E. & DE WIJN, J. R. 1990. The effect of heating by microwave irradiation and by conventional heating on the aldehyde concentration in aqueous glutaraldehyde solutions. *The Histochemical Journal,* 22**,** 389-393.

RUIZ-PEREZ, F. & NATARO, J. P. 2014. Bacterial serine proteases secreted by the autotransporter pathway: classification, specificity, and role in virulence. *Cellular and Molecular Life Sciences,* 71**,** 745-770.

RUPLEY, J. A., GRATTON, E. & CARERI, G. 1983. Water and globular proteins. *Trends in Biochemical Sciences,* 8**,** 18-22.

RYAN, K. J. & BREWER, M. S. 2007. In situ examination of starch granule-soy protein and wheat protein interactions. *Food Chemistry,* 104**,** 619-629.

SAFI, C., CABAS RODRIGUEZ, L., MULDER, W. J., ENGELEN-SMIT, N., SPEKKING, W., VAN DEN BROEK, L. A. M., OLIVIERI, G. & SIJTSMA, L. 2017. Energy consumption and water-soluble protein release by cell wall disruption of Nannochloropsis gaditana. *Bioresource Technology,* 239**,** 204-210.

SAHUTOGLU, A. S. & AKGUL, C. 2015. Immobilisation of Aspergillus oryzae alpha-amylase and Aspergillus niger glucoamylase enzymes as cross-linked enzyme aggregates. *Chemical Papers,* 69**,** 433-439.

SAKINTUNA, B., BUDAK, O., DIK, T., YONDEM-MAKASCIOGLU, F. & KINCAL, N. S. 2003. Hydrolysis of freshly prepared wheat starch fractions and commercial wheat starch using alpha-amylase. *Chemical Engineering Communications,* 190**,** 883-897.

SALEM, M., MAUGUEN, Y. & PRANGE, T. 2010. Revisiting glutaraldehyde cross-linking: the case of the Arg-Lys intermolecular doublet. *Acta Crystallographica Section F-Structural Biology and Crystallization Communications,* 66**,** 225-228.

SALSABIL, M. R., PROROT, A., CASELLAS, M. & DAGOT, C. 2009a. Pre-treatment of activated sludge: Effect of sonication on aerobic and anaerobic digestibility. *Chemical Engineering Journal,* 148**,** 327-335.

SALSABIL, M. R., PROROT, A., CASELLAS, M. & DAGOT, C. 2009b. Pre-treatment of activated sludge: Effect of sonication on aerobic and anaerobic digestibility. *Chemical Engineering Journal,* 148**,** 327-335.

SANDHYA, M., RAMASAMY, D., SUDHAKAR, K., KADIRGAMA, K. & HARUN, W. S. W. 2021. Ultrasonication an intensifying tool for preparation of stable nanofluids and study the time influence on distinct properties of graphene nanofluids - A systematic overview. *Ultrasonics sonochemistry,* 73**,** 105479-105479.

SANGEETHA, K. & EMILIA ABRAHAM, T. 2008. Preparation and characterization of cross-linked enzyme aggregates (CLEA) of Subtilisin for controlled release applications. *International Journal of Biological Macromolecules,* 43**,** 314-319.

SCHÄGGER, H. 2003. 2 - Techniques and Basic Operations in Membrane Protein Purification. *In:* HUNTE, C., VON JAGOW, G. & SCHÄGGER, H. (eds.) *Membrane Protein Purification and Crystallization (Second Edition).* San Diego: Academic Press.

SCHOEVAART, R. & KIEBOOM, T. 2001. Galactose dialdehyde: the forgotten candidate for a protein cross-linker? *Carbohydrate Research,* 334**,** 1-6.

SCHOEVAART, R., SIEBUM, A., VAN RANTWIJK, F., SHELDON, R. & KIEBOOM, T. 2005. Glutaraldehyde cross-link analogues from carbohydrates. *Starch-Starke,* 57**,** 161-165.

SCHOEVAART, R., WOLBERS, M. W., GOLUBOVIC, M., OTTENS, M., KIEBOOM, A. P. G., VAN RANTWIJK, F., VAN DER WIELEN, L. A. M. & SHELDON, R. A. 2004. Preparation, optimization, and structures of cross-linked enzyme aggregates (CLEAs). *Biotechnology and Bioengineering,* 87**,** 754-762.

SCHOLZ, R. W., ULRICH, A. E., EILITTÄ, M. & ROY, A. 2013. Sustainable use of phosphorus: A finite resource. *Science of The Total Environment,* 461-462**,** 799-803.

SELVAKUMAR, P. & SIVASHANMUGAM, P. 2019. Ultrasound assisted oleaginous yeast lipid extraction and garbage lipase catalyzed transesterification for enhanced biodiesel production. *Energy Conversion and Management,* 179**,** 141-151.

SETHUPATHY, A. & SIVASHANMUGAM, P. 2019. Investigation on ultrasonication mediated biosurfactant disintegration method in sludge flocs for enhancing hydrolytic enzymes activity and polyhydroxyalkanoates. *Environmental Technology,* 40**,** 3547-3560.

SHADDEL, S., BAKHTIARY-DAVIJANY, H., KABBE, C., DADGAR, F. & OSTERHUS, S. W. 2019. Sustainable Sewage Sludge Management: From Current Practices to Emerging Nutrient Recovery Technologies. *Sustainability,* 11.

SHAFEE, T. 2015. Organisation of enzyme structure and lysozyme example. Binding sites in blue, catalytic site in red and peptidoglycan substrate in black. (PDB: 9LYZ). Self-published work.

SHAH, S., SHARMA, A. & GUPTA, M. N. 2006. Preparation of cross-linked enzyme aggregates by using bovine serum albumin as a proteic feeder. *Analytical Biochemistry,* 351**,** 207-213.

SHARMA, R., CHISTI, Y. & BANERJEE, U. C. 2001. Production, purification, characterization, and applications of lipases. *Biotechnology Advances,* 19**,** 627-662.

SHELDON, R. A. 2007. Enzyme immobilization: The quest for optimum performance. *Advanced Synthesis & Catalysis,* 349**,** 1289-1307.

SHELDON, R. A. 2011a. Characteristic features and biotechnological applications of cross-linked enzyme aggregates (CLEAs). *Applied Microbiology and Biotechnology,* 92**,** 467-477.

SHELDON, R. A. 2011b. Cross-Linked Enzyme Aggregates as Industrial Biocatalysts. *Organic Process Research & Development,* 15**,** 213-223.

SHELDON, R. A. & VAN PELT, S. 2013. Enzyme immobilisation in biocatalysis: Why, what and how. *Chemical Society Reviews,* 42**,** 6223-6235.

SHENG, G.-P., YU, H.-Q. & YU, Z. 2005. Extraction of extracellular polymeric substances from the photosynthetic bacterium Rhodopseudomonas acidophila. *Applied Microbiology and Biotechnology,* 67**,** 125-130.

SHOW, K. Y., MAO, T. & LEE, D. J. 2007. Optimisation of sludge disruption by sonication. *Water Research,* 41**,** 4741-4747.

SHUDDHODANA, GUPTA, M. N. & BISARIA, V. S. 2018. Effectiveness of cross-linked enzyme aggregates of cellulolytic enzymes in hydrolyzing wheat straw. *Journal of Bioscience and Bioengineering,* 126**,** 445-450.

SIDDIQI, R. A., SINGH, T. P., RANI, M., SOGI, D. S. & BHAT, M. A. 2020. Diversity in Grain, Flour, Amino Acid Composition, Protein Profiling, and Proportion of Total Flour Proteins of Different Wheat Cultivars of North India. *Frontiers in Nutrition,* 7.

SIDDIQUI, K. S., POLJAK, A., GUILHAUS, M., FELLER, G., D'AMICO, S., GERDAY, C. & CAVICCHIOLI, R. 2005. Role of disulfide bridges in the activity and stability of a cold-active alpha-amylase. *Journal of bacteriology,* 187**,** 6206-6212.

SIGMA-ALDRICH. 2020. *Infrared Spectrum Table & Chart* [Online]. Darmstadt, Germany: Merck KGaA. Available: https://www.sigmaaldrich.com/technical-documents/articles/biology/ir-spectrum-table.html#table-by-group [Accessed 2020].

SIM, S.-L., HE, T., TSCHELIESSNIG, A., MUELLER, M., TAN, R. B. H. & JUNGBAUER, A. 2012. Protein precipitation by polyethylene glycol: A generalized model based on hydrodynamic radius. *Journal of Biotechnology,* 157**,** 315-319.

SINHA, S. K., CHAKRABORTY, S. & BANDYOPADHYAY, S. 2008. Thickness of the hydration layer of a protein from molecular dynamics simulation. *Journal of Physical Chemistry B,* 112**,** 8203-8209.

SINIRLIOGLU, Z. A., SINIRLIOGLU, D. & AKBAS, F. 2013. Preparation and characterization of stable cross-linked enzyme aggregates of novel laccase enzyme from Shewanella putrefaciens and using malachite green decolorization. *Bioresource Technology,* 146**,** 807-811.

SMITH, S. R. 2014. How activated sludge has been transformed from a waste to a resource, and the implications of this for the future of the activated sludge process. *In:* HORAN, N. J. (ed.) *Activated Sludge: Past, Present and Future.* Manchester, UK: Aqua Enviro.

SOJITRA, U. V., NADAR, S. S. & RATHOD, V. K. 2017. Immobilization of pectinase onto chitosan magnetic nanoparticles by macromolecular cross-linker. *Carbohydrate Polymers,* 157**,** 677-685.

SOLEIMANI, M., KHANI, A. & NAJAFZADEH, K. 2012. alpha-Amylase immobilization on the silica nanoparticles for cleaning performance towards starch soils in laundry detergents. *Journal of Molecular Catalysis B-Enzymatic,* 74**,** 1-5.

SORARUF, D., ROOSEN-RUNGE, F., GRIMALDO, M., ZANINI, F., SCHWEINS, R., SEYDEL, T., ZHANG, F., ROTH, R., OETTEL, M. & SCHREIBER, F. 2014. Protein cluster formation in aqueous solution in the presence of multivalent metal ions – a light scattering study. *Soft Matter,* 10**,** 894-902.

SÓTI, V., LENAERTS, S. & CORNET, I. 2018. Of enzyme use in cost-effective high solid simultaneous saccharification and fermentation processes. *Journal of Biotechnology,* 270**,** 70-76.

SPONER, J. 1990. Dependence of the cavitation threshold on the ultrasonic frequency. *Czechoslovak Journal of Physics,* 40**,** 1123-1132.

SPONZA, D. T. 2002. Extracellular polymer substances and physicochemical properties of flocs in steady and unsteady-state activated sludge systems. *Process Biochemistry,* 37**,** 983-998.

SRERE, P. A. & UYEDA, K. 1976. [2] Functional groups on enzymes suitable for binding to matrices. *Methods in Enzymology.* Academic Press.

ST CLAIR, N. L. & NAVIA, M. A. 1992. Cross-Linked Enzyme Crystals as Robust Biocatalysts. *Journal of the American Chemical Society,* 114**,** 7314-7316.

STANK, A., KOKH, D. B., FULLER, J. C. & WADE, R. C. 2016. Protein Binding Pocket Dynamics. *Accounts of Chemical Research,* 49**,** 809-815.

STOECKEL, D. M., STELZER, E. A. & DICK, L. K. 2009. Evaluation of two spike-and-recovery controls for assessment of extraction efficiency in microbial source tracking studies. *Water Research,* 43**,** 4820-4827.

STRADNER, A., SEDGWICK, H., CARDINAUX, F., POON, W. C. K., EGELHAAF, S. U. & SCHURTENBERGER, P. 2004. Equilibrium cluster formation in concentrated protein solutions and colloids. *Nature,* 432**,** 492-495.

SUAREZ GARCIA, E., LO, C., EPPINK, M. H. M., WIJFFELS, R. H. & VAN DEN BERG, C. 2019. Understanding mild cell disintegration of microalgae in bead mills for the release of biomolecules. *Chemical Engineering Science,* 203**,** 380-390.

SUBHEDAR, P. B. & GOGATE, P. R. 2013. Intensification of enzymatic hydrolysis of lignocellulose using ultrasound for efficient bioethanol Production: A review. *Industrial & Engineering Chemistry Research,* 52**,** 11816-11828.

SUN, X., YU, C., FU, M., WU, D., GAO, C., FENG, X., CHENG, W., SHEN, X. & TANG, X. 2019. Extruded whole buckwheat noodles: effects of processing variables on the degree of starch gelatinization, changes of nutritional components, cooking characteristics and in vitro starch digestibility. *Food & Function,* 10**,** 6362-6373.

SVENDBY, K. H. 2019. *Effects of Fermented Primary Sludge Supernatant as Carbon Source in an Enhanced Biological Phosphorous Removal Process.* Master.

SZILVESZTER, S., RADULY, B., MIKLÓSSY, I., ÁBRAHÁM, B., SZABOLCS, L. & NICOLAE, D. 2009. Enzymatic activity studies of biological wastewater treatment. *Studia Universitatis Babeș-Bolyai. Chemia*.

TAKEUCHI, I. 1969. Interaction between protein and starch. *Cereal chemistry*.

TALEKAR, S., DESAI, S., PILLAI, M., NAGAVEKAR, N., AMBARKAR, S., SURNIS, S., LADOLE, M., NADAR, S. & MULLA, M. 2013. Carrier free co-immobilization of glucoamylase and pullulanase as combi-cross linked enzyme aggregates (combi-CLEAs). *Rsc Advances,* 3**,** 2265-2271.

TALEKAR, S., GHODAKE, V., GHOTAGE, T., RATHOD, P., DESHMUKH, P., NADAR, S., MULLA, M. & LADOLE, M. 2012. Novel magnetic cross-linked enzyme aggregates (magnetic CLEAs) of alpha amylase. *Bioresource Technology,* 123**,** 542-547.

TANDJAOUI, N., TASSIST, A., ABOUSEOUD, M., COUVERT, A. & AMRANE, A. 2015. Preparation and characterization of cross-linked enzyme aggregates (CLEAs) of Brassica rapa peroxidase. *Biocatalysis and Agricultural Biotechnology,* 4**,** 208-213.

TASSELLI, S., VALENTI, E. & GUZZELLA, L. 2021. Polycyclic musk fragrance (PMF) removal, adsorption and biodegradation in a conventional activated sludge wastewater treatment plant in Northern Italy. *Environmental Science and Pollution Research***,** 11.

TCHOBANOGLOUS, G., BURTON, F. L., STENSEL, H. D., METCALF & EDDY 2014. *Wastewater engineering : treatment and resource recovery,* New York, McGraw-Hill Higher Education.

TEIXEIRA, R. S. S., DA SILVA, A. S., FERREIRA-LEITAO, V. S. & BON, E. P. D. 2012. Amino acids interference on the quantification of reducing sugars by the 3,5-dinitrosalicylic acid assay mislead carbohydrase activity measurements. *Carbohydrate Research,* 363**,** 33-37.

TEO, C. W. & WONG, P. C. Y. 2014. Enzyme augmentation of an anaerobic membrane bioreactor treating sewage containing organic particulates. *Water Research,* 48**,** 335-344.

TEUBER, M. & BRODISCH, K. E. U. 1977. Enzymatic activities of activated sludge. *European journal of applied microbiology and biotechnology,* 4**,** 185-194.

THAN, J. 2020. *Hydrophobic Interactions* [Online]. California, US: LibreTexts. Available: https://chem.libretexts.org/@go/page/1506 [Accessed March 22, 2021 2021].

THEBTI, W., RIAHI, Y. & BELHADJ, O. 2016. Purification and characterization of a new thermostable, haloalkaline, solvent stable, and detergent compatible serine protease from Geobacillus toebii strain LBT 77. *Biomed Research International***,** 8.

TIAN, Y., LIU, Z., LI, X., ZHANG, L., LI, R., JIANG, R. & DONG, F. 2018. The cavitation erosion of ultrasonic sonotrode during large-scale metallic casting: Experiment and simulation. *Ultrasonics Sonochemistry,* 43**,** 29-37.

TIEHM, A., NICKEL, K., ZELLHORN, M. & NEIS, U. 2001. Ultrasonic waste activated sludge disintegration for improving anaerobic stabilization. *Water Research,* 35**,** 2003-2009.

TORABIZADEH, H., TAVAKOLI, M. & SAFARI, M. 2014. Immobilization of thermostable α-amylase from Bacillus licheniformis by cross-linked enzyme aggregates method using calcium and sodium ions as additives. *Journal of Molecular Catalysis B: Enzymatic,* 108**,** 13-20.

TRZCINSKI, A. P. 2018. *Advanced Biological, Physical, and Chemical Treatment of Waste Activated Sludge,* Boca Raton, CRC Press.

TYAGI, V. & LO, S. L. 2013. Sludge: A waste or renewable source for energy and resources recovery. *Renewable and Sustainable Energy Reviews,* 25**,** 708–728.

TYAGI, V. K., LO, S. L., APPELS, L. & DEWIL, R. 2014. Ultrasonic treatment of waste sludge: A review on mechanisms and applications. *Critical Reviews in Environmental Science and Technology,* 44**,** 1220-1288.

TYTŁA, M. 2019. Assessment of Heavy Metal Pollution and Potential Ecological Risk in Sewage Sludge from Municipal Wastewater Treatment Plant Located in the Most Industrialized Region in Poland-Case Study. *Int J Environ Res Public Health,* 16.

TYTLA, M. & ZIELEWICZ, E. 2016. The effect of ultrasonic disintegration process conditions on the physicochemical characteristics of excess sludge. *Archives of Environmental Protection,* 42**,** 19-26.

VALDES, E. C., SOTO, L. W. & ARCAYA, G. A. 2011. Influence of the pH of glutaraldehyde and the use of dextran aldehyde on the preparation of cross-linked enzyme aggregates (CLEAs) of lipase from Burkholderia cepacia. *Electronic Journal of Biotechnology,* 14.

VAN PELT, S., QUIGNARD, S., KUBÁČ, D., SOROKIN, D. Y., VAN RANTWIJK, F. & SHELDON, R. A. 2008. Nitrile hydratase CLEAs: The immobilization and stabilization of an industrially important enzyme. *Green Chemistry,* 10**,** 395-400.

VARDANEGA, R., SANTOS, D. T. & MEIRELES, M. A. A. 2014. Intensification of bioactive compounds extraction from medicinal plants using ultrasonic irradiation. *Pharmacognosy Reviews,* 8**,** 88-95.

VASCONCELOS, A., SILVA, C. J., SCHROEDER, M., GUEBITZ, G. M. & CAVACO-PAULO, A. 2006. Detergent formulations for wool domestic washings containing immobilized enzymes. *Biotechnol Lett,* 28**,** 725-31.

VELASCO-LOZANO, S., LOPEZ-GALLEGO, F., ROCHA-MARTIN, J., GUISAN, J. M. & FAVELA-TORRES, E. 2016. Improving enantioselectivity of lipase from Candida rugosa by carrier-bound and carrier-free immobilization. *Journal of Molecular Catalysis B-Enzymatic,* 130**,** 32-39.

VERLICCHI, P. & ZAMBELLO, E. 2015. Pharmaceuticals and personal care products in untreated and treated sewage sludge: Occurrence and environmental risk in the case of application on soil — A critical review. *Science of The Total Environment,* 538**,** 750-767.

VERSTRAETE, W. & VLAEMINCK, S. E. 2011. ZeroWasteWater: short-cycling of wastewater resources for sustainable cities of the future. *International Journal of Sustainable Development & World Ecology,* 18**,** 253-264.

VIDYA, C. H., KUMAR, B. S. G., CHINMAYEE, C. V. & SINGH, S. A. 2020. Purification, characterization and specificity of a new GH family 35 galactosidase from Aspergillus awamori. *International Journal of Biological Macromolecules,* 156**,** 885-895.

VON BUELOW, S., SIGGEL, M., LINKE, M. & HUMMER, G. 2019. Dynamic cluster formation determines viscosity and diffusion in dense protein solutions. *Proceedings of the National Academy of Sciences of the United States of America,* 116**,** 9843-9852.

VRIENS, L., NIHOUL, R. & VERACHTERT, H. 1989. Activated sludges as animal feed: A review. *Biological Wastes,* 27**,** 161-207.

VRŠANSKÁ, M., VOBĚRKOVÁ, S., JIMÉNEZ JIMÉNEZ, A. M., STRMISKA, V. & ADAM, V. 2017. Preparation and Optimisation of Cross-Linked Enzyme Aggregates Using Native Isolate White Rot Fungi Trametes versicolor and Fomes fomentarius for the Decolourisation of Synthetic Dyes. *Int J Environ Res Public Health,* 15.

WAHAB, R. A., ELIAS, N., ABDULLAH, F. & GHOSHAL, S. K. 2020. On the taught new tricks of enzymes immobilization: An all-inclusive overview. *Reactive and Functional Polymers,* 152**,** 104613.

WALT, D. R. & AGAYN, V. I. 1994. The chemistry of enzyme and protein immobilization with glutaraldehyde. *TrAC Trends in Analytical Chemistry,* 13**,** 425-430.

WANG, B. B., CHANG, Q., PENG, D. C., HOU, Y. P., LI, H. J. & PEI, L. Y. 2014. A new classification paradigm of extracellular polymeric substances (EPS) in activated sludge: Separation and characterization of exopolymers between floc level and microcolony level. *Water Research,* 64**,** 53-60.

WANG, M., QI, W., JIA, C., REN, Y., SU, R. & HE, Z. 2011. Enhancement of activity of cross-linked enzyme aggregates by a sugar-assisted precipitation strategy: Technical development and molecular mechanism. *Journal of Biotechnology,* 156**,** 30-38.

WANG, R., GODOY, L. C., SHAARANI, S. M., MELIKOGLU, M., KOUTINAS, A. & WEBB, C. 2009. Improving wheat flour hydrolysis by an enzyme mixture from solid state fungal fermentation. *Enzyme and Microbial Technology,* 44**,** 223-228.

WANG, Y., BU, C. N., KANG, Q., AHMAD, H. A., ZHANG, J., GAO, B. Y. & NI, S. Q. 2017. Autoclaved sludge as the ideal seed to culture anammox bacteria: Reactor performance and microbial community diversity. *Bioresource Technology,* 244**,** 391-399.

WANG, Y., HU, H., MA, J., YAN, Q., LIU, H. & JIANG, Z. 2020. A novel high maltose-forming α-amylase from Rhizomucor miehei and its application in the food industry. *Food Chemistry,* 305**,** 125447.

WATERBORG, J. H. 2009. The Lowry Method for Protein Quantitation. *In:* WALKER, J. M. (ed.) *The Protein Protocols Handbook.* Totowa, NJ: Humana Press.

WAWRZYNCZYK, J., SZEWCZYK, E., NORRLOW, O. & DEY, E. S. 2007. Application of enzymes, sodium tripolyphosphate and cation exchange resin for the release of extracellular polymeric substances from sewage sludge - Characterization of the

extracted polysaccharides/glycoconjugates by a panel of lectins. *Journal of Biotechnology,* 130**,** 274-281.

WEEMAES, M. P. J. & VERSTRAETE, W. H. 1998. Evaluation of current wet sludge disintegration techniques. *Journal of Chemical Technology & Biotechnology,* 73**,** 83-92.

WETT, B., PHOTHILANGKA, P. & ELADAWY, A. 2010. Systematic comparison of mechanical and thermal sludge disintegration technologies. *Waste Management,* 30**,** 1057-1062.

WILÉN, B. M., JIN, B. & LANT, P. 2003. Relationship between flocculation of activated sludge and composition of extracellular polymeric substances. *Water Sci Technol,* 47**,** 95-103.

WILSON, L., ILLANES, A., ABIAN, O., PESSELA, B. C. C., FERNANDEZ-LAFUENTE, R. & GUISAN, J. M. 2004. Co-aggregation of penicillin G acylase and polyionic polymers: An easy methodology to prepare enzyme biocatalysts stable in organic media. *Biomacromolecules,* 5**,** 852-857.

WINE, Y., COHEN-HADAR, N., FREEMAN, A. & FROLOW, F. 2007. Elucidation of the mechanism and end products of glutaraldehyde crosslinking reaction by X-ray structure analysis. *Biotechnology and Bioengineering,* 98**,** 711-718.

WINGENDER, J., NEU, T. R. & FLEMMING, H.-C. 1999. What are bacterial extracellular polymeric substances? *Microbial Extracellular Polymeric Substances.* Berlin: Springer.

WINGFIELD, P. 2001. Protein precipitation using ammonium sulfate. *Current protocols in protein science,* Appendix 3**,** Appendix-3F.

WINTERS, A. L. & MINCHIN, F. R. 2005. Modification of the Lowry assay to measure proteins and phenols in covalently bound complexes. *Analytical Biochemistry,* 346**,** 43-48.

WOLTER, A., HAGER, A.-S., ZANNINI, E. & ARENDT, E. K. 2013. In vitro starch digestibility and predicted glycaemic indexes of buckwheat, oat, quinoa, sorghum, teff and commercial gluten-free bread. *Journal of Cereal Science,* 58**,** 431-436.

WOODS, A. E. & STIRLING, J. W. 2019. Transmission electron microscopy. *In:* SUVARNA, S. K., LAYTON, C. & BANCROFT, J. D. (eds.) *Bancroft's Theory and Practice of Histological Techniques.* Eighth ed.: Content Repository Only!

WORTHINGTON, C. C., WORTHINGTON, V. & WORTHINGTON, A. 2019. *Introduction to Enzymes* [Online]. Lakewood, US: Worthington Biochemical Corporation. Available: http://www.worthington-biochem.com/introbiochem/effectspH.html [Accessed May, 2021].

WOYENGO, T., AMPAIRE, A. & LI, W. 2018. Growth performance and nutrient digestibility of weaned pigs fed multi-enzyme supplemented corn-soybean meal-based diets. *Journal of Animal Science,* 96**,** 329-329.

WU, J. C. Y., HUTCHINGS, C. H., LINDSAY, M. J., WERNER, C. J. & BUNDY, B. C. 2015. Enhanced Enzyme Stability Through Site-Directed Covalent Immobilization. *Journal of Biotechnology,* 193**,** 83-90.

WU, Y., JIANG, Y., KE, G. & LIU, Y. 2017. Effect of gamma-ray irradiation on the dewaterability of waste activated sludge. *Radiation Physics and Chemistry,* 130**,** 164-170.

XAVIER, J. B., DE KREUK, M. K., PICIOREANU, C. & VAN LOOSDRECHT, M. C. M. 2007. Multi-Scale Individual-Based Model of Microbial and Bioconversion Dynamics in Aerobic Granular Sludge. *Environmental Science & Technology,* 41**,** 6410-6417.

XIANG, Y., WANG, L. & JIAO, Y. 2016a. Disintegration of excess sludge enhanced by a combined treatment of gamma irradiation and modified coal fly ash. *Radiation Physics and Chemistry,* 120**,** 49-55.

XIANG, Y., XIANG, Y. & WANG, L. 2016b. Cobalt-60 gamma-ray irradiation pretreatment and sludge protein for enhancing enzymatic saccharification of hybrid poplar sawdust. *Bioresource Technology,* 221**,** 9-14.

XIAO, B. & LIU, J. 2009. Biological hydrogen production from sterilized sewage sludge by anaerobic self-fermentation. *Journal of Hazardous Materials,* 168**,** 163-167.

XU, F. & LI, Y. 2017. Biomass Digestion. *In:* ABRAHAM, M. A. (ed.) *Encyclopedia of Sustainable Technologies.* Oxford: Elsevier.

XU, M., JI, D., DENG, Y. & AGYEI, D. 2020. Preparation and assessment of cross-linked enzyme aggregates (CLEAs) of β-galactosidase from Lactobacillus leichmannii 313. *Food and Bioproducts Processing,* 124**,** 82-96.

XU, M.-Q., WANG, S.-S., LI, L.-N., GAO, J. & ZHANG, Y.-W. 2018. Combined Cross-Linked Enzyme Aggregates as Biocatalysts. *Catalysts,* 8**,** 460.

YAMAGUCHI, H., KIYOTA, Y. & MIYAZAKI, M. 2018. Techniques for preparation of cross-linked enzyme aggregates and their applications in bioconversions. *Catalysts,* 8.

YAMAGUCHI, M., WAKABAYASHI, S., NAKAMURA, Y., MATSUE, H., HIRAO, T., AOKI, S., YAMASHINA, S., YAMADA, H., MAMIZU, N., FURUKAWA, H. & CHIBANA, H. 2020. Good Ultrastructural Preservation of Human Tissues and Cultured Cells by Glutaraldehyde Fixation, Sandwich Freezing, and Freeze-Substitution. *Cytologia,* 85**,** 15-26.

YAN, J. Y., GUI, X. H., WANG, G. L. & YAN, Y. J. 2012. Improving Stability and Activity of Cross-linked Enzyme Aggregates Based on Polyethylenimine in Hydrolysis of Fish Oil for Enrichment of Polyunsaturated Fatty Acids. *Applied Biochemistry and Biotechnology,* 166**,** 925-932.

YANG, Q., LUO, K., LI, X. M., WANG, D. B., ZHENG, W., ZENG, G. M. & LIU, J. J. 2010. Enhanced efficiency of biological excess sludge hydrolysis under anaerobic digestion by additional enzymes. *Bioresource Technology,* 101**,** 2924-2930.

YAO, Y. 2014. *Use of carbohydrate, protein and fat to characterise wastewater in terms of its major elemental constituents and energy.* Master of Philosophy Thesis, The University of Manchester.

YAO, Y. L., GUAN, J., TANG, P., JIAO, H. P., LIN, C., WANG, J. J., LU, Z. M., MIN, H. & GAO, H. C. 2010. Assessment of toxicity of tetrahydrofuran on the microbial community in activated sludge. *Bioresource Technology,* 101**,** 5213-5221.

YASUDA, K., KATO, D., XU, Z., SAKKA, M. & SAKKA, K. 2010. Effect of ultrasonic frequency on enzymatic hydrolysis of cellulose. *Japanese Journal of Applied Physics,* 49**,** 07HE08.

YE, F. X., PENG, G. & LI, Y. 2011. Influences of influent carbon source on extracellular polymeric substances (EPS) and physicochemical properties of activated sludge. *Chemosphere,* 84**,** 1250-1255.

YIN, Y., LIU, Y. J., MENG, S. J., KIRAN, E. U. & LIU, Y. 2016. Enzymatic pretreatment of activated sludge, food waste and their mixture for enhanced bioenergy recovery and waste volume reduction via anaerobic digestion. *Applied Energy,* 179**,** 1131-1137.

YU, C. Y., LI, X. F., LOU, W. Y. & ZONG, M. H. 2013. Cross-linked enzyme aggregates of Mung bean epoxide hydrolases: A highly active, stable and recyclable biocatalyst for asymmetric hydrolysis of epoxides. *Journal of Biotechnology,* 166**,** 12-19.

YU, G. H., HE, P. J., SHAO, L. M. & LEE, D. 2008. Extracellular enzymes in sludge flocs collected at 14 full-scale wastewater treatment plants. *Journal of Chemical Technology and Biotechnology,* 83**,** 1717-1725.

YU, G. H., HE, P. J., SHAO, L. M. & LEE, D. J. 2007. Enzyme activities in activated sludge flocs. *Applied Microbiology and Biotechnology,* 77**,** 605-612.

YU, G. H., HE, P. J., SHAO, L. M. & ZHU, Y. S. 2009. Enzyme extraction by ultrasound from sludge flocs. *Journal of Environmental Sciences,* 21**,** 204-210.

YUAN, T. Z., LIU, S., REIMER, M., ISAAK, C. & AI, Y. 2021. Evaluation of pasting and gelling properties of commercial flours under high heating temperatures using Rapid Visco Analyzer 4800. *Food Chemistry,* 344**,** 128616.

ZDARTA, J., MEYER, A. S., JESIONOWSKI, T. & PINELO, M. 2018. A General Overview of Support Materials for Enzyme Immobilization: Characteristics, Properties, Practical Utility. *Catalysts,* 8**,** 92.

ZEINALI, M. & LENJANNEZHADIAN, H. 2018. Degradation of urea by entrapped cross-linked urease aggregates: a combinatorial approach to urease stabilization for environmental

and industrial applications. *International Journal of Environmental Science and Technology,* 15**,** 49-56.

ZHANG, G. G., YANG, Z. B., WANG, Y., YANG, W. R. & ZHOU, H. J. 2014a. Effects of dietary supplementation of multi-enzyme on growth performance, nutrient digestibility, small intestinal digestive enzyme activities, and large intestinal selected microbiota in weanling pigs1. *Journal of Animal Science,* 92**,** 2063-2069.

ZHANG, G. M., ZHANG, P. Y., YANG, J. & LIU, H. Z. 2008. Energy-efficient sludge sonication: Power and sludge characteristics. *Bioresource Technology,* 99**,** 9029-9031.

ZHANG, J., ZHANG, Y., LI, W., LI, X. L. & LIAN, X. 2014b. Optimizing detergent formulation with enzymes. *Journal of Surfactants and Detergents,* 17**,** 1059-1067.

ZHANG, P., ZHANG, G. & WANG, W. 2007. Ultrasonic treatment of biological sludge: Floc disintegration, cell lysis and inactivation. *Bioresource Technology,* 98**,** 207-210.

ZHANG, W., ALVAREZ-GAITAN, J. P., DASTYAR, W., SAINT, C. P., ZHAO, M. & SHORT, M. D. 2018. Value-Added Products Derived from Waste Activated Sludge: A Biorefinery Perspective. *Water,* 10**,** 545.

ZHANG, W., LI, L. Y., SHU, Z. X., WANG, P. P., ZENG, X. F., SHEN, W. Y., DING, W. P. & SHI, Y. C. 2021. Properties of flour from pearled wheat kernels as affected by ozone treatment. *Food Chemistry,* 341.

ZHANG, Y. H., REN, H., WANG, Y. L., CHEN, K. N., FANG, B. S. & WANG, S. Z. 2016. Bioinspired Immobilization of Glycerol Dehydrogenase by Metal Ion-Chelated Polyethyleneimines as Artificial Polypeptides. *Scientific Reports,* 6.

ZHEN, Q. N., WANG, M. F., QI, W., SU, R. X. & HE, Z. M. 2013. Preparation of beta-mannanase CLEAs using macromolecular cross-linkers. *Catalysis Science & Technology,* 3**,** 1937-1941.

ZHENG, J. F., CHEN, Y., YANG, L. W., LI, M. C. & ZHANG, J. 2014. Preparation of Cross-Linked Enzyme Aggregates of Trehalose Synthase via Co-aggregation with Polyethyleneimine. *Applied Biochemistry and Biotechnology,* 174**,** 2067-2078.

ZHOU, C., QIN, H. L., CHEN, X. J., ZHANG, Y., XUE, Y. F. & MA, Y. H. 2018a. A novel alkaline protease from alkaliphilic Idiomarina sp C9-1 with potential application for eco-friendly enzymatic dehairing in the leather industry. *Scientific Reports,* 8.

ZHOU, H., ZHANG, Z., WANG, M., HU, T. & WANG, Z. 2017a. Enhancement with physicochemical and biological treatments in the removal of pharmaceutically active compounds during sewage sludge anaerobic digestion processes. *Chemical Engineering Journal,* 316**,** 361-369.

ZHOU, H. D., LIU, J. C., CHEN, X. M., YING, Z. X., ZHANG, Z. & WANG, M. 2018b. Fate of pharmaceutically active compounds in sewage sludge during anaerobic digestions

integrated with enzymes and physicochemical treatments. *Waste Management,* 78**,** 911-916.

ZHOU, L. Y., MOU, H. X., GAO, J., MA, L., HE, Y. & JIANG, Y. J. 2017b. Preparation of cross-linked enzyme aggregates of nitrile hydratase ES-NHT-118 from E. coli by macromolecular cross-linking agent. *Chinese Journal of Chemical Engineering,* 25**,** 487-492.

ZHU, R., LI, C., CHEN, C., XING, S., CAI, Y., ZENG, X. & HE, L. 2021. Effect of cross-linked enzyme aggregate strategy on characterization of sn-1,3 extracellular lipase from Aspergillus niger GZUF36. *Applied Microbiology and Biotechnology,* 105**,** 1925-1941.

ZIELEWICZ, E. 2016a. Effects of ultrasonic disintegration of excess sewage sludge. *Applied Acoustics,* 103**,** 182-189.

ZIELEWICZ, E. 2016b. Effects of ultrasonic disintegration of excess sewage sludge. *Topics in Current Chemistry,* 374.

ZIELINSKI, M., DEBOWSKI, M., KISIELEWSKA, M., NOWICKA, A., ROKICKA, M. & SZWARC, K. 2019. Comparison of ultrasonic and hydrothermal cavitation pretreatments of cattle manure mixed with straw wheat on fermentative biogas production. *Waste and Biomass Valorization,* 10**,** 747-754.

ZINCHENKO, G. 2012. *Optimization of enzymatic hydrolysis of fibre sludge from pulp mill.* Bachelor thesis, Central Ostrobothnia University of Applied Sciences.

ZOHRA, R. R., QADER, S. A., PERVEZ, S. & AMAN, A. 2016. Influence of different metals on the activation and inhibition of α-amylase from thermophilic Bacillus firmus KIBGE-IB28. *Pak J Pharm Sci,* 29**,** 1275-8.

ZOROV, I. N., SEMENOVA, M. V., TSURIKOVA, N. V. & SINITSYN, A. P. 2006. Hydrolysis of wheat flour with amylase preparations and individual enzymes. *Applied Biochemistry and Microbiology,* 42**,** 616-619.

ZOU, J. T., TAO, Y. Q., LI, J., WU, S. Y. & NI, Y. J. 2018. Cultivating aerobic granular sludge in a developed continuous-flow reactor with two-zone sedimentation tank treating real and low-strength wastewater. *Bioresource Technology,* 247**,** 776-783.

Appendix

A- 1 The date of sampling and the corresponding specific energy input level of sonication treatment specific activities in the crude AS enzyme extracts (shown as average values)

Sampling date	AS pH	Specific Energy (kJ/g VS)	Amylase (U/g VS)	Protease (U/g VS)	Lipase (U/g VS)	Cellulase (U/g VS)	Experimental purpose
2018.4.23	7.54	54.54	*39.45	5.84	-	8.95	Optimisation of crude enzyme extraction from activated sludge
2018.5.16	7.13	56.14	*34.87	6.31	-	8.21	
2018.6.13**	6.73	-	*48.57	6.92	-	8.87	
	6.67	-	*44.14	6.79	-	9.21	
	6.66	-	*49.67	7.86	-	9.22	
	6.67	-	*43.56	5.97	-	7.84	
	6.63	-	*49.70	6.08	-	9.86	
2018.6.13	6.57	-	*53.69	6.47	-	10.38	
2018.7.2	7.48	76.19	*35.97	6.59	-	-	Consolidation and stabilisation of crude enzymes by cross-linking
2018.7.30	7.18	67.78	*38.29	4.92	-	-	
2018.9.18	7.23	58.33	*38.80	4.69	-	-	
2018.9.24	-	64.85	-	4.73	-	-	
2018.12.5	6.94	56.52	179.43	3.89	-	-	
2018.12.8	-	54.82	150.48	-	-	-	
2019.2.5	6.67	52.03	263.42	-	-	-	
2019.2.11		56.78	271.19	-	-	-	
2019.2.19	6.76	64.53	393.81	-	-	-	
2019.3.4	6.84	65.34	412.15	8.40	20.09	13.48	
2019.4.3	6.81	58.71	267.98	7.93	14.83	-	
2019.4.10	-	56.19	288.45	8.14	-	-	
2019.5.21	7.49	56.59	220.23	6.99	22.24	30.38	
2019.5.27	-	56.56	241.09	7.16	22.89	30.12	
2019.6.10	7	63.69	230.10	7.60	28.44	34.62	

2019.8.5	7.04	57.76	192.10	6.63	19.19	19.59	
2019.10.7	6.93		217.45	6.55	13.73	25.45	
2019.11.14	7.04	55.23	-	-	-	-	
2020.6.30	6.7	59.92	262.35	7.06	20.96	-	Substrate hydrolysis activity of CLEAs
2020.7.27	6.71	57.28	228.96	5.43	13.41	-	
2020.7.28	-	58.96	-	-	-	-	
2020.10.20	6.61	56.22	254.72	-	-	-	
2020.10.21	-	54.72	-	-	-	-	

Note:* donates α-amylase was measured based on the procedure specified in Section 3.6; ** donates the sludge samples were collected from WWTP2, with other batches of sludge samples collected from WWTP1.

A- 2 First order model validation for flour hydrolysis: residual plots for sTOC (a, b), reducing sugar (c, d), and tyrosine (e, f) concentration against reaction time at CLEA addition = 1:100 (a, c, e) and 1:10 v/v (b, d, f) (blue, orange and grey dots representing three replicated measurements)

(a)

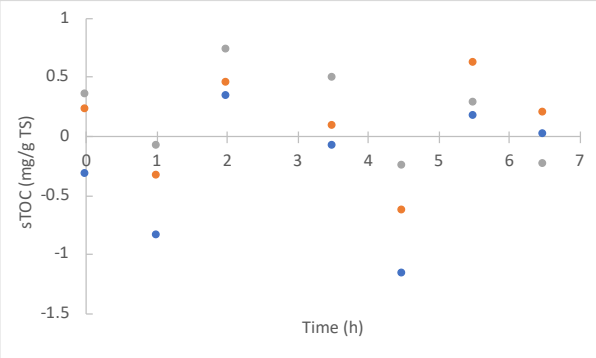

(b)

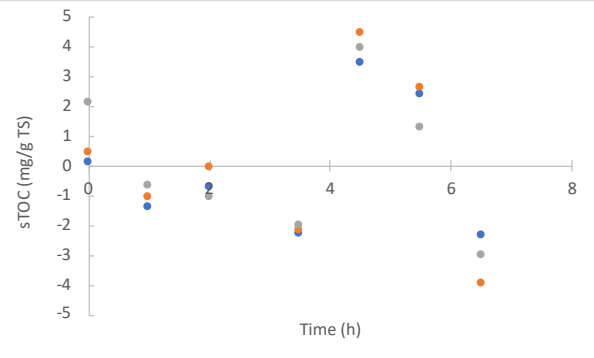

(c)

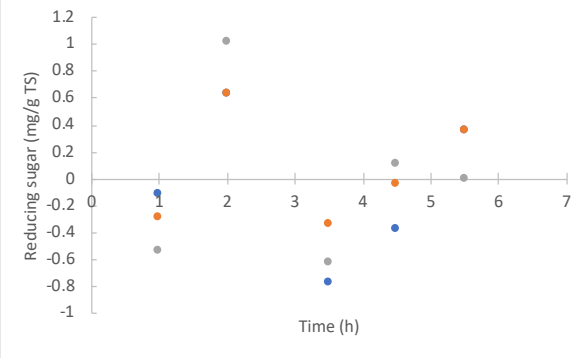

(d)

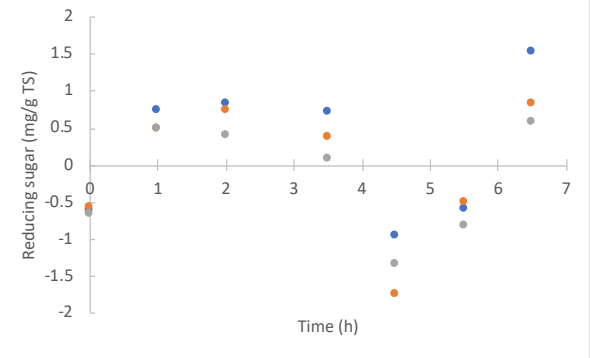

(e)

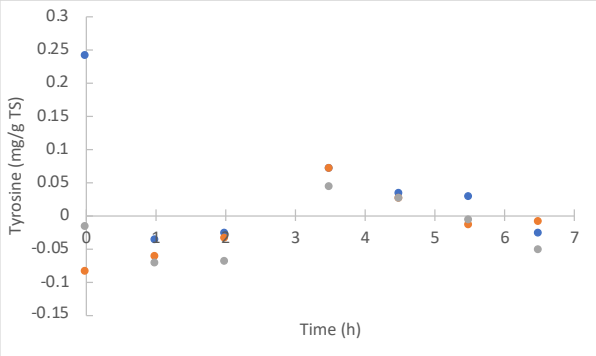

(f)

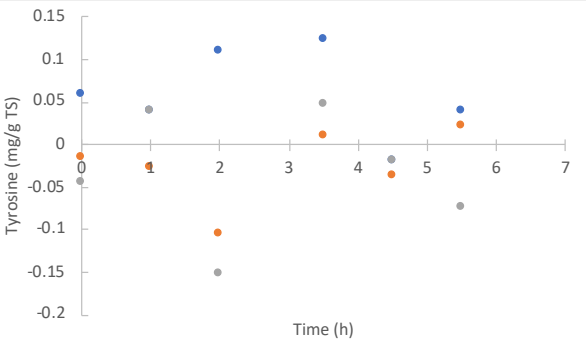

A- 3 First order model validation for hydrolysis of (a) γ-irradiated AS and (b) sonicated AS hydrolysis: residual plots for tyrosine concentration against reaction time (blue, orange and grey dots representing three replicated measurements)

(a) (b)

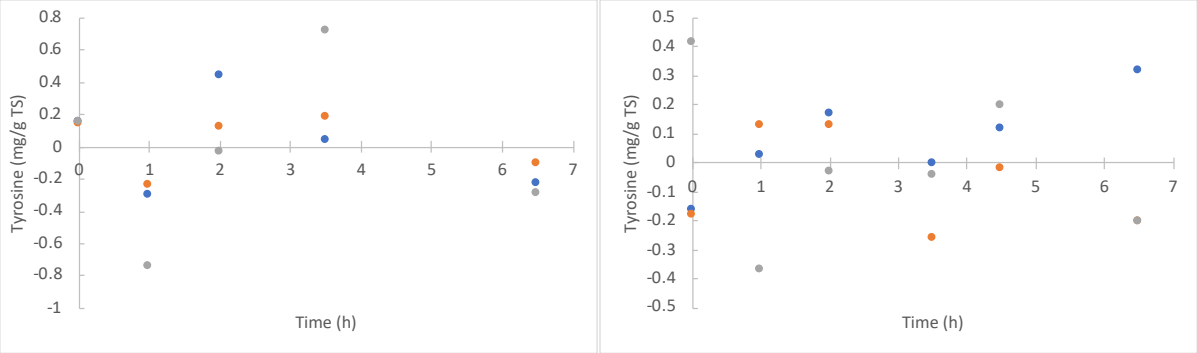

A- 4 UV-Absorbance of activated sludge samples before and after gamma-irradiation (for 10 h at room temperature, with total radiation dose = 1944 Gy at a dose rate of 3.24 Gy/min), measured by an UV-spectrophotometer at wavelength = 190-800 nm